Microbial community characterization and carbon turnover in methane-rich marine environments - case studies in the Gulf of Mexico and the Black Sea

Dissertation
zur Erlangung des Doktorgrades
der Naturwissenschaften
- Dr. rer. nat. -

Am Fachbereich Geowissenschaften
der Universität Bremen

vorgelegt von

Florence Schubotz

Bremen
Oktober 2009

1. Gutachter: Prof. Dr. Kai-Uwe Hinrichs
2. Gutachter: Prof. Dr. Stuart G. Wakeham

Date of defense: October 26, 2009

Science is a way of studying the world around us, not a set of facts.

(Tori Hoehler)

TABLE OF CONTENTS

Abstract Thesis abstract I
Zusammenfassung III

List of Abbreviations V

List of Figures IX

List of Tables XII

Chapter I Introduction and Methods 1
I.1. General Introduction 2
I.2. Objectives of this Thesis 13
I.3. Methods 15
I.4. Contribution to Publications 31
I.5. References 32

Chapter II Detection of microbial biomass by intact polar membrane lipid analysis in the water column and surface sediments of the Black Sea 51
II.1 Summary 52
II.2 Introduction 52
II.3. Results and Discussion 53
II.4. Experimental Procedures 66
II.5. Acknowledgements 68
II.6. References 68
II.S1. Supporting Information 72
II.S2. Supporting Information - References 74

Chapter III Chemosynthetic life at the Chapopote asphalt volcano - insights from stable carbon isotopes and intact polar membrane lipid analyses ... 77
III.1. Abstract 78
III.2. Introduction 78
III.3. Material and Methods 80
III.4. Results and Discussion 84
III.5. Summary and Conclusions 104
III.6. Acknowledgements 105
III.7. References 105

Chapter IV Sulfate-reduction, methanotrophy, and methanogenesis at the Chapopote asphalt volcano deciphered by head group-specific stable carbon isotopic analysis of intact polar membrane lipids 113
IV.1. Abstract 114
IV.2. Introduction 114
IV.3. Material and Methods 115
IV.4. Results 124
IV.5. Discussion 124
IV.6. Summary and Conclusions 131
IV.7. Acknowledgements 132
IV.8. References 132

Chapter V. Determining total petroleum hydrocarbon degradation and weathering by comprehensive GC×GC at an asphalt seep in the southern Gulf of Mexico 141
V.1. Abstract 142
V.2. Introduction 142
V.3. Experimental 143
V.4. Results and Discussion 146
V.5. Acknowledgements 154
V.6. References 155
V.S1. Supplementary Material 158
V.S2. References 162

Chapter VIb. Methane and sulfide fluxes in permanent anoxia: *in-situ* studies at the Dvurechenskii mud volcano (Sorokin Trough, Black Sea) 165

Chapter VIc. Bacterial symbionts of *Bathymodiolus* mussels and *Escarpia* tubeworms from an asphaltic deep-sea environment in the southern Gulf of Mexico 169

Chapter VII. Concluding Remarks and Outlook 173
Summary and Conclusions 174
Outlook 178
References 179

Acknowledgements 183

Appendix 187
Published Manuscript I: Rock weathering creates oases of life in a High Arctic Desert 189
Published Manuscript II: Methane-producing microbial community in a coal bed of the Illinois Basin 193
Curriculum Vitae 196

Thesis Declaration 199

THESIS ABSTRACT

This thesis investigated patterns in the distribution of intact polar membrane lipids (IPLs) in the marine environment. IPL analysis is a relatively new tool in microbial ecology to study (*i*) live microbial biomass and (*ii*) the dominating microbial players. This technique was applied for the first time to study the oxic and anoxic water column of the Black Sea and observed a stratification of IPLs according to geochemical zonation. Export of IPLs to the sediment was found to be selective and the distribution of IPLs in the upper 2 cm of the sediments reflects *de novo* production of IPLs by indigenous microbes, putatively identified as sulfate-reducing bacteria and benthic archaea. The distribution of archaeal IPLs in the anoxic water body did not indicate the abundant presence of methanotrophic archaea, which were presumed in earlier studies due to high estimated methane oxidation rates. The presence of betaine lipids and glycosidic sphingolipids in the anoxic water column could be linked to unknown anaerobic bacteria and is a novel finding as these lipids are primarily known to be produced by eukaryotes.

Investigations of microbial communities associated to the Chapopote asphalt seep in the southern Gulf of Mexico revealed the presence of a diverse array of IPLs from both Bacteria and Archaea. IPL concentrations in the sediments were correlated with the abundant presence of oil and methane, indicating that the petroleum hydrocarbons are a major stimulant for microbial activity. Bacterial IPL concentrations decreased with decreasing sulfate concentrations over depth, whereas archaeal IPLs increased simultaneously and comprised up to 80% of total IPLs at ca. 15 cm sediment depth. Bacterial lipids mainly included phospholipids with the polar head groups phosphatidylethanolamine (PE), phosphatidyl-(N)-methylethanolamine (PME), and phosphatidylglycerol (PG). The assignment of these IPLs to sulfate-reducing bacteria (SRB) was confirmed by the presence of SRB-characteristic fatty acids. Polar head group-specific isotope analysis of the SRB core lipids revealed that the majority of the SRB population is autotrophic and involved in the anaerobic oxidation of methane. However, a large amount of SRB are heterotrophic hydrocarbon-degrading bacteria. The oil-degrading bacteria mainly contained PME as head group. Archaeal IPLs indicated the presence of ANME-1 archaea comprised of diglycosidic glyceroldibiphytanylglyceroltetraethers (2Gly-GDGT) accompanied by ANME-2 archaea suggested by phosphate-based hydroxyarchaeols. Polar head group-specific stable carbon isotope analysis of the archaeal IPLs confirmed the association of those lipids to methanotrophic archaea and could also show that phosphate-based archaeols and GDGTs with mixed glycosidic and phosphate-based head groups were mainly derived from methanogenic archaea. In subsurface sediments of the oil-influenced Chapopote asphalt seep abundant archaeal IPLs were detected close to a sulfate-methane transition zone. Here, bacterial lipids were only a minor part of the total IPLs and were dominated by diether lipids with PE headgroups. Phosphate-based hydroxyarchaeols and diglycosidic GDGTs could be assigned to both methanogenic and methanotrophic sources. Methane is thus a major intermediate in microbial metabolism at the Chapopote asphalt volcano.

Investigations of biological and physical weathering of the deposited asphalts showed that the asphalts are an important substrate for the microbial community. The removal of *n*-alkanes, branched alkanes, isoprenoids and low molecular weight polyaromatic hydrocarbon compounds could be primarily assigned to biodegradation. Biomarkers such as steranes and hopanes were most recalcitrant and were still observed in highly weathered brittle asphalts. Comparison of fresh and weathered asphalts allowed to estimate total petroleum hydrocarbon losses into the environment. Assessment of the potential of total hydrocarbon emission from the Chapopote asphalt seep amounts to up to 1,540 ± 770 tons. However, there is indication that a large fraction of these hydrocarbons are already efficiently recycled by the indigenous microorganisms associated to the asphalts.

ZUSAMMENFASSUNG

In der vorliegenden Arbeit wurde die Verteilung von intakten polaren Membranlipiden (IPL) in marinen Umweltproben untersucht. Die Analyse von IPLs ist eine recht junge Methode der mikrobiellen Ökologie zur Untersuchung von (*i*) lebendiger mikrobieller Biomasse und (*ii*) den vorherrschenden Mikroorganismen. Diese Technik wurde zum ersten Mal angewendet um die sauerstoffreichen und sauerstoffarmen Bereiche der Wassersäule des Schwarzen Meeres zu untersuchen. Wie erwartet, wurde eine Stratifizierung der IPLs in Übereinstimmung mit der geochemischen Zonierung gefunden. Es wurde beobachtet, dass der Export von Lipiden in das Sediment sehr selektiv vonstattengeht und dass die ersten 2 cm des Sediments durch *de novo* Produktion von IPLs gekennzeichnet sind. Als einheimische Mikroorganismen wurden Sulfatreduzierer und benthische Archaeen identifiziert. Die Verteilung der Archaeenlipide im anoxischen Teil der Wassersäule zeigte keine Anzeichen von methanotrophen Archaeen, die aufgrund von früheren Studien basierend auf hohen potentiellen Methanoxidationsraten vorhergesagt wurden. Die Anwesenheit von Betainlipiden und glykosidischen Sphingolipiden im anoxischen Bereich hingegen konnte mit unbekannten anaeroben Bakterien verknüpft werden. Dies ist eine neue Beobachtung, weil diese Lipide bisher nur von Eukaryoten bekannt sind.

Untersuchungen der mikrobiellen Gemeinschaften an der Chapopote Asphaltquelle im südlichen Golf von Mexiko fanden eine große Bandbreite von IPLs von Bakterien und Archaeen. Die Lipidkonzentrationen in den Sedimenten waren mit den großen Mengen an Öl und Gas verknüpft. Hieraus lässt sich schließen, dass das Vorkommen der Kohlenwasserstoffe mikrobielle Aktivität fördert. Die Konzentrationen von Bakterienlipiden nahmen mit sinkender Sulfatkonzentration über die Tiefe ab, wohingegen die Archaeenlipidkonzentrationen gleichzeitig zunahmen und schließlich bis zu 80% der gesamten IPLs in 15 cm Tiefe ausmachten. Die bakteriellen Lipide umfassten hauptsächlich Phospholipide mit den polaren Kopfgruppen Phosphatidylethanolamin (PE), Phosphatidyl-(N)-methylethanolamin (PME) und Phosphatidylglycerol (PG). Die Zuordnung dieser Lipide zu sulfatreduzierenden Bakterien (SRB) wurde durch spezifische Fettsäurekombinationen bestätigt. Eine detaillierte Analyse der Kernlipide nach Auftrennung nach Lipidklassen basierend auf den polaren Kopfgruppen zeigte, dass der größte Teil der SRB autotroph ist und an der anaeroben Oxidation von Methan beteiligt ist. Trotzdem wurde bestimmt, dass ein großer Anteil der SRB heterotrophe Kohlenwasserstoffdegradierende Bakterien sind. Diese Organismen besitzen hauptsächlich PME Kopfgruppen. Diglykosidische Glyceroldibiphytanylglyceroltetraether (2Gly-GDGT) deuteten auf die Anwesenheit von ANME-1 Archaeen hin. Zusätzlich wurden phosphatbasierende Hydroxyarchaeole gefunden, welche für ANME-2 Archaeen spezifisch sind. Die Untersuchung der stabilen Kohlenstoffisotope der Archaeenlipide bestätigte die Zuordnung zu methanotrophen Archaeen und konnte weiterhin zeigen, dass phosphatbasierende Archaeole und GDGTs mit gemischter Zucker/Phosphat Kopfgruppe hauptsächlich von methanogenen Archaeen gebildet werden. In den tief versenkten Sedimenten der öligen Quelle am Chapopote wurden große

Mengen von Archaeenlipiden in der Nähe der Sulfat/Methan-Übergangszone gefunden. Dort machten Bakterienlipide, hauptsächlich in der Form von Dietherlipiden mit PE Kopfgruppe, nur einen kleinen Anteil der Gesamtmenge aus. Phosphatbasierende Hydroxyarchaeole und diglykosidische GDGTs konnten zu methanogenen und methanotrophen Quellen zugeordnet werden. Methan ist somit eine wichtiges Intermediat in der mikrobiellen Verstoffwechslung am Chapopote asphalt volcano.

Weiterhin wurden die biologischen und physikalischen Verwitterungsprozesse der abgelagerten Asphalte untersucht. Es zeigte sich, dass die Asphalte ein bedeutendes Substrat für die mikrobiellen Gemeinschaften darstellen. Der Abbau von unverzweigten und verzweigten Alkanen, Isoprenoiden und niedermolekularen polyaromatischen Kohlenwasserstoffen konnte zu Biodegradation zugeordnet werden. Biomarker wie Sterane und Hopane waren recalcitrant und konnten auch in stark verwitterten Asphalten nachgewiesen werden. Ein Vergleich von frischen und verwitterten Asphaltstücken erlaubte eine Abschätzung der Gesamtmenge an Kohlenwasserstoffen die in die Umwelt abgegeben werden. Eine erste Einschätzung zeigte, dass der Chapopote Asphaltvulkan bis zu 1540 ± 770 Tonnen Kohlenwasserstoffe ausstößt. Allerdings gibt es Hinweise darauf, dass ein großer Anteil dieser Menge bereits von Mikroorganismen im Asphalt abgebaut wird.

LIST OF ABBREVIATIONS

1Gly	Monoglycosyl
2Gly	Diglycosyl
3Gly	Triglycosyl
16S rRNA	Small subunit of ribosomal ribonucleic acid with a sedimentary unit of 16
AEG	Acylether glycerol
ANME	Anaerobic methanotrophic archaea
AOM	Anaerobic oxidation of methane
AP	Asphalt patches
APCI	Atmospheric pressure chemical ionization
API gravity	American Petroleum Institute gravity
AR	Archaeol
BBr_3	Boron tribromide
BL	Betaine lipid
bp	Biphytane
bp3c	Biphytane derived from crenarchaeol
BS	Bubble site
BSTFA	Bis-(trimethylsilyl)trifluoroacetamide
BTEX	Benzene, toluene, ethyltoluene, xylene compounds
C_{16}-PAF	1-O-hexadecyl-2-acetoyl-*sn*-glycero-3-phosphocholine
CARD-FISH	Catalyzed reporter deposition – fluorescent *in-situ* hybridization
CH_4	Methane
C_n-BT	Alkylbenzothiophene
C_n-DBT	Alkyldibenzothiophene
C_n-N	Alkyl-substituted naphthalenes
C_n-P	Phenantrene
COI	Mitochondrial cytochrome oxidase I gene
CO_2	Carbon dioxide
CSIA	Compound-specific isotope analysis
DAG	Diacylglycerol
DAGE	Dialkylgycerolether
DAPI	4′,6-diamidino-2-phenylindol
DCM	Dichloromethane
DEG	Dietherglycerol
DFG	Deutsche Forschungsgemeinschaft
DGTA	Diacylglyceryl-hydroxymethyl-(N,N,N-trimethyl)-*ß*-alanine
DGTS	Diacylglyceryl-(N,N,N)-trimethylhomoserine
DIC	Dissolved inorganic carbon
DMV	Dvurechenskii mud volcano
DNA	Desoxyribonucleic acid
DPG	Diphosphatidylglycerol, cardiolipin

dsrA	Dissimilatory sulfide reductase enzym, subunit A
DSS	*Desulfosarcina/Desulfoccocus* group
ESI	Electrospray ionization
eV	Electron volts
FA	Fatty acid
FID	Flame ionization detector
FISH	Fluorescence *in-situ* hybridization
GC	Gas chromatography
GC-FID	Gas chromatography coupled to flame ionization detector
GC-irMS	Gas chromatography coupled to isotope ratio mass spectrometer
GC-MS	Gas chromatography coupled to mass spectrometer
GC×GC	Comprehensive two-dimensional gas chromatography
GDGT	Glyceroldibiphytanyltetraether
GHSZ	Gas hydrate stability zone
GLOMAR	Global Changes in the Marine Realm
Gly-Cer	Glycosidic ceramides
Gly-dGly	Glycosyl-deoxyglycosyl
GoM	Gulf of Mexico
GRC	Gravity core
Gt	Gigatons (10^9 tons)
H_2	Hydrogen gas
H341-GDGT	IPL-GDGT species with unidentified head group of 341 Da
HC	Hydrocarbon
HG	Heterocyst glycolipids
HPLC	High performance liquid chromatography
ID	Inner diameter
IPL	Intact polar membrane lipid
IS	Internal standard
IT-MS	Ion trap mass spectrometer
KOH	Potassium hydroxide
LMW	Low molecular weight
MAF	Main asphalt field
MAGE	Monoalkylglycerolether
MARUM	Center for Marine Environmental Sciences
mbsf	Meters below seafloor
mbsl	Meters below sea level
MeOH	Methanol
mL	Milliliter
mM	Millimolar
MS^n	Multistage mass spectrometry
MPL	Main polar lipid

m/z	Mass-to-charge ratio
ODP	Ocean drilling program
OH-AR	Hydroxyarchaeol
OH-eAR	Extended hydroxyarchaeol
OL	Ornithine lipid
OlsA	Acyl-*sn*-glycerol-3-phosphate acyltransferase protein
PLFA	Polar lipid-derived fatty acid
PA	Phosphatidic acid
PAH	Polycyclic aromatic hydrocarbons
PC	Phosphatidylcholine
PDME	Phosphatidyl-(N,N)-dimethylethanolamine
PE	Phosphatidylethanolamine
PG	Phosphatidylglycerol
PI	Phosphatidylinositol
PM	Particulate matter
PME	Phosphatidyl-(N)-methylethanolamine
$\mathbf{PO_4}$	Phosphate
POC	Particulate organic carbon
Pr	Pristane
PS	Phosphatidylserine
PUC	Push core
PUFA	Polyunsaturated fatty acid
RCOM	Research center for ocean margins
RNA	Ribonucleic acid
ROV	Remotely operated vehicle
SIM	Selected ion monitoring
SIMS	Secondary ion mass spectrometry
SMTZ	Sulfate-methane transition zone
SR	Sulfate-reduction
SRB	Sulfate-reducing bacteria
SQ-DAG	Sulfoquinovosyl diacylglycerol
TCA	Trichloroacetic acid
TCA	Tricarboxylic acid
TIC	Total ion chromatogram
THF	Tetrahydrofurane
TLE	Total lipid extract
TMS	Trimethylsilyl
TN	Total nitrogen
TOC	Total organic carbon
ToF-MS	Time-of-flight mass spectrometer
Tm	Trisnorhopane

TPH	Total petroleum hydrocarbon
Ts	Trisnorneohopane
UCM	Unresolved complex mixture
UK	Unknown
VPDB	Vienna Pee Dee Belemnite standard

LIST OF FIGURES

Figure I.1. Pictures of a black smoker surrounded by tubeworms at the Endeavour hydrothermal vent site and a cold seep 2
Figure I.2. Global distribution of modern and fossil cold seeps 3
Figure I.3. Scheme of sulfate-methane transition zone in marine sediments 5
Figure I.4. (CARD)-FISH images of different ANME and SRB cells in the marine environment 7
Figure I.5. Cartoons representing the redox zonation and associated electron acceptors accompanying sucessive respiration processes in the marine environment 8
Figure I.6. Aerobic BTEX activation and anaerobic naphthalene biodegradation ... 12
Figure I.7. Schematic structure of a bacterial phospholipid bilayer membrane 15
Figure I.8. Tree of life showing the three domains of life and polar head group and core lipid structures of Archaea and Bacteria 18
Figure I.9. Fragmentation patterns of IPLs in positive and negative ion mode 22
Figure I.10. Example of HPLC-chromatogram, associated density map, and mass spectra of a soil sample from Svalbard 23
Figure I.11. Density map of a preparative HPLC run of a sample mixture from a cold seep and a soil from Svalbard used for method development 24
Figure I.12. Important biomarkers in crude oils, depicting the different numbering system for cheilanthanes, hopanes and steranes, and organic hydrocarbons present in crude oils primarily derived from cracking processes and catagenesis 25
Figure I.13. Alteration of oils during biodegradation showing how the removal of compounds results in a rise of the baseline during GC-FID analysis . 26
Figure I.14. Comparison of mass chromatograms of methylphenantrene isomers and dimethylphenantrene isomers showing alterations during weathering of oils 27
Figure I.15. Separation of compounds by GC×GC showing individual chromatograms in the second dimension 28
Figure I.16. GC-FID and GC×GC chromatogram of a sample from an oil-contaminated site 29
Figure I.17. Conversion of a GC×GC chromatogram into a mass loss table 30

Figure II.1. Depth profile of concentrations of oxygen, methane, hydrogen sulfide, nitrate, POC, TN, PLFA, IPL, and cells 54
Figure II.2. Relative distribution and estimated absolute abundance of IPLs 55
Figure II.3. Relative distrubution, number of rings, and estimated absolute abundance of IPL-GDGTs 60
Figure II.4. Base peak chromatogram and density maps of representatative redox zones in the water column 62
Figure II.5. IPL structures of head groups and core lipids 64
Figure II.S1. Mass spectra of tentatively identified IPLs 73

Figure III.1. Location, bathymetric map, and pictures of samples 81
Figure III.2. Relative and total abundance of hydrocarbon gases, and cross plot of the stable carbon isotopic composition of hydrocarbon gases 85
Figure III.3. Geochemical profiles of concentrations and stable carbon isotopic compositions of hydrocarbon gases, DIC, TOC, IPLs, and UCM 87
Figure III.4. Total ion and mass chromatograms showing the *n*-alkane distribution of asphalts and oil-impregnated sediments 88
Figure III.5. Structures of core lipids and head groups of identified IPLs 91
Figure III.6. Distribution and absolute concentrations of IPLs in deep asphalt samples and surface sediments 92
Figure III.7. Density maps and chromatograms showing the distribution of IPLs 93
Figure III.8. Mass spectra of tentatively identified intact archaeal isoprenoidal ether lipids in positive ion mode 99
Figure III.9. Density map and chromatogram showing the lipid distribution in holothurian digestive tracks 103
Figure III.10. Schematic of hydrocarbon seepage and associated chemosynthetic life at the Chapopote Knoll 104

Figure IV.1. Geochemical profiles of absolute and relative abundances of sulfate, methane, IPL, and δ^{13}C of methane, dissolved inorganic carbon, and total organic carbon at sites GeoB10619 and GeoB10610 119
Figure IV.2. Distribution of PLFA of different head groups from F8-F10 at site GeoB10619 at 2.5-10 cm and 10-15 cm sediment depth 122
Figure IV.3. Core and IPL-GDGT distribution in GRC GeoB10610 124
Figure IV.4. Depth profiles of archaeal and bacterial IPL concentrations and δ^{13}C of IPL-derived apolar derivatives and carbon substrates TOC, DIC and methane at sites GeoB10619 and GeoB10610 127

Figure V.1. Comparison of a conventional GC-MS and GCxGC chromatogram of an asphalt sample from the main asphalt field 147
Figure V.2. Dendrogram of compound classes in all GC×GC ToF-MS analyzed asphalt samples, and compound class quantification of three selected samples with GC×GC FID 148
Figure V.3. Chromatograms of a fresh and rough asphalt sample, and the corresponding difference chromatogram 150
Figure V.4. Chromatogram of a fresh and a brittle asphalt sample, and the generated difference chromatogram 151
Figure V.5. Estimated total petroleum hydrocarbon (TPH) mass losses between fresh/rough and fresh/brittle asphalts 153
Figure V.S1. Map of the asphalt seeps at the Chapopote Knoll and images of the asphalt structures on the seafloor 159
Figure V.S2. Comparison of GC×GC chromatograms of an asphalt sample analyzed with GC×GC ToF-MS and GC×GC-FID 160
Figure V.S3. Spider diagram showing the biomarker ratios of a selection of the analyzed asphalt samples and two oils from the Campeche Shelf and the Sureste Basin 160

Figure V.S4. Mass spectra and distribution of bicyclic sesquiterpanes identified in this study 161

Figure VIa. Bathymetric map of the DMV generated during the M72-2 cruise with sampling stations 166
Figure VIb.1. Fluorescence *in-situ* hybridization (FISH) identification of bacterial symbionts in *Bathymodiolus heckerae* 170
Figure VIb.2. Stable carbon isotope composition of fatty acids extracted from *B. heckerae*, *B. brooksi*, and *Escarpia* sp. tubeworms tissue 170

Figure Appendix 1. The ML-RS1 site in the moraine of Midtre Lovénbreen glacier, Ny Ålesund, Svalbard 190
Figure Appendix 2. Proposed mechanisms of stepwise biodegradation of OM in coal.. 194

LIST OF TABLES

Table I.1. Simplified pathways of organic matter oxdidation and associated free energy yield in marine sediments 4
Table I.2. Summary of $\delta^{13}C$ contents and fractionation factors of different archaeal lipids from methanogens during growth on different substrates under substrate-limited and non-limited conditions 21
Table I.3. $\delta^{13}C$ of biomass and FA of four SRB under different growth conditions. 22

Table II.1. Core lipid structures and likely origin of IPL compound classes in different redox zones of the central Black Sea 57
Table II.S1. Identification of IPLs using complementary evidence gained through data-dependent MS^n experiments 72

Table III.1. Concentration and stable carbon isotopic composition of hydrocarbon gases of asphalts and sediments 86
Table III.2. Hydrocarbon composition and pristane to C_{17} *n*-alkane ratios of different asphalt samples 89
Table III.3. Examples of characteristic fragmentation patterns of IPL 94
Table III.4. Major core lipid composition of IPLs in asphalts and sediments 95

Table IV.1. Recovered fractions after preparative LC, containing IPLs separated according to head group polarity 117
Table IV.2. Stable carbon isotopic composition and relative distribution of most abundant fatty acids, MAGE and DAGE of bacterial IPLs 121
Table IV.3. Stable carbon isotopic composition of archaeal diether and tetraether IPL-derivatives in surface sediments 128
Table IV.4. Stable carbon isotopic composition of archaeal diether and tetraether IPL-derivatives in subsurface sediments 130

Table V.1. Sample list and asphaltene content of analyzed asphalts 146
Table V.2. Relative abundance of total petroleum hydrocarbons and TPH losses in the three asphalts analyzed with GC×GC-FID 153
Table V.S1. Biomarker ratios, bulk $\delta^{13}C$ values of the analyzed asphalt samples ... 158

Chapter I

Introduction and Methods

I.1. GENERAL INTRODUCTION

I.1.1. Cold seeps and their role in the global carbon cycle

I.1.1.1. Oases on the seafloor

Plate tectonics change the face of the Earth in a constantly evolving manner (Wegener et al., 1929; Vine and Matthews, 1963). Volcanic activities and expulsion of reduced gases accompanied by episodic earthquakes go along with subduction, conversion, faulting, and shifting processes during movements of plates, making plate boundaries a hostile environment to live in (McCann et al., 1979; MacDonald, 1982; Condie, 1997). Nevertheless, extreme forms of life have found modes to adapt to such harsh conditions (e.g., Hessler et al., 1985; Kulm et al., 1986; Kennicutt et al., 1985; Junpier and Sinuit, 1987; Van Dover et al., 2002). The major sustaining factor for life far from sunlight is the dependency on chemosynthetic energy in the form of reduced chemical substances (Cavanaugh et al., 1981; Jannasch, 1984; Childress et al., 1986; MacDonald et al., 1990a). Hot vents, which were the first underwater oases to be discovered (Weiss et al., 1977; Corliss et al., 1979), usually occur at convergent plate boundaries where chemosynthetic life is driven by hydrothermal activity pumping electron donors such as hydrogen and hydrogen sulfide to the sediment surface (cf. Jannasch and Mottl, 1985; Kelley et al., 2002; Martin et al., 2008; Fig. I.1a). Cold seeps, first observed at the Florida Escarpment in the Gulf of Mexico (Paull et al., 1984), mainly occur at continental margins and divergent plate boundaries where fluid and gas seepage is not primarily driven by temperature but rather by tectonic processes causing overpressurisation of hydrocarbon-containing sediments (Kulm et al., 1986; Juniper and Sinuit, 1987; Kennicutt et al., 1988). This essentially results in a focused upwards flow of gases along created fissures and faults and leads to expulsion of reduced hydrocarbon gases such as methane and higher hydrocarbons (Brooks et al., 1984; Sassen et al., 1999). These fluids and gases serve as substrate and energy source for a vast array of specially adapted organisms, including microbial mats, bacterial symbiont-hosting tube worms, mussels and clams, but also crabs, shrimps, and sea cucumbers (cf. Sibuet and Olu, 1998; Levin, 2005; Fig. I.1b).

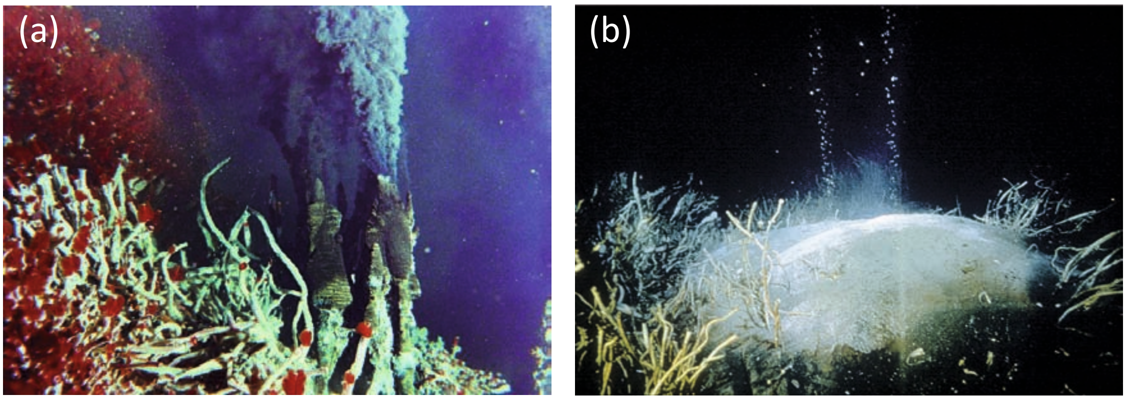

Fig. I.1. Pictures of a black smoker surrounded by tubeworms at (**A**) the Endeavour hydrothermal vent site (V. Tunnicliffe, University of Victoria) and (**B**) a cold seep (MacDonald et al., 2002). The hot vent features black smokers caused by precipitation of metals and associated tube worms; the cold seep shows bubbles of methane seeping out of the ocean floor accompanied by carbonate precipitates and tube worms.

I.1.1.2. Global importance of hydrocarbon emissions

Cold seeps are a globally widespread feature and occur along continental margins in both active and passive systems (Fig. I.2). It is estimated that cold seeps have a contribution of 600,000 tons of spilled hydrocarbon per year (Wilson et al., 1974; Kvenvolden and Cooper, 2003). Furthermore, they pose a great potential of methane emission into the atmosphere, to an extent which is currently poorly constrained (Solomon et al., 2009). Understanding of the sources and sinks of methane is important, considering that methane is a 21 times more efficient greenhouse gas than CO_2 (cf. Wuebbles and Hayhoe, 2002). Large amounts of methane are preserved in the form of gas hydrates at cold seeps in clathrate structures formed from a mixture of natural gas and water (e.g., Brooks et al., 1984; Suess et al. 1999; Milkov and Sassen, 2001). These hydrates are only stable at high pressures and low temperatures in the so-called gas hydrate stability zone (GHSZ; Sloan, 1991; Kvenvolden et al., 1995). Most recent estimates of the total amount of methane stored in gas hydrates may range up to 74,400 Gt of carbon (Klauda and Sandler, 2005), more conservative values range around 3,000 Gt of methane carbon (Buffet and Archer, 2004; Milkov, 2004). Dissociation of these gas hydrates would have catastrophic consequences and could cause significant perturbations in the global climate, as was described in previous studies where a sudden release of methane gas from gas hydrates has been attributed to past global warming events (Dickens et al., 1995; Hesselbo et al., 2000; Hinrichs et al., 2003). Although cold seeps have a high potential of methane emission, current estimates attribute oceanic emissions roughly to less than 1% of global atmospheric input (cf. Reeburgh, 2007). This is explained by a very efficient recycling of methane within the oceanic biosphere by biological activity, consuming methane before it reaches the atmosphere.

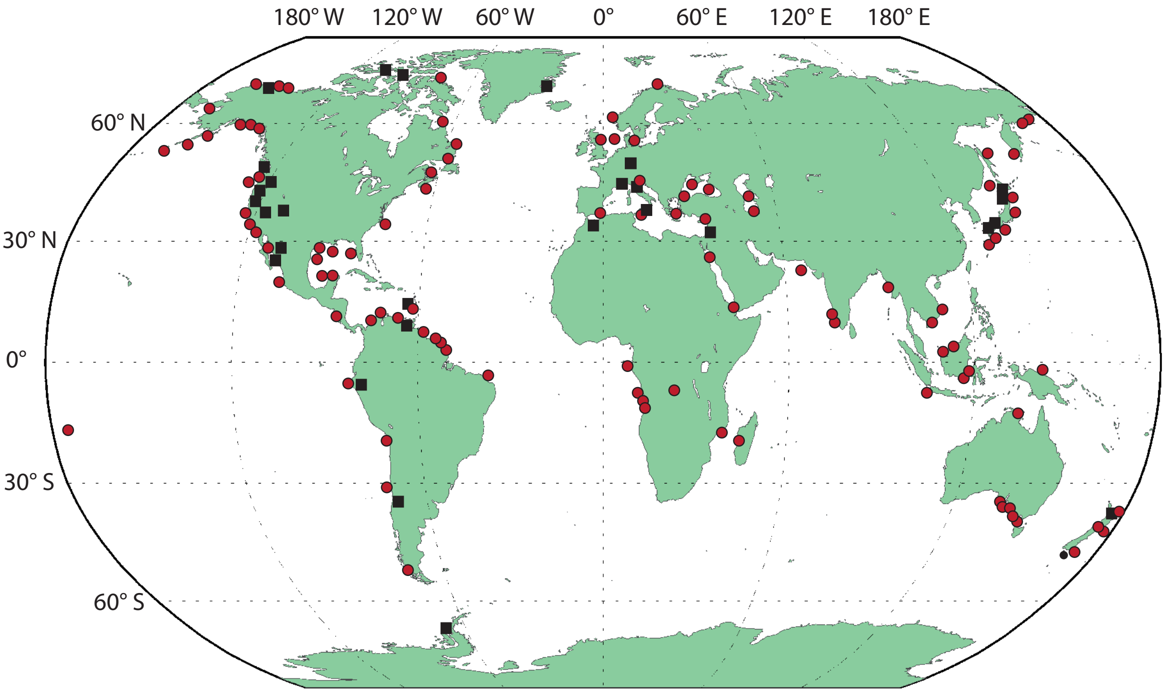

Fig. I.2. Global distribution of modern (red circles) and fossil (black squares) cold seeps, modified after Kvenvolden (2002) and Campbell (2006).

I.1.1.3. Mineralization of organic matter and biological methanogenesis

Organic matter that is deposited on the ocean floor is mineralized by microbes performing a variety of respiratory activities termed early diagenesis (Berner, 1980). These mineralization processes occur in a stepwise manner controlled by the free energy potential of each of those reactions: Organic matter is first oxidized with oxygen as electron acceptor, followed by nitrate, iron(III), manganese(IV), sulfate, and finally CO_2 (Fenchel and Jørgensen, 1977; Froelich et al., 1979, Table I.1). After depletion of all inorganic electron acceptors fermentative processes remain as the only process to mineralize organic matter in deeper sediments. Sulfate is abundantly present in the marine realm and is consequently the most important electron acceptor in marine sediments, when oxygen is depleted. At continental margins sulfate-reducing bacteria (SRB) can account for up to 50% of total organic matter remineralization (Jørgensen, 1982).

One of the most important biological processes in anoxic sediments below the sulfate-reduction zone is biologically-mediated methanogenesis (Whiticar et al., 1986; Capone and Kiene, 1988). To date the only known organisms able to perform methanogenesis belong to the domain of the Archaea. Methanogenic archaea utilize fermentative end products such as acetate or CO_2 together with hydrogen according to the following net reactions:

$$CO_2 + 4\,H_2 \rightarrow CH_4 + 2H_2O\ ,\ \Delta G_0 = -135.6\ \text{kJ mol}^{-1} \qquad \text{Eq. 1}$$

$$CH_3COOH \rightarrow CH_4 + CO_2\ ,\ \Delta G_0 = -31.0\ \text{kJ mol}^{-1} \qquad \text{Eq. 2}$$

Other substrates that can be utilized by methanogenic archaea are methanol, formate or methylamines (cf. Thauer, 1988; Boone et al., 1993 Keltjens and Vogels, 1993). Since methanogens mainly utilize competitive substrates, i.e., substrates that are also readily consumed by other organisms such as SRB, the presence of methanogenic archaea is predominantly restricted to the zone below sulfate-reduction. Biological methane formation can thus be regarded as the terminal process of biomass degradation in aquatic habitats where all other electron acceptors have been depleted.

One method to track methanogenesis in sediments is by analysis of the stable carbon isotopes (cf. Whiticar, 1999). Generally, chemical reactions discriminate against the heavier isotope (in this case ^{13}C), resulting in a so-called isotope fractionation. Isotope fractionations are particularly high during biological processes and increase with decreasing molecular mass

Table I.1. Simplified pathways of organic matter oxdidation and associated free energy yield in marine sediments. Organic matter is symbolized by $[CH_2O]$. Table adopted from Froelich et al. (1979) and Jørgensen (2005).

pathway	reaction	ΔG_0 (kJ mol^{-1} glucose)
oxic respiration	$[CH_2O] + O_2 \rightarrow CO_2 + H_2O$	-3190
denitrification	$5\,[CH_2O] + 4\,NO_3^- \rightarrow 2\,N_2 + 4\,HCO_3^- + CO_2 + 3\,H_2O$	-3030
manganese(IV) reduction	$[CH_2O] + 3\,CO_2 + H_2O + 2\,MnO_2 \rightarrow 2\,Mn^{2+} + 4\,HCO_3^-$	-3090 to -2920
iron(III) reduction	$[CH_2O] + 7\,CO_2 + 4\,Fe(OH)_3 \rightarrow 4\,Fe^{2+} + 8\,HCO_3^- + 3\,H_2O$	-1410/-1330
sulfate reduction	$2\,[CH_2O] + SO_4^{2-} \rightarrow H_2S + 2\,HCO_3^-$	-380
methanogenesis	$4\,H_2 + HCO_3^- + H^+ \rightarrow CH_4 + 3\,H_2O$	-350

(cf. Hayes et al., 2001). Stable carbon isotope values are typically reported in the δ-notation and expressed in ‰ as deviation of the isotope ratio to a reference standard of known isotopic composition. For stable carbon isotopes the Vienna Pee Dee Belemnite (VPDB) standard is used (Slater et al., 2001):

$$\delta X = [(R_{sample} - R_{reference})\text{-}1] * 1000 \qquad \text{Eq. 3}$$

The determination of the stable carbon isotope composition ($\delta^{13}C$) of methane can be used to distinguish between the relative contribution of thermogenic methane (i.e., from petroleum reservoirs) or biogenic methane (i.e., produced during biological methanogenesis) at petroleum seeps. This is due to the fact that cracking of petroleum hydrocarbons, the main precursor of thermogenic methane, is not associated with such strong isotope effects as biological methane formation. Consequently thermogenic methane is always relatively enriched in ^{13}C compared to biogenic methane (e.g., Chung et al., 1988; Sassen et al., 1999).

I.1.1.4. The anaerobic oxidation of methane

The presence of a sulfate-methane transition zone (SMTZ) in porewater profiles of marine sediments has been puzzling for geochemists for a long time (Fig. I.3; Martens and Berner, 1974). Such a depletion of methane concentrations below the sulfate-reduction zone was recognized to be best explained by microbial activity, i.e., by anaerobic oxidation of methane (AOM) most likely with sulfate as electron acceptor (Barnes and Goldberg, 1976; Reeburgh, 1976). The proposed stoichiometry of AOM can be expressed as the following net reaction:

$$CH_4 + SO_4^{2-} \rightarrow HS^- + HCO_3^- + H_2O \qquad \text{Eq. 4}$$

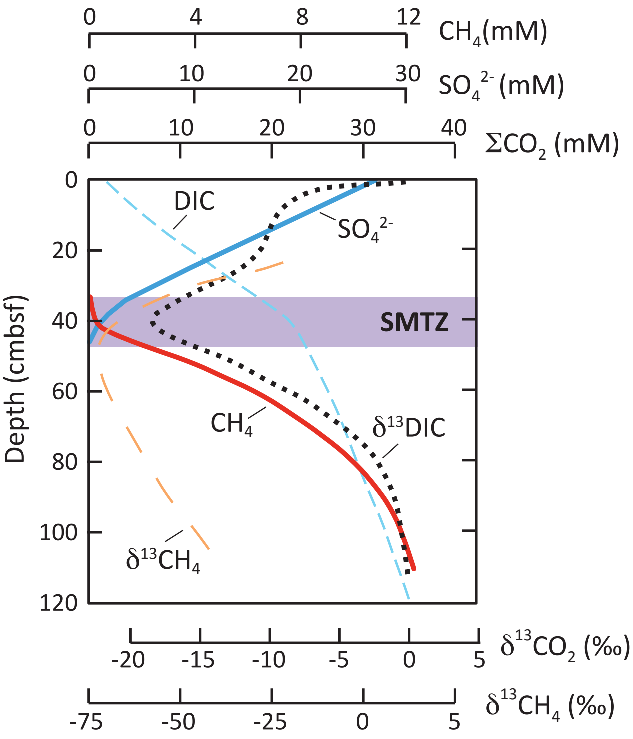

Fig. I.3. Schematic illustration of the sulfate-methane transition zone (SMTZ) in marine sediments and associated representative stable carbon isotope values of CO_2 and CH_4 (modified after Reeburgh, 2007).

(cf. Hayes et al., 2001). Stable carbon isotope values are typically reported in the δ-notation and expressed in ‰ as deviation of the isotope ratio to a reference standard of known isotopic composition. For stable carbon isotopes the Vienna Pee Dee Belemnite (VPDB) standard is used (Slater et al., 2001):

$$\delta X = [(R_{sample} - R_{reference})-1] * 1000 \qquad \text{Eq. 3}$$

The determination of the stable carbon isotope composition ($\delta^{13}C$) of methane can be used to distinguish between the relative contribution of thermogenic methane (i.e., from petroleum reservoirs) or biogenic methane (i.e., produced during biological methanogenesis) at petroleum seeps. This is due to the fact that cracking of petroleum hydrocarbons, the main precursor of thermogenic methane, is not associated with such strong isotope effects as biological methane formation. Consequently thermogenic methane is always relatively enriched in ^{13}C compared to biogenic methane (e.g., Chung et al., 1988; Sassen et al., 1999).

I.1.1.4. The anaerobic oxidation of methane

The presence of a sulfate-methane transition zone (SMTZ) in porewater profiles of marine sediments has been puzzling for geochemists for a long time (Fig. I.3; Martens and Berner, 1974). Such a depletion of methane concentrations below the sulfate-reduction zone was recognized to be best explained by microbial activity, i.e., by anaerobic oxidation of methane (AOM) most likely with sulfate as electron acceptor (Barnes and Goldberg, 1976; Reeburgh, 1976). The proposed stoichiometry of AOM can be expressed as the following net reaction:

$$CH_4 + SO_4^{2-} \rightarrow HS^- + HCO_3^- + H_2O \qquad \text{Eq. 4}$$

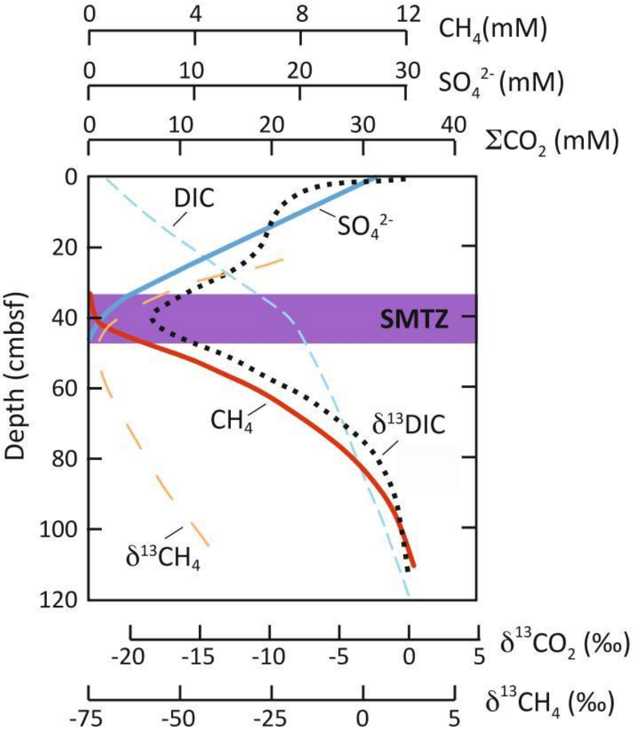

Fig. I.3. Schematic illustration of the sulfate-methane transition zone (SMTZ) in marine sediments and associated representative stable carbon isotope values of CO_2 and CH_4 (modified after Reeburgh, 2007).

Radiotracer experiments with radioactively labeled sulfate and methane could indeed confirm that sulfate was an electron acceptor during oxidation of methane (Devol, 1983; Iversen and Jørgensen, 1985), however, the microorganisms involved in this process remained elusive. Hoehler et al. (1994) postulated that a methanogen/sulfate-reducer consortium, consisting of methanogenic archaea performing reversed methanogenesis and sulfate-reducing bacteria could be responsible for the consumption of methane. The first direct evidence of the existence of methanotrophic archaea came from lipid biomarkers: Hinrichs et al. (1999) found archaeol and hydroxyarchaeol - isoprenoidal lipids characteristic for Archaea - with highly depleted $\delta^{13}C$ values (up to 50‰ relative to methane) in hydrate-rich sediments of the Santa Barbara basin, which could best be explained by biological assimilation of methane. These biomarker observations were supported by the presence of small-subunit ribosomal RNA (16S rRNA) genes of a new archaeal group (the ANaerobic MEthane oxidizers, ANME), which is closely associated to methanogenic archaea of the order *Methanomicrobiales* and *Methanosarcinales*. Biomarker studies from other locations, both of recent and ancient cold seeps followed and could confirm the presence of highly ^{13}C-depleted archaeal lipid biomarkers in association to AOM (Elvert et al., 1999; Peckmann et al., 1999; Thiel et al., 1999). The first microscopic evidence of a closely associated archaeal/bacterial aggregate apparently mediating the anaerobic oxidation of methane was provided by Boetius et al. (2000). These authors used fluorescence in-situ hybridization (FISH) using specific 16S rRNA-targeted oligonucleotide probes to identify the archaeal/bacterial consortium in the sediments. Orphan et al. (2001) then provided direct proof of the extreme ^{13}C depletion of the aggregate biomass by secondary ion mass spectrometry (SIMS) coupled to FISH.

Production of ^{13}C depleted $\sum CO_2$ during AOM can also be typically evidenced in the pore water profiles by a decrease of $\delta^{13}C_{CO_2}$ close to the SMTZ and a corresponding increase in alkalinity in the same horizon (cf. Reeburgh et al., 2007; Fig. I.3). Many studies on AOM performing communities in different environments have followed and revealed the presence of a variety of ANME clades that all cluster within the methanogenic euryarchaea (e.g., Michaelis et al., 2002; Nauhaus et al., 2002; Orphan et al., 2002; Knittel et al., 2005; Lösekann et al., 2007). The ANME archaea can be divided according to their phylogeny into the ANME-1, ANME-2 and ANME-3 groups (cf. Knittel and Boetius, 2009). Not all ANME archaea occur in close association with SRB, for instance ANME-1 archaea are often found as single cells (Fig. I.4a), whereas ANME-2 archaea are either intermixed with SRB (Fig. I.4c-e) or are partially or fully surrounded by an outer shell of SRB (Fig. I.4f,g). ANME-2 cells without a bacterial partner were also reported (Orphan et al., 2002; Treude et al., 2007). ANME-3 archaea were also observed as shell-type aggregates with the SRB partner or as single cells (Niemann et al., 2006; Lösekann et al., 2007; Omoregie et al., 2008). The typical SRB partner of ANME-1 and ANME-2 archaea is found within the *Desulfosarcina/Desulfococcus* (DSS) group, whereas ANME-3 archaea are - if at all - associated to the SRB of the *Desulfobulbus* branch (cf. Knittel and Boetius, 2009). Despite all of these studies, not a single member of the above described groups has been to date obtained as a pure culture. Furthermore, detailed knowledge about

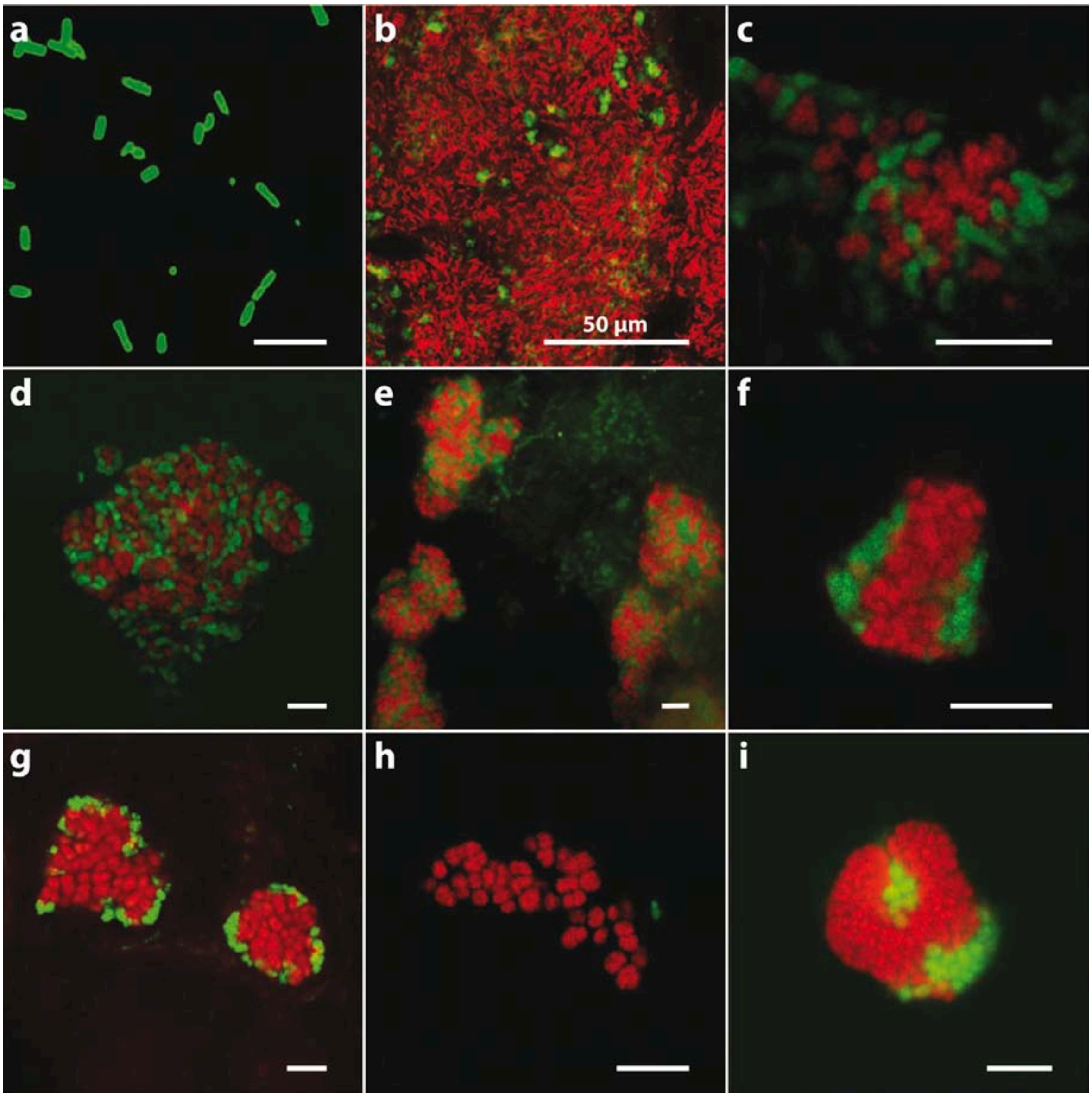

Fig. I.4. (CARD)-FISH images of different ANME and SRB cells in the marine environment adapted from Knittel and Boetius (2009). (**A**) Single ANME cells from a microbial mat in the Black Sea. (**B**) Mat-type consortia of ANME-1 (red) and DSS (green) cells. (**C**)-(**E**) Examples of mixed-type consortia of ANME-2a (red) and DSS (green cells). (**F**)-(**G**) Shell-type consortia of ANME-2c (red) and DSS (green) cells. (**H**) Example of ANME-2c single cells. (**I**) ANME-3/*Desulfobulbus* consortia. Scalebar 5 µm. For abbreviations see text.

the biochemical process of AOM remains unknown, as the intermediate between the methane oxidation and sulfate-reduction partners has not been identified. Recent studies using an investigative ^{13}C-labeling approach, however, could show that the growth of methanotrophic archaea depends on the SRB partner and that the SRB grow autotrophically (Wegener et al, 2008).

In summary, methanotrophic microorganisms are widely distributed in the marine realm and their activity is thought to be responsible for most of the methane removal in the oceanic environment (cf. Reeburgh et al., 2007). Since methane has the potential to cause significant perturbations of the global carbon cycle, it is of vital importance to understand the controls of sources and sinks of methane and generally stresses the importance of microorganisms in global element cycling.

I.1.2. The stratified water column of the Black Sea

The Black Sea is the largest, permanently stratified water body on Earth and thus represents an ideal location to study transitions of aerobic and anaerobic microbial communities and associated processes.

The Black Sea water column extends up to 2200 meter below sea level (mbsl) in the central basin and is primarily controlled by a density gradient caused by elevated salinities in the deeper water body that prevents mixing of surface and deeper water masses (Sorokin, 2002). This permanent halocline at ca. 100 to 200 mbsl was established after the opening of the Bosporus which resulted in the inflow of saline waters from the Mediterranean Sea to the Black Sea about 7150 years ago (Ryan et al., 1997; Gorur et al., 2001). In the vicinity of river mouths, e.g., the Danube, the salinity gradient can extend up to 300 m depth due to freshwater input (Sorokin, 2002). The presence of this halocline together with constant supply of methane from the sediments to the water column resulted in the establishment of a stratified water column supporting a complex biogeochemical structure consisting of different redox zones (cf. Oguz et al., 2000; Wakeham et al., 2007). Major methane sources are methane seeps on the continental margin (Schubert et al., 2006a) and methane-rich mud volcanoes on the abyssal plains of the Black Sea (Ivanov et al., 1998; Schubert et al., 2006a).

In the surface waters (up to ca. 50 mbsl) oxygen is depleted by aerobic respiratory activity by active aerobic planktonic organic matter production and cycling processes (e.g., Oguz et al., 1999; Fig. I.5). Due to a recent shift in the geochemical characteristics of the Black Sea, a 30 m deep suboxic zone has been established, preventing a direct overlap of the sulfidic anoxic bottom waters and the oxygenated surface waters (Murray et al., 1989). This results in a nicely established geochemical zonation where electron acceptors are utilized in a successive manner as determined by the Gibbs energies (Table I.1) during organic matter degradation (Fig. I.5). In the nitrogenous zones a balance between nitrification and denitrification has been described (Ward and Kilpatrick, 1991), and recent work has demonstrated the occurrence

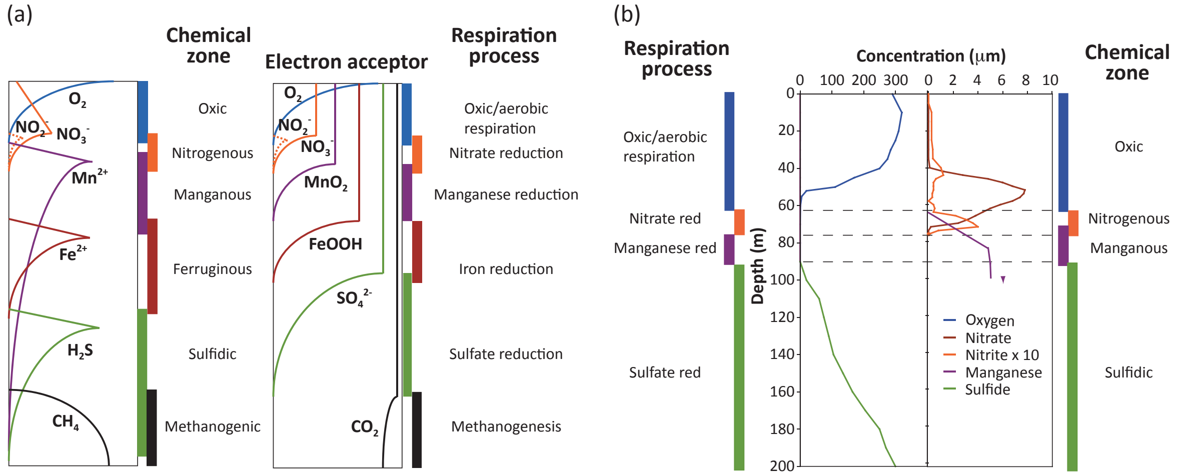
(a)
Chemical zone
Electron acceptor
Respiration process
O_2
NO_2^-
NO_3^-
Mn^{2+}
Fe^{2+}
H_2S
CH_4
Oxic
Nitrogenous
Manganous
Ferruginous
Sulfidic
Methanogenic
O_2
NO_2^-
NO_3^-
MnO_2
FeOOH
SO_4^{2-}
CO_2
Oxic/aerobic respiration
Nitrate reduction
Manganese reduction
Iron reduction
Sulfate reduction
Methanogenesis
(b)
Respiration process
Oxic/aerobic respiration
Nitrate red
Manganese red
Sulfate red
Concentration (μm)
0 100 200 300
0 2 4 6 8 10
Depth (m)
0
20
40
60
80
100
120
140
160
180
200
Oxygen
Nitrate
Nitrite x 10
Manganese
Sulfide
Chemical zone
Oxic
Nitrogenous
Manganous
Sulfidic

Fig. I.5. (**A**) Cartoon representing the redox zonation and associated electron acceptors accompanying sucessive respiration processes in the marine envirnment. (**B**) Cartoon of water column geochemistry in the Black Sea. Figure modified from Canfield and Thamdrup (2009).

of anaerobic ammonium oxidation (anammox; Kuypers et al., 2003), and nitrification by ammonium oxidizing autotrophic planktonic crenarchaea (Coolen et al., 2007; Lam et al., 2007) in the suboxic zone. The upper part of the anoxic zone is dominated by iron and manganese redox chemistry (Lewis and Landing, 1991; Tebo, 1991; Murray et al., 1995), with bacterial manganese oxidation occurring most likely only in zones with lateral intrusions of oxygen (Schippers et al., 2005). Aerobic sulfide- and thiosulfate-oxidizing bacteria also inhabit the lower chemocline and were studied by Tuttle and Jannasch (1973), Jannasch (1991), Jørgensen et al. (1991) and Sorokin et al. (1995). The presence of anoxygenic photosynthetic sulfur bacteria was confirmed by detection of carotenoid pigments from green-sulfur bacteria (Repeta and Simpson, 1991; Repeta, 1993). Manske et al. (2005) showed that green-sulfur bacteria were present up to 100 mbsl and thus represent the most extremely low-light adapted and slowest-growing type of anoxygenic phototrophs known to date. Furthermore, the chemocline of the Black Sea represents a niche for aerobic methanotrophic bacteria, belonging to type I and II methanotrophs (Durisch-Kaiser et al., 2005; Blumenberg et al., 2006; Schubert et al., 2006a, 2006b).

In general, chemoautotrophic production in the chemocline at the oxic-anoxic interface amounts to an estimated 10-32% of photoautotrophic production in surface waters (Karl and Knauer, 1991; Jørgensen et al., 1991; Sorokin et al., 1995). Bottom waters of the Black Sea are characterized by high concentrations of hydrogen sulfide, ammonium, and methane. The increasing concentrations of H_2S in the anoxic zone show the importance of sulfate reduction (Jannasch et al., 1991; Albert et al., 1995). Furthermore, recent work on AOM (Wakeham et al., 2003; Schubert et al., 2006b) suggests that the anoxic zone itself may be further divided into two layers - an upper anoxic zone between about 100 m and 400 m where AOM is mediated by ANME-2 euryarchaeota, and a deep anoxic zone (400-2200 m) where ANME–1 euryarchaeota oxidize methane. Nevertheless, there seems to be a discrepancy between the abundance of anaerobic methanotrophs and high measured rates of AOM in the anoxic zone, averaging to 2 nmol CH_4 mL^{-1} day^{-1} (Reeburgh et al., 1991). Although estimates show that AOM consumes more than 99% of the methane that is released into the water column, recent studies of ANME cell abundance cannot account for the observed methane oxidation Schubert et al. (2006b). It was thus speculated by the authors that there must be other methane-oxidizing communities present in the water column in order to account for such high rates.

Biomarker studies have proved to be very helpful in the investigation of (micro) biological stratification in the Black Sea and are reviewed in detail by Wakeham et al. (2007). However, most of these studies have only focused on the analysis of apolar derivatives of intact polar membrane lipids and therefore possibly represent a mixture of fossil and living material.

I.1.3. Petroleum seeps in the Gulf of Mexico

The Gulf of Mexico (GoM) is an example of a passive margin which is rich in gas and petroleum reservoirs (e.g., Brooks et al., 1986). At the GoM, the upward movement of hydrocarbon-rich gases and fluids is primarily controlled by salt tectonics. Hereby, salt ridges, salt deformations and active faults create conduits that enable rapid gas and fluid transfer to the seafloor (Kennicutt et al., 1988; Aharon et al., 1992; Roberts and Carney, 1997). In the northern GoM a wide variety of distinct cold seep features can be found, these include (*i*) brine pools that are a result of the expulsion of saline-rich fluids (cf. Joye et al., 2009), (*ii*) thermogenic gas hydrates that form at the ocean floor or within surface sediments due to cold bottom water temperatures and high pressures associated with deep water (Brooks et al., 1984; Sassen et al., 1999), and (*iii*) authigenic carbonate minerals with depleted δ^{13}C values that are formed during microbial oxidation of hydrocarbons in surface-near sediments (Anderson et al., 1983; Sassen et al., 2004).

Since the discovery of the first cold seeps at the Florida Escarpment (Paull et al., 1984), researchers have mainly focused on the investigation of hydrocarbon seepage and the associated biocommunities in the northern GoM (e.g., Kennicutt et al., 1985; MacDonald et al., 1990b; Larkin et al., 1994). In the northern GoM, hydrocarbon seeps and outcropping methane hydrates are colonized by dense mats of sulfide-oxidizing bacteria, vestimentiferan tubeworms, methanotrophic mussels and other bivalves, and unique methane hydrate-dwelling worms (Kennicutt et al., 1985; MacDonald et al., 1990a,b; Desbruyéres and Toulmond, 1998; Fischer et al., 2000; MacAvoy et al., 2002). Studies of AOM were conducted at (Mills et al., 2003) and in (Orcutt et al., 2004) gas hydrates that abundantly occur at the GoM cold seeps and showed that AOM is an important process. Investigation of AOM in the hydrocarbon-rich sediments showed that rates of sulfate-reduction were largely decoupled from rates of AOM (Joye et al., 2004; Orcutt et al., 2005), indicating that SRB also degrade the oil and are not only associated to AOM. Furthermore, it was observed that rates of methanogenesis accounted up to ~10% of AOM rates, despite a dominance of ANME-1 and to a lesser extent ANME-2 phylotypes in the archaeal community. This observation was supported in laboratory experiments where it was interpreted as the ability of ANME phylotypes to switch between methanotrophy and methanogenesis (Orcutt et al., 2008). Other studies showed that hypersaline sediments are inhabited only by ANME-1 archaea, indicating a special adaptation of these AOM-performing archaea to higher salinities (Lloyd et al., 2006). Distributions of Bacteria on the other hand were phylogenetically diverse and are consistent with previous results, indicating that most of them are likely involved in the degradation of petroleum hydrocarbons. Investigation of lipid biomarkers that were less depleted in δ^{13}C than expected from solely AOM-performing SRB confirmed that a majority of SRB are involved in petroleum hydrocarbon degradation (Zhang et al., 2002; Orcutt et al., 2005). ^{13}C-depleted archaeol and hydroxyarchaeol were consistent with the presence of ANME-2 archaea in the study by Orcutt et al. (2005). However, the dominance of ANME-1 (by analysis of the hydrocarbon fraction, i.e., biphytanes) could not be corroborated due to interference of the oil, which was causing a strong background of an unresolved complex mixture during gas chromatographic analysis. Similar analytical problems were also encountered in a previous study by Zhang et al. (2002). Joye et al. (2009) could show that AOM plays only a minor role at mud volcanoes and seafloor brines in the northern GoM, i.e., sites that are characterized by high fluid flow and vigorous discharge of mud, gas, brine and oil. Instead, at the brine pool acetogenesis and sulfate-reduction rates were found to be elevated. At the mud volcano acetoclastic and CO_2-reducing methanogens are most important and methane is primarily emitted into the ocean.

The less studied southern GoM recently became the center of attention as extensive asphalt deposits were observed on the surface of salt structures as the Campeche Knolls (MacDonald et al., 2004). At one of the Knolls, the Chapopote Knoll, these asphalt deposits are covered by vast chemosynthetic communities such as vestimentiferan tubeworms, clams, sponges, crabs and sea cucumbers (Bohrmann et al., 2008; Brüning et al., 2009). The energetic basis of the establishment of these cold seep communities seems to be not only derived from reduced gases, but also from the presence of heavy oil. Microbial degradation of oil must hereby be the primary factor for the establishment of such a rich and unique ecosystem. The heavy oil likely originates from within a shallow reservoir in ca. 300 m depth where seismic reflectors revealed an area of potential hydrocarbon accumulation (Ding et al., 2008). Investigations of authigenic carbonates from the Chapopote revealed enriched $\delta^{13}C$ values (-28.6‰ to -17.9‰) indicating oil oxidation as the major source of carbon, however, the simultaneous detection of $\delta^{13}C$-depleted lipids of AOM-performing organisms point to at least a partial contribution of AOM to the precipitation of carbonates (Nähr et al., 2009).

I.1.4. Modes of biodegradation

Aerobic degradation of petroleum hydrocarbons can either be performed by Bacteria or Eukarya (Cerniglia et al., 1978; Jerina et al., 1968; Habe and Omori, 2003). In the marine environment the most widespread eukaryotic hydrocarbon-degraders are found within the fungi (cf. Leahy and Colwell, 1990). Additionally, a wide variety of aerobic bacteria, including members from the proteobacteria, high G+C gram-positive bacteria, and *Flavobacterium* in the group of the Cytophageles-green sulfur bacteria, are known to degrade hydrocarbons, (cf. Wackett, 2006). Metabolic pathways of hydrocarbon degradation differ between Eukarya and Bacteria. Most Bacteria, however, show similarities in their catabolic pathways during biodegradation. For instance BTEX compounds, i.e., benzene, toluene, ethylbenzene and xylenes, which are common constituents of petroleum hydrocarbon mixtures (Tissot and Welte, 1984) are oxidized to a catechol intermediate during the aerobic metabolism (Fig. I.6a; cf. Wackett, 2006). This enzymatic conversion from hydrocarbons to alcohols as metabolic intermediates is essential to activate the compound for further metabolic consumption.

Petroleum hydrocarbons can also be degraded anaerobically by sulfate-reducing and denitrifying bacteria (cf. Widdel et al., 2006). It is of interest for petroleum exploration geochemists to gain a better understanding of pathways and rates of oil biodegradation. Petroleum degradation by SRB is for instance highly undesirable as high amounts of toxic sulfides are produced (Bastin et al., 1926), however, methanogenic oil-degradation is of particulate interest, as it increases the yield of methane as a potential energy source (Suflita et al., 2004). The degradation of *n*-alkanes to methane and carbon dioxide in the absence of nitrate and sulfate could first be shown by Zengler et al. (1999) in methanogenic enrichment cultures. This process was later demonstrated to have a potentially strong contribution to methane-formation in subsurface reservoirs (Anderson and Lovley, 2000; Jones et al., 2008). During methanogenic oil-degradation the *n*-alkane-degrading bacteria, assumed to consist of acetogenic (syntrophic) bacteria within the subclass of proteobacteria, convert the *n*-alkane to acetate and H_2. These products are then utilized by acetoclastic methanogenic archaea, converted to methane and CO_2, and the remaining CO_2 is finally reduced to methane by CO_2-reducing methanogenic archaea (Zengler et al., 1999). Primary activation of alkanes during anaerobic biodegradation most likely occurs via the addition of fumarate yielding methyl-substituted succinates (cf. Widdel et al., 2006; Grossi et al., 2008). Similarly, alkyl-substituted aromatic hydrocarbons, e.g., toluene, xylene, and ethylbenzene were observed to be activated by the addition of fumarate, resulting in the respective succinates. Benzylsuccinates were first observed in sulfate-reducing enrichment cultures (Beller et al., 1992) and a denitrifying strain (Evans et al., 1992) and were later identified as a direct intermediate formed from toluene and fumarate (Biegert et al., 1996; Heider, 2007). The activation of benzene first occurs by the addition of a methyl-group to form toluene (cf. Widdel et al., 2006). Consequently, it is widely accepted that the anaerobic degradation of alkylbenzenes occurs via addition of fumarate. Similarly, succinates were also identified as metabolite intermediate during degradation of 2-methylnapthalene in a sulfate-reducing enrichment culture and was identified as naphtyl-2-methylsuccinic acid (Annweiler et al., 2000). However, for unsubstituted aromatic hydrocarbons, such as naphthalene and phenantrene, the exact pathway of anaerobic degradation is currently not well understood and must proceed via a different route: (*i*) addition of fumarate is energetically unfavorable because this reaction would involve the energy-intensive cleavage of a C-H bond (Reed and Kass, 2000), and (*ii*) methylsuccinates have to date never been observed during the degradation of naphthalene (cf. Musat et al., 2009). Therefore, the proposed pathway is either primary methylation of the unsubstituted aromatic hydrocarbon (Safinowski and Meckenstock, 2006; Safinowski et al., 2006) or alternatively carboxylation of the multiring aromatic hydrocarbon (Fig. I.6b; Zhang and Young, 1997; Annweiler et al., 2002; Caldwell and Suflita, 2000; Davidova et al., 2007; Musat et al., 2009). The presence of such metabolic intermediates -

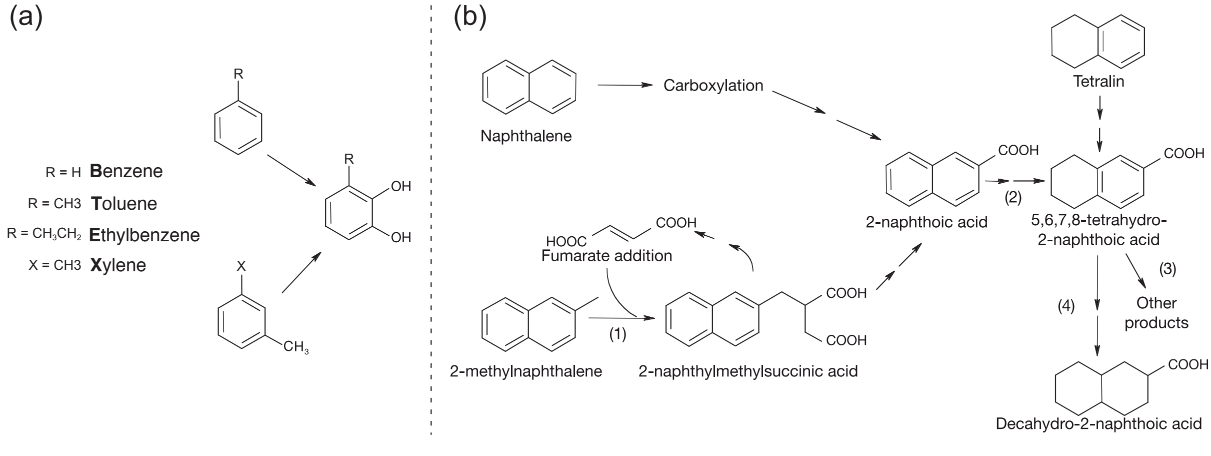
(a)
R
R = H Benzene
R = CH3 Toluene
R = CH3CH2 Ethylbenzene
X = CH3 Xylene
R
OH
OH
X
CH3
(b)
Naphthalene
Carboxylation
Tetralin
COOH
COOH
2-naphthoic acid
(2)
5,6,7,8-tetrahydro-2-naphthoic acid
HOOC
COOH
Fumarate addition
(3)
Other products
(4)
COOH
COOH
(1)
2-methylnaphthalene
2-naphthylmethylsuccinic acid
COOH
Decahydro-2-naphthoic acid

Fig. I.6. (**A**) Aerobic bacterial BTEX activation during biodegradation, after Wackett (2006). (**B**) Anaerobic naphthalene biodegradation (Figure from Aitken et al., 2004. For details refer to text.

particularly metabolites that are specific for either aerobic or anaerobic processes - can be used as tracers for active hydrocarbon degradation. Detection of these compounds in biodegraded subsurface oil reservoirs by Aitken et al. (2004) showed that anaerobic hydrocarbon degradation is a common process.

Both aerobic and anaerobic bacteria produce biosurfactants during hydrocarbon degradation, in order to increase the surface area and facilitate enzymatic uptake of the apolar petroleum hydrocarbons (Zon and Rosenberg, 2002). This emulsification of crude oil is strongly dependant on the availability of nutrients (Reisfeld et al., 1972). Indeed, in laboratory and environmental studies it was observed that amendment of fertilizers stimulated production of biosurfactants and enhanced oil dispersion and degradation (e.g., Xu and Obbard, 2004; Nikolopoulou et al., 2007). Treatment of oil contaminated sites or hydrocarbon containing model systems with surfactants has proven to be effective in supporting bioremediation (Oberbremer et al., 1990; Vasheghane-Farhani and Mehrnia, 2000). However, sometimes these amendments yielded opposite results and hindered oil degradation (e.g., Bachoon et al., 2001). This demonstrates the complexity of bioremediation in the environment and calls for more studies in order to understand the function of oil-degrading bacteria in natural systems.

I.2. OBJECTIVES OF THIS THESIS

The objective of this thesis is to develop and apply novel techniques in organic geochemistry in order to study microbial communities and their carbon turnover in methane-fueled environments.

The analysis of intact polar membrane lipids (IPLs) to study live microbial biomass has been recently established as a tool in microbial ecology. However, even though substantial knowledge on the distribution of IPLs in cultured organisms exists, their distribution in the environment is only poorly constrained. One of the aims of this thesis is therefore to investigate the IPL inventories in a variety of different environments and link variations in IPL distribution to different microbial communitities. Furthermore, I anticipate to exploit the full potential of molecular isotopic information encoded in the IPLs in order to unravel carbon flow in the microbial communities. The second aim is to investigate the importance of the newly discovered asphalt seeps in the southern Gulf of Mexico for the associated chemosynthetic community and to decipher mechanistic details of asphalt degradation on the seafloor.

The specific questions (together with a rationale) I want to adress in this thesis are:

(1) Can IPLs be used to fingerprint viable microbial communities?

IPLs are an important constituent of cellular membranes of all living organisms and are taxonomically specific. The Black Sea represents an ideally-suited natural laboratory to study IPL stratification according to changes in the microbial community composition.

(2) What additional information can be gleaned from IPL analysis compared to other molecular techniques?

IPL analysis can provide quantitative information on the dominating microbes and can *distinguish between different groups of organisms. Furthermore, IPLs can be used to gain head group-specific* $\delta^{13}C$ *values of core lipids.*

(3) How does asphalt seepage sustain benthic life?
Microbes that feed on petroleum hydrocarbons provide the basis of the trophic food web at the Chapopote asphalt seep. Benthic life might harbour novel metabolic pathways and capabilites that provide a special adaption to the seepage of heavy oil.

(4) What are the biological controls on methane at the Chapopote asphalt volcano?
Both methanogenesis and methanotrophy are important processes in the marine realm. Constraining the balance or imbalance of these two processes is important for the understanding of the global carbon cycle. It is known that oil degradation can be coupled to methane production, but methane is typically efficiently recycled by microbial activity within the sediments.

(5) What are the compositional changes in the asphalts caused by biological or physical weathering processes?
Biodegradation is in some cases able to efficiently remediate oil spills in the environment. The Chapopote asphalt seep presents a natural system where long term weathering and biodegradation of heavy oil can be assessed.

(6) Is it possible to quantify hydrocarbon emission rates of the Chapopote asphalt seep by GCxGC analysis?
Every year huge amounts of hydrocarbons are emitted into the environment by both natural seeps and anthropogenic influences. However, there are still great uncertainties to the amount of hydrocarbons expelled into the environment and how efficiently it is recycled. To fully assess the importance of natural hydrocarbon emissions, systems such as the Chapopote asphalt seep need to studied.

These questions have been adressed in total in four first-author manuscripts (*Chapters II* to *V*) and two second-author manuscript (*Chapter VIa* and *VIb*). Hereby, *Chapter II* mainly adresses questions (1) and (2), *Chapters III, IV* and *VIc* aim to answer the questions (2), (3) and (4), and *Chapter V* focuses mainly on questions (5) and (6). *Chapter VIa* is related to question (4) and (6) and investigates methane emissions at a mud volcano in the Black Sea.

I.3. METHODS

I.3.1. Intact polar membrane lipids – extending the biomarker approach

I.3.1.1. Functions and structures of membrane lipids

Lipids are an integral part of every cellular membrane. The membrane-forming lipids are typically comprised of a hydrophilic polar head group and a hydrophobic tail, a structural property that leads to the arrangement of a lipid bilayer that separates the inside of a cell from the outside environment (Fig. I.7). Besides their function as a permability barrier, membrane lipids also provide a stabilizing matrix for transmembrane proteins and help to regulate membrane fluidity by adapting the lipid composition to external variations in pressure, temperature, pH, or other factors (e.g., Hazel and Wiliams, 1990; Russel et al., 1995). Membrane lipids are also involved in a multitude of processes such as transport of nutrients into the cell, signal transduction, intracellular protein transport, and maintenance of the proton-motive force (cf. Dowhan and Bogdanov, 2002; Eyster, 2007; Haucke and Di Paolo, 2007).

Evolutionary adaptations have led to the formation of a variety of membrane lipids that have different functional roles. Variations are both observed in the hydrophilic polar head group as well as the hydrophobic tail or core lipid. The most abundant membrane lipids are phospholipids, i.e., membrane lipids that contain a phosphate-based polar head group. Other membrane lipids contain glycosidic-, amino- or sulfate-based head groups (cf. Kates, 1989; Dembitsky, 1996; Hölzl and Dörmann, 2007). These polar membrane lipids can be divided into two groups with either anionic or zwitterionic head groups at physiological pH. Widespread anionic phospholipid head groups are phosphatidylglycerol (PG), diphosphatidylglycerol (DPG, or cardiolipin), phosphatidylinositol (PI), and phosphatidylserine (PS). The zwitterionic phospholipids comprise the head groups phosphatidylcholine (PC), phosphatidylethanolamine (PE), phosphatidyl-(N)-ethanolamine (PME), and phosphatidyl-(N, N)-ethanolamine (PDME). The importance of anionic lipids in the thylakoid membranes of phototrophic organisms was demonstrated as growth of cyanobacteria was significantly repressed during PG deprivation

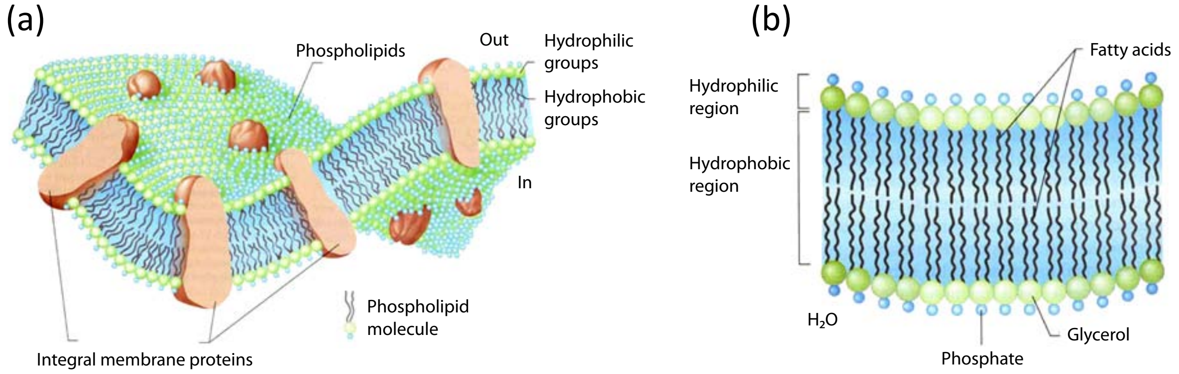

Fig. I.7. Schematic structure of a bacterial phospholipid bilayer membrane. (**A**) Cytoplasmic membrane showing the lipid molecules and transmembrane proteins. The inner surface faces the cytoplasm and the outer part faces the environment. (**B**) Detailed view of the lipid bilayer. The polar headgroups are hydrophilic and face outwards to the aqueous environment, while the apolar fatty acids are hydrophobic and make up the interior of the membrane. Figure adopted from Madigan et al. (2003).

(e.g., Sato et al., 2000; Sakurai et al., 2003; wada and Murata, 2007). It was also observed that during phosphate limitation other non phosphorous-containing anionic lipids, such as sulfoquinovosyl diacylglycerol (SQ-DAG) substitute for PG (Benning et al., 1995; Güler et al., 1996) and if both of these anionic lipids were suppressed, photoautrophic growth was severely hindered (Yu and Benning, 2003). A similar observation was made for the zwitterionic PE, which was replaced in marine algae by the non-phosphorous-containing zwitterionic betaine lipid diacylglycerol-(N,N,N)-trimethylhomoserine (DGTS) under phosphate-limiting conditions (Khozin-Goldberg and Cohen, 2006). Other adaptation processes are found when pressure and temperature were changed: During an increase in temperature, thermophilic bacteria shifted from synthesis of PE to PG, which was assigned to a lower melting point of PG (Hasegawa et al., 1980). In piezophilic bacteria, PG was observed to be abundantly associated to long chain polyunsaturated fatty acids (PUFAs) such as $C_{20:5}$ and $C_{22:6}$ (Fang et al., 2000). PUFAs also have lower melting points and help to maintain membrane fluidity (e.g., DeLong and Yayanos, 1986; Nichols et al., 1997; Yano et al., 1998; Valentine and Valentine, 2004). Adaptive changes in fatty acids were reviewed by Zhang et al. (2008). Generally, double bond introduction and synthesis of long chain fatty acids increases membrane fluidity, whereas short chain and unsaturated fatty acids are synthesized by bacteria adapted to low temperatures (e.g., Männistö and Puhakka, 2001). The modification of a double bond to a cyclopropane ring is primarily observed in Bacteria adapted to acid stress and a replacement of a cis to trans unsaturation also increases the membrane transition temperature (cf. Zhang et al., 2008).

I.3.1.2. The concept of intact polar membrane lipids as chemotaxonomic markers

The synthesis of certain lipids is not only dependent on environmental factors, but is also characteristic for different groups of organisms that are either phylogenetically related or have similar metabolisms (e.g., Goldfine, 1984; Langworthy and Pond, 1986; Kaneda et al., 1991; Itoh et al., 2001).

Studies in surficial marine sediments have shown that the polar head groups of the membrane-lipids are quickly hydrolyzed after cell death (White et al., 1979; Harvey et al., 1986), therefore the detection of the Intact Polar membrane Lipids (IPLs) is generally thought to reflect the presence of intact cells and thus viable biomass. In deep marine sediments where turnover times of living cells are very low and likely occurs on geological time scales (cf. Parkes et al., 2000), it is still under dispute if IPLs represent a marker for living organisms (cf. Lipp and Hinrichs, 2009). Nevertheless, IPLs have been successfully applied as markers in microbial ecology in a variety of aquatic environments, including marine sediments (Rütters et al., 2002a, 2002b; Zink et al., 2003, Biddle et al., 2006; Fredricks and Hinrichs, 2007; Lipp et al., 2009), cold seeps (Sturt et al., 2004; Rossel et al., 2008), oceanic surface waters (VanMooy et al., 2006, 2009) and a meromictic lake (Ertefai et al., 2008).

These studies have provided a step forward in comparison to conventional biomarker analyses that have mainly focused on the polar lipid-derived fatty acids (PLFA) and other core lipids that are derived from IPLs (e.g., Summit et al., 2000; Orcutt et al., 2005; Mills et

AL., 2006; WAKEHAM ET AL., 2007). In combination with core lipid analysis, the additional taxonomic information encoded in the head group can (*i*) provide more insight on the type of microbial communities present, (*ii*) distinguish between dead and alive biomass, and (*iii*) give a quantitative overview on the major dominating microbial groups of organisms (e.g., FANG ET AL., 2000; RÜTTERS ET AL., 2002; STURT ET AL., 2004; BIDDLE ET AL., 2006; LIPP ET AL., 2008; LIPP AND HINRICHS, 2009).

I.3.1.2.1. Differences in IPLs on a domain level - evolutionary considerations. Generally within the three domains of life, the Eukarya, the Bacteria and the Archaea, certain distinct differences in membrane composition are observed (Fig. I.8). Organisms from all domains produce glycerol-based lipids. The most intrinsic difference between the three domains is found in the biosynthetic pathways of membrane formation: whereas the hydrophobic carbon chains of Eukarya and Bacteria are bonded at the *sn*-1 and *sn*-2 position of the glycerol backbone, the Archaea synthesize the hydrophobic carbon chains on glycerol positions *sn*-2 and *sn*-3 (e.g., KATES, 1978). Eukarya and some Bacteria can synthesize sphingolipids, which are composed of an alkyl chain and a fatty acid linked via an amide-bond to the alkyl chain (OLSEN AND JANTZEN, 2001). Furthermore, some Bacteria also synthesize ornithine lipids which are comprised of an amide bound 3-hydroxy fatty acid esterified via its hydroxyl group to another fatty acid (e.g., LÓPEZ-LARA ET AL., 2003). The synthesis of polar head groups is not very distinct between the domains, but some taxonomic significance is observed. However, inherent differences between the domains are observed in the hydrophobic core lipids: Archaeal core lipids differ from those of Bacteria and Archaea in that they are composed of isoprenoidal carbon units bound to the glycerol backbone via ether bonds (e.g., LANGWORTHY AND POND, 1986, DEROSA AND GAMBACORTA,1988, ITOH ET AL., 2001). This membrane characteristic results in very rigid cell membranes that can withhold high stress factors, such as high temperatures, salinities and pressure. This is also consistent with the fact that Archaea root very deeply in the phylogenetic tree, indicating closest relationships with a thermophilic ancestor (WOESE ET AL., 1990; STETTER, 1996). Isoprenoidal ether lipids are not known to occur in any of the other domains than Archaea. However, ether-lipids are also observed in Bacteria, particularly in the deeply-branching, thermophilic bacteria, which is also in agreement with the rigid membrane structure that ether lipids provide to help withstand cell stress and temperature (HUBER ET AL., 1992; STURT ET AL., 2004). Overall bacterial and eukaryal lipids show the greatest resemblance, they are both mainly composed of fatty acids as core lipids. Differences between these two domains are mainly observed in the carbon chain length and degree of unsaturation. Eukaryal fatty acids are predominantly even carbon numbered, i.e., contain mainly C_{14}, C_{16}, C_{18}, and C_{20} fatty acids (e.g., LECHEVELIER AND LECHEVALIER, 1988), whereas Bacteria are characterized by high relative abundance of additional odd carbon-numbered fatty acids, i.e., C_{15} and C_{17} (e.g., FULCO ET AL., 1983; LECHEVELIER AND LECHEVALIER, 1988). C_{19} fatty acids are rare, but were found in acidophilic bacteria (e.g., GROGAN AND CRONAN, 1997; FANG ET AL., 2007). Furthermore, many Eukarya contain a lot of PUFAs (e.g., BRETT AND MÜLLER-NAVARRA, 1997), whereas these are

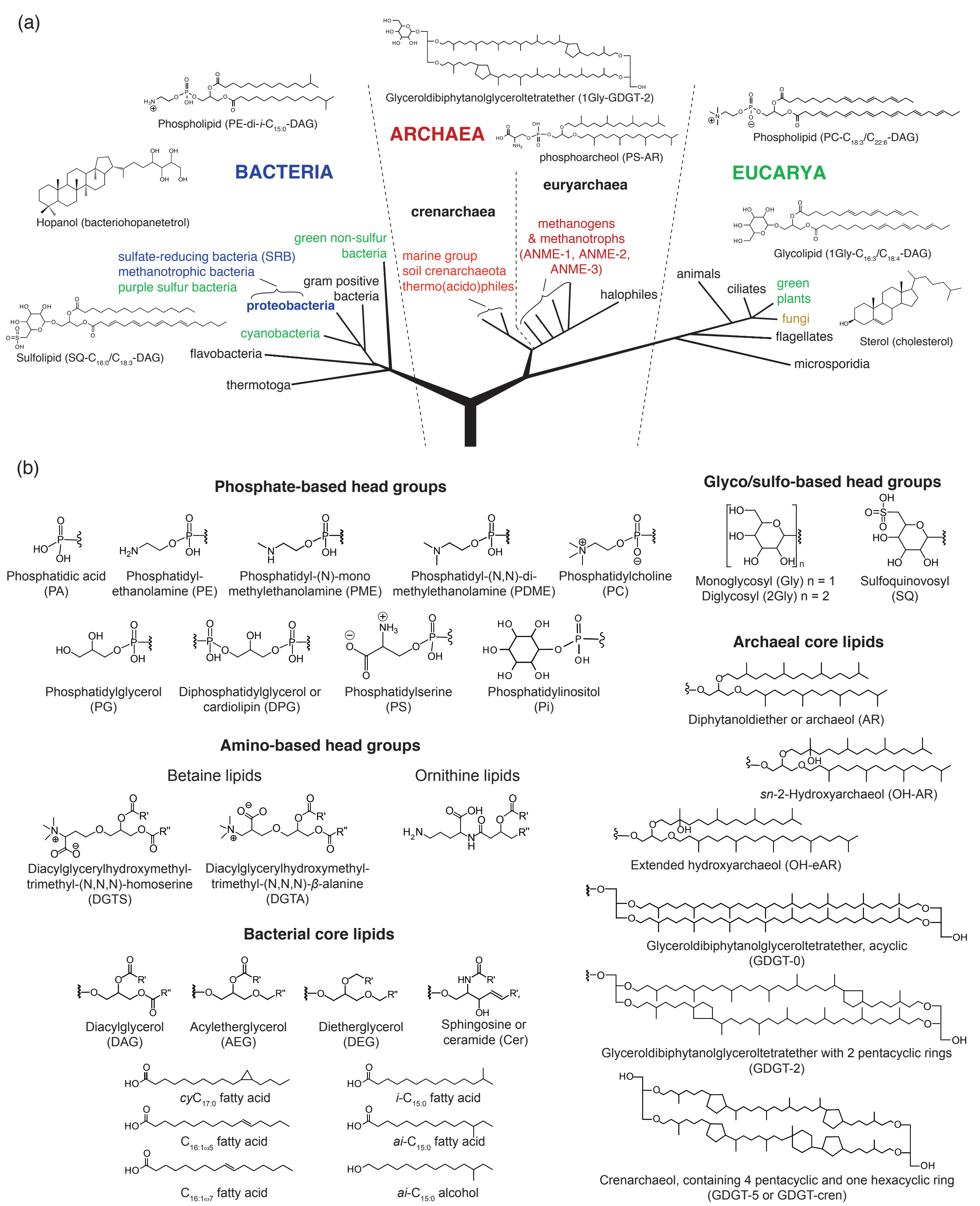
(a)
Glyceroldibiphytanolglyceroltetratether (1Gly-GDGT-2)
Phospholipid (PE-di-*i*-$C_{15:0}$-DAG)
ARCHAEA
phosphoarcheol (PS-AR)
Phospholipid (PC-$C_{18:3}$/$C_{22:6}$-DAG)
Hopanol (bacteriohopanetetrol)
BACTERIA
euryarchaea
EUCARYA
crenarchaea
Glycolipid (1Gly-$C_{16:3}$/$C_{18:4}$-DAG)
green non-sulfur bacteria
methanogens & methanotrophs (ANME-1, ANME-2, ANME-3)
sulfate-reducing bacteria (SRB)
methanotrophic bacteria
purple sulfur bacteria
proteobacteria
gram positive bacteria
marine group
soil crenarchaeota
thermo(acido)philes
halophiles
animals
ciliates
green plants
fungi
flagellates
microsporidia
Sterol (cholesterol)
cyanobacteria
flavobacteria
thermotoga
Sulfolipid (SQ-$C_{16:0}$/$C_{18:3}$-DAG)
(b)
Phosphate-based head groups
Phosphatidic acid (PA)
Phosphatidyl-ethanolamine (PE)
Phosphatidyl-(N)-mono methylethanolamine (PME)
Phosphatidyl-(N,N)-di-methylethanolamine (PDME)
Phosphatidylcholine (PC)
Glyco/sulfo-based head groups
Monoglycosyl (Gly) n = 1
Diglycosyl (2Gly) n = 2
Sulfoquinovosyl (SQ)
Phosphatidylglycerol (PG)
Diphosphatidylglycerol or cardiolipin (DPG)
Phosphatidylserine (PS)
Phosphatidylinositol (Pi)
Archaeal core lipids
Diphytanoldiether or archaeol (AR)
Amino-based head groups
Betaine lipids
Ornithine lipids
sn-2-Hydroxyarchaeol (OH-AR)
Diacylglycerylhydroxymethyl-trimethyl-(N,N,N)-homoserine (DGTS)
Diacylglycerylhydroxymethyl-trimethyl-(N,N,N)-β-alanine (DGTA)
Extended hydroxyarchaeol (OH-eAR)
Glyceroldibiphytanolglyceroltetratether, acyclic (GDGT-0)
Bacterial core lipids
Diacylglycerol (DAG)
Acyletherglycerol (AEG)
Dietherglycerol (DEG)
Sphingosine or ceramide (Cer)
Glyceroldibiphytanolglyceroltetratether with 2 pentacyclic rings (GDGT-2)
cy$C_{17:0}$ fatty acid
i-$C_{15:0}$ fatty acid
$C_{16:1\omega5}$ fatty acid
ai-$C_{15:0}$ fatty acid
$C_{16:1\omega7}$ fatty acid
ai-$C_{15:0}$ alcohol
Crenarchaeol, containing 4 pentacyclic and one hexacyclic ring (GDGT-5 or GDGT-cren)

Fig. I.8. (**A**) Phylogenetic tree of life showing the three domains of life adapted from Woese et al. (1990) and modified after Stetter et al. (1996), Könneke et al. (2005), and Knittel and Boetius (2009). Representative lipids of the three domains are shown. (**B**) Polar head group and core lipid structures of Archaea and Bacteria as discussed in the text.

only found in Cyanobacteria (cf. Wada and Murata, 1998), and in some deep-sea psychrophilic bacteria where they help to regulate membrane fluidity (e.g., Fang et al., 2000). Another distinction of Eukarya and Bacteria from Archaea is the presence of steroids and hopanoids, respectively, which have been proposed to mainly act as membrane rigidifiers (cf. Ourisson et al., 1987). Hopanoids are exclusively synthesized by Bacteria and can in some instances be genus- or species-specific (cf. Rohmer et al., 1984; Rohmer, 1993). The synthesis of steroids is restricted to the domain of Eukarya with one exception: 4-methyl steroids were observed in methanotrophic bacteria and can thus be applied as characteristic markers for these Bacteria (Bouvier et al., 1976; Schouten et al., 2000)

In the following I will discuss some of the characteristic lipids in different groups of organisms and focus mainly on the organisms that are relevant for this thesis.

I.3.1.2.2. *Phototrophic organisms.* Photosynthetic membranes of plants and cyanobacteria primarily contain non-phosphorous glycolipids, with the exception of PG (cf. Siegenthaler et al., 1998; Wada and Murata, 1998). Additionally, all phototrophic organisms produce very similar fatty acids, which are dominated by polyunsaturated fatty acids (PUFAs) with 3 to 4 unsaturations and carbon chain lengths of C_{14} to C_{18} (cf., Siegenthaler et al., 1998). Marine algae additionally synthesize long chain PUFAs, such as $C_{20:5}$ and $C_{22:6}$ (Brett and Müller-Navarra, 1997). Although some marine algae are also able to synthesize PE, PME and PDME lipids, a characteristic trait of almost all algae is that they also abundantly synthesize betaine lipids (Sato, 1992; Dembitsky, 1996; Kato et al., 1996), which is most likely an evolutionary adaptation to the generally low phosphate concentrations in the ocean (Van Mooy et al., 2006; 2009). Similarly to the oxygenic phototrophs, anoxygenic phototrophic organisms, such as the green sulfur and purple sulfur bacteria, also mainly synthesize glycolipids and PG. However, in some instances also DPG and ornithine lipids were observed; notably other phospholipids such as PE are of minor importance (Imhoff and Bias-Imhoff, 1995).

I.3.1.2.3. *Sulfate-reducing bacteria.* Studies of SRB from a variety of genera showed that overall the synthesis of polar head groups is very similar and consisted of predominantly PG, PE and DPG (e.g., Makula and Finnerty, 1974; Rütters et al., 2001; Sturt et al., 2004, Seidel, 2009). Furthermore, in some strains ornithine lipids were observed (e.g., Makula and Finnerty, 1975, Seidel, 2009). A characteristic trait of SRB is the synthesis of branched fatty acids, such as 10me$C_{16:0}$, anteiso and iso $C_{15:0}$ and $C_{17:0}$ which were observed to be genus specific (e.g., Boon et al., 1977; Ueki and Suto, 1979; Taylor and Parkes, 1983; Dowling et al., 1986; Kohring et al., 1994). Some strains of mesophilic SRB also synthesize monoether lipids (Rütters et al., 2001), and diether lipids were also observed in thermophilic SRB (Sturt et al., 2004).

I.3.1.2.4. *Methanotrophic bacteria.* Methanotrophic bacteria, which utilize methane as carbon source under aerobic conditions can be classified into three groups: type I, and type II and type X methanotrophic bacteria (cf. Hanson and Hanson, 1996). Fang et al. (2000) used IPLs and the associated fatty acid composition to identify differences in lipid synthesis of the three groups. The authors observed subtle difference in IPL production, e.g., type I methanotrophs mainly contained PE and PG as head groups with predominantly $C_{16:1}$ fatty acids, type II methanotrophs mainly PG, PME and PDME with mainly $C_{18:1}$ fatty acids, and type X methanotrophs were predominantly comprised of PE phospholipids. However, considering that these are very widespread head groups and fatty acids among the Bacteria, the observed lipids are only of minor taxonomic relevance. Furthermore, early studies by Makula (1978), do not confirm the observations by Fang et al. (2000) and instead show that type I and type II methanotrophs essentially produce similar IPLs and are additionally also able to synthesize DPG and PC phospholipids. However, methanotrophic bacteria produce very specific hopanoids and steroids that - together with $\delta^{13}C$ analysis - can be ideally used to trace their presence in a given environment (Bouvier et al., 1976; Schouten et al., 2000; Hinrichs et al., 2003; Birgel and Peckmann, 2008; Elvert and Niemann, 2008).

I.3.1.2.5. *Methanogenic and methanotrophic archaea.* Methanogenic and methanotrophic archaea are found within the euryarchaea and are phylogenetically closely related microorganisms (cf. Knittel and Boetius, 2009). Lipids of methanogenic archaea have been extensively studied (e.g., Koga et al., 1993; Koga et al., 1998; Koga and Nakano, 2008). Distinct differences between different subgroups of methanogenic archaea have been observed, but some general comments can be made regarding the distribution of polar head groups and core lipids in methanogens: all methanogens contain core lipids comprised of archaeols (isoprenoidal diether lipids) with glycosidic headgroups being most abundant. Furthermore, widespread lipids among the methanogens are acyclic glyceroldibiphytanyltetraethers (GDGTs) and hydroxyarchaeols. Common phospho-based head groups are PE, PG, PS and PI. Insights on the IPL composition of methanotrophic archaea greatly relies on environmental studies, because to date no methanotrophic archaea exists in culture (cf. Knittel and Boetius, 2009). Nevertheless, a study by Rossel et al. (2008) could successfully identify different patterns of IPL distribution in ANME-1 or ANME-2 dominated environments. Here, methane seeps dominated by the ANME-1 group mainly contained IPLs with 2Gly-GDGT structures, whereas methane seeps dominated by the ANME-2 group were dominated by phosphate-based archaeols and hydroxyarchaeols. These results are generally consistent with observations from previous studies that focused only on the apolar IPL moeties (cf. Hinrichs and Boetius, 2002; Blumenberg et al., 2004; Niemann and Elvert, 2008). The similarity of IPL synthesis between methanotrophic and methanogenic archaea is most likely based on their phylogenetic relationship.

I.3.1.2.6. *Planktonic and benthic crenarchaea.* Crenarchaea have been found to be ubiquitously distributed in the ocean, proving that Archaea not only inhabit very extreme environments, such as hydrothermal systems or regions with elevated salinities (e.g., Karner et al., 2001). A distinct feature of the crenarchaea is the synthesis of crenarchaeol as core lipid, which to date has not been found in any other organism (Sinninghe Damsté et al., 2002). However, although previously assumed, the synthesis of crenarchaeol is not only restricted to planktonic crenarchaea, but was also observed in thermophilic relatives in hot springs (De la Torre et al., 2008). The first planktonic crenarchaea that could be cultivated was found to be an autotrophic ammonium oxidizer (Könneke et al., 2005). Schouten et al. (2008) analyzed the IPL composition of this crenarchaeon and showed that it is not only composed of 1Gly- and 2Gly-GDGTs, but also contains phospho hexose-based GDGTs. The primary synthesis of glycolipids could be an indication that these organisms have evolutionary adapted to nutrient-depleted environments.

Only recently benthic crenarchaea are found in increasing numbers in the deep biosphere in subsurface sediments (cf. Teske and Sørensen, 2008). Although no cultured representative exists, IPL analysis has revealed that GDGTs found in subsurface sediments could be tentatively linked to crenarchaea due to the presence of crenarchaeol (Biddle et al. 2006; Lipp et al., 2008). Here, crenarchaeol-containing GDGTs were also found with 1Gly- and 2Gly-GDGTs (cf. Lipp and Hinrichs, 2009).

I.3.1.3. Compound specific stable carbon isotopes as metabolic tracer

Studies on the IPL composition in cultures are crucial for interpreting lipid distributions in the environment. However, not many of the environmentally most relevant microorganisms are available as cultures. Therefore lipid geochemists often turn to other tools in order to make inferences on the respective source organisms. One such powerful technique is compound-specific isotope analysis (CSIA). The concept of CSIA is based on the observation that biological uptake of carbon is associated with specific isotope fractionations that typically discriminate against the heavier isotope, i.e., ^{13}C (cf. Hayes et al., 2001). For instance, the first direct evidence of anaerobic oxidation of methane came from CSIA of archaeal lipids that were found to be highly depleted in ^{13}C, which was associated to a strong fractionation during uptake of methane (Elvert et al., 1999; Hinrichs et al., 1999; Hinrichs and Boetius, 2002). Nevertheless, this technique also relies on laboratory investigations of the respective processes. Recent studies have revealed some important insights on substrate to lipid fractionations for both methanogenic archaea and SRB of different phyla or genera (Londry et al., 2004, 2008). The results can be used to trace heterotrophic uptake of substrates according to different metabolic cycles in the environment and shows that CSIA is a useful tool to track carbon assimilation processes in the environment.

Table I.2. Summary of $\delta^{13}C$ contents and fractionation factors of different archaeal lipids from methanogens during growth on different substrates under substrate-limited and non-limited conditions. Table from Londry et al. (2008).

	Substrate $\delta^{13}C$	Biomass $\delta^{13}C$	$\delta^{13}C$ initial CH_4	$\delta^{13}C$ final CH_4	$\delta^{13}C$ PMI	$\delta^{13}C$ archaeol	$\delta^{13}C$ *sn*-2	$\Delta_{S\text{-}CH4}$[a]	$\Delta_{S\text{-}biomass}$[b]	$\Delta_{S\text{-}PMI}$[c]	$\Delta_{S\text{-}archaeol}$[d]	$\Delta_{S\text{-}sn\text{-}2}$[e]
H_2/CO_2												
Abundant H_2	-31.2	-45.1	-76.6	-71.5	-50.7	-42.5	-45.6	45.4	13.9	19.5	11.3	14.4
Limited H_2	-28.5	-44.1	-108.0	-79.6	-75.5	-71.7	-74.3	79.5	15.6	47.0	43.2	45.8
Acetate												
Abundant	-30.9	-38.2	-65.7	-53.8	-37.2	-35.8	-33.0	34.8	7.3	6.3	4.9	2.1
Limited	-30.9	-31.4		-25.7	-24.3	-22.7			0.5	-5.2	-6.6	-8,2
Methanol												
Abundant	-46.2	-77.3	-129.6	-100.0	-78.7	-98.4	-92.0	83.4	31.1	32.5	52.2	45.8
Limited	-46.2	-46.1		-51.2	-53.1	-53.0			-0.1	5.0	6.9	6.8
TMA												
Abundant	-29.5	-54.3	-96.0	-86.8	-69.2	-72.8	-71.9	66.5	24.8	39.7	43.4	42.4
Limited	-29.5	-41.6	-96.1		-50.7	-42.2	-53.2	66.6	12.1	21.2	12.7	23.7

[a] difference between $\delta^{13}C$ substrate and $\delta^{13}C$ for initially produced methane
[b] difference between $\delta^{13}C$ substrate and $\delta^{13}C$ biomass
[c] difference between $\delta^{13}C$ substrate and $\delta^{13}C$ PMI
[d] difference between $\delta^{13}C$ substrate and $\delta^{13}C$ achaeol
[e] difference between $\delta^{13}C$ substrate and $\delta^{13}C$ *sn*-2 hydroxyarchaeol

Table I.3. δ^{13}C of biomass and FA of four SRB grown under two different conditions. Table adopted from Londry et al. (2004).

Organism	Growth condition	δ^{13}C organic substrate[a]	δ^{13}C CO_2	δ^{13}C biomass	δ^{13}C FA[b]	$\Delta\delta^{13}$C FA to substrate[c]	$\Delta\delta^{13}$C FA to biomass
Desulfovibrio desulfuricans	Mixotrophic	-34.2 ± 0.8	-27.4 ± 0.1	-32.1 ± 0.2	-36.2 ± 1.0	-2.0	-4.1
	Heterotrophic	-29.1 ± 0.8		-29.3 ± 0.1	-41.0 ± 0.3	-11.9	-11.7
Desulfotomaculum acetoxidans	Autotrophic		-27.1 ± 0.6	-55.6 ± 1.5	-64.4 ± 3.4	-37.3	-8.8
	Heterotrophic	-34.2 ± 0.8		-25.4 ± 0.9	-24.7 ± 1.3	9.5	0.7
Desulfobacter hydrogenophilus	Autotrophic		-24.5 ± 0.3	-40.4 ± 0.3	-52.2 ± 0.3	-24.4	-11.8
	Heterotrophic	-34.2 ± 0.8		-34.9 ± 0.6	-48.1 ± 0.4	-13.9	-13.3
Desulfobacterium autotrophicum	Autotrophic		-27.3 ± 0.2	-36.9 ± 0.4	-47.4 ± 2.4	-20.1	-10.5
	Heterotrophic	-34.2 ± 0.8		-34.8 ± 0.3	-48.6 ± 1.2	-14.4	-13.8

[a] all δ^{13}C values reported as ‰ relative to VPDB
[b] δ^{13}C FA is the weighted average of the isotopic values of the individual FA
[c] $\Delta\ \delta^{13}$C is the difference between FA and the CO_2 for autotrophic growth, acetate or lactate for heterotrophic growth, or acetate for mixotrophic growth

For methanogenic archaea it was shown that δ^{13}C fractionation varies significantly according to the availability of hydrogen. For instance, isotopic fractionations from methane to lipid can be as high as 47‰ under H_2-limiting conditions (Table I.2; Londry et al., 2008). This is an interesting finding, since it was typically assumed that such high fractionations only occur during anaerobic oxidation of methane (cf. Hinrichs and Boetius, 2002; Niemann and Elvert, 2008). Another exceptional observation was made by comparison of isotopic fractionation factors of SRB from the deltaproteobacteria and firmicutes during heterotrophic growth: the fatty acids of *Desulfotomaculum*, belonging to the phyla of the firmicutes, became isotopically enriched compared to the substrate acetate (Table I.3; Londry et al., 2004). This was assigned to the use of the reversed tricarboxylic acid [TCA] cycle during carbon assimilation.

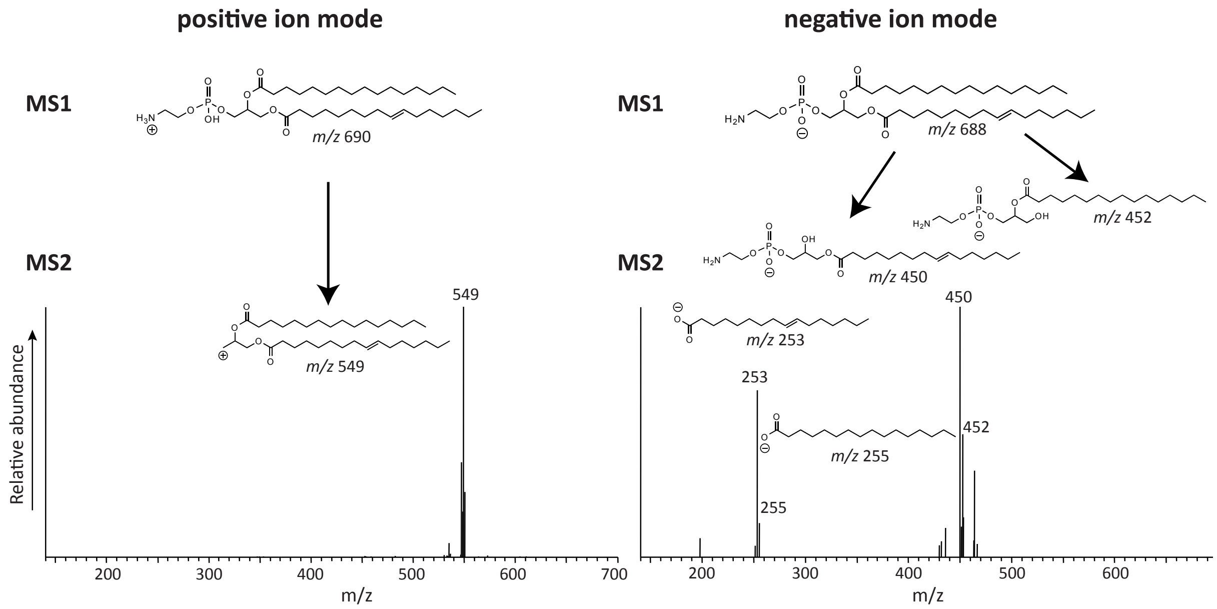

Fig. I.9. Fragmentation patterns of IPLs in positive and negative ionization mode. In the positive mode, the parent ion loses its head group in the MS^2, whereas in the negative mode the fatty acid chains are lost and form characteristic fragments in MS^2.

I.3.1.4. IPL analysis

In this study IPLs were extracted from sediments, pure biomass, or filtered particulate organic matter according to a modified Bligh and Dyer method (after White and Ringelberg, 1998; Sturt et al., 2004). Measurement and Identification of IPLs occurred by high-performance liquid chromatography coupled to multistage mass spectrometry via an electrospray ionization interface (HPLC-ESI-MS^n). This technique enables the analysis of IPLs from all three domains of life in the same analytical window and is ideal to assess the relative importance of the individual domains in the environment. Samples were measured in positive and negative ion mode to facilitate structural elucidation of compounds (Fig. I.9). When the mass spectrometer is operating in positive ion mode, the IPL parent ion formed in the ion source typically loses its polar head group upon fragmentation. This results in a characteristic MS^2 spectrum from which a head group-diagnostic neutral mass loss can be calculated, e.g., for PE this is 141 Da (cf. Sturt et al., 2004). During fragmentation in negative ion mode the IPL parent ion tends to loose the fatty acids of the hydrophobic side chains which can be identified according to characteristic fragments in the MS^2 spectra, e.g., *m/z* 255 for the $C_{16:0}$ fatty acid (Fig. I.9).

A helpful visualization of the data is presented in the form of density maps (cf. Fig. I.10). The top panel (Fig. I.10a) shows an example of a HPLC chromatogram in two dimensions,

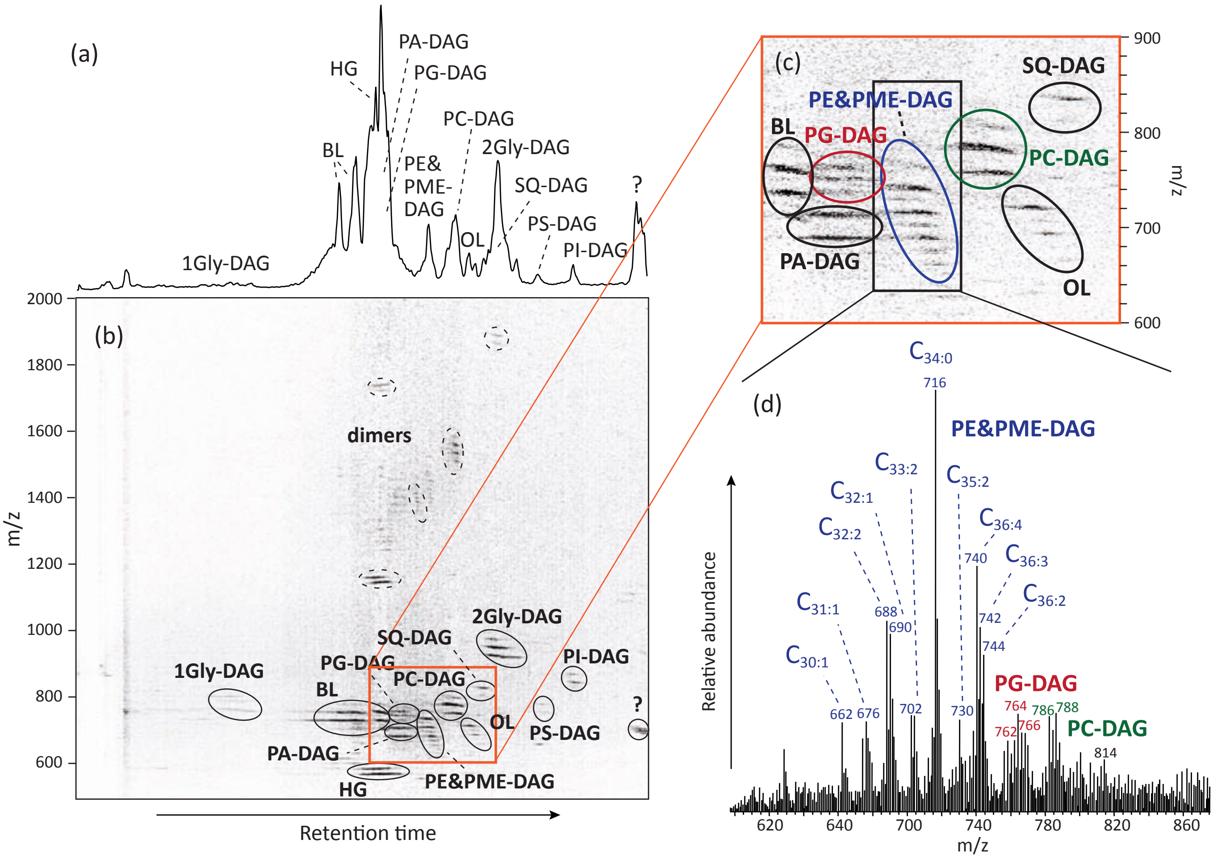

Fig. I.10. Example of HPLC-chromatogram, associated density map, and mass spectra of a soil sample from Svalbard. (**A**) Base peak chromatogram, (**B**) three-dimensional density map showing additionally the *m/z*, (**C**) cut-out of density map of (**B**) showing the elution windows of PE and PME IPLs, and (**D**) MS^1 mass spectra showing parent ion masses of PE and PME. For abbreviations see text and Fig. I.8, HG = heterocyst glycolipids, ? = unidentified compound. Carbon chain lengths and number of unsaturations are noted as the sum of both fatty acid chains.

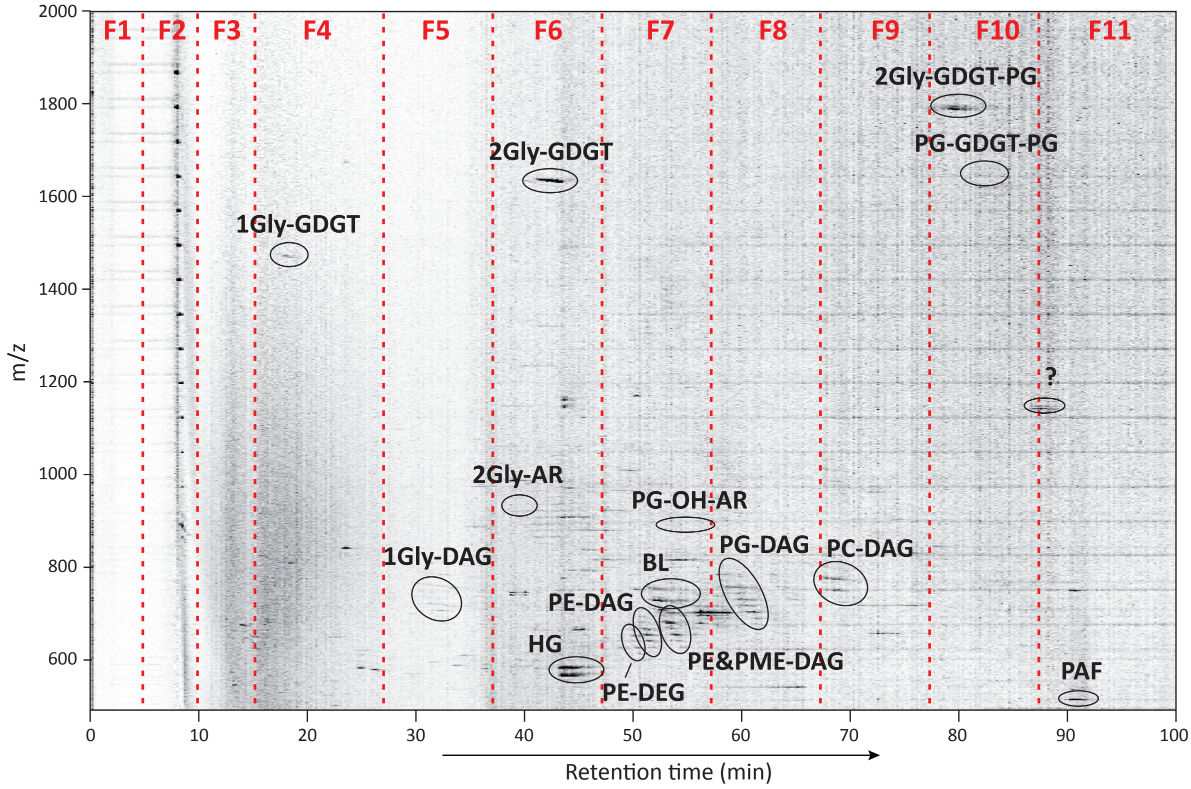

Fig. I.11. Density map of a preparative HPLC run of a mixture of sample extracts from a sample mixture of a cold seep from the Gulf of Mexico and a soil from Svalbard used for method development. Fraction collector time windows are shown in red dashed lines. Major compounds are indicated. For abbreviations refer to text and Fig. I.8, HG = heterocyst glycolipids, PAF = platelet activation factor, ? = unidentified compound. Fraction collection (F1-F11) according to IPL retention times is indicated by red dashed lines.

where peaks of individual compounds co-elute and cannot be clearly distinguished. The lower panel (Fig. I.10b) shows a three dimensional density map with retention time on the x-axis, the *m/z* values of the IPL parent ions on the y-axis, and darker colors denoting higher relative intensities in the third dimension. In the density map individual peaks containing different fatty acid side chains are clearly visualized, further aiding sample comparison (Figs. I.10c,d). Additionally dimers can be easily attributed to the individual IPL compound classes, dimers are formed during ionization when the analyte concentration is very high. Density maps thus provide a “fingerprint” of the IPL composition of the environmental sample.

HPLC also opens up new avenues for CSIA: with the use of preparative-HPLC compounds can be separated according to their polarity and collected in different fractions, i.e. time windows according to IPL retention. As a results each fraction contains IPLs with different head groups (Fig. I.11). This is a methodological advance to the conventional CSIA analysis that are typically performed on the bulk IPLs (e.g., Summit et al., 2004; Orcutt et al., 2005; Mills et al., 2006; Wakeham et al., 2007) and has been applied in a recent study by Biddle et al. (2006). Assuming that different types of organisms produce distinct head groups this technique has the potential to help unravel complex microbial community structures. In concert with the quantification of relative and absolute abundances of IPLs, IPL-specific CSIA could potentially also be used to track the carbon flow in complex environmental systems.

I.3.2. Comprehensive two-dimensional gas chromatography

I.3.2.1. Composition of petroleum hydrocarbons

Petroleum is composed of a complex mixture of hydrocarbons that are comprised of (*i*) biomarkers that can function as molecular fossils and reflect the depositional environment of the organic matter, and (*ii*) complex organic molecules composed of aliphatic and aromatic hydrocarbons derived from thermal alteration, cracking, and catagenesis of organic matter over time and burial (Fig. I.12; cf. Tissot and Welte, 1984, Peters and Moldowan, 1993; Killops and Killops, 2005). After oil generation there are a variety of secondary processes that can affect and alter the composition of petroleum hydrocarbons. One of the processes that causes most profound alterations is microbially-mediated biodegradation (cf. Connan, 1984; Head et al., 2003). During this process petroleum hydrocarbons are removed in a stepwise manner, where first the short chain and then the long chain *n*-alkanes are consumed, followed by branched and isoprenoid aliphatic compounds, and finally aromatic hydrocarbons. This sequential removal of compounds is a consequence of lower rates of degradation of the high molecular-weight alkanes and aromatic compounds, which causes the illusion of a sequential degradation (Head et al., 2006). The removal of hydrocarbon compounds in crude oils during biodegradation leads to a relative enhancement of the residual compounds. During conventional gas chromatographic analysis this process is observed as a gradual rise in the baseline (Fig. I.13) and finally results in the presence of a hump in the chromatogram which is composed of a complex mixture

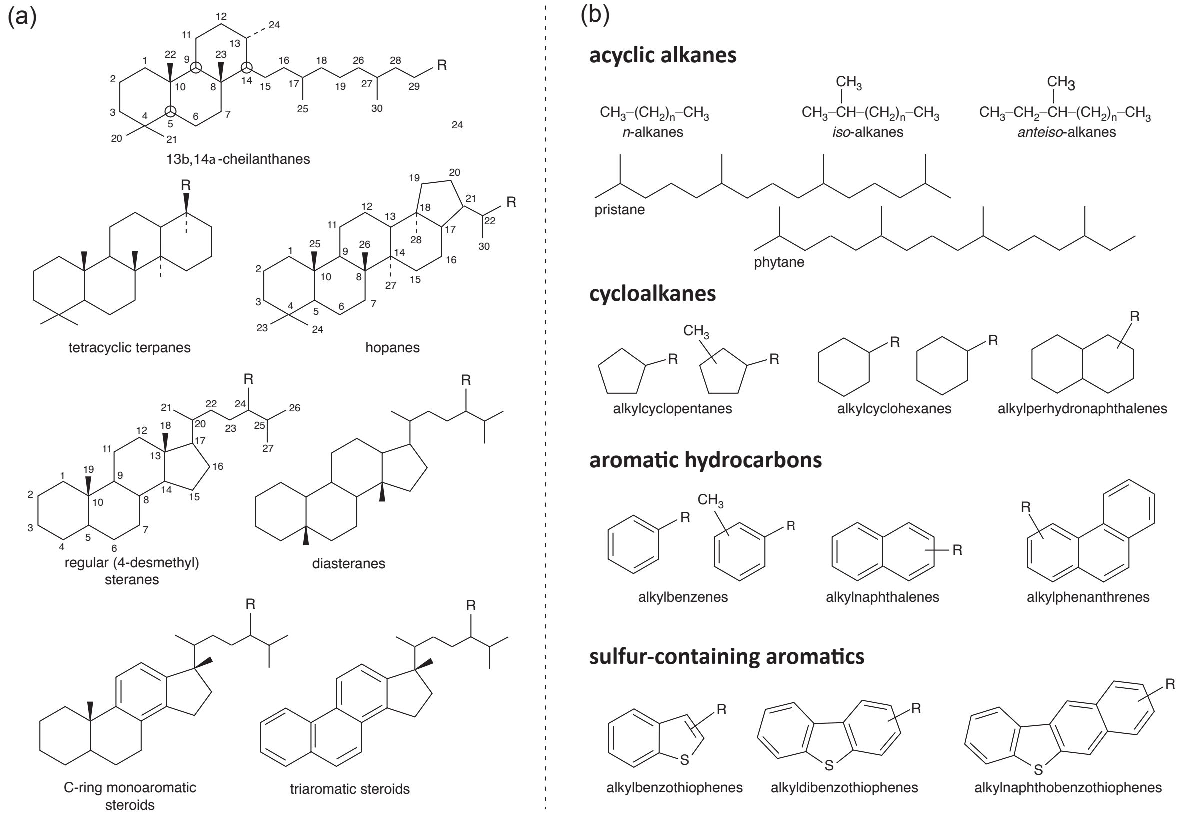
(a)
13b,14a -cheilanthanes
tetracyclic terpanes
hopanes
regular (4-desmethyl) steranes
diasteranes
C-ring monoaromatic steroids
triaromatic steroids
(b)
acyclic alkanes
$CH_3-(CH_2)_n-CH_3$
n-alkanes
$CH_3-CH(CH_3)-(CH_2)_n-CH_3$
iso-alkanes
$CH_3-CH_2-CH(CH_3)-(CH_2)_n-CH_3$
anteiso-alkanes
pristane
phytane
cycloalkanes
alkylcyclopentanes
alkylcyclohexanes
alkylperhydronaphthalenes
aromatic hydrocarbons
alkylbenzenes
alkylnaphthalenes
alkylphenanthrenes
sulfur-containing aromatics
alkylbenzothiophenes
alkyldibenzothiophenes
alkylnaphthobenzothiophenes
R
S
CH_3

Fig. I.12. (**A**) Important biomarkers in crude oils, depicting the different numbering system for cheilanthanes, hopanes and steranes. (**B**) Organic hydrocarbons present in crude oils primarily derived from cracking processes and catagenesis. R denotes alkyl group. Both figures modified after Killops and Killops (2005).

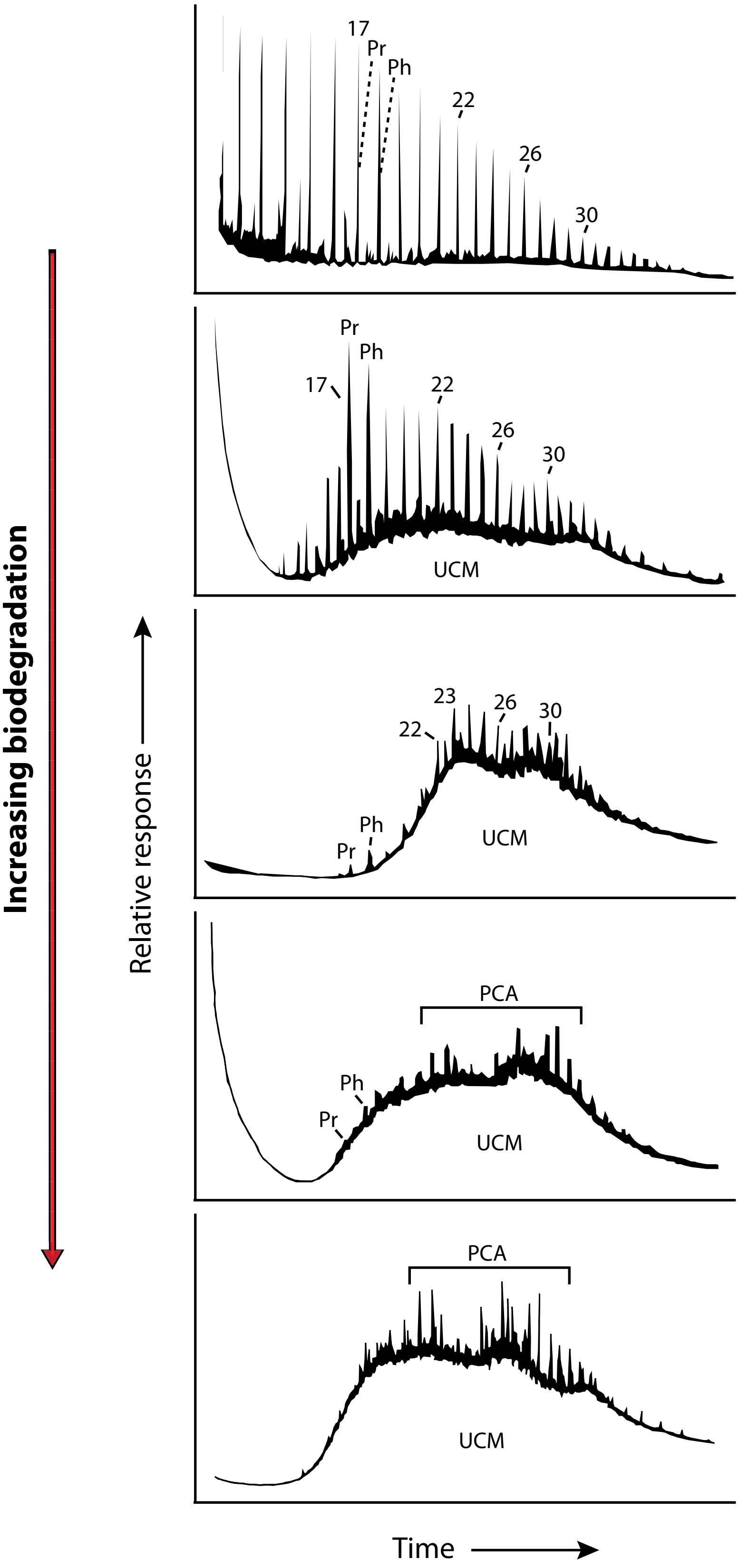

Fig. I.13. Alteration of oils during biodegradation showing how the removal of compounds results in a rise of the baseline during GC-FID analysis. Figure from Hostettler and Kvenvolden (1994). Pr - Pristane, Ph - Phytane, PCA - polycyclic aliphatics, UCM - unresolved complex mixture. Numbers depict carbon chain length of *n*-alkanes.

of hydrocarbon compounds that cannot be further resolved, it is thus termed the unresolved complex mixture (UCM).

Gas chromatography coupled to mass spectrometry (GC-MS) enables the extraction of specific mass chromatograms and therefore can be a useful tool to gain insights on the composition of the UCM (cf. Wang et al., 1999). GC-MS analyses have been widely applied in the investigation of oil weathering after anthropogenic oils spills (e.g., Hostettler and Kvenvolden, 1994; Wang and Fingas, 1995; Bence et al., 1996; Boehm et al., 1997; Munoz et al., 1997a; Bakarat et al., 2002). Hostettler and Kvenvolden (1994) analyzed petroleum hydrocarbons two to four years after the *T/V Exxon Valdez* oil spill of 1989 and found that degradation processes have effectively attacked and partly removed the n-alkanes, isoprenoids, and many of the polycyclic aromatic hydrocarbons. The terpane, sterane and aromatic sterane distribution was not greatly affected by degradation processes and was still correlated with the original *Exxon Valdez* oil. Polycyclic aromatic hydrocarbons (PAHs) changed over time in a characteristic pattern where first the low-molecular weight compounds were consumed, i.e., naphthalenes and flourenes, followed by phenantrenes and finally dibenzothiophenes and chrysenes. Furthermore, differences within the compound classes were observed (Fig. I.14). These observations were very

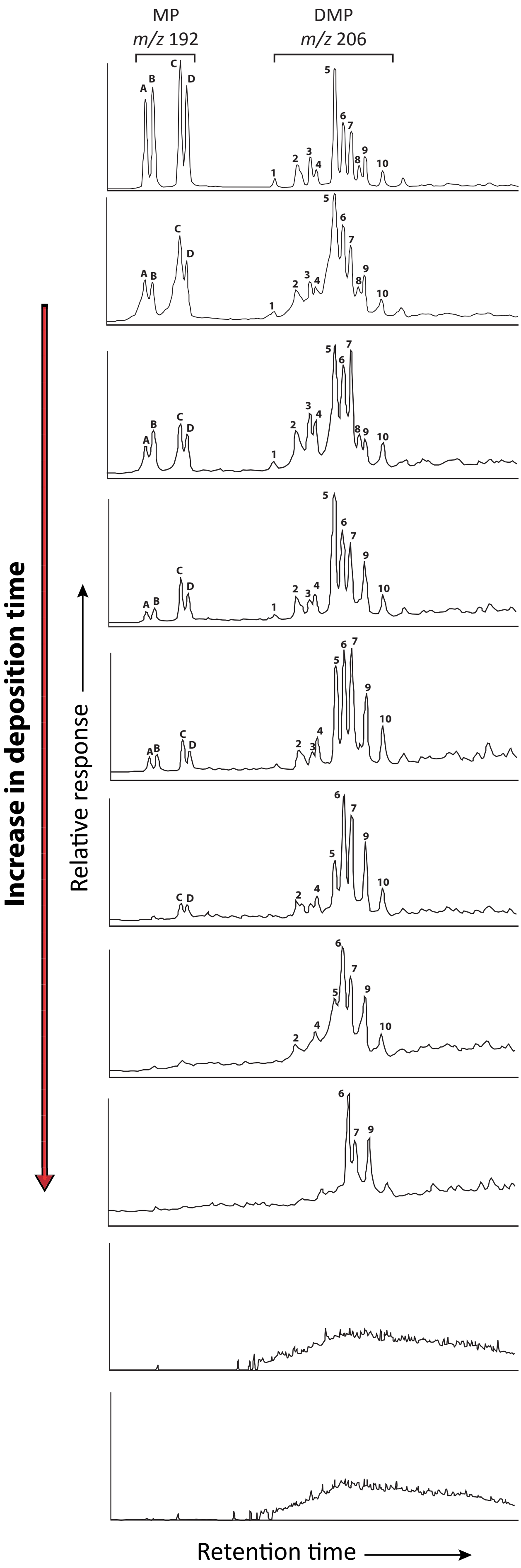

Fig. I.14. Comparison of mass chromatograms of methylphenantrene isomers (MP; A-D) and dimethylphenantrene isomers (DMP; 1-10) showing alterations during weathering of oils. Figure adapted from Hostettler and Kvenvolden (1994).

useful in the assessment of bioremediation of spilled oil where characteristic patterns can be used to distinguish biodegradation from weathering, as the latter shows a more unselective removal of petroleum compounds (cf. WANG ET AL., 1998). Nevertheless, problems of co-elution of hydrocarbon compounds that are very similar in structure also cannot be sufficiently resolved during extraction of mass chromatograms by conventional GC-MS analysis. Methods offering an increased resolution power of complex hydrocarbon mixtures include high resolution GC-MS (SIM) and metastable reaction monitoring (GC-MS-MS; e.g., MUNOZ ET AL., 1997B). Another significant methodological advance in the separation of complex hydrocarbon mixtures is the application of comprehensive two-dimensional gas chromatography (GC×GC), which separates compounds according to two orthogonal chemical properties during one analytical run (e.g., GAINES ET AL., 1999; FRYSINGER AND GAINES, 2001).

I.3.2.2. Separation of complex petroleum hydrocarbons by GC×GC

The set-up of GC×GC basically consists of two columns that contain different phases and are interconnected by a modulator. The modulator tube is positioned at the interface between the two capillary columns and requires an abrupt termination of the stationary phase. Compounds on the first column are typically separated according to volatiliy, similarly to conventional GC analysis. Hence, compounds are eluted at the end of the first column by elevated temperatures (ca. 300°C) and need to be quickly cooled down before they are subjected to the second column (cf. GAINES ET AL., 1999; NELSON ET AL., 2006). This takes place within the modulator where cooling is performed via liquid nitrogen. Fig. I.15 depicts how compounds are separated according to their retention time on the first and second dimension by GC×GC. Compounds that have the same boiling point due to structural similarities would co-elute during separation according to volatility only (primary retention). However, proper separation is achieved by addition of a polar second column in the GC×GC analysis. In Fig. I.15 the secondary chromatogram is 3 s long, which means that every 3 s (= period of one modulation) compounds that elute from the first column are subjected to separation on the second column. Consequently, this separation technique results in the generation of multiple secondary chromatograms that are, however, all

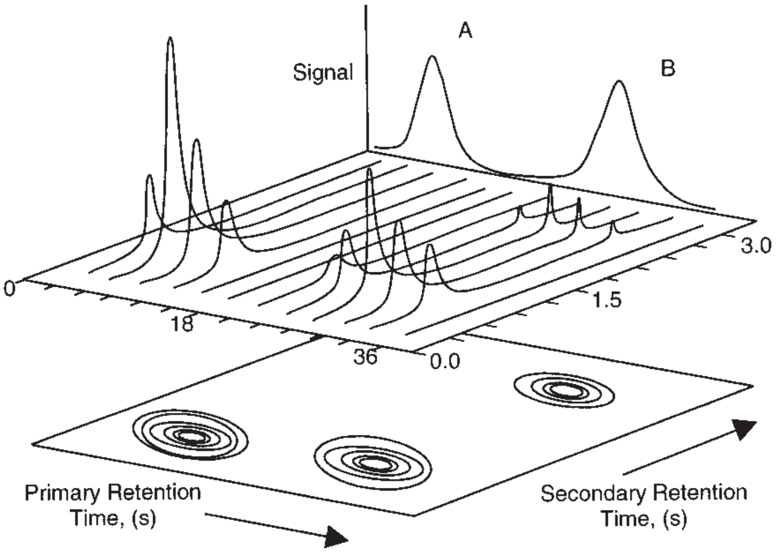

Fig. I.15. Separation of compounds by GC×GC showing individual chromatograms in the second dimension. A one-dimensional GC trace is on the back plane (A, B), and a contour plot of the GC×GC data appears on the bottom plane. Figure from GAINES ET AL. (1999).

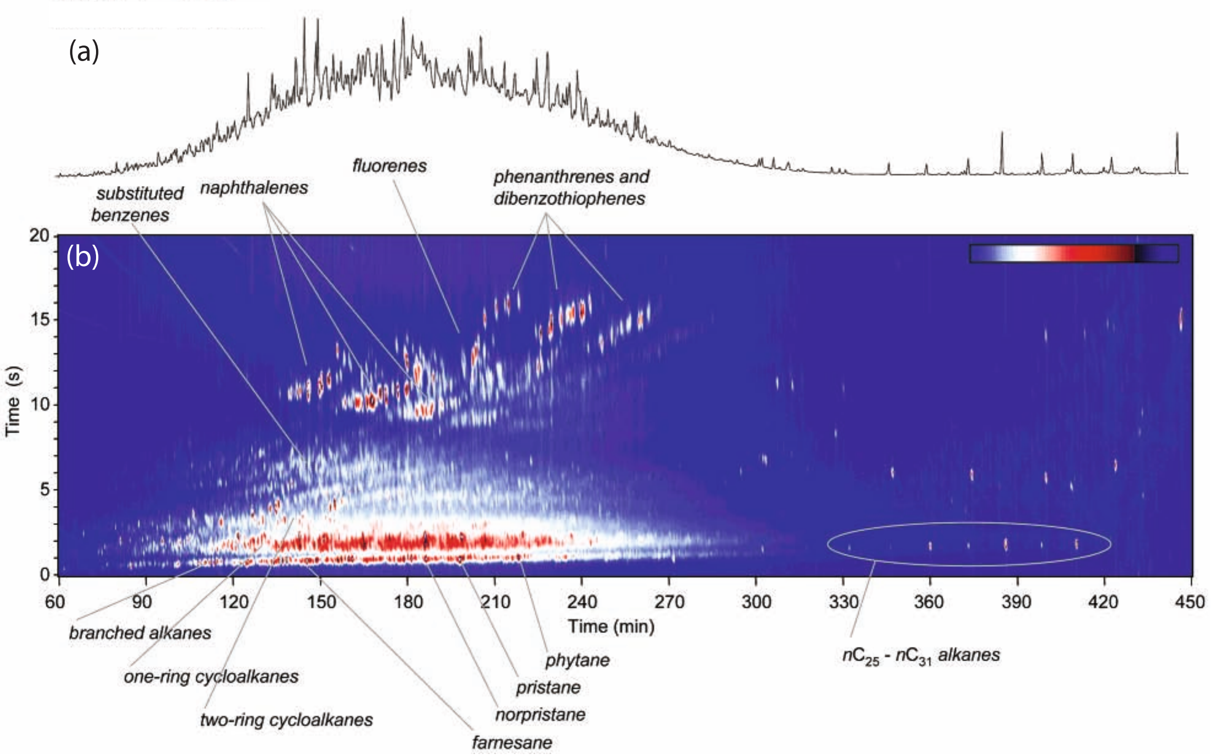

Fig. I.16. (**A**) GC-FID and (**B**) GC×GC chromatogram contour plot of a sample from an oil-contaminated site. In the first dimension (x-axis) the compounds are separated according to volatility and in the second dimension according to polarity. The background is blue. Peak intensity is scaled from white to red and then to blue (most intense). Figure from Reddy et al. (2002).

actually just one peak in the first chromatographic dimension.

Fig. I.16 shows an example of the resolution power of GC×GC of a natural sample from an oil-contaminated site, adapted from Reddy et al. (2002). In the upper panel the resolution power by conventional GC is depicted, showing a rise in the baseline, i.e., the presence of an UCM. GC×GC was able to separate the UCM according to volatility and polarity of the petroleum-forming hydrocarbon compounds. The applied chromatographic separation has lead to a separation of hydrocarbon compounds according to chain length elongation on the x-axis, leading to the elution of C_{19} compounds (e.g., pristane) before C_{20} compounds (e.g., phytane). The separation on the secondary axis is according to polarity, which can be seen in that aromatic compounds with increasing ring numbers elute at a later time, e.g., naphthalenes before phenantrenes. GC×GC separation results in the separation of compounds according to characteristics of compound classes, i.e., two-ring and three-ring compounds cluster closely together.

This increase in the resolving power of complex hydrocarbon mixtures has opened new possibilities during investigations of oils spills in the environment (e.g., Gaines et al., 1999; Reddy et al., 2002, Nelson et al., 2006; Peacock et al., 2007). Arey et al., (2007) made use of the GC×GC chromatographic analysis to decipher details of weathering processes between different samples of the same source. According to the separation of compounds by volatility on the the first dimension, he postulated that similarly, compounds that are most susceptible to evaporation would be removed along a path perpendicular to the retention time on the first dimension (Fig. I.17). Likewise, dissolution should remove compounds along a path perpendicular to solubility contours or dissolution lines (Fig. I.17c), primarily removing the smaller, more soluble aromatic compounds. The solubility contours were determined according to known aqueous solubilities of individual aromatic compounds (cf. Arey et al., 2007). The application of this concept is pretty straightforward as it enables deciphering different processes that affect the weathering alterations of oils and has been successfully applied in recent studies off the coast of Santa Barbara (e.g., Wardlaw et al., 2008; Farwell et al., 2009).

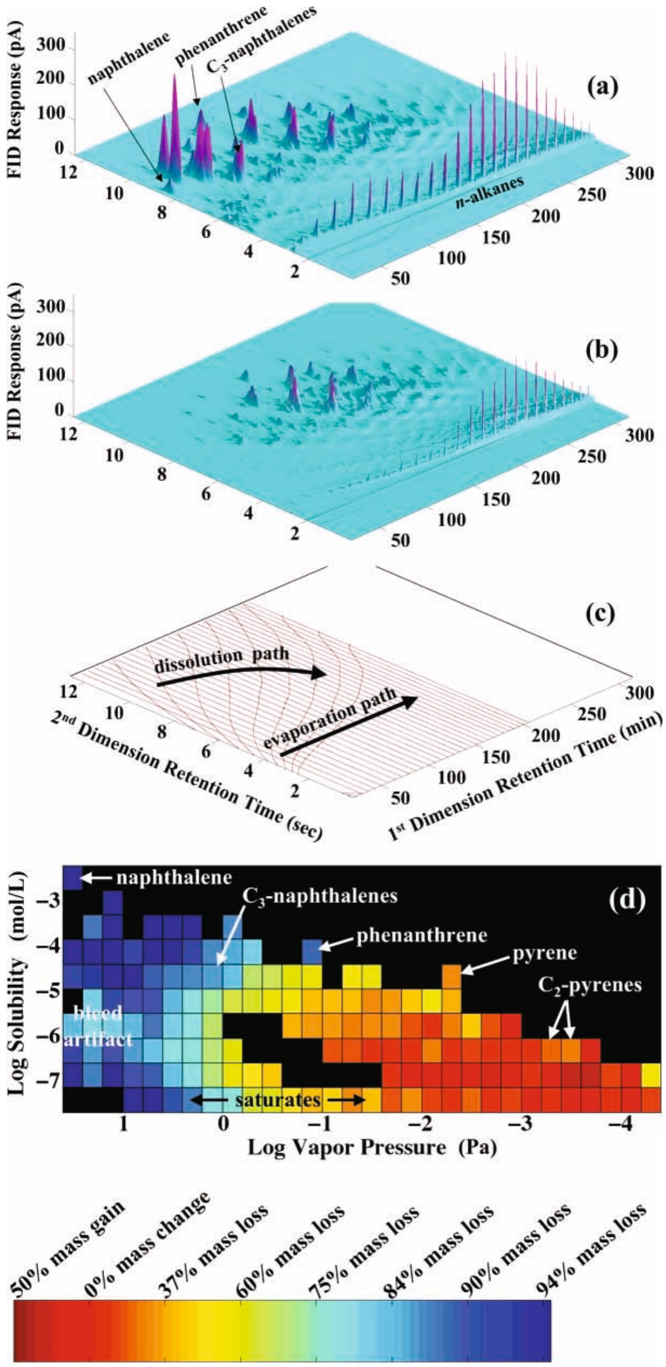

Fig. I.17. Conversion of a GC×GC chromatogram into a mass loss table. (**A**) GC×GC mountain plot of crude oil and (**B**) of weathered oil showing differences in hydrocarbon composition. (**C**) Contours of hydrocarbon vapor pressure (straight lines) overlaid with contours of hydrocarbon aqueous solubility (curved lines). Evaporation and dissolution are expected to remove hydrocarbon mass along a path that is perpendicular to the corresponding partitioning property contour lines, as shown by the bold arrows. (**D**) Mass loss table created by subtracting the first from the second chromatogram. For details see Arey et al. (2007).

I.4. CONTRIBUTIONS TO PUBLICATIONS

This thesis includes the complete versions of four first-author manuscripts for publication in international journals (*Chapters II-V*), one of which is already published (*Chapter II*). *Chapters VIa* and *VIb* include abstracts of two co-author manuscripts that are also part of this thesis but are not included in full for reasons of length. *Chapters VIa* is submitted to an international journal and *Chapter VIb* is ready as a draft version close to submission.

Chapter II – full manuscript

Detection of microbial biomass by intact polar membrane lipid analysis in the water column and surface sediments of the Black Sea
Florence Schubotz, Stuart G. Wakeham, Julius S. Lipp, Helen F. Fredricks, and Kai-Uwe Hinrichs
S.G.W. and K.-U.H. designed the project. S.G.W. collected samples, extracted, and performed sample clean-up on TLE of filters of particulate organic matter. H.F.F. and F.S. measured and identified IPLs with help from J.S.L. F.S. and S.G.W. wrote the paper with input from all co-authors. Published in *Environmental Microbiology*, vol. 11, no. 10, page 2720-2734, doi:10.1111/j.1462-2920.2009.01999.x © Society for Applied Microbiology and Blackwell Publishing Ltd, Oct. 2009.

Chapter III – full manuscript

Chemosynthetic life at the Chapopote asphalt volcano – insights from stable carbon isotopes and intact polar membrane lipid analyses
Florence Schubotz, Julius S. Lipp, Marcus Elvert, Sabine Kasten, Matthias Zabel, Elva Escobar, Gerhard Bohrmann, Kai-Uwe Hinrichs
F.S. and K.-U.H. designed the project and collected samples with help from S.K., M.Z., E.E. and G.B. F.S., K.-U.H and M.E. measured and identified hydrocarbon gases. S.K. and M.Z. measured sulfate, and S.K. provided samples for δ^{13}C hydrocarbon gas analysis. F.S. prepared samples for δ^{13}C DIC and TOC analysis and extracted IPLs from sediment, asphalt and soft tissue samples. F.S. conducted TLE clean-up and compound specific δ^{13}C analysis and interpreted the results with help from J.S.L., M.E. and K.-U.H.. F.S. wrote the paper with input from all co-authors. In preparation for *Geochimica et Cosmochimica Acta*.

Chapter IV – full manuscript

Sulfate-reduction, methanotrophy, and methanogenesis at the Chapopote asphalt volcano deciphered by head group-specific stable carbon isotopic analysis of intact polar membrane lipids
Florence Schubotz, Julius S. Lipp, Marcus Elvert, Kai-Uwe Hinrichs
F.S. designed the project under supervision of K.-U.H. F.S extracted IPLs from sediment, and developed a new analytical protocol for IPL head group-specific δ^{13}C analysis with help from J.S.L. GC-MS interpretation was supervised by M.E. F.S. wrote the paper with input from all co-authors. In preparation for *Geochimica et Cosmochimica Acta*.

Chapter V – full manuscript

Determining total petroleum hydrocarbon degradation and weathering by comprehensive GC×GC at an asphalt seep in the southern Gulf of Mexico
Florence Schubotz, G. Todd Ventura, Robert K. Nelson, Christopher M. Reddy, Kai-Uwe Hinrichs
F.S. and K.-U.H. designed the project. F.S. extracted asphalt samples and conducted TLE clean-up. C.M.R. provided the laboratory facilities and R.K.N. analyzed the samples. F.S. processed and interpreted the data with help from G.T.V. and R.K.N. F.S. wrote the paper with input from all co-authors. In preparation for *Environmental Science and Technology*.

Chapter VIb – abstract only

Methane and sulfide fluxes in permanent anoxia: in-situ studies at the Dvurechenskii mud volcano (Sorokin Trough, Black Sea)
Anna Lichtschlag, Janine Felden, Frank Wenzhöfer, Florence Schubotz, Tobias Ertefai, Antje Boetius, Dirk de Beer
A.L. together with D.dB. and A.B. designed the project. All authors were involved in sample collection. A.S. and J.F. performed in-situ experiments under the supervision of F.W. and D.dB. F.S. provided measurements of δ^{13}C DIC and T.E. of δ^{13}C methane. A.L. wrote the paper with input from all co-authors. Submitted to *Geochimica et Cosmochimica Acta*.

Chapter VIc – abstract only

Bacterial symbionts of Bathymodiolus mussels and Escarpia tubeworms from an asphaltic deep-sea environment in the southern Gulf of Mexico
Luciana Raggi, Florence Schubotz, Kai-Uwe Hinrichs and Nicole Dubilier
N.D. designed the project. L.R. conducted all microbiological and genetic analyses. F.S. and K.-U.H were involved in sample collection. F.S. conducted lipid analysis (IPL and CSIA δ^{13}C) under the supervision of K.-U.H. L.R. wrote the paper with input from all co-authors. In preparation for *Marine Ecology Progress Series*.

I.5. REFERENCES

Aharon, P., Roberts, H.H., Snelling, R. (1992) Submarine venting of brines in the deep Gulf of Mexico: observations and geochemistry. *Geology* **20**: 483-486.

Aitken, C.M., Jones, D.M., Larter, S.R. (2004) Anaerobic hydrocarbon biodegradation in deep subsurface oil reservoirs. *Nature* **43**: 291-294.

Albert, D.B., Taylor, C., Martens, C.S. (1995) Sulfate reduction rates and low molecular weight fatty acid concentrations in the water column and surficial sediments of the Black Sea. *Deep-Sea Res I* **42**: 1239-1260.

Anderson, R.K., Scalan, R.S., Parker, P.L. (1983) Seep oil and gas in Gulf of Mexico slope sediment. *Nature* **222**: 619-621.

Anderson, R.T., Lovley, D.R. (2000) Anaerobic bioremediation of benzene under sulfate-reducing conditions in a petroleum-contaminated aquifer. *Environ Sci Technol* **34**: 2261-2266.

Anweiler, E., Materna, A., Safinowski, M., Kappler, A., Richnow, H.H., Michaelis, W., Meckenstock, R.U. (2000) Anaerobic degradation of 2-methylnapthalene by a sulfate-reducing enrichment culture. *Appl Environ Microbiol* **66**: 5329-5333.

Annweiler, E., Michaelis, W., Meckenstock, R.U. (2002) Identical ring cleavage products during anaerobic degradation of naphthalene, 2-methylnaphthalene and tetralin indicate a new metabolic pathway. *Appl Environ Microbiol* **68**: 852-858.

Arey, J.S., Nelson, R.K., Reddy, C.M. (2007) Disentangling oil weathering using GC×GC. 1. Chromatogram analysis. *Environ Sci Technol* **41**: 5738-5746.

Bachoon, D.S., Araujo, R., Molina, M., Hodson, R.E. (2001) Microbial community dynamics and evaluation of bioremediation strategies in oil-impacted salt marsh sediment microcosms. *J Ind Microbiol Biotechnol* **27**: 72-79.

Bakarat, A.O., Mostafa, A.R., Qian, Y., Kennicutt, M.C. (2002) Application of petroleum fingerprinting in oil spill investigations – Gulf of Suez, Egypt. *Spill Sci Tech Bull* **7**: 229-239.

Barnes, R.O., Goldberg, E.D. (1976) Methane production and consumption in anoxic marine sediments. *Geology* **4**: 297-300.

Bastin, E.S., Greer, F.E., Merrit, C.A., Moulton, G. (1926) The presence of sulphate-reducing bacteria in oil field waters. *Science* **63**: 21-24.

Beller, H., Reinhard, M., Grbic-Galic, D. (1992) Metabolic byproducts of anaerobic toluene degradation by sulfate-reducing enrichment cultures. *Appl Environ Microbiol* **58**: 3192-3195.

Bence, A.E., Kvenvolden, K.A., Kennicutt II, M.C. (1996) Organic geochemistry applied to environmental assessments of Prince William Sound, Alaska, after the *Exxon Valdez* oil spill – a review. *Org Geochem* **24**: 7-42.

Benning, C., Beatty, J.T., Prince, R.C., Somerville, C.R. (1993) The sulfolipid sulfoquinovosyldiacylglycerol is not required for photosynthetic electron transport in *Rhodobacter sphaeroides* but enhances growth under phosphate limitation. *Proc Natl Acad Sci USA* **90**: 1561-1565.

Benning, C., Huang, Z.H., Gage, D.A. (1995) Accumulation of a novel glycolipid and a betaine lipid in cells of *Rhodobacter sphaeroides* grown under phosphate limitation. *Arch Biochem Biophys* **317**: 103-111.

Berner, R.A. (1980) *Early Diagenesis, a Theoretical Approach*. Princeton University Press, Princeton, New Jersey.

Biddle, J.F., Lipp, J.S., Lever, M.A., Lloyd, K.G., Sørensen, K.B. Anderson, R., Fredricks, H.F., Elvert, M., Kelly, T.J., Schrag, D.P., Sogin, M.L., Brenchley, J.E., Teske, A., House, C.H., Hinrichs, K.-U. (2006) Heterotrophic Archaea dominate sedimentary subsurface ecosystems off Peru. *Proc Natl Acad Sci USA* **103**: 3846-3851.

Biegert, T., Fuchs, G., Heider, J. (1996) Evidence that anaerobic oxidation of toluene in the denitrifying bacterium *Thauera aromatica* is initiated by formation of benzylsuccinate from toluene and fumarate. *Eur J Biochem* **238**: 661-668.

Birgel, D., Peckmann, J (2008) Aerobic methanotrophy at ancient marine methane seeps: a synthesis. *Org Geochem* **39**: 1659-1667.

Blumenberg, M., Seifert, R., Reitner, J., Pape, T., Michaelis, W. (2004) Membrane lipid patterns typify distinct anaerobic methanotrophic consortia. *Proc Natl Acad Sci USA* **101**:11111-11116.

Blumenberg, M., Krüger, M., Nauhaus, K., Talbot, H.M., Oppermann, B.I., Seifert, R., Pape, T., Michaelis W. (2006) Biosynthesis of hopanoids by sulfate-reducing bacteria (genus *Desulfovibrio*). *Environ Microbiol* **8**: 1220-1227.

Boehm, P.D., Douglas, G.S., Burns, W.A., Mankiewicz, P.J., Page, D.S., Bence, A.E. (1997) Application of petroleum hydrocarbon chemical fingerprinting and allocation techniques after the Exxon Valdez oil spill. *Mar Poll Bull* **34**: 599-613.

Boetius, A., Ravenschlag, K., Schubert, C.J., Rickert, D., Widdel, F., Gieseke, A., Amann, R., Jørgensen, B.B., Witte, U., Pfannkuche, O. (2000) A marine microbial consortium apparently mediating the anaerobic oxidation of methane. *Nature* **407**: 623-626.

Bohrmann, G., Spiess, V., M67/2 cruise Participants (2008) Report and preliminary results of R/V Meteor cruise M67/2a and 2b, Balboa – Tampico – Bridgetown, 15 March – 24 April 2006. Fluid seepage in the Gulf of Mexico, Berichte, No.263, Fachbereich Geowissenschaften, Universität Bremen, Bremen, Germany.

Boon, J.J., De Leeuw, J.W., V. D. Hoek, G.J., Vosjan, J.H. (1977) Significance and taxonomic value of iso and anteiso monoenoic fatty acids and branched *β*-hydroxy acids in *Desulfovibrio desulfuricans*. *J Bacteriol* **129**: 1183-1191.

Boone, D.R., Whitman, W.B., Rouviere, P. (1993) *Diversity and taxonomy of methanogens*, p. 35-80. In J.G. Ferry (ed.), Methanogenesis: ecology, physiology, biochemistry, and genetics. Chapman & Hall, New York.

Bouvier P., Rohmer, M., Benveniste P., Ourisson, G. (1976) Delta8(14)-steroids in the bacterium *Methylococcus capsulatus*. *Biochem J* **159**: 267-271.

Brett, M.T., Müller-Navarra D.C. (1997) The role of highly unsaturated fatty acids in aquatic foodweb processes. *Freshw Biol* **38**: 483-499.

Brooks, J.M., Kennicutt II, M.C., Fay, R.R., T.J. MacDonald (1984) Thermogenic gas hydrates in the Gulf of Mexico. *Science* **225**: 409-411.

Brooks, J.M., Cox, H.B., Bryant, W.R., Kennicutt II, R., Mann, G., MacDonald, D.J. (1986) Association of gas hydrates and oil seepage in the Gulf of Mexico. *Org Geochem* **10**: 221-234.

Brüning, M., Sahling, H., MacDonald, I. R, Ding, F, Bohrmann, G. Origin, distribution, and alteration of asphalts at Chapopote Knoll, Southern Gulf of Mexico (2009). *Mar Petrol Geol,* accepted September 2009.

Buffet B., Archer, D. (2004) Global inventory of methane clathrate: sensitivity to changes in the deep ocean. *Earth Planet Sci Lett* **227**: 185-199.

Caldwell, M.E., Suflita, J.M. (2000) Detection of phenol and benzoate as intermediates of anaerobic benzene biodegradation under different terminal electron-accepting conditions. *Environ Sci Technol* **34**: 1216-1220.

Canfield, D.E., Thamdrup, B. (2009) Towards a consistent classification scheme for geochemical environments, or, why we wish the term ‘suboxic’ would go away. *Geobiology* **7**: 385-392.

Capone, D.G., Kiene, R.P. (1988) Comparison of microbial dynamics in marine and freshwater sediments: Contrasts in anaerobic carbon catabolism. *Limnol Oceanogr* **33**: 725-749.

Cavanaugh, C.M., Gardiner, S.L., Jones, M.L., Jannasch, H.W., Waterbury, J.B. (1981) Prokaryotic cells in the hydrothermal vent tube worm *Riftia pachyptila* Jones: possible chemoautotrophic symbionts. *Science* **213**: 340-342.

Cerniglia, C.E., Hebert, R.L., Szaniszlo, P.J., Gibson, D.T. (1978) Fungal transformation of naphthalene. *Arch Microbiol* **117**: 135-143.

Childress, J.J., Fisher, C.R., Brooks, J.M., Kennicutt, M.C. II, Bidigare, R., Anderson, A. (1986) A methanotrophic marine mulluscan symbiosis: mussels fueled by gas. *Science* **233**: 1306-1308.

Chung, H.M., Gormly, J.R., Squires, R.M. (1988) Origin of gaseous hydrocarbons in subsurface environments: Theoretical considerations of carbon isotope distribution. *Chem Geol* **71**: 97-103.

Condie, K.C. (1997) Plate tectonics and crustal evolution. Pergamon Press, Oxford.

Connan, J. (1984) Biodegradation of crude oils in reservoirs. In: Brooks, J., Welte, D. (eds.) Advances in petroleum geochemistry, Vol. 1. Academic Press, London, pp. 299-335.

Coolen, M.J.L., Abbas, B., van Bleijswijk, J., Hopmans, E., Kuypers, M.M.M., Wakeham, S.G., Sinninghe Damsté, J.S. (2007) Putative ammonia-oxidizing Crenarchaeota in suboxic waters of the Black Sea: a basin-wide ecological study using 16S ribosomal and functional genes and membrane lipids. *Environ Microbiol* **9**: 1001-1016.

Corliss, J.B., Dymond, J., Gordon, L.I., Edmond, J.M., von Herzen, R.P., Ballard, R.D., Green, K., Williams, D., Bainbridge, A., Crane, K., van Andel, T.H. (1979) Submarine thermal springs on the Galápagos Rift. *Science* **203**: 1073-1083.

Davidova, I.A., Gieg, L.M., Duncan, K.E., Suflita, J.M. (2007) Anaerobic phenantrene mineralization by a carboxylating sulfa-reducing bacterial enrichment. *ISME J* **1**: 436-442.

De la Torre, J., Walker, C.B., Ingalls, A.E., Könneke, M., Stahl, D.A. (2008) Cultivation of a thermophilic ammonia oxidizing archaeon synthesizing crenarchaeol. *Env Microbiol* **10**: 810-818.

DeLong, E.F., Yayanos, A.A. (1986) Biochemical function and ecological significance of novel bacterial lipids in deep-sea prokaryotes. *Appl Environ* **51**: 730-737.

De Rosa, M., Gambacorta, A. (1988) The lipids of archaebacteria. *Progr Lipid Res* **27:** 153-175.

Dembitsky, V.M. (1996) Betaine ether-linked glycerolipids: chemistry and biology. *Prog Lipid Res* **35**: 1-51.

Desbruyéres, D., Toulmond, A. (1998) A new species of hesionid worm, *Hesiocoeca methanolica* n. sp. (Plychaeta: Hesionidae) living in ice-like methane hydrates in the deep Gulf of Mexico. *Cahiers Biol Mar* **39**: 93-98. Ding, F., Spiess, V., Brüning, M., Fekete, N., Keil, H., Bohrmann, G. (2008) A conceptual model for hydrocarbon accumulation and seepage processes around Chapopote asphalt site, southern Gulf of Mexico: From high resolution seismic point of view. *J Geophys Res* **113**: DOI:10.1029/2007JB005484.

Devol, A.H. (1983) Methane oxidation rates in the anaerobic sediments of Saanich Inlet. *Limn Oceanogr* **28**: 738-742.

Dickens, G.R., O'Neal, J.R., Rea, D.K., Owen, R.M. (1995) Dissociation of oceanic methane hydrate as a cause of the carbon isotope excursion at the end of the Paleocene. *Paleoceanogr* **10**: 965-971.

Ding, F., Spiess, V., Brüning, M., Fekete, N., Keil, H., Bohrmann, G. (2008) A conceptual model for hydrocarbon accumulation and seepage processes around Chapopote asphalt site, southern Gulf of Mexico: From high resolution seismic point of view. *J Geophys Res* **113**: DOI:10.1029/2007JB005484.

Dowhan, H., Bogdanov, M. (2002) Functional roles of lipids in membranes. In: D.E. Vance and J.E. Vance (eds) Biochemistry of Lipids, Lipoproteins and Membranes (4th Edition) Elsevier Science, 2002, pp. 1-35.

Dowling, N.J.E., Widdel, F., White, D.C. (1986) Phospholipid ester-linked fatty acid biomarkers of acetate-oxidizing sulphate-reducing and other sulphide-forming bacteria. *J Gen Microbiol* **132**: 1815-1825.

Durisch-Kaiser, E., Klauser, L., Wehrli, B., Schubert, C. (2005) Evidence of intense archaeal and bacterial methanotrophic activity in the Black Sea water column. *Appl Environ Microbiol* **71**: 8099-8106.

Elvert, M., Suess, S., Whiticar, M.J. (1999) Anaerobic methane oxidation associated with marine gas hydrates: superlight C-isotopes from saturated and unsaturated C_{20} and C_{25} irregular isoprenoids. *Naturwissenschaften* **86**: 295-300.

Elvert, M., Niemann, H. (2008) Occurrence of unusual steroids and hopanoids derived from aerobic methanotrophs at an active marine mud volcano. *Org Geochem* **39**: 167-177.

Ertefai, T.F., Fisher, M.C., Fredricks, H.F., Lipp, J.S., Pearson, A., Birgel, D., Udert, K.M., Cavanaugh, C.M., Gschwend, P.M., Hinrichs, K.-U. (2008) Vertical distribution of microbial lipids and functional genes in chemically distinct layers of a highly polluted meromictic lake. *Org Geochem* **39**: 1572-1588.

Eyster K. (2009) The membrane and lipids as integral participants in signal transduction: lipid signal transduction for the non-lipid biochemist. *Advan Physiol Edu* **31**: 5-16.

Evans, P.J., Ling, W., Goldschmidt, B., Ritter, E.R., Young, L.Y. (1992) Metabolites formed during anaerobic transformation of toluene and o-xylene and their proposed relationship to the initial steps of toluene mineralization. *Appl Environ Microbiol* **58**: 496-501.

Fang, J., Barcelona, M.J., Semrau, J.D. (2000) Characterization of methanotrophic bacteria on the basis of intact phospholipid profiles. *FEMS Microbiol Let* **189**: 67-72.

Fang, J.S., Hasiotis, S.T., Das Gupta, S., Brake, S.S., Bazylinski, D.A. (2007) Microbial biomass and community structure of a stromatolite from an acid mine drainage system as determined by lipid analysis. *Chem Geol* **243**: 191-204.

Farwell C., Reddy, C.M., Peacock, E., Nelson, R.K., Washburn, L., Valentine, D.L. (2009) Weathering and the fallout plume of heavy oil from strong petroleum seeps near Coal Oil Piont, CA. *Environ Sci Technol* **43**: 3542-3548.

Fenchel, T. and Jørgensen, B.B. (1977) Detritus food chains of aquatic ecosystems: The role of bacteria. In *Advances in Microbial Ecology*. Alexander, M. (ed). New York: Plenum Press, pp. 1-58.

Fischer, C.R., MacDonald, I.R., Sassen, R., Young, C.M., Macko, S.A., Hourdez, S., Carney, R.S., Joye, S., McMullin, E. (2000) Methane ice worms: *hesiocaeca methanicola* colonizing fossil fuel reserves. *Naturwissenschaften* **87**: 184-187.

Fredricks, H. F., Hinrichs, K.-U. (2007) Data Report: Intact Membrane Lipids as Indicators of Subsurface Life in Cretaceous and Paleogene Sediments from Sites 1257 and 1258. *Proc ODP Sci Res* **207**.

Froelich, P. N., Klinkhammer, G. P., Bender, M. L., Luedtke, N. A., Heath, G. R., Cullen, D., Dauphin, P., Hammond, D., Hartman, B., Maynard, V. (1979). Early oxidation of organic matter in pelagic sediments of the eastern equatorial Atlantic: suboxic diagenesis. *Geochim Cosmochim Acta.* **43**: 1075-1090.

Frysinger, G.S., Gaines, R.B. (2001) Separation and identification of petroleum biomarkers by comprehensive two-dimensional gas chromatography. *J Sep Sci* **24**: 87-96.

Fulco, A. J. (1983). Fatty acid metabolism in bacteria. *Progr Lipid Re*s **22**, 133-160.

Gaines, R.B., Frysinger, G.S., Hendrick-Smith, M.S., Stuart, J.D. (1999) Oil spill source identification by comprehensive two-dimensional gas chromatography. *Environ Sci Technol* **33**: 2106-2112.

Goldfine, H. (1984) Bacterial membranes and lipid packing theory. *J Lip Res* 25: 1501-1507.

Gorur, N., Cagatay, M.N., Emre, O., Alpar, B., Sakine, M., Islamogly, Y., Algan, O., Erkal, T., Kecer, M., Akkok, R., Karlik, G. (2001) Is the abrupt drowning of the Black Sea shelf at 7150 yr a myth? *Mar Geol* **176**: 65-73.

Grogan, D.W., Cronan, J.E. (1997) Cyclopropane ring formation in membrane lipids of bacteria. *Microbiol Mol Biol Rev* **61**: 429-436.

Grossi, V., Cravo-Laureau, C., Guyoneaud, R., Ranchou-Peyruse, A.R., Réa, A.H. (2008) Metabolism of *n*-alkanes and *n*-alkenes by anaerobic bacteria: A summary. *Org Geochem* **39**: 1197-1203.

Güler, S., Seeliger, A., Härtl, H., Renger, G., Benning, C. (1996) A null mutant of *synechococcus* sp. PCC7942 deficient in the sulfolipid sulfoquinovosyldiacylglycerol. *J Biol Chem* **271**: 7501-7507.

Habe, H., Omori, T. (2003) Genetics of polycyclic aromatic hydrocarbon metabolism in diverse aerobic bacteria. *Biosci Biotechnol Biochem* **67**: 225-243.

Hanson, R.S., Hanson, T.E. (1996) Methanotrophic bacteria. *Microbiol Rev* **60**: 439-471.

Harvey, H.R., Fallon, R.D., Patton, J.S. (1986) The effect of organic matter and oxygen on the degradation of bacterial membrane lipids in marine sediments. *Geochim Cosmochim Acta* **50**: 795-804.

Hasegawa, J., Kawada, N., Nosoh, J. (1980) Change in chemical composition of membrane of *Bacillus caldotenax* after shifting the growth temperature. *Arch Microbiol* **126**: 103-108.

Haucke, V., DiPaolo, G. (2007) Lipids and lipid modifications in the regulation of membrane traffic. *Curr Opin Cell Biol* **19**: 426-435.

Hazel, J.R., Williams, E. (1990) The role of alterations in membrane lipid composition in enabling physiological adaptation of organisms to their physical environment. *Prog Lipid Res* **29**: 167-227.

Hayes, J.M. (2001) Fractionation of the isotopes of carbon and hydrogen in biosynthetic processes. *Rev Mineral Geochem* **43**: 225-277.

Head, J.M., Jones, D.M., Larter, S.R. (2003) Biological activity in the deep subsurface and the origin of heavy oil. *Nature* **426**: 344-352.

Head, I.M., Jones, D.M., Röling, W.F.M. (2006) Marine microorganisms make a meal of oil. *Nature* **4**: 173-182.

Heider, J. (2007) Adding handles to unhandy substrates: anaerobic hydrocarbon activation mechanisms. *Curr Opin Chem Biol* **11**: 188-194.

Hesselbo, S.P., Gröcke, D.R., Jenkyns, H.C., Bjerrum, C.J., Farrimond, P., Morgans Bell, H.S., Green, O.R. (2000) Massive dissociation of gas hydrate during a Jurassic oceanic anoxic event. *Nature* **406**: 392-395.

Hessler, R.R., Smithey, W.M., Keller, C.H. (1985) Spatial and temporal variation of giant clams, tubeworms and mussels at deep-sea hydrothermal vents. *Bull Biol Soc Wash* **6**: 411-428.

Hinrichs, K.-U., Hayes, J.M., Sylva, S.P., Brewer, P.G., DeLong, E.F. (1999) Methane-consuming archaebacteria in marine sediments. *Nature* **398**: 802-805.

Hinrichs, K.-U., Boetius, A. (2002) The anaerobic oxidation of methane: New insights in microbial ecology and biogeochemistry. In *Ocean Margin Systems*, eds. Wefer G., Billet, D., Hebbeln, D., Jørgensen, B. B., Schlüter, M. & van Weering, T. (Springer, Berlin), pp. 457–477.

Hinrichs, K.-U., Hmelo, L.R., Sylva, S.P. (2003) Molecular fossil record of elevated methane levels in late Pleistocene coastal waters. *Science* **299**: 1214-1217.

Hoehler, T.M., Alperin, M.J., Albert, D.B., Martens, C.S. (1994) Field and laboratory studies of methane oxidation in an anoxic marine sediment: Evidence for a methanogen-sulfate reducer consortium. *Global Biochem Cyc* **8**: 451-463.

Hölzl, G., Dörmann, P. (2007) Structure and function of glycoglycerolipids in plants and bacteria. *Progr Lipid Res* **46**: 225-243.

Hostettler, F.D., Kvenvolden, K.A. (1994) Geochemical changes in crude oil spilled from the Exxon Valdez supertanker into Prince William Sound, Alaska. *Org Geochem* **21**: 927-936.

House, C.H., Schopf, J.W., Stetter, K.O. (2003) Carbon isotopic fractionation by archaeans and other thermophilic prokaryotes. *Org Geochem* **34**: 345-356.

Huber, R., Wilharm, T., Huber, D., Trincone, A., Burggraf, S., Rachel, R., Rockinger, I., Frickel, H., Stetter, K.O. (1992) *Aquifex pyrophilus* gen. nov. sp. nov., represents a novel group of marine hyperthermophilic hydrogen-oxidizing bacteria. *Syst Appl Microbiol* **15**: 340-351.

Imhoff, J.F. Bias-Imhoff, U. (1995) Lipids, quinones and fatty acids of anoxygenic phototrophic bacteria. In Anoxygenic Photosynthetic Bacteria. Blankenship, R.E., Madigan, M.T., Bauer, C.E. (eds.), pp. 179-205. 1995 Kluwer Academic Publishers. Printed in The Netherlands.

Itoh, Y.H., Sugai, A., Uda, I., Itoh, T. (2001) The evolution of lipids. *Adv Space Res* **4**: 719-724.

Iversen, N., and Jørgensen, B.B. (1985) Anaerobic methane oxidation rates at the sulfate-methane transition in marine sediments from Kattegat and Skagerrak (Denmark). *Limnol Oceanogr* **30:** 944–955.

Ivanov, M.K, Limonov, A.F., Woodside, J.M. (1998) *Extensive deep fluid flux through the seafloor on the Crimean continental margin (Black Sea).* In: Henriet, J.-P., Mienat, J. (eds.), Gas hydrates: relevance to world-margin stability and climate change, Geological Society London, 1998.

Jannasch, H.W. (1984) Chemosynthesis: the nutritional basis for life at deep-sea vents. *Oceanus* **27**: 73-78.

Jannasch, H.W., Mottl, M.J. (1985) Geomicrobiology of deep-sea hydrothermal vents. *Science* **229**: 717-725.

Jannasch, H.W., Wirsen, C.O., Molyneaux, S.J. (1991) Chemoautotrophic sulfur-oxidizing bacteria from the Black Sea. *Deep-Sea Res I* **38** (Suppl. 2): 1105-1120.

Jerina, D.M., Daly, J.W., Witkop, B., Zaltzman-Nirenberg, P., Udenfriend, S. (1968) Role of the Arene Oxide-Oxepin system in the metabolism of aromatic substances. I. In vitro conversion of benzene oxide to a premercapturic acid and a dihydrodiol. *Arch Biochem Biophys* **128**: 176-183.

Jørgensen, B.B. (1982) Mineralization of organic matter in the sea bed – the role of sulphate reduction. *Nature* **296**: 643-645.

Jørgensen, B.B., Fossing, H., Wirsen, C.O., Jannasch, H.W. (1991) Sulfide oxidation in the anoxic Black Sea chemocline. *Deep-Sea Res I* **38** (Suppl. 2): 1083-1103.

Jones, D.M., Head, I.M., Gray, N.D., Adams, J.J., Rowan, A.K., Aitken, C.M., Bennett, B., Huang, H., Brown, A., Bowler, B.F.J., Oldenburg, T., Erdmann, M., Larter, S.R. (2008) Biodegradation via methanogenesis in subsurface petroleum reservoirs. *Nature* **451**: 176-180.

Joye, S.B., Boetius, A., Orcutt, B.N., Montoya, J.P., Schulz, H.N., Erickson, M.J., Lugo, S.K. (2004) The anaerobic oxidation of methane and sulfate reduction in sediments from Gulf of Mexico cold seeps. *Chem Geol* **205**: 219-238.

Joye, S.B., Samarkin, V.A., Orcutt, B.N., MacDonald, I.R., Hinrichs, K.-U., Elvert, M., Teske, A.P., Lloyd, K.G., Lever, M.A., Montoya, J.P., Meile, C.D. (2009) Metabolic variability in seafloor brines revealed by carbon and sulphur dynamics. *Nat Geosci* **2**: 349-354.

Juniper, S.K., Sinuit, M. (1987) Cold seep benthic communities in Japan subduction zones: spatial organization, trophic strategies and evidence for temporal evolution. *Mar Evol Prog Ser* **40**:115-126.

Kaneda, T. (1991) Iso- and anteiso-fatty acids in bacteria: Biosynthesis, function, and taxonomic significance. *Microbiol Rev* **55**: 288-302.

Karl, D.M., Knauer, G.A. (1991) Microbial production and particle flux in the upper 350 m of the Black Sea. *Deep-Sea Res* **38**: 921-942.

Karner, M.B., DeLong, E.F., Karl, D.M. (2001) Archaeal dominance in the mesopelagic zone of the Pacific Ocean. *Science* **409**: 507-510.

Kates, M. (1979) The phytanyl ether-linked polar lipids and isoprenoid neutral lipids of extremely halophilic bacteria. *Prog. Chem. Fats and Other Lipids* **15**: 206-208.

Kates, M. (1989) *The sulfolipids of diatoms*. In: Marine biogenic lipids, fats, and oils, volume 1, CRC Press, Inc., Florida.

Kato, M., Sakai, M., Adachi, K., Ikemoto, H., Sano, H. (1996) Distribution of betaine lipids in marine algae. *Phytochemistry* **42**: 1341-1345.

Kelley, D.S., Baross, J.A., Delaney, J.R. (2002) Volcanoes, fluids, and life at mid-ocean ridge spreading centers. *Annu Rev Earth Planet Sci* **30**: 385-491.

Keltjens, J.T., Vogels, G.S. (1993) *Methanogenesis* (Ferry J.G., eds), p. 253, Chapman & Hall, New York.

Kennicutt, M.C. II, Brooks, J.M., Bidare, R.R., Fay, R.R., Wade, T.L., MacDonald, T.J. (1985) Vent-type taxa in a hydrocarbon seep region on the Lousiana Slope. *Nature* **317**: 351-353.

Kennicutt II, M.C., Brooks, J.M., Denoux, G.J. (1988) Leakage of deep, reservoired petroleum to the near surface on the Gulf of Mexico continental slope. *Marine Chem* **24**: 39-59.

Khozin—Goldberg, I., Cohen, Z. (2006) The effect of phosphate starvation on the lipid and fatty acid composition of the fresh water eustigmatophyte *Monodus subterraneus*. *Phytochem* **67**: 696-701.

Killops, S.D., Killops, V.J. (2005) Introduction to Organic Geochemistry, 2nd ed., Blackwell Publishing, Malden, Mass.

Klauda, J.B., Sandler, S.I. (2005) Global distribution of methane hydrate in ocean sediment. *Energy & Fuels* **19**: 459-470.

Knittel., K. Lösekann, T., Boetius, A., Kort, R., Amann, R. (2005) Diversity and Distribution of methanotrophic archaea at cold seeps. *Appl Environ Microbiol* **71**, 467-479.

Knittel., K., Boetius, A. (2009) Anaerobic oxidation of methane: Progress with an unknown process. **63**: 311-334.

Könneke, M., Bernhard, A.E., de la Torre, J.R., Walker, C.B., Waterbury, J.B., Stahl, D.A. (2005) Isolation of an autotrophic ammonia-oxidizing marine archaeon. *Nature* **437**: 543-546.

Koga, Y., Morii, H., Akagawa-Matsushita, M., Ohga, M. (1998) Correlation of polar lipid composition with 16S rRNA phylogeny in methanogens. Further analysis of lipid component parts. *Biosci Biotechnol Biochem* **69**: 230-236.

Koga, Y., Nakano, M. (2008) A dendrogram of archaea based on lipid component parts composition and its relationship to rRNA phylogeny. *Syst App. Microbiol* **31**: 169-182.

Kohring, L.L., Ringelberg, D.B., Devereux, R., Stahl, D.A., Mittelman, M.W., White, D.C. (1994) Comparison of phylogenetic relationships based on phospholipid fatty acid profiles and ribosomal RNA sequence similarities among dissimilatory sulfate-reducing bacteria. *FEMS Microbiol Lett* **119**: 303-308.

Könneke, M., Bernhard, A.E., de la Torre, J.R., Walker, C.B., Waterbury, J.B., Stahl, D.A. (2005) Isolation of an autotrophic ammonia-oxidizing marine archaeon. *Nature* **437**: 543-546.

Kulm, L.D., Suess, E., Moore, J.C., Carson, B., Lewis, B.T., Ritger, S.S., Kadko, D.C., Thornburg, T.M., Embley, R.W., Rugh, W.D., Massoth, G.J., Langseth, M.G., Cochrane, G.R., Scamman, R.L. (1986) Oregon Subduction Zone: Venting, fauna, and carbonates. *Science* **231**: 561-231.

Kuypers, M.M.M, Sliekers, A.O., Lavik, G., Schmid, M., Jørgensen, B.B., Sinninghe Damsté, J.S., Strous, M., Jetten, M.S.M. (2003) Anaerobic ammonium oxidation by anammox bacteria in the Black Sea. *Nature* **422**: 608-611.

Kvenvolden, K.A. (1995) A review of the geochemistry of methane in natural gas hydrate. *Org Geochem* **23**: 997-1008.

Kvenvolden, K.A., Cooper, C.K. (2003) Natural seepage of crude oil into the marine environment. *Geo-Mar Lett* **23**: 140-146.

Lam, P., Jensen, M.M., Lavik, G., McGinnis, D.F., Müller, B., Schubert, C.J., Amann, R., Thamdrup, B., Kuypers, M.M.M (2007) Linking crenarchaeal and bacterial nitrification to anammox in the Black Sea. *Proc Natl Acad Sci USA* **104**: 7104-7109.

Langworthy, T.A., Pond, J.L. (1986) Archaebacterial etherlipids and chemotaxonomy. *Syst Appl Microbiol* **7**: 253-257.

Larkin, J., Aharon, P., Henk, M.C. (1994) Beggioatoa in microbial mats at hydrocarbon vents in the Gulf of Mexic and warm mineral springs, Florida. *Geo-Mar Lett* **14**:97-103.

Lechevalier, H., Lechevalier, M.P. (1988) *Chemotaxonomic use of lipids – an overview*. In: Ratledge, S.G., Wilkinson (eds), Microbial Lipids 1, p 369-902. Academic Press, London.

Leahy, J.G., Colwell, R.R. (1990) Microbial degradation of hydrocarbons in the environment. *Microbiol Mol Biol Rev* **54**: 305-315.

Levin, L.A. (2005) Ecology of cold seep sediments: interactions of fauna with flow, chemistry and microbes. *Oceanogr Mar Biol: Anu Rev* **43**: 1-46.

Lewis, B.L., Landing, W.M. (1991) The biogeochemistry of manganese and iron in the Black Sea. *Deep-Sea Res A* **38**: 773-803.

Lipp, J.S., Morono, Y., Inagaki, F., Hinrichs, K.-U. (2008) Significant contribution of Archaea to extant biomass in marine subsurface sediments. *Nature* **454**: 991-994.

Lipp, J.S., Hinrichs K.-U. (2009) Structural diversity and fate of intact polar lipids in marine sediments. *Geochim Cosmochim Acta* DOI:10.1016/j.gca.2009.08.003.

Lloyd, K.G., Lapham, L., Teske, A. (2006) An anaerobic methane-oxidizing community of ANME-1b Archaea in Hypersaline Gulf of Mexico sediments. *Appl Environ Microbiol* **72**: 7218-7230.

Lösekann, T., Knittel, K., Nadalig, T., Fuchs, B., Niemann, H., Boetius, A., Amann, R. (2007) Diversity and abundance of aerobic and anaerobic methane oxidizers at the Haakon Mosby Mud Volcano, Barents Sea. *Appl Environm Microbiol* **73:** 3348–3362.

Londry, K.L., Jahnke, L.L., Des Marais, D.J. (2004) Stable carbon isotope ratios of lipid biomarker of sulfate-reducing bacteria. *Appl Environm Microbiol* **70**: 745-751.

Londry, K.L., Dawson, K.G., Grover, H.D., Summons, R.E., Bradley, A.S. (2008) Stable carbon isotope fractionation between substrates and products of *Methanosarcina barkeri* **39**: 608-621.

López-Lara, I.M., Sohlenkamp, C., Geiger, O. (2003) Membrane lipids in plant-associated bacteria: Their biosyntheses and possible functions. *Mol Plant Microbe Int* 16: 567-579.

MacAvoy, S.E., Macko, S.A., Joye, S.B. (2002) Fatty acid carbon isotope signatures in chemosynthetic mussels and tube worms from Gulf of Mexico hydrocarbon seep communities. *Chem Geol* **185**: 1-8.

MacDonald, K.C. (1982) Mid-ocean ridges: fine scale tectonic, volcanic and hydrothermal processes within the plate boundary zone. *Ann Rev Earth Planet Sci* **10**: 155-190.

MacDonald, I.R., Reilly, J.F. II, Guinasso, N.L. Jr., Brooks, J.M., Carney, R.S., Bryant, W.A., Bright, T.J. (1990a) Chemosynthetic mussels at a brine-filled pockmark in the northern Gulf of Mexico. *Science* **238**: 1096-1099.

MacDonald, I.R., Guinasso, N.L., Reilly, J.F., Brooks, J.M., Callender, W.R., Gabrielle, S.G. (1990b) Gulf of Mexico hydrocarbon seep-communities: VI. Species composition and habitat characteristics. *Geo-Mar Lett* **10**: 244-252.

MacDonald, I.R., Bohrmann, G., Escobar, E., Abegg, F., Blanchon, P., Blinova, V., Brückmann, W., Drews, M., Eisenhauer, A., Han, X., Heeschen, K., Meier, F., Mortera, C., Nähr, T., Orcutt, B., Bernard, B., Brooks, J., de Faragó, M. (2004) Asphalt volcanism and chemosynthetic life in the Campeche Knolls, Gulf of Mexico. *Science* **304**: 999-1002.

Makula, R.A., Finnerty, W.R. (1974) Phospholipid composition of *Desulfovibrio* species. *J Bacteriol* **120**: 1279-1283.

Makula, R.A., Finnerty, W.R. (1975) Isolation and characterization of an ornithine-containing lipid from *Desulfovibrio gigas*. *J Bacteriol* **123**: 523-529.

Makula, R.A. (1978) Phospholipid composition of methane-utilizing bacteria. *J Bacteriol* **143**: 771-777.

Männistö, M.K., Puhakka, J.A. (2001) Temperature- and growth-phase regulated changes in lipid fatty acid structures of psychrotolerant groundwater proteobacteria. *Arch Microbiol* **177**: 41-46.

Manske, A.K., Glaeser, J., Kuypers, M.M., Overmann, J. (2005) Physiology and phylogeny of green sulfur bacteria forming a monospecific phototrophic assemblage at a depth of 100 meters in the Black Sea. *Appl Environ Microbiol* **71**: 8049-8060.

Martens, C.S., Berner, R.A. (1974) Methane production in the interstitial waters of sulfate-depleted marine sediments. *Nature* **185**: 1167-1169

Martin, W., Baross, J., Kelley, D., Russell, M.J. (2008) Hydrothermal vents and the origin of life. *Nat Rev Microbiol* **6**: 805-814.

Michaelis, W., Seifert, R., Nauhaus, K., Treude, T., Thiel, V., Blumenberg, M., Knittel, K., Gieseke, A., Peterknecht, K., Pape, T., Boetius, A., Amann, R., Jørgensen, B.B., Widdel, F., Peckmann, J., Pimenov, N.V., Gulin, M.B. (2002) Microbial reefs in the Black Sea fueled by anaerobic oxidation of methane. *Science* **297:** 1013–1015.

Milkov, A.V., Sassen, R. (2001) Estimate of gas hydrate resource, northwestern Gulf of Mexico continental slope. *Mar Geol* **179**: 71-83.

Milkov, A.V. (2004) Global estimates of hydrate-bond gas in marine sediments: how much is really out there? *Earth-Sci Rev* **66**: 183-197.

Mills, H.J., Hodges, C., Wilson, K., MacDonald, I.R., Sobecky, P.A. (2003) Microbial diversity in sediments associated with surface-breaching gas hydrate mounds in the Gulf of Mexico. *FEMS Microbiol Ecol* **46**: 39-52.

Mills, C.T., Dias, R.F., Graham, D., Mandernack, K.W. (2006) Determination of phospholipid fatty acid structures and stable carbon isotope compositions of deep-sea sediments of the Northwest Pacific, ODP site 1179. *Mar Chem* **98**: 197-209.

Munoz, D., Guilliano, M., Doumenq, P., Jacquot, F., Scherrer, P., Mille, G. (1997a) Long term evolution of petroleum biomarkers in mangrove soil (Guadeloupe). *Mar Poll Bull* **34**: 868-874.

Munoz, D., Doumenq, P., Guiliano, M., Jacquot, F., Scherrer, P., Mille, G. (1997b) New approach to study spilled oils using high resolution GC-MS (SIM) and metastable reaction monitoring GC-MS-MS. *Talanta* **45**: 1-12.

Murray, J.W., Jannasch, H.W., Honjo, S., Anderson, R.F., Reeburgh, W.S., Top, Z., Friedrich, G.E., Codispoti, L.A., Izdar, E. (1989) Unexpected changes in the oxic/anoxic interface in the Black Sea. *Nature* **338**: 411-413.

Murray, J.W., Codispoti, L.,A., Friedrich, G.E. (1995) Oxidation-reduction environments: the suboxic zone in the Black Sea. In Aquatic chemistry: Interfacial and interspecies processes ACS Advances in Chemistry Series. Vol 244. Oxford University Press, New York, NY, pp. 157-176.

Musat, F., Galushko, A., Jacob, J., Widdel, F., Kube, M., Reinhardt, R., Wilkes, H., Schink, B., Rabus, R. (2009) Anaerobic degradation of naphthalene and 2-methylnaphthalene by strains of marine sulfate-reducing bacteria. *Environ Microbiol* **11**: 209-219.

Nähr, T.H., Birgel, D., Bohrmann, G., MacDonald, I.R., Kasten, S. (2009) Biogeochemical controls on authigenic carbonate formation at the Chapopote "asphalt volcano", Bay of Campeche. *Chem Geol* **266**: 399-411.

Nauhaus, K., Boetius, A., Krüger, M., Widdel, F. (2002) In vitro demonstration of anaerobic oxidation of methane coupled to sulphate reduction in sediments from a marine gas hydrate area. *Environ Microbiol* **4**: 296-305.

Nelson, R.K., Kile, B.M., Plata, D.L., Sylva, S.P., Xu, L., Reddy, C.M., Gaines, R.B., Frysinger, G.S., Reichenbach, S.E. (2006) Tracking the weathering of an oil spill with comprehensive two-dimensional gas chromatography. *Environ Forensics* **7**: 33-44.

Nichols, D.S., Nichols, P.D., Russel, N.J., Davies, N.W. McMeekin, T.A. (1997) Polyunsaturated fatty acids in the psychrophilic bacterium *Shewanella gelidimarina* ACAM 456^{T}: molecular species analysis of major phospholipids and biosynthesis of eicosapentaenoic acid. *Biochim Biophys Acta* **1347**: 164-176.

Niemann, H., Lösekann, T., De Beer, D., Elvert, M., Nadalig, T., Knittel, K., Amann, R., Sauter, E.J., Schlüter, M., Klages, M., Foucher, J.P., Boetius, A. (2006) Novel microbial communities of the Haakon Mosby mud volcano and their role as a methane sink. *Nature* **443**: 854-858.

Niemann, H., Elvert, M. (2008) Diagnostic lipid biomarker and stable carbon isotope signatures of microbial communities mediating the anaerobic oxidation of methane with sulphate. *Org Geochem* **39**: 1668-1677.

Nikolopoulou, M., Pasadakis, N., Kalogerakis, N. (2007) Enhanced bioremediation of crude oil utilizing lipophilic fertilizers. *Desalination* **211**: 286-295.

Oberbremer, A., Müller-Hurtig, R., Wagner, F. (1990) Effect of the addition of microbial surfactants on hydrocarbon degradation in a soil population in a stirred reactor. *Appl Microbiol Biotechnol* **32**: 485-489.

Oguz, T., Ducklow, H.W., Malanotte.Rizzoli, P., Murray J.W., Shushkina, E.A., Vedernikov, V.I., Unluata, U. (1999) A physical-biochemical model of plankton productivity and nitrogen cycling in the Black Sea. *Deep-Sea Res I* **46**: 597-636.

Oguz, T., Ducklow, H.W., Malanotte-Rizzoli, P. (2000) Modeling distinct vertical biogeochemical structure of the Black Sea: dynamical coupling of the oxci, suboxic, and anoxic layers. *Global Biogeochem Cycles* **14**: 1331-1352.

Olsen, I., Jantzen, E. (2001) Sphingolipids in bacteria and fungi. *Anaerobe* **7**: 103-112.

Omoregie, E. O., Mastalerz ,V., de Lange, G., Straub, K. L., Kappler, A., Røy, H., Stadnitskaia, A., Foucher, J. P., Boetius, A. (2008) Biogeochemistry and community composition of iron- and sulfur-precipitating microbial mats at the Chefren Mud Volcano (Nile Deep Sea Fan, Eastern Mediterranean), *Appl Environ Microbiol* **74**: 3198–3215.

Orcutt, B.N., Boetius, A., Lugo, S.K., MacDonald, I.R., Samarkin, V.A., Joye, S.B. (2004) Life at the edge of methane ice: microbial cycling of carbon and sulfur in Gulf of Mexico gas hydrates. *Chem Geol* **205**: 239-251.

Orcutt, B., Boetius, A., Elvert, M., Samarkin, V., Joye, S.B. (2005) Molecular biogeochemistry of sulfate reduction, methanogenesis and the anaerobic oxidation of methane at Gulf of Mexico cold seeps. *Geochim Cosmochim Acta* **69**: 4267-4281.

Orcutt, B., Samarking, V., Boetius, A., Joye, S. (2008) On the relationship between methane production and oxidation by anaerobic methanotrophic communities from cold seeps of the Gulf of Mexico. *Environ Microbiol* **10**: 1108-1117.

Orphan, V.J., House, C., Hinrichs, K.-U., McKeegan, K.D., DeLong, E.F. (2001) Methane-consuming archaea revealed by directly coupling isotopic and phylogenetic analysis. *Science* **293**: 484-487.

Orphan, V.J., House, C., Hinrichs, K.-U., McKeegan, K.D., DeLong, E.F. (2002) Multiple archaeal groups mediate methane oxidation in anoxic cold seep sediments. *Proc Natl Acad Sci USA* **99**: 7663-7668.

Ourisson, G., Rohmer, M., Poralla, K. (1987) Prokaryotic hopanoids and other polyterpenoid sterol surrogates. *Ann Rev Microbiol* **41**: 301-333.

Parkes, R.J., Cragg, B.A., Wellsbury, P. (2000) Recent studies on bacterial populations and processes in subseafloor sediments: A review. *Hydrogeol J*. **8**: 11–28.

Paull, C.K., Hecker, B., Commeau, R., Freedman-Lynde R.P., Neumann, C., Corso, W.P., Golubic, S., Hook, J.E., Sikes, E., Curray, J. (1984) Biological communities at the Florida Escarpment resemble hydrothermal vent taxa. *Science* **226**: 965-967.

Peckmann, J., Thiel, V., Michaelis, W., Clari, P., Gaillard, C., Martire, L., Reitner, J. (1999) Cold seep deposits of Beauvoisin (Oxfordian; southeastern France) and Marmorito (Miocene; northern Italy): microbially induced authigenic carbonates. *Int J Earth Sci* **88**: 60-75.

Peters, K.E., Moldowan, J.M. (1993) *The Biomarker Guide*. Prentice Hall, New York, 1993.

Peacock, E.E., Hampson, G.R., Nelson, R.K., Xu, L., Frysinger, G.S:, Gaines, R.B., Farrington, J.W., Tripp, B.W., Reddy, C.M. (2007) The 1974 spill of the *Bouchard 65* oil barge: Petroleum hydrocarbons persist in Windsor Cove salt marsh sediments. *Mar Pollut Bull* **54**: 214-225.

Reddy, C.M., Eglinton, T.I., Hounshell, A., White, H.K., Xu, L., Gaines, R.B., Frysinger, G.S. (2002) The West Falmouth Oil spill after thirty years: The persistence of petroleum hydrocarbons in marsh sediments. *Environ Sci Technol* **36**: 4754-4760.

Reeburgh, W.S. (1976) Methane consumption in Cariaco Trench waters and sediments. *Earth Planet Sci Lett* **28:** 337–344.

Reeburgh, W.S. (2007) Oceanic methane biogeochemistry. *Chem Rev* **107**: 486-513.

Reed, D.R., Kass, S.R. (2000) Experimental determination of the α and β C-H bond dissociation energies in naphthalene. *J Mass Spectrom* **35**: 534-539.

Reisfeld, A., Rosenberg, E., Gutnick, D. (1972) Microbial degradation of crude oil: factors affecting the dispersion in sea water by mixed and pure cultures. *Appl Microbiol* **24**: 363-368.

Repeta, D.J., Simpson, D.J. (1991) The distribution and recycling of chlorophyll, bacteriochlorophyll and carotenoids in the Black Sea. *Deep Sea Res A* **38**: 969-984.

Repeta, D.J. (1993) A high resolution historical record of Holocene anoxygenic primary production in the Black Sea. *Geochim Cosmochim Acta* **57**: 4337-4342.

Roberts, H.H., Carney, R.S. (1997) Evidence of episodic fluid, gas, and sediment venting on the northern Gulf of Mexico continental slope. *Econ Geol* **92**: 863–879.

Rohmer, M., Bouvier-Nave, P., Ourisson, G. (1984) Distribution of hopanoid triterpenes in prokaryotes. *J Gen Microbiol* **130**: 1137-1150.

Rohmer, M. (1993) The biosynthesis of triterpenoids of the hopane series in the Eubacteria: A mine of new enzyme reactions. *Pure Appl Chem* **65**: 1293-1298.

Rossel, P.E., Lipp, J.S., Fredricks, H.F., Arnds, J., Boetius, A., Elvert, M., Hinrichs, K.-U. (2008) Intact polar lipids of anaerobic methanotrophic archaea and associated bacteria. *Org Geochem*. **39**: 992-999.

Russell, N.J., Evans, R.I., ter Steeg, P.F., Hellemons, J., Verheul, A., Abee, T. (1995) Membranes as a target for stress adaptation. *Int J Food Microbiol* **28**: 255-261.

Rütters, H., Sass, H., Cypionka, H., Rullkötter, J. (2001) Monoalkylether phospholipids in the sulfate-reducing bacteria *Desulfosarcina variabilis* and *Desulforhabdus amnigenus*. *Arch Microbiol* **176**: 435-442.

Rütters, H., Sass, H., Cypionka, H., Rullkötter, J. (2002) Phospholipid analysis as a tool to study complex microbial communities in marine sediments. *J Microbiol Meth* **48**: 149-160.

Ryan, W.B.F., Pitman, W.C., III, Major, C.O., Shimkus, K., Moskalenko, V., Jones, J.A., Diomitrov, P., Gorur, N., Sakine, M., Yuce, H. (1997) An abrupt drowning of the Black Sea shelf. *Mar Geol* **138**: 119-126**.**

Safinowski, M., Meckenstock, R.U. (2006) Methylation is the initial reaction in anaerobic naphthalene degradation by a sulfate-reducing enrichment culture. *Environ Microbiol* **8**: 347-352.

Safinowski, M., Griebler, C., Meckenstock, R.U. (2006) Anaerobic cometabolic transformation of polycyclic and heterocyclic aromatic hydrocarbons: evidence from laboratory and field studies. *Environ Sci Technol* **40**: 4165-4173.

Sakurai, I., Hagio, M., Gombos, Z., Tyystjärvi, T., Paakarinen, V., Aro, E.-M., Wada, H. (2003) Requirement of phosphatidylglycerol for maintenance of photosynthetic machinery. *Plant Physiol* **133**: 1376-1384.

Sassen, R., Joye, S., Sweet, S.T., DeFreitas, D.A., Milkov, A.V., MacDonald, I.R. (1999) Thermogenic gas-hydrates and hydrocarbon gases in complex chemosynthetic communities, Gulf of Mexico, continental slope. *Org Geochem* **30**: 485-497.

Sassen, R., Roberts, H.H., Aharon, P., Carnay, R., Milkov, A.V., DeFreitas, D.A., Lanoil, B., Zhang, C. (2004) Free hydrocarbon gas, gas hydrate, and authigenic minerals in chemosynthetic communities of the northern Gulf of Mexico continental slope: relation to microbial processes. *Chem Geol* **205**: 195-217.

Sato, N. (1992) Betaine lipids. *Bot Mag* **105**: 185-197.

Sato, N., Hagio, M., Wada, H., Tsuzuki, M. (2000) Requirement of phosphatidylglycerol for photosynthetic function of thylakoid membranes. *Proc Natl Aca Sci USA* **97**: 10655-10660.

Schippers A., Neretin, L.N., Lavik, G., Leipe, T., Pollehne, F. (2005) Manganese(II) oxidation driven by lateral oxygen intrusions in the western Black Sea. *Geochim Cosmochim Acta* **69**: 2241-2252.

Schouten, S., Bowman, J.P., Rijpstra, W.I.C., Sinninghe-Damsté, J.S. (2000) Sterols in a psychrophilic methanotroph, *Methylosphaera hansonii*. **186**: 193-195.

Schouten, S., Hopmans, E.C., Baas, M., Boumann, H., Standfest, S., Könneke, M., Stahl, D.A., Sinninghe Damsté, J.S. (2008) Intact membrane lipids of *Candidatus Nitrosopumilus maritimus*, a cultivated representative of the cosmopolitan mesophilic Group I Crenarchaeota. *Appl Environ Microbiol* **74**: 2433-2440.

Schubert, C.J., Durisch-Kaiser, E., Klauser L., Vazquez, F., Wehrli, B., Holzner, Kipfer, R., Schmale, O., Greinert, J., Kuypers, M.M. (2006a) Recent studies on sources and sinks of methane in the Black Sea. In: L.N. Neretin (ed) Past and Present Water column anoxia. 2006, Springer, The Netherlands, p. 419-441.

Schubert, C.J., Coolen, M.J.L., Neretin, L.N., Schippers, A., Abbas, B., Durisch-Kaiser, E., Wehrli, B., Hopmans, E.C., Sinninghe Damsté, J.S., Wakeham, S.G., Kuypers, M.M.M. (2006b) Aerobic and anaerobic methanotrophs in the Black Sea water column. *Environ Microbiol* **8**: 1844-1856.

Seidel, M. (2009) Intakte polare Membranlipide als Biomarker zur Charakterisierung mikrobieller Lebensgemeinschaften in Wattsedimenten. *PhD thesis*, University of Oldenburg, Germany.

Sibuet, M., Olu, K. (1998) Biogeography, biodiversity and fluid dependence of deep-sea cold-seep communities at active and passive margins. *Deep Sea Res II* **45**: 517-567.

Siegenthaler, P.-A. (1998) Molecular organization of acyl lipids in photosynthetic membranes of higher plants. In Lipids in photosynthesis. Siegenthaler P.-A., Murata, N. (eds). Kluwer Academic Publishers, Dordrecht, The Netherlands, pp 199-144.

Sinninghe Damsté, J.S., Schouten, S., Hopmans, E.C., van Duin, A.C.T., and Geenevasen, A.J. (2002) Crenarchaeol: the characteristic core glycerol dibiphytanyl glycerol tetraether membrane lipid of cosmopolitan pelagic crenarchaeota. *J Lipid Res* **43**: 1641–16451.

Slater, C., Preston, T., Weaver, L.T. (2001) Stable isotopes and the international system of units. *Rapid Comm Mass Spectrom* **15**: 1270-1273.

Sloan , E.D. (1991) Natural gas hydrates. *J Petrol Technol* **43**: 1414-1417.

Solomon, E.A., Kastner, M., MacDonald, I.R., Leifer, I. (2009) Considerable methane flux to the atmosphere from hydrocarbon seeps in the Gulf of Mexico. *Nat Geosci* **2**: 561-565.

Sorokin, Y.I., Sorokin, P.Y., Audeev, D.Y., Sorokin, D.Y., Ilchenko, S.V. (1995) Biomass, production and activity of bacteria in the Black Sea with special reference to chemosynthesis and the sulfur cycle. *Hydrobiologia* **308**: 61-76.

Sorokin, Y.I. (2002) The Black Sea, ecology and oceanography. Leiden, Backhuys Publishers.

Stadnitskaia, A., Bouloubassi, I., Elvert, M., Hinrichs, K.-U., Sinninghe Damsté, J.S. (2008) Extended hydroxyarchaeol, a novel lipid biomarker for anaerobic methanotrophy in cold seepage habitats. *Org Geochem* **39**: 1007-1014.

Stetter, K.O. (2006) Hyperthermophilic prokaryotes. *FEMS Microbiol Rev* **18**: 149-158.

Sturt, H.F., Summons, R.E., Smith, K., Elvert, M., Hinrichs, K.U. (2004) Intact polar membrane lipids in prokaryotes and sediments deciphered by high-performance liquid chromatography/electrospray ionization multistage mass spectrometry – new biomarkers for biogeochemistry and microbial ecology. *Rap Comm Mass Spec* **18**: 617-628.

Suess, E., Torres, M.E., Bohrmann, G., Collier, R.W., Greinert, J., Linke, P., Rehder, G., Trehu, A., Wallmann, K., Winckler, G., Zuleger, E. (1999) Gas hydrate destabilization: enhanced dewatering, benthic material turnover and large methane plumes at the Cascadia convergent margin. *Earth Planet Sci* **170**: 1-15.

Suflita, J.M., Davidova, I.A., Gieg, I.M., Nanny, M., Prince, R.C. (2004) Anaerobic hydrocarbon biodegradation and the prospects for microbial enhanced energy production. In: R. Vazquez-Duhalt, R. Quintero-Ramirez (eds) Studies in Surface Science and Catalysis. 2004, p. 283-304.

Summit, M., Peacock, A., Ringelberg, D., White, D.C., Baross, J.A. (2000) Phospholipid Fatty Acid-derived Microbial Biomass and Community Dynamics in hot, hydrothermally influenced Sediments from the Middle Valley, Juan de Fuca Ridge. Proc ODP Sci Res **169**.

Taylor, J., Parkes, R.J. (1983) The cellular fatty acids of the sulphate-reducing bacteria, *Desulfobacter* sp., *Desulfobulbus* sp. and *Desulfovibrio desulfuricans*. *J Gen Microbiol* **129**: 3303-3309.

Tebo, B.M. (1991) Manganese(II) oxidation in the suboxic zone of the Black Sea. *Deep Sea Res A* **38**: 883-905.

Teske, A., Sørensen, K.B. (2008) Uncultured archaea in deep marine subsurface sediments: have we caught them all? *The ISME J* **2**: 3-18.

Thauer, R.K. (1988) Citric-acid cycle, 50 years on. Modifications and alternative pathway in anaerobic bacteria. *Eur. J. Biochem* **176**: 497-508.

Thiel, V. Peckmann, J., Seifert, R., Wehrung, P., Reitner, J., Michaelis, W. (1999) Highly isotopically depleted isoprenoids: molecular markers for ancient methane venting. *Geochim Cosmochim Acta* **63**: 3959-3966.

Tissot, B.P., Welte, D.H. (1984) Petroleum Formation and Occurrence. Springer Verlag Berlin Heidelberg.

Treude, T., Orphan, V., Knittel, K., Gieseke, A., House, C. and Boetius, A. Consumption of methane and CO2 by methanotrophic microbial mats from gas seeps of the anoxic Black Sea- *Appl Environ Microbiol* **73**: 2271-2283.

Tunnicliffe, University of Victoria: http://www.dfo-mpo.gc.ca/media/infocus-alaune/2003/endeavour/photo-eng.htm

Tuttel, J.H., Jannasch, H.W. (1973) Sulfide and thiosulfate-oxidizing bacteria in anoxic marine basins. *Mar Biol* **20**: 64-70.

Ueki, A., Suto, T. (1979) Cellular fatty acid composition of sulfate-reducing bacteria. *J Gen Appl Microbiol* **25**: 185-196.

Valentine, R.C., Valentine, D.L. (2004) Omega-3 fatty acids in cellular membranes: a unified concept. *Prog Lipi Res* **43**: 383-402.

Van Dover, C.L., German, C.R., Speer, K.G., Parson, L.M., Vrijenhoek, R.C. (2002) Evolution and biogeography of deep-sea vent and seep invertebrates. *Science* **295**: 1253-1257.

Van Mooy, B.AS., Rocap, G., Fredricks, H.F., Evans, C.T., Devol., A.H. (2006) Sulfolipids dramatically decrease phosphorous demand by picocyanobacteria in oligotrophic marine environments. *Proc Nat Acad Sci USA* **103**: 8607-8612.

Van Mooy, B.A.S., Fredricks, H.F., Pedler, B.E., Dyhrman, S.T., Karl, D.M., Koblizek, M., Lomas, M.W., Mincer, T.J., Moore, L.R., Moutin, T., Rappé, M.S., Webb, E.A. (2009) Phytoplankton in the ocean use non-phosphorous lipids in response to phosphorus scarcity. *Nature* **458**: 69-72.

Vasheghani-Farahani, E., Mehrnia, M. (2000) Bio-physicochemical treatment of oil contaminated sea water. *J Petrol Sci Eng* **26**: 179-185.

Vine, F.J., Matthews, D.H. (1963) Magnetic anomalies over oceanic ridges. *Nature* **199**: 947-949.

Wackett, L.P. (2006) The metabolic pathways of biodegradation. *The Prokaryotes* **2**: 956-968.

Wada, H., Murata, N. (1998) Membrane Lipids in cyanobacteria. In: Lipids in photosynthesis: structure, function and genetics. Siegenthaler P., Murata N. (eds.) Kluwer Academic Publishers, pp. 65-81.

Wada, H., Murata, N. (2007) The essential role of phosphatidylglycerol in photosynthesis. *Photosynth Res* **92**: 205-215.

Wakeham, S.G., Lewis, C.M., Hopmans, E.C., Schouten, S., Sinninghe Damsté, J.S. (2003) Archaea mediate anaerobic oxidation of methane in deep euxinic waters of the Black Sea. *Geochim Cosmochim Acta* **67**: 1359-1374.

Wakeham, S.G., Amann, R., Freeman, K.H., Hopmans, E.C., Jørgensen, B.B., Putnam, I.F., Schouten, S., Sinninghe Damsté, J.S., Talbot, H.M., Woebken, D. (2007) Microbial ecology of the stratified water column of the Black Sea as revealed by a comprehensive biomarker study. *Org Geochem* **38**: 2070-2097.

Wang, Z., Fingas, M. (1995) Study of the effects of weathering on the chemical composition of a light crude oil using GC/MS GC/FID. *J Microcol Sep* **7**: 617-639.

Wang, Z., Fingas, M., Blenkinsopp, S., Sergy, G., Landriault, M., Sigouin, L., Foght, J., Semple, K., Westlake, D.W.S. (1998) Comparison of oil composition changes due to biodegradation and physical weathering in different oils. *J Chrom A* **809**: 89-107.

Wang, Z., Fingas, M., Page, D.S. (1999) Oil spill identification. *J Chrom A* **843**: 369-411.

Ward, B.B., Kilpatrick, K.A. (1991) In: Black Sea Oceanography, Iydar, E., Murray, J.W. (eds)., p. 111-124, Kluwer, Dordrecht, The Netherlands.

Wardlaw, G.D., Arey, J.S., Reddy, C.M., Nelson, R.K., Ventura, G.T., Valentine, D.L. (2008) Disentangling oil weathering at a marine seep using GCxGC: broad metabolic specificity accompanies subsurface petroleum biodegradation. *Environ Sci Technol* **42**: 7166-7173.

Wegener, A. (1929) *Die Entstehung der Kontinente und Ozeane*. Vieweg, Braunschweig, 1929.

Wegener, G., Niemann, H., Elvert, M., Hinrichs, K.-U., Boetius, A. (2008) Assimilation of methane and inorganic carbon by microbial communities mediating the anaerobic oxidation of methane. *Environ Microbiol* **10**: 2287-2298.

Weiss, R.F., Lonsdale, P., Lupton, J.E., Bainbridge, A.E., Craig, H. (1977) Hydrothermal plumes in the Galapagos Rift. *Nature* **267**: 600-603.

Widdel, F., Boetius, A., Rabus, R. (2006) Anaerobic biodegradation of hydrocarbons including methane. *The Prokaryotes* **2**: 1028-1049.

White, D.C., Davis, W.M., Nickels, J.S., King, J.D., Bobbie, R.J. (1979) Determination of the sedimentary microbial biomass by extractable lipid phosphate. *Oecologia* **40**: 51-62.

White, D. C., Ringelberg, D. B. (1998) *Signature lipid biomarker analysis*. In: Techniques in Microbial Ecology (eds. Burlage, B. S., Atlas, R., Stahl, D.), pp. 255-259 (Oxford University Press: New York).

Whiticar, M.J., Faber, E., Schoell, M. (1986) Biogenic methane formation in marine and freshwater environments: CO_2 reduction *vs.* acetate fermentation-Isotopic evidence. *Geochim Cosmochim Acta* **50**:693-709.

Whiticar, M.J., (1999) Carbon and hydrogen isotope systematics of bacterial formation and oxidation of methane. *Chem Geol* **161**: 291-314.

Wilson, R.D., Monaghan, P.H., Osanik, A., Price, L.C., Rogers, M.A. (1974) Natural marine oil seepage. *Science* **184**: 857-865.

Woese, C.R., Kandler, O., Wheelos, M.L. (1990) Towards a natural system of organisms: Proposal for the domains, Archaea, Bacteria and Eukarya. *Proc Natl Acad Sci USA* **87**: 4576-4569.

Wuebbles, D.J., Hayhoe, K. (2002) Atmospheric methane and global change. *Earth-Sci Rev* **57**: 177-210.

Xu, R., Obbard, J.P. (2004) Bioremediation and Biodegradation. *J Environ Qual* **33**, 861-867.

Yano, Y. Nakayama, A., Ishihara, K., Saito, H. (1998) Adaptive changes in membrane lipids of barophilic bacteria in response to changes in growth pressure. *Appl Environ Microbiol* **64**: 479-485.

Yu, B., Benning, C. (2003) Anionic lipids are required for chloroplast structure and function in *Arabidopsis*. *Plant J* **36**: 762-770.

Zengler, K., Richnow, H.H., Rosselló-Mora, Michaelis, W., Widdel, F. (1999) Methane formation from long-chain alkanes by anaerobic microorganisms. *Nature* **401**: 266-269.

Zhang, X., Young, L.Y. (1997) Carboxylation as an initial reaction in the anaerobic metabolism of naphthalene and phenantrene by sulfidogenic consortia. *Appl Environ Microbiol* **63**: 4759-4764.

Zhang, C.L., Li, Y., Wall, J.D., Larsen, L., Sassen, R., Huang, Y., Wang, J., Peacock, A., White, D.C., Horita, J., Cole, D.R. (2002) Lipid and carbon isotopic evidence of methane-oxidizing and sulfate-reducing bacteria in association with gas hydrates from the Gulf of Mexico. *Geology* **30**: 239-242.

Zhang, Y.-M., Rock , C.O. (2008) Membrane lipid homeostasis in bacteria. *Nat Rev Microbiol* **6**: 222-233.

Zink, K.-G., Wilkes, H., Disko, U., Elvert, M., Horsfield, B. (2003) Intact phospholipids-microbial „life markers” in marine deep subsurface sediments. *Org Geochem* **34**: 755-769.

Zon, E.Z., Rosenberg, E. (2002) Biosurfactants and oil bioremediation. *Curr Opin Biotechnol* **13**: 249-252.

Chapter II

Detection of microbial biomass by intact polar membrane lipid analysis in the water column and surface sediments of the Black Sea

Florence Schubotz[1*], Stuart G. Wakeham[2], Julius Sebastian Lipp[1],
Helen F. Fredricks[3†], and Kai-Uwe Hinrichs[1,3]

Published in *Environmental Microbiology*

vol. 11, no. 10, page 2720-2734, doi:10.1111/j.1462-2920.2009.01999.x

© Society for Applied Microbiology and Blackwell Publishing Ltd, Oct. 2009

* Corresponding author.
[1] *Department of Geosciences, University of Bremen, D-28359 Bremen, Germany*
[2] *Skidaway Institute of Oceanography, Savannah, GA 31411, USA*
[3] *Woods Hole Oceanographic Institution, Department of Geology and Geophysics, Woods Hole, MA 02543, USA*

[†] *Present address: Woods Hole Oceanographic Institution, Department of Marine Chemistry and Geochemistry*

Keywords
Chemocline, anoxic, glycolipids, phospholipids, betaine lipids, GDGT, sphingolipids, ornithine lipids, suspended particulate matter

PRINTED MANUSCRIPT

II.1. SUMMARY

The stratified water column of the Black Sea produces a vertical succession of redox zones, stimulating microbial activity at the interfaces. Our study of intact polar membrane lipids (IPL) in suspended particulate matter and sediments highlights their potential as biomarkers for assessing the taxonomic composition of live microbial biomass. Intact polar membrane lipids in oxic waters above the chemocline represent contributions of bacterial and eukaryotic photosynthetic algae, while anoxygenic phototrophic bacteria and sulfate-reducing bacteria comprise a substantial amount of microbial biomass in deeper suboxic and anoxic layers. Intact polar membrane lipids such as betaine lipids and glycosidic ceramides suggest unspecified anaerobic bacteria in the anoxic zone. Distributions of polar head groups and core lipids show planktonic archaea below the oxic zone, methanotrophic archaea are only a minor fraction of archaeal biomass in the anoxic zone, contrasting previous observations based on the apolar derivatives of archaeal lipids. Sediments contain algal and bacterial IPLs from the water column, but transport to the sediment is selective; bacterial and archaeal IPLs are also produced within the sediments. IPL distributions in the Black Sea are stratified in accordance with geochemical profiles and provide information on vertical successions of major microbial groups contributing to suspended biomass. This study vastly extends our knowledge of the distribution of complex microbial lipids in the ocean.

II.2. INTRODUCTION

The Black Sea is the largest anoxic basin on Earth and offers an excellent opportunity to study microbial community dynamics under oxic and anoxic conditions (Oguz *et al.*, 2000; Wakeham et al., 2007). Oxygen is quickly consumed by respiration in the upper 40 to 60 m of the water column, giving way to microbially mediated redox reactions in the suboxic zone where both O_2 and H_2S are barely detectable (Murray et al., 1995). Overlapping layers of sulfide- and thiosulfate-oxidation, nitrification and denitrification, Fe and Mn redox chemistry, aerobic methanotrophy and anoxygenic photosynthesis all co-occur at the redox interface (for a review see Wakeham et al., 2007). The ~30 m thick chemocline is stabilized by a permanent halocline and characterized by high microbial activity and biomass; here chemosynthetic new production may be equivalent to 10 to 32% of photoautotrophic production in surface waters (Karl and Knauer, 1991; Sorokin et al., 1995). Anoxic waters below the chemocline contain high amounts of sulfide, ammonium, and methane (Reeburgh et al., 1991). Microbial processes occurring in the anoxic zone are sulfate reduction (Albert et al., 1995) and anaerobic oxidation of methane (Reeburgh et al., 1991).

Gene-based fingerprinting techniques gave first insights into the taxonomic composition of relevant microorganisms throughout the water column and point to the contribution of diverse functional groups of archaea and bacteria to the microbial assemblage (Vetriani et al., 2003; Lin et al., 2006; Wakeham et al., 2007). In this study we apply a culture- and gene-independent approach for assaying the community composition using the taxonomic value encoded in intact polar membrane lipids (IPL), the building blocks of every cellular membrane. IPL analysis is considered to explicitly target viable organisms since the polar head groups hydrolyze quickly after cell death (White et al., 1979; Harvey et al., 1986). A wide array of different IPLs exists in nature. Most widespread are glycerolipids that are present in all domains of life (for a review see Christie, 2003). Sphingolipids comprise a second group and are commonly found in eukarya but only in a few bacteria (Olsen and Jantzen, 2001), whereas ornithine lipids are restricted to bacteria (López-Lara et al., 2003). Previous lipid biomarker investigations in the Black Sea mainly focused on the hydrolysable apolar derivatives of IPLs (for a review see Wakeham et al., 2007). By including the analysis of lipids in the intact form a more complete picture of microbial community composition can be gained (e.g., Sturt et al., 2004). Since this method is rather non-selective compared to gene-based methods, IPLs provide valuable information complementary to other culture-independent techniques (e.g., Biddle et al., 2006, Lipp et al., 2008). A powerful extension of this approach is isotopic analysis of IPLs as a means to constrain further metabolic details of the corresponding organisms (e.g., Biddle et al., 2006).

IPL analysis is a relatively new tool in microbial ecology yet has been successfully applied in several environments, including marine sediments (e.g., Rütters et al., 2002; Zink et al., 2003; Biddle et al., 2006; Lipp et al., 2008), microbial mats (Rossel et al., 2008), a meromictic lake (Ertefai et al., 2008), and surface waters of the ocean (Van Mooy et al., 2006). At this point the use of IPLs as taxonomic markers in natural settings is limited by the available information on IPL inventories in cultures. Therefore exploratory studies of IPLs in environments with well-defined chemical conditions and microbiological background data such as the Black Sea are valuable and will aid establishment of links to the source organisms. Here, we examine the distribution and significance of IPLs in the oxic and anoxic water column and surface sediments of the central Black Sea. We will discuss production, preservation and export into the sediment and evaluate application of IPLs as biomarkers for the qualitative and quantitative assessment of biomass composition in such ecosystems.

II.3. RESULTS AND DISCUSSION

II.3.1. Water column chemistry and quantitative distribution of IPLs

Water column chemistry of the investigated site in the central Black Sea is shown in Fig. II.1A and in more detail reported by Wakeham et al. (2007). Oxygen concentrations drop from ~300 µM to below 10 µM at ~60 meters below sea level (mbsl) as a consequence of aerobic respiration. A nitrate peak at ~60 mbsl (4 µM) resulting from organic matter degradation is surrounded by two nitrite peaks at ~42 mbsl and ~77 mbsl reflective of microbial nitrification and denitrification processes. Ammonia is first detectable (0.02 µM) at ~75 mbsl, and the first detection of sulfide (~0.3 µM) at ~94 mbsl is associated with a density of σ_θ=16.2, that marks the permanent halocline (Konovalov and Murray, 2001). Consequently, the suboxic zone is defined between ~60 and ~90 mbsl, spanning a depth of ~30 m. In the anoxic zone, hydrogen sulfide, ammonium, and methane concentrations increase to maximal values of

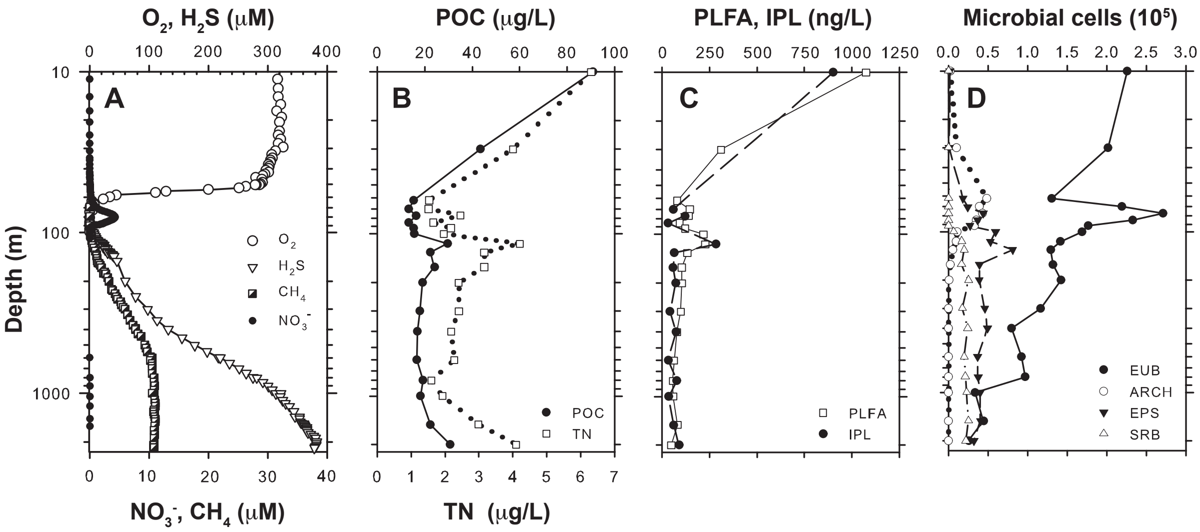

Fig. II.1. (**A**) Depth profile of oxygen, methane, hydrogen sulfide and nitrate concentrations at the study site in the central Black Sea (Station 5, R/V *Knorr* cruise 172/8, May 2005). The full data set of geochemical profiles was determined by J.W. Murray and G.W. Luther (available online at http://www.ocean.washington.edu/cruises/Knorr2003) and is re-plotted from Wakeham et al. (2007). **(B)** Distribution of POC and TN are reprinted from Wakeham et al. (2007). (**C**) Total PLFA depth profile and total estimated IPL depth profile of filtered biomass at Station 5. (**D**) Distributions (10^5 cells/mL) of eubacteria (EUB), archaea (ARCH), epsilonproteobacteria (EPS) and sulfate-reducing bacteria (SRB) are obtained by catalyzed reporter deposition-fluorescent in situ hybridization (CARD-FISH) and are replotted from Lin et al. (2006) and Wakeham et al. (2007). Probes used: bacteria (EUB338), archaea (CREN554+EURY806), epsilonproteobacteria (EPS549) and sulfate-reducing bacteria (DSS658).

~380 μM, ~100 μM, and ~15 μM in bottom waters, respectively. Intact polar membrane lipid and polar lipid-derived fatty acid (PLFA) concentration profiles track each other, suggesting that both represent identical pools of microbial biomass. The observed concentration differences between PLFAs and IPLs are not regarded as significant since the reported IPL concentrations are semi-quantitative and represent first-order estimates of the actual values (see experimental procedures). The concentration of archaeal IPLs, which do not contain fatty acids, are in such low amounts that overall they do not affect the correspondence between IPL and PLFA concentrations (Fig. II.2). Lipid concentrations (IPL and PLFA) track trends of particulate organic carbon (POC) and total nitrogen (TN), until 1000 mbsl (Fig. II.1B,C). The increase of POC and TN in the last 1000 m of the anoxic water column might be due to the presence of a bottom nepheloid layer. This increase in POC and TN is likely caused by re-suspension of sinking particles and is not reflected in the IPL and PLFA profile since these particles do not reflect live biomass. Concentrations of IPLs and PLFAs are, with values around 1 mg/L, highest in the oxygenated surface waters due to eukaryotic contributions, and decrease more than 10-fold by 62 mbsl as oxygen levels decrease. Cell counts by CARD-FISH of bacteria peak at 77 mbsl in the suboxic zone (Lin et al., 2006, Wakeham et al., 2007; Fig. II.1D), accompanied by an increase in IPL and PLFA concentrations. Pronounced peaks in lipid concentration at 115 mbsl are mirrored in peaks in POC and TN profiles, below the maximum of bacterial cell counts and possibly result from accumulation of organic matter at the density discontinuity at the top of the anoxic zone. IPL and PLFA concentrations remain constantly low at 50 ng/L and 100 ng/L, respectively, throughout the anoxic zone.

The vertical distribution and structural composition of individual IPLs are summarized in Table II.1 and Figs. II.2 and II.3. Representative chromatograms of IPLs for the different geochemical zones are visualized in density plots (Fig. II.4).

Three IPL compound classes, betaine lipids (BL), monoglycosyldiacylglycerols (Gly-DAG) and diacylglycerol phosphatidylglycerols (PG-DAG) are present as major IPLs at all depths. Other IPLs are restricted to specific depth intervals. Diglycosyldiacylglycerols (2Gly-DAG), sulfoquinovosyldiacylglycerols (SQ-DAG) and diacylglycerol phosphatidylcholines (PC-DAG) are only present in the oxygenated water column. Archaeal glycosidic glyceroldibiphytanyltetraethers (Gly-GDGTs) with one and two sugars as head groups (Gly-GDGT and 2Gly-GDGT) and an unknown head group (H341-GDGT) were only detected in the suboxic and anoxic zone. Diacylglycerol phosphatidyl-(N,N)-dimethylethanolamines (PDME) occur only in the oxic and upper suboxic zone, whereas diether and diacyl-based phosphatidylethanolamines (PE-DEG/-DAG) and phosphatidyl-(N)-methylethanolamines (PME-DEG/-DAG) and glycosidic ceramides are significant IPLs throughout the lower suboxic and anoxic zone. Minor contributions to the total IPL assemblage are composed by diphosphatidylglycerols (DPG) and glycosyl-deoxyglycosyl-diacylglycerol (Gly-dGly-DAG) which are restricted to the suboxic zone and ornithine lipids (OL) which are only observed in the anoxic zone. We note that the IPL approach as carried out here (Sturt et al., 2004) targets

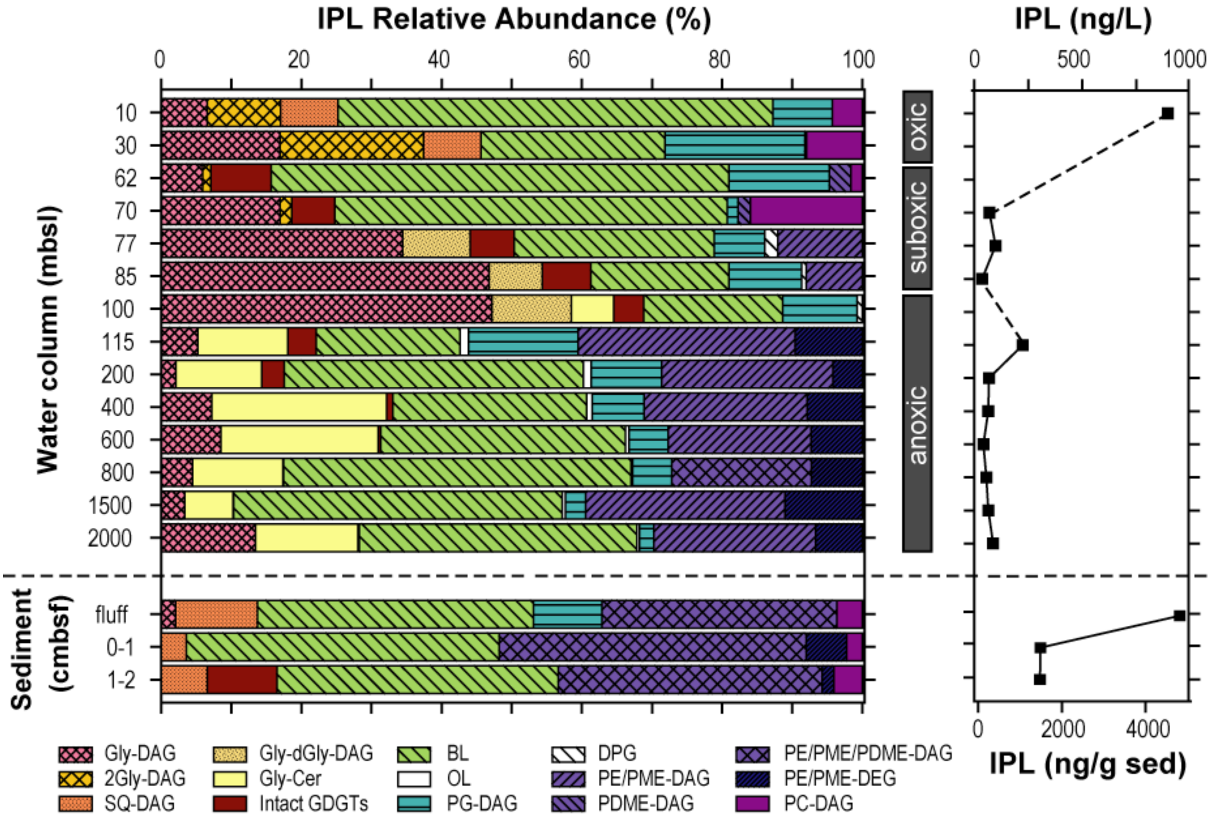

Fig. II.2. Relative distribution and estimated absolute abundance of IPLs in the water column and in surface sediments in the central Black Sea (station 5, R/V *Knorr* cruise 172/8). The same analytical response is assumed for individual IPL classes (analytical error see experimental procedures). For abbreviations of IPL compound classes see text and Fig. II.5. *At 2000 mbsl also PG-DEG was observed. **Admixtures of PE/PME/PDME-AEG could be present (see *Experimental procedures*).

at the comprehensive and nonselective detection of major compounds and will therefore provide a molecular view of the dominant organisms within the microbial community. Community members contributing less than 0.1% to the total community are unlikely to be registered unless very diagnostic lipids are present and targeted selectively. For instance, although small amounts of the apolar ladderane lipids of anammox bacteria are present in our samples (0.02-4.6 ng/L; Wakeham et al., 2007), we could not detect ladderane lipids in their intact form. Given results from a recent study in which ladderane IPL concentrations were between one and two orders of magnitude lower than those of their apolar derivatives (Jaeschke et al., 2009), ladderane IPLs are likely below our analytical level of detection and will therefore not be further discussed.

II.3.2. IPL classes present in the water column

II.3.2.1. Betaine lipids (BL)

BL are the most abundant IPLs in the upper water column, where they amount to 25% and 65% of total IPLs. Between 77 and 115 mbsl, BL decrease in relative abundance to ~20% of total IPLs, but remain an important IPL class in the anoxic part of the water column at 25 to 45% of total IPLs. BL are common constituents in lower plants and marine algae (Dembitsky, 1996; Kato et al., 1996). However, only limited information on the distribution of BL in environmental samples exists (e.g., Ertefai et al., 2008). BL in the oxic water column are probably derived from algal sources as diatoms, dinoflagellates, coccolithophores and green algae dominate the surface waters (Oguz and Merico, 2006).

The presence of BL throughout the water column (Fig. II.2) is not related to export of algal material from the photic zone as indicated by a distinct change of fatty acid composition in BL (Table II.1). In the oxic zone, the core structures of BL are dominated by combinations of $C_{14:0}$ and $C_{16:0}$ with $C_{16:1}$ and $C_{18:1}$ fatty acids, whereas in the suboxic zone combinations of mainly $C_{16:0}$ and $C_{16:1}$ fatty acids are observed. In the anoxic zone fatty acids with odd numbers of carbon atoms become dominant, e.g., $C_{15:0}$ and $C_{17:0}$ in combination with $C_{18:1}$. Betaine lipids have not been widely reported in bacteria, and to our knowledge they are only known in the purple non-sulfur bacteria *Rhodobacter sphaeroides* (Benning et al., 1995) and the plant-nodule forming *Sinorhizobium meliloti* (Geiger et al., 1999). Both species produce the betaine lipid diacylglyceryl-(N,N,N)-trimethylhomoserine (DGTS) *de-novo* when grown under phosphate limiting conditions. Genes coding for the enzymes involved in the biosynthesis of DGTS have to date only been detected in members of the alphaproteobacterial subdivision (López-Lara et al., 2003). In the suboxic and anoxic parts of the central Black Sea, alphaproteobacteria have been detected in small amounts with CARD-FISH (~5% of total DAPI-positive cells; Lin et al., 2006) and in bacterial clone libraries (Vetriani et al., 2003). Yet, the recent observation of BL in the sulfate-reducing firmicute *Desulfotomaculum putei* (K.-U. Hinrichs, H.F. Fredricks, J.F. Biddle, and C.H. House, unpubl. data) suggest that BL are more widely distributed in the bacterial domain. We therefore suggest that unknown anaerobic bacteria other than those belonging to alphaproteobacteria might also be the producers of betaine lipids in the anoxic zone.

Table II.1. Core lipid structures and likely origin of IPL compound classes in different redox zones in the water column and surface sediment of the central Black Sea.

Zonation	IPL compound class	Major core structure	Likely biological origin
Oxic (0-60 mbsl)	Gly-DAG, 2Gly-DAG, SQ-DAG, PG-DAG	14:0/16:0; 14:0/16:1; 14:0/18:1; 14:0/18:2; 16:0/16:1; 16:0/18:1; 16:1/16:1; 18:1/18:1	Eukaryotic algae[1,2] and cyanobacteria[2,3,4]
	PG-DAG, PDME-DAG, PC-DAG	14:0/14:0; 14:0/15:0; 14:0/16:0; 14:0/16:1; 14:0/18:1; 16:0/16:1; 16:0/18:1; 16:1/16:1; 18:1/18:1	Eukaryotic algae[1,2] and Bacteria[5], e.g., nitrifying[6] and heterotrophic[5] bacteria
	2Gly-DAG, SQ-DAG, PG-DAG	16:0/18:3; 16:0/18:4	Eukaryotic algae[1,2] and cyanobacteria[2,3,4]
	Gly-DAG, 2Gly-DAG	16:4/18:5; 18:4/18:5	
	PC -DAG	16:0/18:2; 16:0/18:5; 16:0/22:6; 18:0/20:5; 20:5/22.6; 22:6/22:6	Eukaryotic algae[1,2]
	BL	14:0/16:1; 14:0/18:1; 16:0/18:1; 16:0/16:1; 16:0/22:0	Eukaryotic algae[7,8]
Suboxic (60-90 mbsl)	Gly-DAG, 2Gly-DAG	14:0/16:1; 16:4/18:5; 18:4/18:5	Eukaryotic algae[1,2] and cyanobacteria[2,3,4]
	PC -DAG	16:0/20:5; 16:0/22:6; 18:1/22:6	Eukaryotic algae[1,2]
	BL	16:0/16:1; 16:1/16:1	Eukaryotic algae[7,8] and Bacteria (this study*)
	PG-DAG, PDME-DAG, PC-DAG	14:0/16:0; 14:0/16:1; 16:0/16:0; 16:0/16:1; 16:1/16:1	Bacteria[5], e.g., nitrifying[6] and heterotrophic[5] bacteria
	PE/PME-DAG, DPG	14:0/16:1; 15:0/15:1; 15:0/16:1; 16:0/16:1; 16:1/16:1	Bacteria[5], e.g., CH$_4$[9,10], Fe[11], S[12] oxidizing bacteria
	Gly-DAG, Gly-dGly-DAG, PG-DAG, DPG, *lyso*-DPG	16:0/16:1; 16:1/16:1	Bacteria[5], e.g., green sulfur bacteria[13]
	Gly-GDGT	GDGT-0; GDGT-5	Archaea, e.g., (nitrifying[14]) crenarchaea[15] and methanotrophic euryarchaea[16]
	2Gly-GDGT	GDGT-1; GDGT-2	
	H341-GDGT	GDGT-2; GDGT-3	
Anoxic (90-2200 mbsl)	PG-DAG, PE/PME-DAG	14:0/16:0; 14:0/16:1; 15:0/15:0; 15:0/15:1; 15:0/16:0; 15:0/16:1; 15:0/17:1; 15:0/17:0; 16:0/16:1	Bacteria[5], e.g., sulfate-reducing[17,18], and fermenting[5,19] bacteria
	PE/PME-DEG	o-15:0/o-16:0; o-16:0/o-16:0; o-16:0/o-16:1; o-16:0/o-17:0	Sulfate-reducing bacteria[17,18]
	OL	OH-17:0/15:0; OH-17:0/17:0	Bacteria[20], e.g., sulfate-reducing[21] bacteria
	BL	15:0/17:0; 15:0/18:1; 16:0/18:1; 17:0/18:1	Anaerobic bacteria (this study*)
	Gly-DAG	12:0/20:0; 13:0/18:0; 13:0/20:0; 14:0/17:0; 15:0/16:0; 15:0/17:0; 15:0/18:0	Anaerobic bacteria (this study*)
	Gly-Cer	d21:0/15:0; d21:0/16:0; d22:0/14:0; d22:0/16:0; d22:0/17:0; d23:0/16:0	Anaerobic bacteria (this study*)
	Gly-GDGT	GDGT-0; GDGT-5	Archaea, e.g., cren-[15] and methanotrophic euryarchaea[16]
	2Gly-GDGT	GDGT-1; GDGT-2	
	H341-GDGT	GDGT-2; GDGT-3	
Sediment	Gly-DAG, SQ-DAG	14:0/14:0; 14:0/16:0; 14:0/16:1	Plankton detritus and bacteria
(fluff-2 cmbsf)	BL	16:0/16:0; 16:0/18:1; 18:1/18:1	
	PC-DAG	30:1; 32:0; 33;0; 36:2	(this study*)
	PG-DAG	32:0; 32:1; 32:2; 33:1	
	PE-/PME-/PDME-DAG	15:0/17:1; 16:0/16:0; 16:0/16:1	Plankton detritus and bacteria[5], e.g., sulfate-reducing[17,18] bacteria
	PE-/PME-DEG	o-30:0	
	2Gly-GDGT	GDGT-1; GDGT-2	Archaea, e.g., crenarchaea and euryarchaea[22,23]
	H341-GDGT	GDGT-2; GDGT-3	

* For interpretation refer to the text of this study.

Core structures are depicted as combinations of fatty acids (e.g., 14:0/16:1) or sum of fatty acids (e.g., 30:1) ether-lipids (e.g., o-16:0), hydroxy-fatty acids (e.g., OH-17:0), dihydroxy base or sphinganine (e.g., d22:0) or GDGTs with different rings (e.g., GDGT-2). Main core structures are underlined. Selected references: (1) Harwood, 1998; (2) Brett and Müller-Navarra, 1997; (3) Wada and Murata, 1998; (4) Hölzl and Dörmann, 2007; (5) Goldfine, 1984; (6) Goldfine 1968; (7) Dembitsky, 1996; (8) Kato et al., 1996; (9) Makula, 1978; (10) Fang et al., 2000; (11) Barridge and Shively, 1968; (12) Short et al., 1969; (13) Imhoff and Bias-Imhoff, 1995; (14) Schouten et al., 2008; (15) Sinninghe Damsté et al., 2002; (16) Wakeham et al., 2003; (17) Rütters et al., 2001; (18) Sturt et al., 2004; (19) Siervo and Reynolds, 1975; (20) López-Lara et al., 2003; (21) Makula and Finnerty, 1975; (22) Biddle et al., 2006; (23) Lipp et al., 2008.

II.3.2.2. Monoglycosyldiacylglycerols (Gly-DAG)

Gly-DAG comprise 7 to 18% of total IPLs in the oxic part of the water column and increase in relative abundance in the lower suboxic and upper anoxic zone (77 to 100 mbsl) to almost 50% of total IPLs. Below 115 mbsl Gly-DAG comprise only a minor fraction (2 to 15%) of total IPLs. Gly-DAG is the most widespread glyceroglycolipid in nature and is typically found in all phototrophic membranes (Hölzl and Dörmann, 2007). Photosynthetic algae are probably its primary biological source in the oxygenated photic zone. This conclusion is supported by the main core structures of Gly-DAG, which consist of the major algal fatty acids (Table II.1). Additionally, Gly-DAG contain combinations of polyunsaturated fatty acids (PUFA) $C_{16:4}$ and $C_{18:4}$ that are a widespread in algae (Brett and Müller-Navarra, 1997), and $C_{18:5}$ which was identified as a characteristic marker for some dinoflagellates and coccolithophores (Okuyama et al., 1993). Cyanobacteria are an additional source for Gly-DAG in the oxic zone, as their membrane lipid distribution resembles that of eukaryotic algae (Wada and Murata, 1998). Indeed, cyanobacteria constitute a major fraction of the bacterioplankton in the surface waters of the Black Sea (Uysal, 2006). As for the BL, the dominance of Gly-DAG in the suboxic/upper anoxic parts of the water column (Fig. II.2) does not result from export of algal material from surface waters because the fatty acid composition of Gly-DAG is distinct to that in surface waters (Table II.1). $C_{14:0}$, $C_{18:1}$ fatty acids and PUFAs are barely detectable. Instead, mixtures of $C_{16:0}$ and $C_{16:1}$ become dominant. Anoxygenic phototrophic bacteria are likely responsible for the high relative abundance at the chemocline (Hölzl and Dörmann 2007). In particular, low-light adapted green sulfur bacteria have been observed in the lower suboxic/upper anoxic zone of the Black Sea (e.g., Repeta et al., 1989; Manske et al., 2005). Since green sulfur bacteria account for only up to 10% of total bacterial cells (Bird and Karl, 1991), other sources are likely contributing to the large Gly-DAG pool in the chemocline. Candidates include members of the gram-positive firmicutes and actinobacteria and some alphaproteobacteria (Hölzl and Dörmann, 2007). At 115 mbsl there is again a distinct change in the fatty acid composition of Gly-DAG, where its structural composition is dominated by combinations of long and short chain fatty acids, e.g., $C_{12:0}/C_{20:0}$, $C_{13:0}/C_{18:0}$, $C_{13:0}/C_{20:0}$ and combinations of fatty acids with odd numbers of carbon atoms, e.g., $C_{14:0}/C_{17:0}$, $C_{15:0}/C_{16:0}$, and $C_{15:0}/C_{17:0}$. Combinations of $C_{12:0}$, $C_{13:0}$ and $C_{20:0}$ fatty acids are peculiar and not commonly reported in bacteria, so the taxonomic relevance of these fatty acid combinations needs to be investigated in more detail in the future. As with the betaine lipids discussed above we suggest an uncultured anaerobic bacterial source for Gly-DAG in the anoxic zone.

II.3.2.3. Phosphatidylglycerols (PG)

PG with DAG as core lipids is the only phospholipid that is present throughout the water column. PG is, together with PE, the most widespread phospholipid class in eukarya and bacteria (Goldfine, 1984; Dowhan, 1997) and is present in all photosynthetic membranes (Wada and Murata et al., 2007). In surface waters and the suboxic zone, the fatty acid composition of

PG-DAG resembles that of BL and Gly-DAG (Table II.1), but contains fewer PUFAs than Gly-DAG. As for BL and Gly-DAG, the likely biological sources for PG-DAG in the oxic zone are algae and cyanobacteria. Non photosynthetic sources could contribute to PG-DAG in surface waters, for example heterotrophic bacteria such as members of alphaproteobacteria and cytophaga-flavobacteria, which were detected in the oxic waters (Lin et al., 2006). In the suboxic zone, a number of bacteria known to exist in the chemocline are all potential sources. PG-DAG are found in both aerobic and anaerobic sulfur bacteria, including green sulfur bacteria (Barridge and Shively, 1968; Imhoff and Bias-Imhoff, 1995), but also in nitrifying bacteria (Goldfine and Hagen, 1968), methanotrophic bacteria (Makula et al., 1978; Fang et al., 2000) and metal oxidizing bacteria (Short et al., 1969). The fatty acid distribution dominated by ubiquitous $C_{16:0}$ and $C_{16:1}$ does not further discriminate between potential sources. In the anoxic zone, combinations of fatty acids with odd and even carbon numbers dominate the core lipids; at 2000 mbsl also diether-based PG were observed. Plausible sources for PG in anoxic waters are sulfate-reducing bacteria (SRB) (Rütters et al., 2001, Sturt et al., 2004) or fermenting bacteria (Siervo and Reynolds, 1975).

II.3.2.4. Diglycosyldiacylglycerols (2Gly-DAG), sulfoquinovosyldiacylglycerols (SQ-DAG) and phosphatidylcholines (PC)

2Gly-DAG and SQ-DAG are main constituents of photosynthetic membranes (Siegenthaler, 1998), and were present only in the oxic and upper suboxic zones of the water column. PC plays an essential role in the lipid bilayer of the outer chloroplast envelope and is therefore found in almost all eukaryotic algae but is absent in cyanobacteria (Harwood, 1998; Wada and Murata, 1998). Similarities in core lipid structures of 2Gly-DAG, SQ-DAG, Gly-DAG, PG-DAG and BL in the oxic zone (Table II.1) imply common biological sources for these IPLs. PC-DAG is the only IPL containing the long-chain PUFAs $C_{20:5}$ and $C_{22:6}$ typically found in eukaryotic algae (Brett and Müller-Navarra, 1997). Vertically migrating phytoplankton species (Happey-Wood, 1976) may be responsible for PC-DAG and small amounts of 2Gly-DAG with similar core structures as in the oxic zone in the upper suboxic zone (at 62 and 70 mbsl). Nitrifying bacteria, significant mediators of nitrification in the suboxic zone of the Black Sea (Lam et al., 2007), are an additional source of PC-DAG, PG-DAG, as well as PE-DAG and PDME-DAG (see below) (Goldfine and Hagen, 1968).

II.3.2.5. Phosphatidylethanolamines (PE) and its methylated derivatives (PME, PDME)

A variety of PE derivatives were detected that signify a change in microbial community composition from the suboxic zone into the anoxic zone. Low levels of PDME-DAG of presumed bacterial origin occur in the upper suboxic zone (<5% of total IPLs) with a predominant compound being a diacyl $C_{16:1}/C_{16:1}$ derivative. Together with PC it is a major IPL in nitrifying bacteria (Goldfine and Hagen, 1968) but also present in some sulfide oxidizing (Barridge and Shively, 1968) and methanotrophic bacteria (Makula et al., 1978; Fang et al., 2000), all of which are potential sources given the biogeochemical conditions. Below 77 mbsl, after the

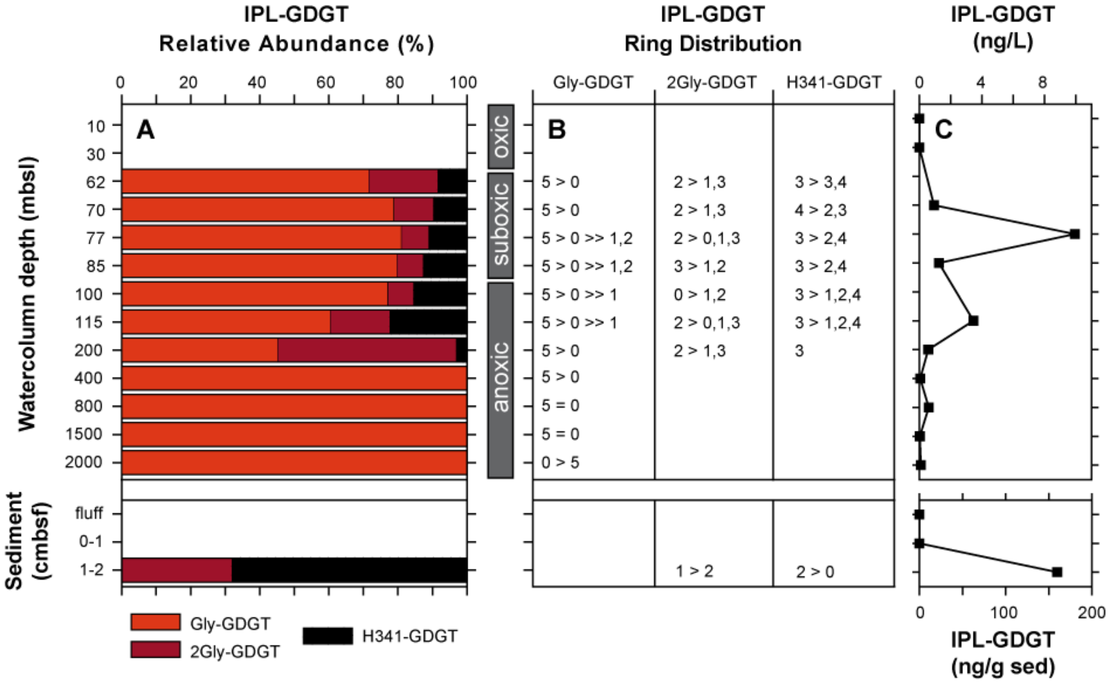

Fig. II.3. (**A**) Relative distribution, (**B**) number of rings in the GDGT core lipid and (**C**) estimated absolute abundance of IPL-GDGTs in the water column and in surface sediments of the central Black Sea (station 5, R/V *Knorr* cruise 172/8).

first detection of ammonia, PE and PME become the most abundant phospholipids along with PG whereas PDME and PC drop below the detection limit. At this depth, we expect to find microorganisms mediating processes such as anaerobic oxidation of sulfide coupled to both denitrification and anoxygenic photosynthesis (Jørgensen et al., 1991) and anammox (Kuypers et al., 2003). PE and PME are common phospholipids in sulfide oxidizers (Barridge and Shively, 1968) as well as metal oxidizing bacteria (Short, 1969) and methanotrophic bacteria (Makula et al., 1978; Fang et al., 2000). However, PE is not a common lipid class in green sulfur bacteria (Imhoff and Bias-Imhoff, 1995), which could explain its absence at 100 mbsl where these organisms are present (Manske et al., 2005). The core lipids of PE and PME in the suboxic zone are dominated by mixtures of saturated and monounsaturated fatty acids with odd and even carbon numbers, e.g., $C_{16:1}/C_{16:1}$, $C_{15:0}/C_{16:1}$ and $C_{16:0}/C_{16:1}$. PE and PME comprise 30 to 40% of total IPLs in the anoxic zone, a major fraction of which is present as ether lipids, i.e., of dietherglycerol (DEG) type (Figs. II.2, II.5). Related acylether glycerol (AEG) and DEG phospholipids are known from members of SRBs (Rütters et al., 2001; Sturt et al., 2004). Sulfate-reducing bacteria account for 8% of total DAPI-stained cells in the suboxic zone (Lin et al., 2006, Wakeham et al., 2007) and are probably the major source of PE and PME.

II.3.2.6. Diphosphatidylglycerols (DPG) and glycosyl-deoxyglycosyldiacylglycerols (Gly-dGly-DAG)

The occurrence of DPG, *lyso*-DPG, and the tentatively identified Gly-dGly-DAG in the lower suboxic/upper anoxic zone (above the particle maximum at 115 mbsl) distinctly coincides with maximal values of Gly-DAG, which also has a similar core lipid structure (Table II.1). As DPG is common in green sulfur bacteria (Imhoff and Bias-Imhoff, 1995) and glycolipids are typical constituents of phototrophic membranes, we assign the presence of these lipids at these depths to phototrophic bacteria. An additional potential source of DPG are methanotrophic bacteria (Makula, 1978), which are present in the lower suboxic/upper anoxic zone (Wakeham et al., 2007). Deoxyglyceroglycolipids have to our knowledge not been reported before in nature, but green sulfur bacteria contain a number of glycolipids, which still await structural elucidation (Imhoff and Bias-Imhoff, 1995).

II.3.2.7. Polar archaeal glyceroldibiphytanyltetraether (GDGT) derivatives

Polar archaeal GDGTs were detected, below 62 mbsl throughout the suboxic and anoxic zone and are present as mono- or diglycosidic species (Gly-GDGT and 2Gly-GDGT), combined with a previously detected IPL-GDGT species with unidentified head group of 341 Da (H341-GDGT) (Sturt et al., 2004; Biddle et al., 2006; Schouten et al., 2008). Gly-GDGTs are the most abundant archaeal IPLs, whereas 2Gly-GDGTs and H341-GDGTs comprise only 10 to 30% of total IPL-GDGTs (Fig. II.3). Below 200 mbsl 2Gly-GDGTs and H341-GDGTs are no longer detected. A peak concentration of total intact GDGTs occurs at 77 mbsl in the suboxic zone where they make up ~7% of total IPLs. They decrease to <1% of total IPLs below 800 mbsl. These relative proportions of archaeal IPLs to total IPLs closely matches archaeal vs. bacterial abundances determined independently in the central Black Sea by both FISH (Wakeham et al., 2007) and rDNA copy numbers (Schubert et al., 2006).

The ring distribution in core lipids distinguishes individual GDGT-IPLs. Gly-GDGTs contain predominantly acyclic GDGT-0 and pentacyclic GDGT-5, which has previously been identified as crenarchaeol by core lipid analysis (Wakeham et al., 2007). 2Gly-GDGT and H341-GDGT are comprised of core lipids with zero to four rings (GDGT-0 to GDGT-4), with GDGT-2 and GDGT-3 being dominant. Planktonic crenarchaeota were shown to be actively involved in the nitrogen cycle in the Black Sea (Coolen et al., 2007; Lam et al., 2007). Thecore lipid of crenarchaeol, putative biomarker of crenarchaeota (Sinninghe Damsté et al., 2002), has been found in high abundances in the suboxic zone of the Black Sea, agreeing with the presence of nitrifying archaea at these depths (Wakeham et al., 2003; 2007; Coolen et al., 2007). The first detection of intact GDGTs at 62 mbsl coincides with a peak in nitrate and maximal GDGT abundances at 77 mbsl coincide with the second nitrite peak (Fig. II.1). Crenarchaeota have been shown to outnumber euryarchaeota in the suboxic zone (Vetriani et al., 2003; Lin et al., 2006). The GDGT-IPL distribution is largely similar to that of *Nitrosopumilus maritimus* (Schouten et al., 2008), the only isolated representative of Marine Group I crenarchaeaota (Könnecke et al., 2005). The only exception is Gly-phosphate-GDGT, which is a significant constituent of *N. maritimus* but was not detected in our study.

In the deeper anoxic zone the presence of methane oxidizing archaea (ANME) was documented by gene-based studies (Vetriani et al., 2003) and isotopic analyses of archaeal membrane lipids (Wakeham et al., 2003). Schubert et al. (2006), however, showed that ANME account for only a tiny fraction of the total archaeal rDNA pool. The archaeal IPL distribution in deep anoxic waters is consistent with this finding. Neither archaeol-based IPL,

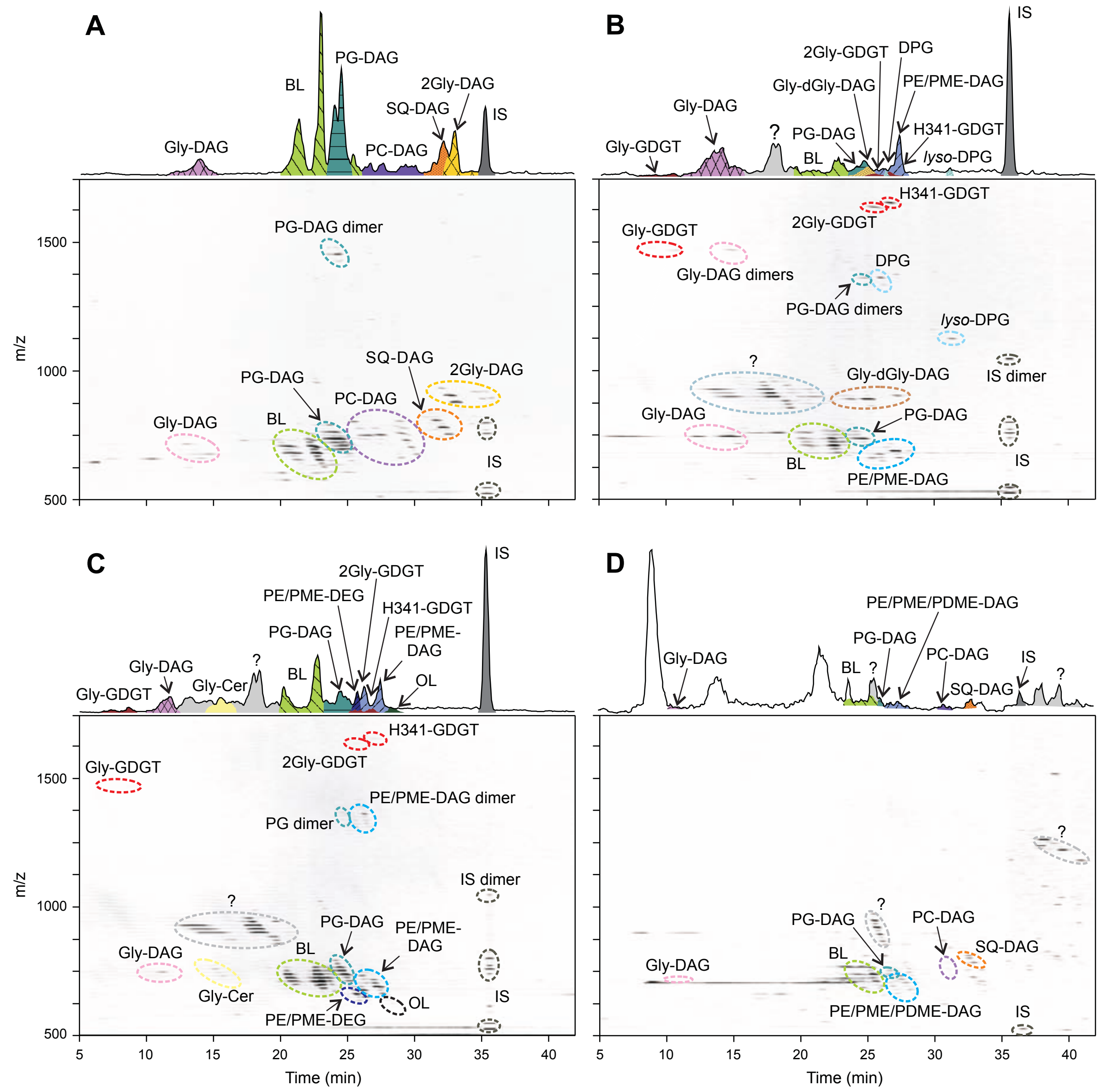

Fig. II.4. Base peak chromatograms and density maps of representative redox zones in the water column: (**A**) 10 mbsl; oxic zone (**B**) 77 mbsl; suboxic zone (**C**) 115 mbsl; anoxic zone (**D**) and fluff layer overlying the sediment. Density maps allow a three-dimensional view on the chromatographic separation. Different peak intensities within one compound class represent differences in core lipid chain length, whereas decreasing chain lengths elute with increasing polarity. Dimers of IPL compound classes form under high analyte concentrations (for abbreviations see text or Fig. II.5; IS = injection standard). Unidentified compounds are marked with ?.

typical for ANME-2 archaea nor 2Gly-GDGTs, the major IPLs in ANME-1 (Rossel et al., 2008) were detected at all or in samples below 200 mbsl, respectively. Moreover, core lipid distributions in Gly-GDGT, the only archaeal IPL detected below 200 mbsl, are indicative of a planktonic archaeal source due to the predominance of GDGT-0 and crenarchaeol (GDGT-5) core lipids rather than an euryarchaeotal ANME-1 source with abundant GDGT-1 to -3 (Rossel et al., 2008). This results are in good agreement with CARD-FISH data from Lin et al. (2006) who had observed that crenarchaeota were more abundant than euryarchaeota in the Black Sea water column.

By contrast, both the ring distribution and stable carbon isotopic composition of apolar GDGT core lipids in the Black Sea (Wakeham et al., 2003) are suggestive of a strong contribution of methanotrophic archaea to the bulk apolar GDGT pool. The combined evidence derived from IPL-GDGTs, their apolar derivatives, and gene-based indications of low ANME contribution to the total archaeal pool suggest accumulation of fossil methanotrophic archaeal biomass in the latter pool. A fossil contribution of apolar GDGT derivatives is additionally supported by concentration data (cf. Wakeham et al., 2003, 2007). Total apolar GDGT concentrations in the deep-water column are around 10 ng L^{-1}, i.e., more than an order of magnitude higher than corresponding IPLs (Fig. II.3) and similar to concentrations of major bacterial fatty acids (Wakeham et al., 2003, 2007), even though fatty acids were analyzed after saponification and thus represent the sum of free and PLFA-derived fatty acids. Processes concentrating GDGT core lipids relative to bacterial fatty acids in the deep water column are probably linked to the higher persistence of GDGTs but the mechanisms for preferentially preserving the signals of methanotrophic archaea relative to those of planktonic archaea in the "fossil GDGT pool" remain elusive. Association of ANME archaea vs. planktonic archaea with particles of different size and chemical composition would provide one explanation. Earlier lipid studies in the Black Sea did indeed observe that ANME GDGTs were preferentially associated with small sized, i.e., slowly sinking or suspended particles as were most bacterial lipids, whereas planktonic GDGTs were present in a larger and faster sinking particle size class that could be collected in sediment traps and thus contribute more to the sediment record (Wakeham and Beier, 1991; Wakeham et al., 2003).

II.3.2.8. Ornithine lipids (OL)

OL comprise less than 5% of total IPLs and are most abundant in the upper anoxic part of the water column, with a peak at 115 mbsl. The detected ornithine lipid types are comprised of an amide-bound C_{17} 3-hydroxyfatty acid that is esterified via its hydroxyl group with mainly saturated C_{15} and C_{17} fatty acids. OL and the corresponding coding gene *OlsA* have not yet been detected in eukarya or archaea, which suggests that OL are limited to the domain of bacteria (López-Lara et al., 2003). OL are widespread among gramnegative bacteria (Asselineau, 1991) and have been identified in the sulfate-reducing bacterium *Desulfovibrio gigas* (Makula and Finnerty 1975) and in some iron and sulfur oxidizing bacteria (e.g., Shively and Knoche, 1969). Based on known sources of OL and observations of OL in environments with active sulfur cycles (Bühring, Schubotz, Hinrichs et al., unpubl. data), we suggest that sulfur-metabolizing bacteria are the most likely source of OL in the anoxic water column.

II.3.2.9. Glycosylceramides (Gly-Cer)

Glycosylceramides (Gly-Cer), also called cerebrosides, belong to the class of glycosphingolipids. Tentatively identified Gly-Cer first occur at the onset of the anoxic zone (at 100 mbsl) and account for 5 to 20% of total IPLs throughout the anoxic zone. Its core lipids are mainly composed of a C_{21} or C_{22} sphinganine backbone to which a fatty acid (C_{15}, C_{16} or C_{17}) is linked via an amide-bond. The occurrence of sphingolipids in bacteria seems to be genus/species-specific, stressing its potential value as taxonomic biomarker (Olsen and Jantzen, 2001).

Phosphosphingolipids are relatively common in anaerobic bacteria, e.g., in the *Bacteroides* group (Kato et al., 1995), whereas glycosphingolipids are rare among bacteria. Glycosphingolipids were identified in some gramnegative bacteria (Kawahara et al., 1999) and in the fermenting alphaproteobacterium *Zymomonas mobilis* (Tahara and Kawazu, 1994). Kawahara et al., (1999) suggested that the unique cellular properties of glycosphingolipids facilitate the uptake of more hydrophobic substrates such as aromatic hydrocarbons and could thus enhance competitive adaptation for survival in ecological niches. To our knowledge, this is the first report of glycosphingolipids in complex natural samples. The distribution pattern in the water column suggests production by an obligate anaerobe.

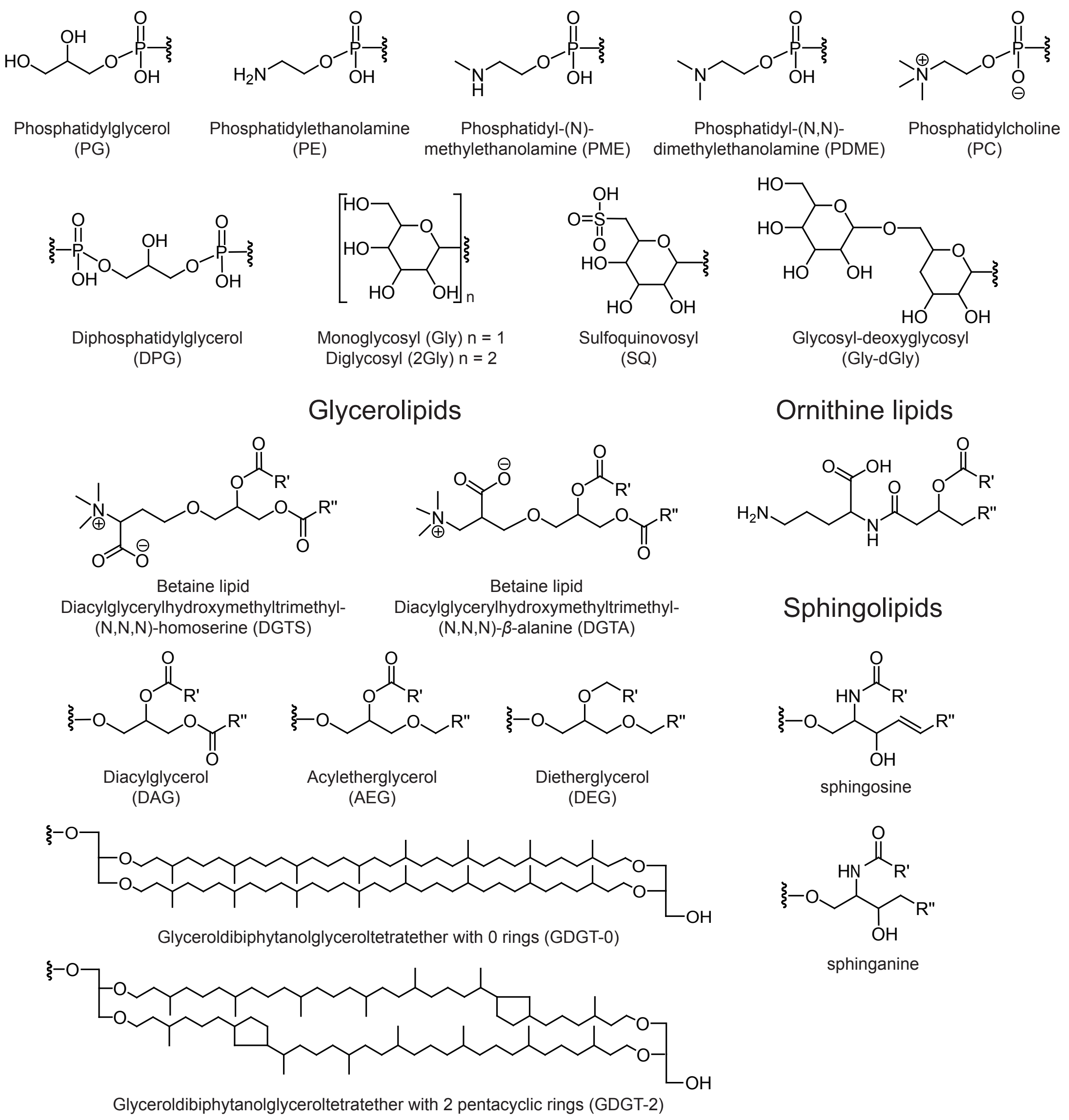
Phosphatidylglycerol (PG)
Phosphatidylethanolamine (PE)
Phosphatidyl-(N)-methylethanolamine (PME)
Phosphatidyl-(N,N)-dimethylethanolamine (PDME)
Phosphatidylcholine (PC)
Diphosphatidylglycerol (DPG)
Monoglycosyl (Gly) n = 1
Diglycosyl (2Gly) n = 2
Sulfoquinovosyl (SQ)
Glycosyl-deoxyglycosyl (Gly-dGly)
Glycerolipids
Ornithine lipids
Betaine lipid Diacylglycerylhydroxymethyltrimethyl-(N,N,N)-homoserine (DGTS)
Betaine lipid Diacylglycerylhydroxymethyltrimethyl-(N,N,N)-β-alanine (DGTA)
Sphingolipids
Diacylglycerol (DAG)
Acyletherglycerol (AEG)
Dietherglycerol (DEG)
sphingosine
sphinganine
Glyceroldibiphytanolglyceroltetratether with 0 rings (GDGT-0)
Glyceroldibiphytanolglyceroltetratether with 2 pentacyclic rings (GDGT-2)

Fig. II.5. IPL structures of head groups and core lipids identified in this study. The type of hexose-moiety for glycolipids was not determined. Note that the identification of the deoxyglycolipid and the sphingolipids in this study are tentative and that we could not distinguish between the betaine lipids DGTA and DGTS based on mass spectrometry. GDGT core lipids were found with zero to 5 rings (GDGT-0 to GDGT-5), whereas GDGT-5 was identified as crenarchaeol in a previous study (Wakeham et al., 2007), containing 4 pentacyclic rings and one hexacyclic ring. R', R'' = hydrocarbon chain with different chain length and unsaturations.

II.3.3. Sedimentary IPLs

IPL concentrations are highest (~5 µg/g sediment) in the unconsolidated "fluff" layer on top of the sediment and decrease to ~2 µg/g sediment in the first two centimeters of sediment (Fig. II.2). The composition of the fluff layer is slightly distinct from the underlying sediments: PG-DAG and Gly-DAG are only detected in the fluff layer, whereas diether PE and PME were first detected in the consolidated sediment. The main IPL compound classes in both layers are BL (composing ~40% of total IPLs) and PE in combination with PME and PDME (also ~40% of total IPLs), minor IPLs are SQ-DAG and PC-DAG. The core structures of all IPLs are dominated by $C_{14:0}$, $C_{16:0}$ and $C_{18:0}$ and $C_{16:1}$ and $C_{18:1}$ fatty acids, except for PE, PME and PDME which mainly contain combinations of $C_{16:0}$, $C_{16:1}$, $C_{15:0}$ and $C_{17:1}$ fatty acids. Based on the high relative abundance of BL, SQ-DAG, PC-DAG, PG-DAG and Gly-DAG with predominately even-numbered fatty acids, we conclude that possibly a large fraction of these lipids is associated with algal material rapidly exported from surface waters (Fowler and Knauer, 1986). The presence of PE-DAG, PME-DAG and PDME-DAG, which are observed in different relative abundances than in the overlying water column, argues for *in-situ* production, most likely by heterotrophic bacteria. The occurrence of PE-DEG and PME-DEG in the underlying sediment signals the presence of indigenous sulfate-reducing bacteria (Rütters et al., 2001, Sturt et al., 2004).

IPL-GDGTs were not detected in the fluff and the 0-1 cm sediments and were first observed at 12 cm sediment depth, where they account for almost 10% of total IPLs. They are composed of 2Gly-GDGT and H341-GDGT with GDGT-0 to GDGT-2 as core structures, as commonly found in benthic archaea (Biddle et al., 2006; Lipp et al., 2008).

II.3.4. IPL turnover, export, and preservation

The well-defined vertical zonation of IPLs along the redox gradients within the water column in the Black Sea is analogous to recent observations in a shallow meromictic pond (4.5 m depth; Ertefai et al., 2008) and suggests rapid turnover of IPLs. Additionally, the low concentrations of IPL-GDGTs (0.03-10 ng/L) and, by inference, IPL-ladderanes (not detectable) compared to approximately 1-3 orders of magnitude higher concentrations of their less polar core lipid derivatives (3-70 ng/L and 0.024.6 ng/L, respectively; Wakeham et al., 2007) are consistent with high turnover of IPLs and relatively long residence times of their less polar derivatives that, in the case of core GDGTs, selectively record signals from persistent but low-rate biogeochemical processes such as AOM (Wakeham et al., 2003), which is mediated by a relatively minor proportion of the microbial community (Schubert et al., 2006). This pattern suggests that (1) hydrolysis of glycosidic and phosphateester bonds between head groups and IPLs proceeds relatively rapidly, even in anoxic settings, and (2) retention and presumably some hydrological mixing affects distributions of the more stable lipid derivatives in the deep anoxic water column.

Even though overall turnover of IPLs seems to be high in the water column, we observe some typical algal signals in the fluff and surface sediments, probably due to delivery of fresh organic material into surface sediments via large, rapidly sinking particles (Fowler and

Knauer, 1986). The observation that not all algal IPLs are exported from the surface waters in equal amounts, e.g., 2Gly-DAG is missing and Gly-DAG is observed in much lower amounts than in surface waters, indicates that a combination of selective preservation, fractionation and modification during sedimentation and additional sources in the deeper water column and surface sediments impacts the intact membrane lipid pool of the surface sediments. Gly-DAG and PG-DAG are only observed in the fluff and are not detected in the underlying sediments, indicating a rapid decay of these lipids. Export of IPLs from planktonic archaea, on the other hand, does not appear to be linked to zooplankton grazing. The most abundant archaeal IPL type in the water column, Gly-GDGT, was not detected in the surface sediments and IPL-GDGTs typically associated with benthic archaea (Lipp et al., 2008) were only detected below 1 cmbsf.

II.4. EXPERIMENTAL PROCEDURES

II.4.1. Samples

Particulate matter (PM) samples were collected in the central basin of the Black Sea by *in-situ* filtration in May 2003, at station 5 (43°06.33'N, 34°00.6'E) during cruise 172, leg 8, of R/V *Knorr* (KN178/2) (Wakeham et al., 2007). Volumes filtered ranged from 160-900 L. Double glass fiber filters (Gelman A/E, nominal pore size 0.7 µm, ashed at 500°C for 6 hr) were used to maximize retention of small particles and the microbial biomarkers they contain. Nevertheless a small loss of single cells (diameter 0.2-0.7 mm) cannot be excluded; leading to IPL concentration that likely underestimate the real values. Particulate organic carbon (POC) and total nitrogen (TN) were measured on "plugs" (14 mm diameter) taken with a cork-borer from each 142 mm filter (actual filtration area 130 mm diameter) and treated by vapor-phase HCl acidification prior to elemental analysis. Sediments were collected using a multicorer during the same cruise. Upon recovery of the corer, the uppermost "fluff" layer (Wakeham and Beier, 1991) was removed with a solvent-rinsed spatula, and the remaining core was extruded and sectioned in 1.0 cm intervals. All samples were stored frozen until extraction.

II.4.2. Analysis

Lipid extraction and fractionation into neutral lipids, glycolipids and phospholipids have been described in Wakeham et al. (2007). Briefly, samples were soxhlet extracted using dichloromethane:methanol (DCM:MeOH; 9:1 v:v). Neutral, glyco- and phospholipid fractions were obtained by chromatography on silica gel (7 g of activated Merck silica gel 60) with chloroform, acetone and methanol, respectively. The glyco- and phospholipid fractions were saponified to release polar lipid fatty acids (PLFA) and were subjected to gas chromatography-mass spectrometry as methyl esters (Wakeham et al., 2007). Glyco- and phospholipid fractions were analyzed for their IPL composition and concentrations on a ThermoFinnigan Surveyor high performance liquid chromatography system coupled to a ThermoFinnigan LCQ DecaXP Plus ion-trap mass spectrometer via electrospray interface (HPLC-ESI-IT-MS^n) under conditions described previously (Sturt et al., 2004). Individual fractions were measured in positive and negative ionization modes with automated data-dependent fragmentation of base peak ions up to MS^3.

II.4.3. Mass spectral interpretation

Identification of IPLs is tentatively based on mass spectral fragmentation and was verified by authentic standards where available. Typically, identification is based on the neutral loss of the characteristic mass of the polar head group or a diagnostic fragment ion in positive ionization mode, and by the complementary core lipid and fatty acid fragments in positive and negative ion mode (for details see Sturt et al., 2004 and Supplementary Material Fig. II.S1). Authentic standards were available for PE-DAG, PDME-DAG, PG-DAG, PC-DAG, Gly-DAG, 2Gly-DAG, Gly-Cer, and *Thermoplasma acidophilum* main polar lipid (Gly-GDGT-PG; Avanti Polar Lipids, AL, USA; Matreya, PA, USA). Identification of SQ-DAG, BL, OL, DPG, Gly-Cer, and diether phospholipids was done according to published mass spectra (e.g., Kim et al., 1997, Geiger et al., 1999; Sturt et al., 2004). We could not distinguish between the betaine lipids DGTS, DGTA due to the structural similarity of their polar head group and we could also not decipher PE- and PME-DAG and -AEG core structures due to co-elution of compounds with the same *m/z* in the ion trap. Gly-dGly-DAG was tentatively identified due to compelling mass spectral evidence. For a complete list of IPL structures and mass spectrometric identification see Fig. II.5 and Supplementary Material Table II.S1 and Fig. II.S1.

II.4.4. Quantification

Three years after primary qualitative analysis the samples were spiked with C_{16}-PAF (1-O-hexadecyl-2-acetoyl-*sn*-glycero-3-phosphocholine) as injection standard and rerun for quantification. Slight changes in the relative distribution of IPLs were observed within the two runs. In particular the differences were identified as a selective loss of the glycolipids Gly-DAG, Gly-Cer, Gly-GDGT, and 2Gly-GDGT (data not shown). We interpret this loss as a sign of selective degradation of glycolipids during storage; hence the calculated absolute lipid concentrations likely underestimate the real values. We did not account for varying response factors of different lipid classes, due to the lack of commercially available standards for several of the analyzed lipids (e.g., SQ-DAG, BL, 2Gly-GDGT, and OL). Analysis of authentic standards from various IPL compound classes showed that the response factors of individual IPLs relative to the injection standard (PAF) span a range of 0.5 to 2 for all analyzed IPL compound classes and 0.5-1 for the IPL compound classes reported in this study, resulting in a similar extrapolated maximal error. The detection limit is determined for each individual run using the same approach as shown in Lipp et al. (2008), for the water column the limit of detection ranges between 0.01 and 0.2 ng/L, and for the surface sediments and the fluff it varies between 10 to 26 ng/g sediment.

II.5. ACKNOWLEDGEMENTS

We thank the captain and the crew of R/V Knorr 172-8 and the chief scientists James Murray and George Luther III. We are also thankful to Krisa Arzayus, Isabell Putnam and Tobias F. Ertefai for help in the laboratory. This work was supported by NSF grants (S.G.W. OCE-0117824 and OCE-0550654), the Deutsche Forschungsgemeinschaft (F.S., K.-U.H. through MARUM Center for Marine Environmental Sciences), the GLOMAR graduate school (to F.S.), and a grant by The Seaver Institute to K.-U.H. at Woods Hole Oceanographic Institution.

II.6. REFERENCES

Adams, J., Ann, Q. (1993) Structure determination of sphingolipids by mass spectrometry. *Mass Spectrom Rev* **12**: 51-85.

Albert, D.B., Taylor, C., Martens, C.S. (1995) Sulfate reduction rates and low molecular weight fatty acid concentrations in the water column and surficial sediments of the Black Sea. *Deep-Sea Res I* **42**: 1239-1260.

Asselineau J. (1991) Bacterial lipids containing amino acids or peptides linked by amide bonds. *Fortschr Chem Org Naturst* **56**: 1-85.

Barridge, J.K., Shively, J.M. (1968) Phospholipids of the *Thiobacilli*. *J Bacteriol* 95: 2182-2185.

Benning, C., Huang, Z.H., Gage, D.A. (1995) Accumulation of a novel glycolipid and a betaine lipid in cells of *Rhodobacter sphaeroides* grown under phosphate limitation. *Arch Biochem Biophys* **317**: 103-111.

Biddle, J.F., Lipp, J.S., Lever, M.A., Lloyd, K.G., Sørensen, K.B. Anderson, R., Fredricks, H.F., Elvert, M., Kelly, T.J., Schrag, D.P., Sogin, M.L., Brenchley, J.E., Teske, A., House, C.H., Hinrichs, K.-U. (2006) Heterotrophic Archaea dominate sedimentary subsurface ecosystems off Peru. *Proc Natl Acad Sci USA* **103**(10): 3846-3851.

Bird, D.F., Karl, D.M. (1991) Microbial biomass and population diversity in the upper water column of the Black Sea. *Deep-Sea Res* **38** (Suppl. 2): S1069-1082.

Brett, M.T., Müller-Navarra D.C. (1997) The role of highly unsaturated fatty acids in aquatic foodweb processes. *Freshw Biol* **38**: 483-499.

Christie, W.W. (2003) Lipid Analysis. 3rd edition. Oily Press, Bridgewater, UK.

Coolen, M.J.L., Abbas, B., van Bleijswijk, J., Hopmans, E., Kuypers, M.M.M., Wakeham, S.G., Sinninghe Damsté, J.S. (2007) Putative ammonia-oxidizing Crenarchaeota in suboxic waters of the Black Sea: a basin-wide ecological study using 16S ribosomal and functional genes and membrane lipids. *Environ Microbiol* **9**: 1001-1016.

Dembitsky, V.M. (1996) Betaine ether-linked glycerolipids: chemistry and biology. *Prog Lipid Res* **35**: 1-51.

Dowhan, W. (1997) Molecular basis for membrane phospholipid diversity: Why are there so many lipids? *Annu Rev Biochem*. **66**: 199-232.

Ertefai, T.F., Fisher, M.C., Fredricks, H.F., Lipp, J.S., Pearson, A., Birgel, D., Udert, K.M., Cavanaugh, C.M., Gschwend, P.M., Hinrichs, K.-U. (2008) Vertical distribution of microbial lipids and functional genes in chemically distinct layers of a highly polluted meromictic lake. *Org Geochem* **39**: 1572-1588.

Fang, J., Barcelona, M.J. (1998) Structural determination and quantitative analysis of bacterial phospholipids using liquid chromatography / electrospray ionization / mass spectrometry. *J Microbiol Meth* **33**: 23-35.

Fang, J., Barcelona, M.J., Semrau, J.D. (2000) Characterization of methanotrophic bacteria on the basis of intact phospholipid profiles. *FEMS Microbiol Let* **189**: 67-72.

Fowler, S.W., Knauer, G.A. (1986) Role of large particles in the transport of elements and organic compounds through the oceanic water column. *Prog Oceanogr* 16: 147-194.

Geiger O., Röhrs, V., Weissenmayer, B., Finan, T.M., Thomas-Oates, J.E. (1999) The regulator gene *phoB* mediates phosphate stress-controlled synthesis of the membrane lipid diacylglyceryl-N,N,N-trimethylhomoserine in *Rhizobium* (*Sinorhizobium*) *meliloti*. *Mol Microbiol* **32**: 63-73.

Goldfine, H., Hagen, P.-O. (1968) N-methyl groups in bacterial lipids. *J Bacteriol* **95**: 367-375.

Goldfine, H. (1984) Bacterial membranes and lipid packing theory. *J Lip Res* 25: 1501-1507.

Harwood, J.L. (1998) Membrane lipids in algae. In Lipids in photosynthesis: Structure, function and genetics. Siegenthaler, P., Murata, N. (eds.) Kluwer Academic Publishers. pp. 53-64.

Harvey, H.R., Fallon, R.D., Patton, J.S. (1986) The effect of organic matter and oxygen on the degradation of bacterial membrane lipids in marine sediments. *Geochim Cosmochim Acta* **50**: 795-804.

Happey-Wood, C.M. (1976) Vertical migration patterns in phytoplankton of mixed species composition. *Euro J Phycol* **11**: 355-369.

Hölzl, G., Dörmann, P. (2007) Structure and function of glycoglycerolipids in plants and bacteria. *Progr Lipid Res* **46**: 225-243.

Imhoff, J.F. Bias-Imhoff, U. (1995) Lipids, quinones and fatty acids of anoxygenic phototrophic bacteria. In Anoxygenic Photosynthetic Bacteria. Blankenship, R.E., Madigan, M.T., Bauer, C.E. (eds.), pp. 179-205. 1995 Kluwer Academic Publishers. Printed in The Netherlands.

Jaescke. A., Rooks, C., Trimmer, M., Nicholls, J.C., Hopmans, E.C., Schouten, S., Sinninghe-Damsté, J.S. (2009) Comparison of ladderane phospholipid and core lipids as indicators for anaerobic ammonium oxidation (anammox) in marine sediments. *Geochim Cosmochim Acta* **73**: 2077-2088.

Jørgensen B.B., Fossing H., Wirsen C.O., Jannasch H.W. (1991) Sulfide oxidation in the anoxic Black Sea chemocline. *Deep-Sea Res* **38** (Suppl. 2): S1083-S1103.

Karl, D.M., Knauer, G.A. (1991) Microbial production and particle flux in the upper 350 m of the Black Sea. *Deep-Sea Res* **38** (Suppl. 2): S921-S942.

Kato, M, Muto, Y., Tanaka-Bandoh, K., Watanabe, K., Ueno, K. (1995) Sphingolipid composition in *Bacteriodes* species. *Anaerobe* **1**: 135-139.

Kato, M., Sakai, M., Adachi, K., Ikemoto, H., Sano, H. (1996) Distribution of betaine lipids in marine algae. *Phytochemistry* **42**: 1341-1345.

Kawahara, K., Kuraishi, H., Zähringer, U. (1999) Chemical structure and function of glycosphingolipids of *Sphingomonas spp.* and their distribution among members of the a-4 subclass of Proteobacteria. *J Ind Microbiol Biotech* **23**: 408-413.

Kim, Y.H., Yoo, J.S., Kim, M.S. (1997) Structural characterization of Sulfoquinovosyl, Monoglactosyl and Digalactosyl Diacylglycerols by FAB-CID-MS/MS. *J Mass Spectrom* **32**: 968-977.

Konovalov, S.K., Murray, J.W. (2001) Variations in the chemistry of the Black Sea on a timescale of decades (1960-1995). *J Mar Syst* **31**: 217-243.

Könneke, M., Bernhard, A.E., de la Torre, J.R., Walker, C.B., Waterbury, J.B., Stahl, D.A. (2005) Isolation of an autotrophic ammonia-oxidizing marine archaeon. *Nature* **437**: 543-546.

Kuypers, M.M.M, Sliekers, A.O., Lavik, G., Schmid, M., Jørgensen, B.B., Sinninghe Damsté, J.S., Strous, M., Jetten, M.S.M. (2003) Anaerobic ammonium oxidation by anammox bacteria in the Black Sea. *Nature* **422**: 608-611.

Lam, P., Jensen, M.M., Lavik, G., McGinnis, D.F., Müller, B., Schubert, C.J., Amann, R., Thamdrup, B., Kuypers, M.M.M (2007) Linking crenarchaeal and bacterial nitrification to anammox in the Black Sea. *Proc Natl Acad Sci USA* **104**: 7104-7109.

Lin, X., Wakeham, S.G., Putnam, I.F., Astor, Y.M., Scranton, M.I., Chistoserdov, A.Y., Taylor, G.T. (2006) Vertical distributions of prokaryotic assemblages in the anoxic Cariaco Basin and Black Sea compared using fluorescence in situ hybridization (FISH) techniques. *Appl Environ Microbiol* **72**: 2679-2690.

Lipp, J.S., Morono, Y., Inagaki, F., Hinrichs, K.-U. (2008) Significant contribution of Archaea to extant biomass in marine subsurface sediments. *Nature* **454**: 991-994.

López-Lara, I.M., Sohlenkamp, C., Geiger, O. (2003) Membrane lipids in plant-associated bacteria: Their biosyntheses and possible functions. *Mol Plant Microbe Int* 16: 567-579.

Madigan, M. T., Martinko, J. M., Parker, J. (2003). *Brock - Biology of Microorganisms*. Prentice Hall, Upper Saddle River, New Jersey.

Makula, R.A. (1978) Phospholipid composition of methane-utilizing bacteria. *J Bacteriol* **143**: 771-777.

Makula, R.A., Finnerty, W.R. (1975) Isolation and characterization of an ornithine-containing lipid from *Desulfovibrio gigas*. *J Bacteriol* **123**: 523-529.

Manske, A.K., Glaeser, J., Kuypers, M.M., Overmann, J. (2005) Physiology and phylogeny of green sulfur bacteria forming a monospecific phototrophic assemblage at a depth of 100 meters in the Black Sea. *Appl Environ Microbiol* **71**(12): 8049-8060.

Murray, J.W., Codispoti, L.,A., Friedrich, G.E. (1995) Oxidation-reduction environments: the suboxic zone in the Black Sea. In Aquatic chemistry: Interfacial and interspecies processes ACS Advances in Chemistry Series. Vol 244. Oxford University Press, New York, NY, pp. 157-176.

Okuyama, H., Kogame, K., Takeda, S. (1993) Phylogenetic significance of the limited distribution of octadecapentaenoic acid in prymnesiophytes and photosynthetic dinoflagellates. *Proc NIPR Symp Polar Biol* **6**: 21-26.

Olsen, I., and Jantzen, E. (2001) Sphingolipids in bacteria and fungi. *Anaerobe* 7: 103-112.

Oguz T., Ducklow H.W., Rizzoli-Mamotte P. (2000) Modeling distinct vertical biogeochemical structure of the Black Sea: Dynamic coupling of the oxic, suboxic and anoxic layers. Global Biogeochemical Cycles **14**: 1331-1352.

Oguz, T., Merico, A. (2006) Factors controlling the summer *Emiliania huxleyi* bloom in the Black Sea: A modeling study. *J Mar Syst* 59: 173-188.

Reeburgh, W.S., Ward, B.B., Whalen, S.C., Sandbeck, K.A., Kilpatrick, K.A., Kerkhof, L.J. (1991) Black Sea methane geochemistry. *Deep-Sea Res* **38** (Suppl. 2: S1189-S1210.

Repeta, D.J. Simpson, D.J., Jørgensen, B.B., Jannasch, H.W. (1989) Evidence for anoxygenic photosynthesis from the distribution of bacteriochlorophylls in the Black Sea. *Nature* **342**: 69-72.

Rossel, P.E., Lipp, J.S., Fredricks, H.F., Arnds, J., Boetius, A., Elvert, M., Hinrichs, K.-U. (2008) Intact polar lipids of anaerobic methanotrophic archaea and associated bacteria. *Org Geochem*. **39**: 992-999.

Rütters, H., Sass, H., Cypionka, H., Rullkötter, J. (2001) Monoalkylether phospholipids in the sulfate-reducing bacteria *Desulfosarcina variabilis* and *Desulforhabdus amnigenus*. *Arch Microbiol* **176**: 435-442.

Rütters, H., Sass, H., Cypionka, H., Rullkötter, J. (2002) Phospholipid analysis as a tool to study complex microbial communities in marine sediments. *J Microbiol Meth* **48**: 149-160.

Schouten, S., Hopmans, E.C., Baas, M., Boumann, H., Standfest, S., Könneke, M., Stahl, D.A., Sinninghe Damsté, J.S. (2008) Intact membrane lipids of *Candidatus Nitrosopumilus maritimus*, a cultivated representative of the cosmopolitan mesophilic Group I Crenarchaeota. *Appl Environ Microbiol* **74**: 2433-2440.

Schubert, C.J., Coolen, M.J.L., Neretin, L.N., Schippers, A., Abbas, B., Durisch-Kaiser, E., Wehrli, B., Hopmans, E.C., Sinninghe Damsté, J.S., Wakeham, S.G., Kuypers, M.M.M. (2006) Aerobic and anaerobic methanotrophs in the Black Sea water column. *Environ Microbiol* **8**: 1844-1856.

Shively, J.M., Knoche, H.W. (1969) Isolation of an ornithine-containing lipid from *Thiobacillus thiooxidans*. *J Bacteriol* **98**: 829-830.

Short, S.A., White, D.C., Aleem, M.I.H. (1969) Phospholipid metabolism in *Ferrobacillus ferrooxidans*. *J Bacteriol* **99**: 142-150.

Siegenthaler, P.-A. (1998) Molecular organization of acyl lipids in photosynthetic membranes of higher plants. In Lipids in photosynthesis. Siegenthaler P.-A., Murata, N. (eds). Kluwer Academic Publishers, Dordrecht, The Netherlands, pp 199-144.

Siervo, A.J., Reynolds, J.W. (1975) Phospholipid composition and cardiolipin synthesis in fermentative and nonfermentative marine bacteria. *J Bacteriol* **123**: 294-301.

Sinninghe Damsté, J.S., Schouten, S., Hopmans, E.C., van Duin, A.C.T., and Geenevasen, A.J. (2002b) Crenarchaeol: the characteristic core glycerol dibiphytanyl glycerol tetraether membrane lipid of cosmopolitan pelagic crenarchaeota. *J Lipid Res* **43**: 1641–1651.

Sorokin, Y.I., Sorokin, P.Y., Audeev, D.Y., Sorokin, D.Y., Ilchenko, S.V. (1995) Biomass, production and activity of bacteria in the Black Sea with special reference to chemosynthesis and the sulfur cycle. *Hydrobiologia* **308**: 61-76.

Sturt, H.F., Summons, R.E., Smith, K., Elvert, M., Hinrichs, K.U. (2004) Intact polar membrane lipids in prokaryotes and sediments deciphered by high-performance liquid chromatography/electrospray ionization multistage mass spectrometry – new biomarkers for biogeochemistry and microbial ecology. *Rap Comm Mass Spec* **18**: 617-628.

Tahara, Y., Kawazu, M. (1994) Isolation of glucuronic acid-containing glycosphingolipid from *Zymomonas mobilis*. *Biosci Biotech Biochem* **58**: 586-587.

Uysal, Z. (2006) Vertical distribution of marine cyanobacteria *Synechococcus* sp. in the Black, Marmara, Aegean, and eastern Mediterranean seas. *Deep-Sea Res II* **53**: 1976-1987.

Van Mooy, B.AS., Rocap, G., Fredricks, H.F., Evans, C.T., Devol., A.H. (2006) Sulfolipids dramatically decrease phosphorous demand by picocyanobacteria in oligotrophic marine environments. *Proc Nat Acad Sci USA* **103**: 8607-8612.

Vetriani, C., Tran, H.V., Kerkhof, L.J. (2003) Fingerprinting microbial assemblages from the oxic/anoxic chemocline of the Black Sea. *Appl Environ Microbiol* **69**: 6481-6488.

Wada, H., Murata, N. (1998) Membrane Lipids in cyanobacteria. In Lipids in photosynthesis: structure, function and genetics. Siegenthaler P., Murata N. (eds.) Kluwer Academic Publishers, pp. 65-81.

Wada, H., Murata, N. (2007) The essential role of phosphatidylglycerol in photosynthesis. *Photosynth Res* **92**: 205-215.

Wakeham, S.G., Beier, J. A. (1991) Fatty acid and sterol biomarkers as indicators of particulate organic matter source and alteration processes in the water column of the Black Sea. *Deep-Sea Res.* **38** (Suppl. 2): S943-S968.

Wakeham, S.G., Lewis, C.M., Hopmans, E.C., Schouten, S., Sinninghe Damsté, J.S. (2003) Archaea mediate anaerobic oxidation of methane in deep euxinic waters of the Black Sea. *Geochim Cosmochim Acta* **67**: 1359-1374.

Wakeham, S.G., Amann, R., Freeman, K.H., Hopmans, E.C., Jørgensen, B.B., Putnam, I.F., Schouten, S., Sinninghe Damsté, J.S., Talbot, H.M., Woebken, D. (2007) Microbial ecology of the stratified water column of the Black Sea as revealed by a comprehensive biomarker study. *Org Geochem* **38**: 2070-2097.

White, D.C., Davis, W.M., Nickels, J.S., King, J.D., Bobbie, R.J. (1979) Determination of the sedimentary microbial biomass by extractable lipid phosphate. *Oecologia* **40**: 51-62.

Zink, K.-G., Wilkes, H., Disko, U., Elvert, M., Horsfield, B. (2003) Intact phospholipids-microbial „life markers" in marine deep subsurface sediments. *Org Geochem* **34**: 755-769.

II.S1. SUPPORTING INFORMATION

(available online: http://www3.interscience.wiley.com/journal/122514874/suppinfo)

Table II.S1. Identification of IPLs using complementary evidence gained through data dependent MS^n experiments in positive and negative ionization modes by HPLC-IT-ESI-MS.

	Pos ion mode		Neg ion mode		
IPL	MS^1	MS^2	MS^1	MS^2	Selected Ref.
PE-DAG/AEG	$[M+H]^+$	141 Da loss	$[M-H]^-$	FAs, *lyso*-IPLs	1,2
PME-DAG	$[M+H]^+$	155 Da loss	$[M-H]^-$	FAs, *lyso*-IPLs	1
PDME-DAG	$[M+H]^+$	169 Da loss	$[M-H]^-$	FAs, *lyso*-IPLs	1
PC-DAG	$[M+H]^+$	*m/z* 184	$[M+HCOO]^-$	FAs, *lyso*-IPLs	1,2
PG-DAG	$[M+NH_4]^+$	189 Da loss	$[M-H]^-$	FAs, *lyso*-IPLs	1,2
DPG	$[M+NH_4]^+$		$[M-H]^-$	FAs, *lyso*-IPLs	1,2
PE-DEG	$[M+H]^+$	43 Da loss	$[M-H]^-$		2
PME-DEG	$[M+H]^+$	59 Da loss	$[M-H]^-$		this study, Fig. II.S1
PG-DEG	$[M+NH_4]^+$	75 Da loss	$[M-H]^-$		2
Gly-DAG	$[M+NH_4]^+$	179; 197 Da loss glycerol + FAs	$[M+HCOO]^-$	FAs, *lyso*-IPLs	3
2Gly-DAG	$[M+NH_4]^+$	341; 359 Da loss, glycerol + FAs	$[M+HCOO]^-$	FAs, *lyso*-IPLs	3
SQ-DAG	$[M+NH_4]^+$	261 Da loss, glycerol + FAs	$[M+HCOO]^-$	FAs, *lyso*-IPLs	3
Gly-dGly-DAG	$[M+NH_4]^+$	179; 197; 325; 343 Da loss, glycerol + FAs	$[M+HCOO]^-$	FAs, *lyso*-IPLs	this study, Fig. II.S1
BL	$[M+H]^+$	*m/z* 236, glycerol + FAs	$[M-H]^-$	FAs, *lyso*-IPLs	4
OL	$[M+H]^+$	Ornithine + OH-FA, *m/z* 115 (MS^3)	$[M-H]^-$	FAs, *lyso*-IPLs	4
Gly-Cer	$[M+H]^+$	162; 180 Da loss 36 Da loss + long chain base ions (MS^3)	$[M+HCOO]^-$	208 Da loss	5
Gly-GDGT	$[M+NH_4]^+$	179 Da loss	$[M+HCOO]^-$	FAs, *lyso*-IPLs	2
2Gly-GDGT	$[M+NH_4]^+$	341 Da loss	$[M+HCOO]^-$	FAs, *lyso*-IPLs	2
H341-GDGT	$[M+NH_4]^+$	359 Da loss	$[M+HCOO]^-$	FAs, *lyso*-IPLs	2

(1) Fang and Barcelona, 1998; (2) Sturt et al., 2004; (3) Kim et al., 1997; (4) Geiger et al., 1999; (5) Adams and Ann, 1993.

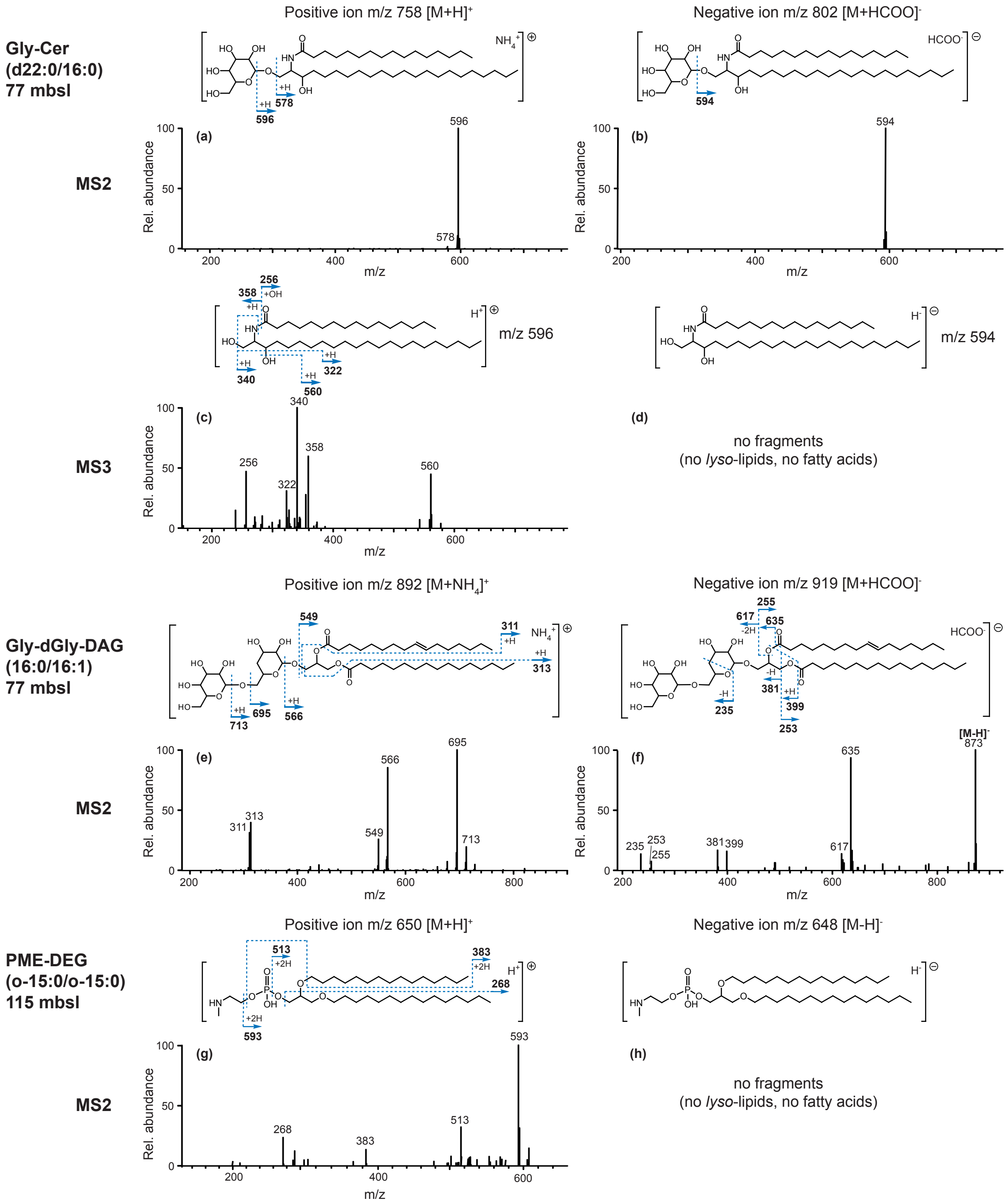

Fig. II.S1. Mass spectra of tentatively identified glycosyl-ceramide (Gly-Cer), Glycosyl-deoxyglycosyl-diacylglycerol (Gly-dGly-DAG) and phosphatidyl-(N)-methylethanolamine-dietherglycerol (PME-DEG) with the aid of data dependent MS^n experiments. **(A)** MS^2 of Gly-Cer with a 22:0 sphinganine backbone (d22:0) and 16:0 fatty acid in positive ionization mode and **(B)** MS^2 in negative ionization mode shows the loss of the sugar head group. **(C)** MS^3 in positive ionization mode of the MS^2 base peak (*m/z* 596) of Gly-Cer (d22:0/16:0) shows the fragmentation of the core lipid thus indicating the different chain lengths. **(D)** No clear fragmentation pattern is observed of the MS^2 base peak (*m/z* 594) of Gly-Cer (d22:0/16:0) in the MS^3 of the negative ionization mode, possibly due to the stable amide-bond structure of the ceramide. Verification of the fragmentation patterns (A)-(D) was conducted by analysis of a Gly-Cer (d18:2/OH-16:0, <98% purity) standard (Avanti Polar Lipids, AL, USA) and by comparison to published mass spectra (ADAMS AND ANN, 1993). **(E)** MS^2 of Gly-dGly-DAG with 16:0 and 16:1 fatty acids in positive ionization mode, note that the position of the double bond cannot be determined. The fragmentation pattern is similar to 2Gly-DAG, as compared with analysis of a standard (Avanti Polar Lipids, AL, USA), except

for a mass difference of 16 Da after the loss of the first sugar, indicating the presence of a deoxy sugar attached directly to the glycerol backbone. **(F)** MS^2 of Gly-dGly-DAG (16:0/16:1) in negative ionization mode, we tentatively identified fragment *m/z* 235 in the MS^2 of the negative ionization mode as the deoxy counterpart of fragment $^{0,4}A_2$ described in Kim *et al.* (1997). A_2 indicates the sugar attached to the glycerol and "0,4" indicates the break of the sugar between carbon position C_0 and C_4 of the sugar. We tentatively propose the deoxy sugar fragments at position "0,3" and not at "0,4" due to the deoxy group at C_4. **(G)** MS^2 of PME-DEG with diether 15:0 in positive ionization mode, showing the loss of only the (N)-methylethanolamine and not of the entire PME head group as described by Sturt *et al.* (2004). **(H)** No fragments were observed in the MS^2 of PME-DEG (o15:0/o15:0) in the negative ionization mode, likely due to the stable structure of the ether-lipid.

II.S2. SUPPORTING INFORMATION - REFERENCES

Adams, J., Ann, Q. (1999) Structure determination of sphingolipids by mass spectrometry. *Mass Spectrom Rev* **12**: 51-85.

Fang, J., Barcelona, M.J. (1998) Structural determination and quantitative analysis of bacterial phospholipids using liquid chromatography / electrospray ionization / mass spectrometry. *J Microbiol Meth* **33**: 23-35

Geiger O., Röhrs, V., Weissenmayer, B., Finan, T.M., Thomas-Oates, J.E. (1999) The regulator gene *phoB* mediates phosphate stress-controlled synthesis of the membrane lipid diacylglyceryl-N,N,N-trimethylhomoserine in *Rhizobium (Sinorhizobium) meliloti*. *Mol Microbiol* **32**: 63-73.

Kim, Y.H., Yoo, J.S., Kim, M.S. (1997) Structural characterization of Sulfoquinovosyl, Monogalactosyl and Digalactosyl Diacylglycerols by FAB-CID-MS/MS *J Mass Spectrom* **32**: 968-977.

Sturt, H.F., Summons, R.E., Smith, K., Elvert, M., Hinrichs, K.U. (2004) Intact polar membrane lipids in prokaryotes and sediments deciphered by high-performance liquid chromatography/electrospray ionization multistage mass spectrometry – new biomarkers for biogeochemistry and microbial ecology. *Rap Comm Mass Spec* **18**: 617-628.

Chapter III

Chemosynthetic life at the Chapopote asphalt volcano – insights from stable carbon isotopes and intact polar membrane lipid analyses

Florence Schubotz[1*], Julius Sebastian Lipp[1], Marcus Elvert[1], Sabine Kasten[2], Matthias Zabel[1], Elva Escobar[3], Gerhard Bohrmann[1], Kai-Uwe Hinrichs[1]

In preparation for *Geochimica et Cosmochimica Acta*

**Corresponding author. Tel: +49-421-218-65711; Fax: +49-421-218-65715*

E-mail address: schubotz@uni-bremen.de

[1]Department of Geosciences and MARUM Center for Marine Environmental Sciences, University of Bremen, D-28359 Bremen, Germany

[2]Alfred Wegener Institute for Polar and Marine Research, 27570 Bremerhaven, Germany

[3]Instituto de Geología, Universidad Nacional Autónoma de México, Ciudad Universitaria, Coyoacán 04510, México

III.1. ABSTRACT

At the Chapopote Knoll in the southern Gulf of Mexico deposits of asphalt form the basis of a prolific cold seep ecosystem extensively colonized by chemosynthetic communities. This study investigates microbial life and associated biological processes inside the asphalts and surrounding oil-impregnated sediments by analysis of intact polar membrane lipids (IPLs) and stable carbon isotopes (^{13}C) of hydrocarbon gases. All asphalts and sedimentary oils are highly biodegraded, showing that petroleum-derived hydrocarbons are an important substrate for the chemosynthetic communities. In the sediments, oil and hydrocarbon gases significantly enhance and control microbial activity and biomass. Oil which is found in subsurface sediments likely stimulates methanogenic hydrocarbon degradation where sulfate is present as indicated by low $\delta^{13}C$ values for methane (-75‰) accompanied by an increase in archaeal biomass close to a sulfate-methane transition zone (6 mbsf). Bacterial IPLs dominate oil-impregnated surface sediments, but decline as sulfate is depleted, whereas archaeal IPLs increase in relative abundance with increasing sediment depth. Here, phospho hydroxyarchaeols and mixed phospho-diglycosidic archaeal tetraethers point to the presence of abundant methanotrophic and methanogenic archaea. Inside gas hydrate-containing asphalts the presence of intact microbial cells could be confirmed by the detection of bacterial diester and diether phospholipids. Biological methanogenesis, however, only contributes a small fraction to the total methane gas hydrates occluded in the asphalts ($\delta^{13}C$ of -55‰). On top of the asphalts grazing macrofauna feed on microbial mats evidenced by aerobic and anaerobic methanotrophic biomarkers in digestive tracks of sea cucumbers; thus demonstrating a close link of energy transfer from the asphalts to benthic life.

III.2. INTRODUCTION

The Gulf of Mexico (GoM) is well known for its naturally occurring hydrocarbon seepage (Brooks *et al.*, 1984; MacDonald *et al.*, 1993; Solomon *et al.*, 2009). Migration of oil and gas from deeper reservoirs to surface sediments occurs along faults that are created by salt tectonic movements (Martin and Case, 1975; Kennicutt et al., 1988). Recurring geological seep formations on the sea floor of the northern shelf are brine pools, mud volcanoes and gas hydrates breaching the seafloor, either dominated by methane or oil seepage (e.g., Sassen et al., 2003; Joye et al., 2009). Hydrocarbon seepage on the seafloor is often evidenced by chemosynthetic life forms, such as microbial mats, symbiont-hosting mussels and tubeworms, filter-feeding shrimp and grazing crabs that colonize these formations (e.g., MacDonald et al., 1990; Sassen et al., 1993, 2004).

Cold seep ecosystems have been extensively studied along the continental margins of the northern GOM: Here, advective transport of reduced gases, primarily methane, to surficial sediments stimulates microbial activity within sediments and at the seafloor in the form of sulfate reduction and methanotrophy (Joye et al., 2004; Orcutt et al., 2005; Lloyd et al., 2006). The anaerobic oxidation of methane (AOM), mediated by a syntrophic consortium of methanotrophic archaea and sulfate-reducing bacteria (SRB) (Hinrichs et al., 1999; Boetius et

AL., 2000, ORPHAN ET AL., 2001), is a widespread biological process in marine sediments where high fluxes of methane are present. The AOM reaction zone varies in depth according to methane flux and sulfate depletion by organoclastic sulfate reduction and sedimentation/accumulation rate (BOROWSKI ET AL., 1996; RIEDINGER ET AL., 2005). Sulfide is abundantly produced during anaerobic degradation of organic matter and AOM and is utilized by sulfide-oxidizing bacteria on top of the sediments, often covering the seafloor over a large area as microbial mats (e.g., SASSEN ET AL., 1993, 2004).

In the southern Gulf of Mexico, a new form of hydrocarbon seepage has been discovered at the Campeche Knolls (MACDONALD ET AL., 2004), which are characterized by intense salt diapirism (e.g., GARRISON AND MARTIN, 1973). At one of the knolls, the Chapopote Knoll, situated at the northern end of the area, deposits of solidified asphalts in 3000 m water depth extend on the seafloor over an area of more than 1 km^2 and are colonized by prominent chemosynthetic communities (MACDONALD ET AL., 2004; BOHRMANN ET AL., 2008; BRÜNING ET AL., 2009). This new form of oil seepage was termed asphalt volcanism, since the structures of the asphalt beds resemble that of solidified lava. In 2006, the Chapopote Knoll was revisited to answer questions of asphalt migration, deposition and microbial and macrofaunal colonization associated with this unique ecological niche. DING AND COWORKERS (2008) could show with high resolution shallow seismic reflectors that the highly viscous asphalts might have originated from a shallow reservoir, situated 200 to 300 m below the crest of the Knoll. Asphalts are saturated with methane and higher hydrocarbons, which results in the formation of gas hydrates (KLAPP ET AL., 2009). Such high methane concentrations are also likely the driving factor in stimulation of abundant and diverse microbial communities.

One way to study microbial activity is by analysis of the stable carbon isotopic ($\delta^{13}C$) composition of microbial metabolites such as dissolved inorganic carbon (DIC), methane and higher hydrocarbon compounds. The underlying concept of $\delta^{13}C$ analysis is that microbial processes are associated with a kinetic isotope effect where the microbes typically discriminate against the heavier isotope (^{13}C) and preferentially metabolize ^{12}C (HAYES, 2001). Carbon isotope fractionations are particularly high for the uptake and production of low-molecular-weight compounds such as methane and CO_2, making this method ideal for tracking their turnover in marine sediments (WHITICAR, 1999). The presence of live microbial communities can be traced by distributions of intact polar membrane lipids (IPLs). After cell death the covalently bound polar head group of the IPLs is quickly hydrolyzed (WHITE ET AL., 1979; HARVEY ET AL., 1986), thus IPLs represent viable cells and are increasingly used to characterize microbial populations in marine sediments (e.g., RÜTTERS ET AL., 2001; STURT ET AL. 2004; LIPP ET AL., 2008). There are inherent differences of IPLs from the major domains of life: the Archaea contain isoprenoidal glycerolether lipids, whereas bacterial IPLs are typically composed of diacylglycerol lipids (DAG; fatty acids; LANGWORTHY AND POND, 1986; ITOH ET AL., 2001). The combined taxonomic information encoded in the core lipids and type of polar head group allows to infer the source organisms and gives an overview on the major microbial communities contributing to biomass (e.g., STURT ET AL., 2004; ERTEFAI ET AL., 2008; SCHUBOTZ ET AL., 2009, *CHAPTER II*).

In this study we apply molecular and isotopic studies on metabolic intermediates in combination with IPLs as tracers for viable microbial cells. This combined approach enables to track the distribution of biological activity in the asphalts and sediments stimulated by asphalt volcanism.

III.3. MATERIAL AND METHODS

III.3.1. Sampling

Sediment, asphalt, and gas hydrate samples were retrieved from the Chapopote Knoll during Meteor expedition M67/2 in March to April 2006 (Fig. III.1a; Bohrmann et al., 2008). The asphalt beds of the main asphalt site were penetrated by gravity coring (GRC; core GeoB10618, 21°53.95’N, 93°26.21’E; GeoB10623, 21°53.96’N, 93°26.22’E). The up to 1.5 m long asphalt cores were interspersed with gas hydrates (Fig. III.1b). Surface asphalts (GeoB10625-16) and macrofaunal samples were collected by the remotely operated vehicle ROV QUEST 4000 with a suction sampler (Fig. III.1c). Selected asphalts samples were retrieved by the rigmaster (GeoB10617-6) or collected in an In-Situ Pressure Seafloor Sampler (GeoB10621; Bohrmann et al., 2008). Sampling locations are pinpointed in Brüning et al. (2009), who mapped the asphalt flow on Chapopote in detail. Sediment cores were recovered by either GRC or by ROV operated push coring (PUC). Push cores (PUCs) GeoB10619 (21°53.99’N, 93°26.18’E) and GeoB10625 (21°53.90’N, 93°26.20’E) were recovered in close vicinity of the main asphalt site and contained oil admixed to the sediments (Fig. III.1c). Patches of tubeworms surrounded site GeoB10619, whereas microbial mats covered sediments from site GeoB10625. The GRC GeoB10610 (21°54.25’N, 93°25.88’E) was retrieved ~1 km northwest of the main asphalt site, in the trough of the Chapopote Knoll ‘crater’. Here oil slicks were observed on the surface of the water.

III.3.2. C_1 to C_6 hydrocarbons

A selection of samples was analyzed for their hydrocarbon (HC) gas composition, including asphalt samples collected from the top and up to 1 m inside of the asphalt mound, a gas hydrate occluded inside the asphalts, and a variety of oil-impregnated and oil-free sediment samples from different depths.

III.3.2.1. Quantification and composition of HC gases

Gas concentrations of sediment samples and asphalts were measured immediately after sampling on-board according to a protocol commonly used during expeditions of the Ocean Drilling Program (ODP Leg 201 Shipboard Scientific Party, 2003). Hereby, a defined sediment or asphalt volume, typically 3-5 mL wet sediment or 1 g of asphalt, was retrieved with cut-off syringes or a spatula, and then transferred to a 20 mL headspace vial and crimp-sealed gas-tight. The sample was subsequently heated at 70°C for 20 to 30 minutes prior to analysis by gas chromatography after cooling to room temperature. Gas hydrate was stored in liquid nitrogen immediately after recovery. Before analysis it was transferred via headspace gas exchange to 20 mL headspace vials filled with saturated NaCl solution. For quantitative analysis of hydrocarbon gases, 200 µL of headspace sample were injected with a 250 µL gas-tight syringe into an Agilent 6890N series gas chromatograph equipped with an Optima 5 capillary column (50 m x 0.32 mm ID) and a flame ionization detector. The injector was set at 180°C, the oven was programmed to hold 45°C for 4 min, then ramp to 155°C at 15°C min^{-1}, hold for 2 min, then heat to 240°C at 25°C min^{-1}, hold for 7 min. Injection of known quantities of standards (methane 100 ppm; C_1 to C_6 mixture, 1000 ppm, Air Liquide, Germany) enabled the calculation of hydrocarbon gas concentrations.

Identification of unknown hydrocarbon gases was performed onshore by GC-MS analysis with a TraceGC (ThermoFinnigan) and TraceDSQ mass spectrometer (ThermoFinnigan), equipped with an Alltech AT-Q packed capillary column (30 m x 0.32 mm ID). The temperature program was: -20°C for 4 min, by cooling with liquid nitrogen, then ramp to 240°C by 20°C min^{-1}, hold for 1 min. Helium as carrier gas was set to a constant flow of 2 mL min^{-1}, scan range was from *m/z* 10 to 150.

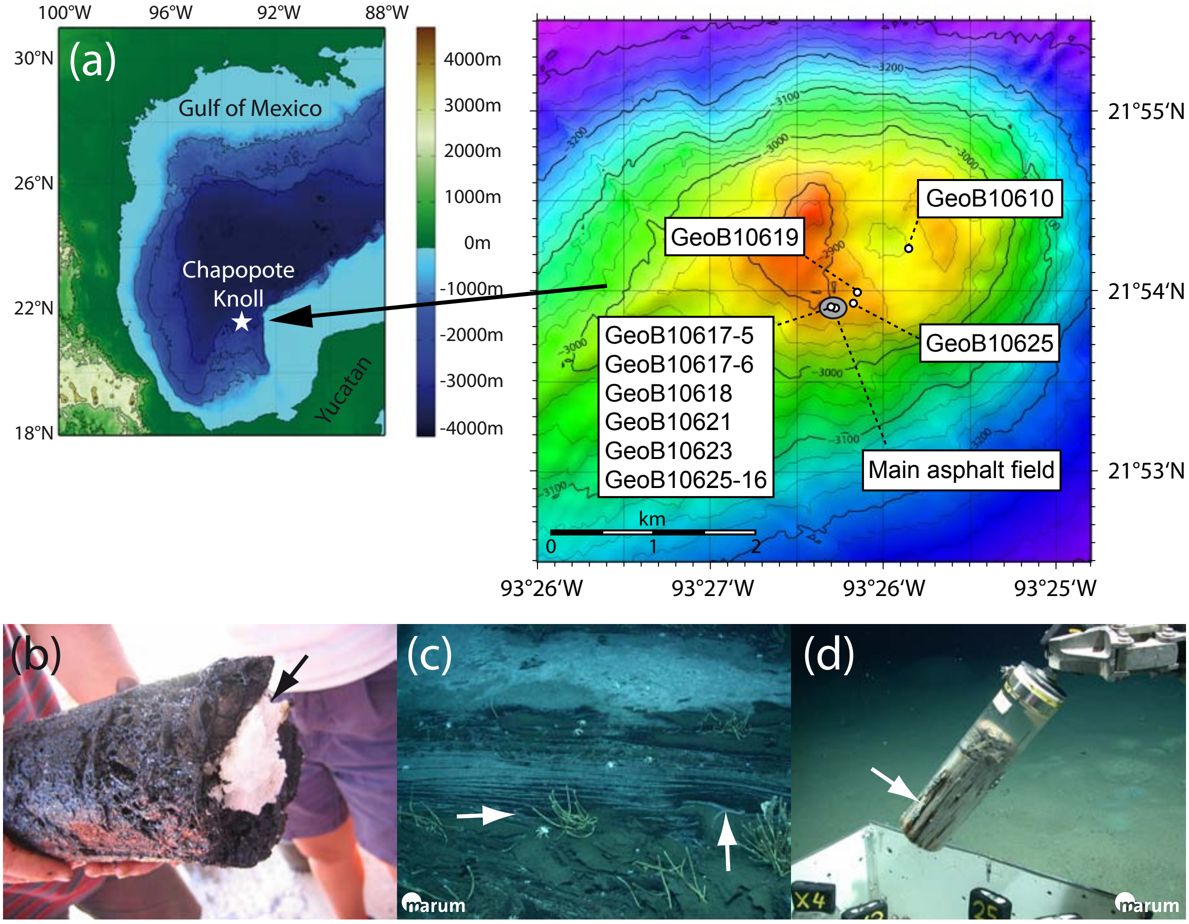
100°W
96°W
92°W
88°W
30°N
26°N
22°N
18°N
(a)
Gulf of Mexico
Chapopote Knoll
Yucatan
4000m
3000m
2000m
1000m
0m
-1000m
-2000m
-3000m
-4000m
GeoB10610
GeoB10619
GeoB10625
GeoB10617-5
GeoB10617-6
GeoB10618
GeoB10621
GeoB10623
GeoB10625-16
Main asphalt field
km
0
1
2
21°55′N
21°54′N
21°53′N
93°26′W
93°27′W
93°26′W
93°25′W
(b)
(c)
(d)
marum
marum

Fig. III.1. (**A**) Location (white star) and bathymetric map of the Chapopote Knoll with sediment and asphalt sample locations (left map based on ETOPO2 topography, U.S. Department of Commerce, National Oceanic and Atmospheric Administration (2001), right map modified from Bohrmann et al., 2008). (**B**) Gravity core GeoB10618 penetrating the asphalt bed and revealing gas hydrates (black arrow) captured inside of the asphalt. (**C**) High resolution photo of surficial asphalt beds, covered by microbial mats, crabs and tube worms, and holothuria (white arrows). (**D**) High resolution photo of oil-impregnated push core at site GeoB10625, white arrow points to oil.

III.3.2.2. Stable carbon isotope analyses

For shore-based isotopic analysis a defined sediment volume, typically 5 mL wet sediment, was collected with cut-off syringes, and then transferred to either a 20 mL headspace vial and spiked with 5 mL of 1N-NaOH, or a 50 mL headspace vial containing 20 mL of saturated NaCl solution and spiked with NaN_3 solution. The headspace vials were crimp-sealed gas tight, stored upside down and kept frozen at -20°C until isotopic analysis. Stable carbon isotope analysis of hydrocarbon gases was performed on a ThermoFinnigan gas chromatograph (Trace GC) coupled to a ThermoFinnigan Deltaplus XP mass spectrometer via a ThermoFinnigan GC Combustion III interface. The GC was equipped with a Supelco Carboxen 1006 Plot fused-silica capillary column (30 m x 0.32 mm ID) for C_1 analysis and an Alltech AT-Q packed capillary column (30 m x 0.32 mm ID) for the analysis of C_2 to C_6 compounds. The initial oven temperature was set to 40°C for C_1 analysis and 20°C for analysis of higher HC gases, held for 4 min, heated by 20°C min^{-1} to 240°C and held for 1 min, with a constant flow of Helium (2 mL min^{-1}) as carrier gas. Carbon isotope ratios are reported in the δ-notation as per mil deviation from Vienna Pee Dee Belemnite standard (VPDB). Analytical precision was determined by repeated injections of commercially available standards (methane 100 ppm; C_1 to C_6 mixture, 1000 ppm, Air Liquide) and was typically better than 1‰.

III.3.3. Lipid biomarkers

III.3.3.1. Extraction of asphalts, sediment and soft tissue

For petroleum-hydrocarbon analysis by GC, small amounts of asphalt (20-40 mg) were dissolved in DCM:MeOH (9:1). For the analysis of intact polar lipids (IPLs) by liquid chromatography (LC), asphalts (2 to 10 g), freeze-dried or frozen sediment (2 to 50 g) and soft tissue samples (1 to 2 g) were extracted with a modified Bligh and Dyer method following the protocol of Sturt et al. (2004). Hereby samples were dispersed in 4 mL per gram sediment or soft tissue of a mixture of DCM:MeOH:buffer (1:2:0.8; v/v) and ultrasonically extracted for 10 minutes in four steps. For the first two extraction steps, a phosphate buffer was used (pH 7.4), in the last two steps the phosphate buffer was replaced by a TCA buffer (50 g/L, pH 2). After each extraction step the centrifuged supernatants were combined in a separatory funnel. The supernatants were washed three times with deionized MilliQ water and collected as total lipid extract (TLE). The TLE was gently evaporated to dryness under a stream of nitrogen in a water bath at 37°C and stored at -20°C until analysis.

III.3.3.2. LC-MS

For the analysis of IPLs, an aliquot of the TLE was dissolved in DCM:MeOH (5:1) and injected on to a ThermoFinnigan Surveyor HPLC System equipped with a LiChrosphere diol column (2.1 x 150 mm; Alltech, Germany) coupled to a ThermoFinnigan LCQ Deca XP Plus ion trap mass spectrometer using an electrospray ionization (ESI) source. Instrument settings were previously described in Sturt et al. (2004). Identification of compounds was based on mass spectral information including specific fragmentation patterns in positive and negative ion mode and verification with standards and previously published data (Sturt et al., 2004; Schubotz et al., 2009, *Chapter II*; Rossel, 2009). Quantification was based on relative response of the analyte compared to an injection standard (di-C_{19}-PC). Values were corrected by response factors of different IPLs relative to the injection standard. Response factors were directly determined for commercially available standards (di-C_{17}-PG, di-C_{16}-PA, di-C_{16}-PE, di-C_{16}-PS, 1Gly-DAG, 2Gly-DAG, PC-AR, Gly-GDGT-PG; Matreya, USA, Avanti Polar Lipids, USA), for other IPLs, the mean response factor was used for correction. The range of response factors for different IPL classes relative to the injection standard varied between 0.5 and 1.3. The quantification is therefore to be considered as semi-quantitative.

III.3.3.3. GC-MS and GC-irMS

For quantification of the total GC-amenable hydrocarbons the asphalt and sediment TLE were derivatized with bis-(trimethylsilyl)trifluoroacetamide (BSTFA, Merck, Germany) in pyridine at 70°C for 1 h. Sample clean-up of asphalt, sediment and soft tissue samples was performed on an aliquot of the TLE, which was first subjected to asphaltene separation, separating hexane-insoluble asphaltenes from hexane-soluble maltenes. The maltenes were further separated by column chromatography on a SPE cartridge (Supelco LC-NH_2, 500 mg sorbent) into four fractions: hydrocarbons, esters and ketones, alcohols and free fatty acids after Hinrichs et al. (2000). Alcohols and free fatty acids were derivatized with bis-(trimethylsilyl)trifluoroacetamide (BSTFA, Merck, Germany) in pyridine at 70°C for 1 h to synthesize trimethylsilyl-(TMS)-derivatives. The hydrocarbons and TMS-derivative alcohols and fatty acids were dissolved in hexane and analyzed on a ThermoFinnigan Trace GC coupled to a ThermoFinnigan TraceMS for structural identification through mass spectral information. Determination of double bond positions was achieved via formation of dimethyldisulfide adducts after Elvert et al. (2003). For quantification, injection standards (behenic acid methylester, 2-methyloctadecanoic acid, nonadecanol) were added and the GC was coupled to a flame ionization detector (FID). The GC was operated in electron impact mode at 70 eV with a full scan mass range of *m/z* 400-800. The initial oven temperature was held at 60°C for 1 min, increased to 150°C with a rate of 10°C min^{-1}, then raised to a temperature of 310°C with a rate of 4°C min^{-1} and held at 310°C for 35 min. The carrier gas was helium with a constant flow of 1.0 ml min^{-1}. Compound-specific stable carbon isotopic compositions were measured on a ThermoFinnigan GC coupled to a ThermoFinnigan Deltaplus XP isotope ratio MS. The isotopic compositions of the TMS-derivatives were corrected for the additional methyl groups introduced during derivatization (47.2‰). The standard deviation of replicate analysis was <1‰. All isotopic values are reported in the delta notation ($\delta^{13}C$) relative to the Vienna PeeDee Belemnite Standard.

III.3.4. $\delta^{13}C$ of TOC and DIC

Stable carbon isotope values of TOC were analyzed after decalcification with 3N HCl on a Leco CS200 analyzer. Pore waters for determination of $\delta^{13}C$ DIC were extracted from the sediment cores by a pore water press and from samples either killed with Hg_2Cl after sampling and stored without head space at 4°C or frozen directly after sampling with a minimal air head space to avoid the breaking of the vial. Analysis occurred after treatment with phosphoric acid under helium atmosphere with a GasBench automated sampler, interfaced to a ThermoFinnigan MAT 251 mass spectrometer. Analyses were calibrated with a known standard of defined isotopic value, standard deviation was estimated to be less than 0.1‰.

III.4. RESULTS AND DISCUSSION

III.4.1. Distribution of hydrocarbons in asphalts and sediments – indicators of biological activity

III.4.1.1. C_1 to C_6 hydrocarbon gases

All asphalt samples contain high amounts of methane and C_{2+} hydrocarbon (HC) gases that can potentially serve as carbon and energy substrates for microbial communities where electron acceptors are present (Fig. III.2a, Table III.1). The C_{2+} HC gases are mainly composed of ethane, propane, butane, pentane and hexane, and their respective regioisomers, *iso*-butane (*i*-C_4), *iso*-pentane (*i*-C_5), cyclo-pentane (cy-C_5), 2-methyl-pentane (2me-C_5), and 3-methyl-pentane (3me-C_5). Highest total gas concentrations are observed in deeper layers of the asphalt beds (GeoB10618; 250 mmol kg^{-1} at ~1.5 mbsf) where the asphalt was interspersed with gas hydrates (Fig. III.1b). For the pure gas hydrate, no absolute concentrations could be determined due to quick dissolution of the hydrate structure after recovery. Samples retrieved from the surface of the asphalt beds (GeoB10617-5, GeoB10621, GeoB10625-16) range from 50 to 150 mmol kg^{-1}, with the maximum value representing the *in-situ* gas concentration, determined upon sample retrieval by an autoclave device (Bohrmann et al., 2008). From this observation it can be inferred that during the sampling procedure roughly two thirds of the actual gas is lost due to out-gassing. Surface asphalts, visually devoid of gas hydrates (GeoB10617-5, GeoB10621, no out-gassing or bubbling, density heavier than water) mainly contain C_2 to C_6 HC gases and only 5 to 22% methane. In asphalts with gas hydrates (GeoB10625-16, GeoB10618, GeoB10623), methane is the most abundant gas and C_2 to C_6 gases comprise only up 50% of total HC gases. The $\delta^{13}C$ of methane in the asphalts is 40‰, ethane is slightly more enriched in ^{13}C with 33‰, and the C_3 to C_6 gases range from 27‰ to 29‰, the latter resembling $\delta^{13}C$ values of asphalt TOC (27‰; Fig. III.2b). Reported values for thermogenic methane in the northern Gulf of Mexico range between 40‰ and 50‰ (Chung et al., 1988; Berner and Faber, 1996; Whiticar et al., 1999). Conclusively, the observed values together with the low observed $C_1/(C_2+C_3)$ ratios are consistent with a thermogenic origin of the asphalt-derived HC gases. The asphalt-occluded gas hydrate was predominantly composed of methane (95.2%), followed by ethane (2.6%), propane (1.3%) and C_4 to C_6 HC gases (<1%). Methane of the pure gas hydrate is slightly depleted in ^{13}C compared to the asphalt with δ values of 55‰, the $\delta^{13}C$ values of C_2 to C_6 HC gases resemble those of the asphalt (Fig. III.2b). The slightly more negative methane $\delta^{13}C$ values in the gas hydrate suggest an admixture of biologically produced methane (Whiticar et al., 1999). A possible source could be long chain *n*-alkane degrading methanogenic consortia, composed of *Synthrophus sp.* and *Methanosaeta* (Zengler et al., 1999), which were found by DNA analysis close to the asphalt-occluded gas hydrates (G. Wegener, K. Knittel et al., pers. comm.).

In contrast to the asphalts the HC gases in the sediments are predominantly composed of methane (77% to 98% of total HC gases) with absolute HC gas concentrations between <1 to 8 mmol kg^{-1} (Fig. III.2a, Table III.1). In general, increased gas concentrations and lower $C_1/(C_2+C_3)$ ratios are correlated with the presence of oil in the sediments (cf. Fig. III.3). Biological methane production is apparent in subsurface sediments close to a sulfate-methane transition zone (SMTZ) at 6 mbsf with δ^{13}C values of methane of up to 75‰ and in surface sediments where methane δ^{13}C values range between 60‰ an 68‰ (Fig. III.2b). Biological activity linked to hydrocarbon degradation in the shallow sediments is furthermore indicated by changes in the carbon isotopic values of the higher hydrocarbon gases: In PUC GeoB10625 more ^{13}C depleted values of n-C_4 and n-C_5 relative to i-C_4 and i-C_5, respectively, are consistent with a favored biological uptake of straight chain relative to branched alkanes (Welte et al., 1982; Vieth and Wilkes, 2006). In both shallow cores, GeoB10619 and GeoB10625, propane seems to be consumed preferentially to the other hydrocarbon gases as suggested by a pronounced relative enrichment in ^{13}C.

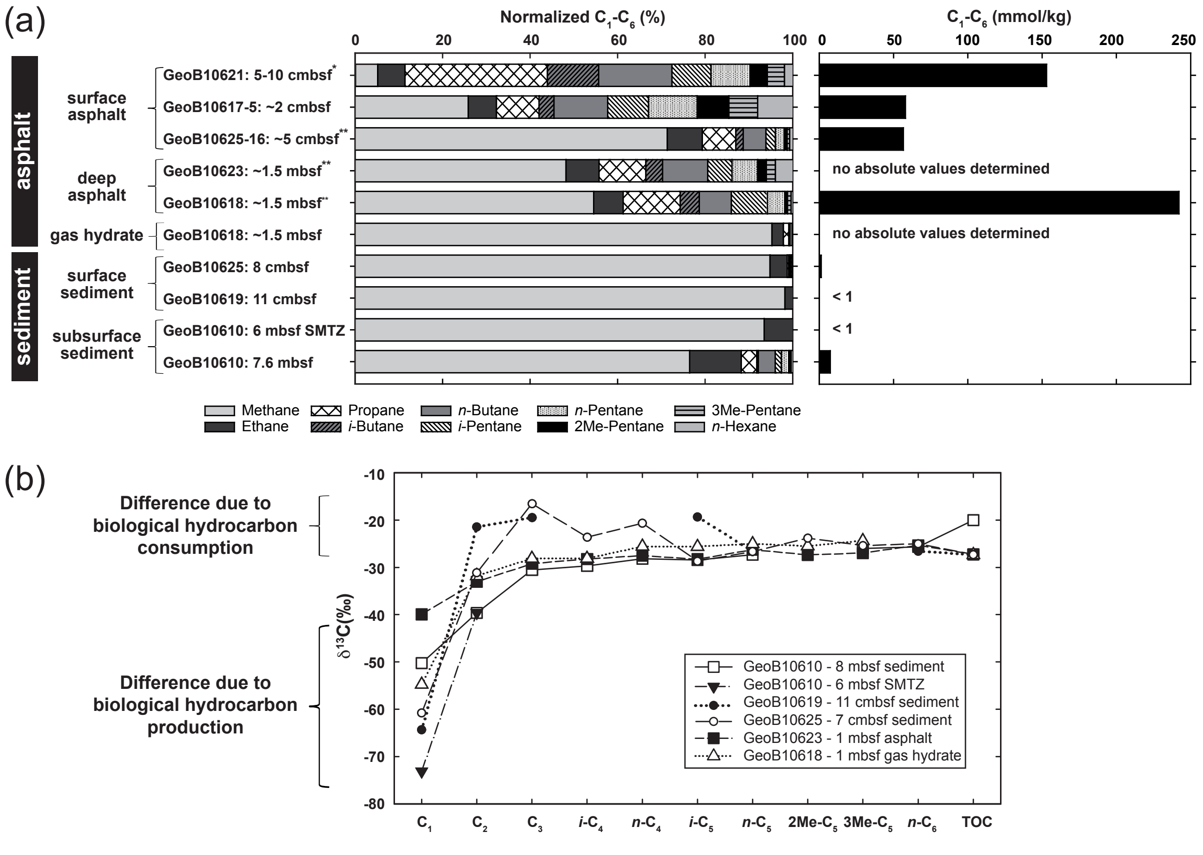

Fig. III.2. (**A**) Relative and total abundance of hydrocarbon gases in the asphalts and sediments. (**B**) Cross plot of the stable carbon isotopic composition of hydrocarbon gases in the asphalts and sediments. * Sample was collected with an autoclave device and represent *in-situ* gas concentrations, all other samples are affected by gas loss during recovery. ** These samples contained gas hydrates.

Table III.1. Concentration and stable carbon isotopic composition of hydrocarbon gases of asphalts and sediments.

		Surface asphalt			Deep asphalt		Gas hydrate	Surface sediments		Subsurface sediments	
		GeoB10617-5 2 cmbsf	GeoB10621 5-10 cmbsf	GeoB10625-16 5 cmbsf	GeoB10623 1.5 mbsf	GeoB10618 1.5 mbsf	GeoB10618 8 mbsf	GeoB10619 7 cmbsf	GeoB10625 11 cmbsf	GeoB10610 7.6 cmbsf	GeoB10612 7.65 mbsf
C_1-C_6	(mmol kg^{-1})	50.0	153.0	56.6	-	242.2	-	0.02	1.65	7.3	1.3
C_1	δ^{13}C in ‰ (relative abundance in %)	nd (30.0)	nd (5.2)	nd (71.3)	-39.9 (48.2)	nd (54.5)	-54.8 (95.3)	-65.4 (98.2)	-58.9 (94.9)	-50.3 (76.5)	-54.2 (96.5)
C_2		nd (7.5)	nd (6.2)	nd (8.0)	-33.1 (7.6)	nd (6.7)	-31.8 (2.6)	-19.7 (1.8)	-31.5 (3.9)	-39.6 (11.8)	-39.9 (3.2)
C_3		nd (11.3)	nd (32.5)	nd (7.7)	-29.2 (10.7)	nd (13.0)	-28.1 (1.3)	-24.6 (ta)	-17.8 (0.4)	-30.6 (3.6)	-29.4 (0.3)
i-C_4		nd (4.0)	nd (11.7)	nd (1.7)	-28.5 (3.8)	nd (4.4)	-28.1 (0.2)	nd (-)	-23.3 (0.3)	-29.7 (0.3)	-25.7 (ta)
n-C_4		nd (14.3)	nd (16.8)	nd (5.2)	-27.4 (10.3)	nd (7.3)	-25.6 (0.5)	nd (-)	-20.7 (0.2)	-28.2 (3.9)	-25.9 (ta)
i-C_5		nd (10.8)	nd (8.9)	nd (2.1)	-28.3 (5.6)	nd (8.2)	-25.6 (ta)	-20.6 (ta)	-23.5 (0.3)	-28.5 (1.4)	nd (-)
n-C_5		nd (12.9)	nd (8.9)	nd (2.0)	-26.3 (5.9)	nd (3.9)	-25.0 (ta)	-26.6 (ta)	nd (0.2)	-27.3 (1.7)	nd (-)
2me-C_5		nd (8.4)	nd (3.9)	nd (0.7)	-27.4 (2.0)	nd (0.6)	-25.5 (ta)	nd (-)	-23.3 (0.3)	(0.3)	nd (-)
3me-C_5		nd (7.6)	nd (3.9)	nd (0.6)	-27.0 (2.1)	nd (0.8)	-24.4 (ta)	nd (-)	-24.5 (ta)	(0.2)	nd (-)
n-C_6		nd (9.3)	nd (1.9)	nd (0.7)	-25.3 (3.9)	nd (0.4)	nd (ta)	-25.8 (ta)	-23.4 (ta)	(0.3)	nd (-)

nd – not detected or not determined
ta – trace amounts

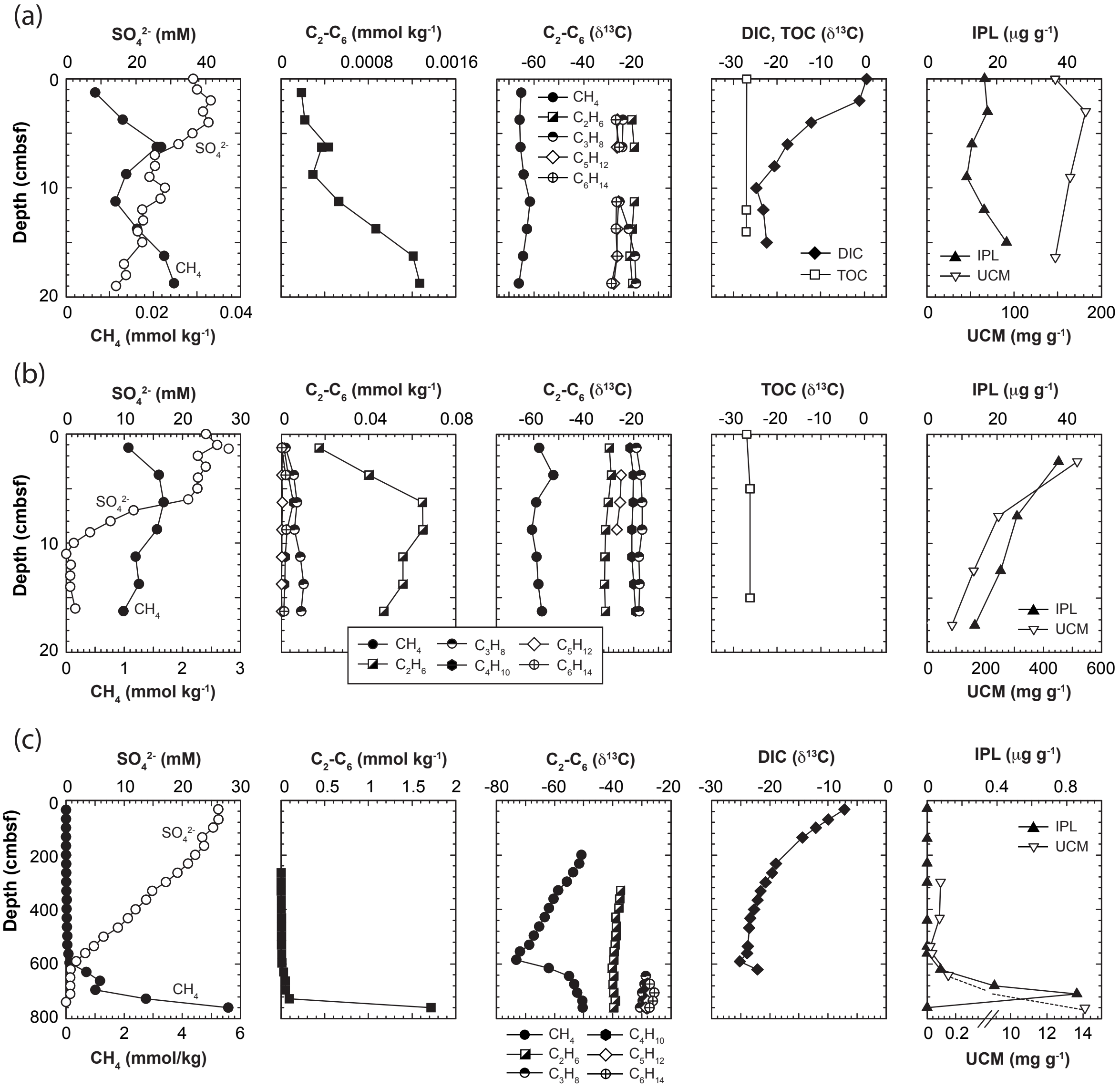

Fig. III.3. Geochemical profiles of concentrations and/or stable carbon isotopic compositions of hydrocarbon gases (methane to hexane), dissolved inorganic carbon (DIC), total organic carbon (TOC), sulfate, intact polar membrane lipids (IPLs), and petroleum-derived hydrocarbons (UCM) in the shallow push cores (**A**) GeoB10619 and (**B**) GeoB10625 and (**C**) the deep gravity core GeoB10610.

III.4.1.2. Petroleum-derived hydrocarbons

Petroleum-derived hydrocarbons in the asphalts and oil-impregnated sediments are characterized by the presence of an unresolved complex mixture (UCM), which cannot be readily resolved using conventional GC analysis (Fig. III.4). In the asphalts the UCM is found in the elution range of C_{14} to C_{40} *n*-alkanes and comprises between 260 to 340 mg g^{-1} asphalt, (Table III.2). UCMs are typically observed in biodegraded petroleum samples, and are formed after other oil-derived compounds have been selectively removed (cf. Peters and Moldowan, 1993). In the deeper layers of the asphalts (ca. 2 cm to 1 m asphalt depth) *n*-alkanes and isoprenoids are still present and distribute a unimodal distribution with a peak at C_{18} (Fig. III.4a). Closer to the asphalt surface a bimodal distribution of *n*-alkanes is observed, indicating that the short chain hydrocarbons (C_{14} to C_{25}) are being removed by hydrocarbon degradation (Fig. III.4b).

In accordance, the pristane to n-C_{17} ratio, commonly used as an indicator of the level of biodegradation (e.g., PETERS AND MOLDOWAN, 1993; WENGER AND ISAKSEN, 2002), increases from 0.33 to 0.71 in asphalts from deeper layers towards the surface (Table III.2). The presence of *n*-alkane and a comparably low Pr/n-C_{17} ratio in deeper asphalts despite the presence of the UCM can be explained by a combination of two processes, (*i*) a large heterogeneity of anaerobic biodegradation inside the asphalts and (*ii*) on-going recharge with pristine undegraded oil after initial biodegradation (i.e., formation of the UCM). It is unclear whether recharge is occurring inside the already deposited asphalt beds or in a potential shallow reservoir prior to seafloor eruption. On the asphalt surface nutrients from the seawater and the presence of oxygen facilitate the degradation of hydrocarbons by aerobic bacteria. Here, all *n*-alkanes and

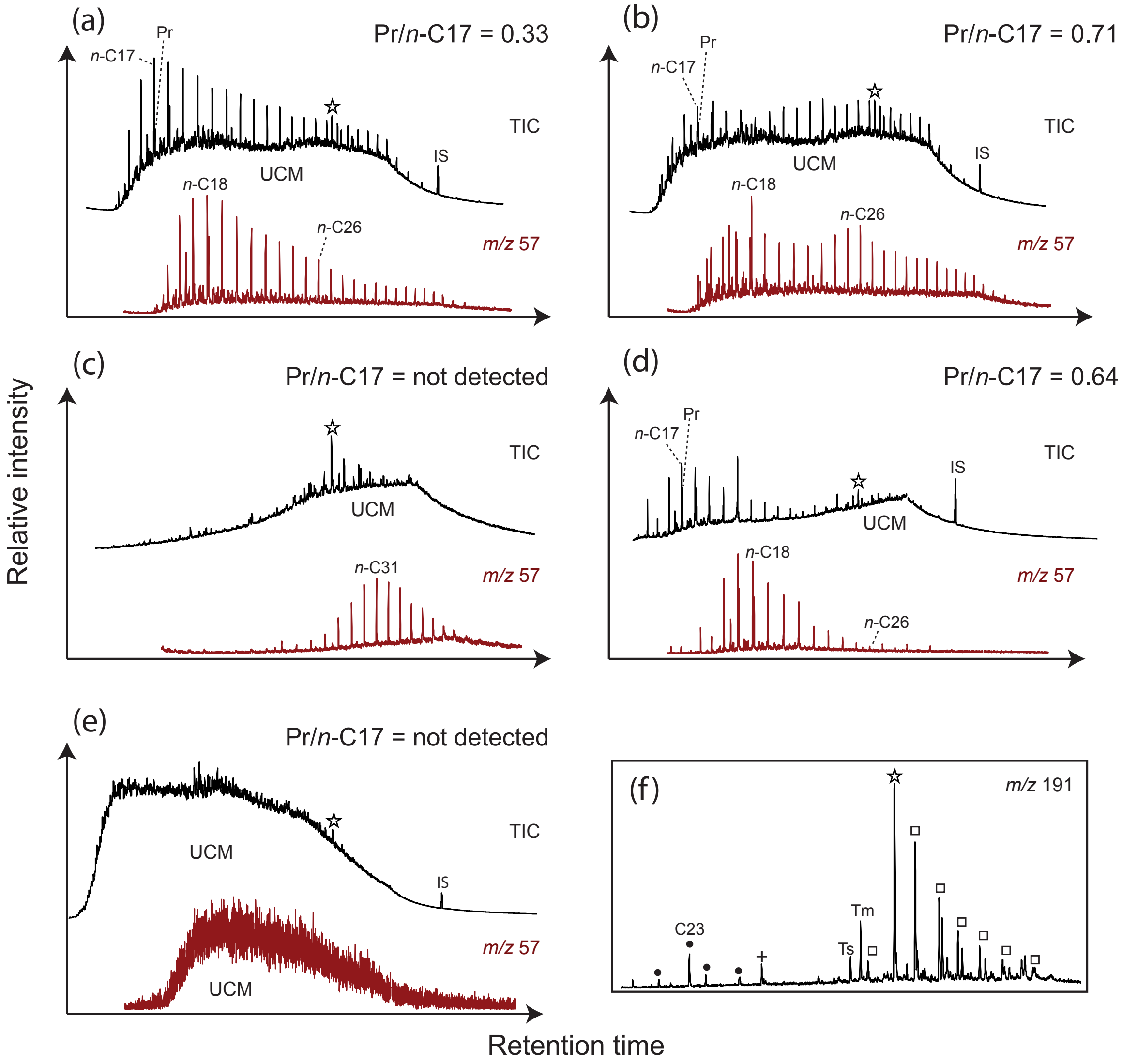

Fig. III.4. Total ion chromatograms (TIC) and mass chromatogram *m/z* 57, showing the *n*-alkane distribution of asphalts and oil-impregnated sediments. (**A**) Deep asphalt GeoB10623, 1.5 m asphalt depth, (**B**) shallow asphalt GeoB10617-6, 3 cm asphalt depth, (**C**), surface asphalt GeoB10619-17, (**D**) subsurface sediment GeoB10610, 7.6 m sediment depth, and (**E**) surface sediment GeoB10619, 5 cm sediment depth. (**F**) Extracted mass chromatogram *m/z* 191, it is the same for all asphalt and sediment samples. Abbreviations: UCM – unresolved complex misture, Pr – pristane, IS – injection standard, star – norhopane, filled circles – tricyclic terpanes (C_{22}-C_{25}), cross – C_{24} tetracyclic terpane, Ts - trisnorneohopane, Tm - trisnorhopane, open squares – 17α21β 22R and S hopane series (C_{28}-C_{35}).

Table III.2. Hydrocarbon composition and pristane (Pr) to C_{17} *n*-alkane (*n*-C_{17}) ratios of different asphalt samples.

Sample type, depth	Sample ID	Pr/*n*-C_{17}	mg Maltenes g^{-1} asphalt
Surface asphalt, 1 cm	GeoB10617-6	0.71	273
Surface asphalt, 2 cm	GeoB10617-6	0.53	264
Surface asphalt, 3 cm	GeoB10617-6	0.38	326
Surface asphalt, 1-10 cm	GeoB10621	0.41	278
Surface asphalt*	GeoB10625-16	0.33	309
Deep asphalt*, ~1.5 m	GeoB10618	0.43	326
Deep asphalt*, ~1.5 m	GeoB10623	0.31	280

* These samples contained gas hydrates.

isoprenoids in the carbon range C_{14} to C_{30} have been degraded, and also the lighter end of the UCM in the carbon number range C_{14} to C_{30} is lost (Fig. III.4c). Besides aerobic biodegradation other physicochemical processes such as water washing have likely contributed to a more unselective removal of the UCM-forming hydrocarbons after exposure of asphalts on the sea floor (e.g., WARDLAW ET AL., 2008; SCHUBOTZ ET AL., IN PREP., *CHAPTER V*).

The oils in subsurface sediments show a similar unimodal *n*-alkane distribution as the deeper asphalts. Comparably high pristine to *n*-C_{17} ratios of 0.64 indicate that anaerobic hydrocarbon degradation is occurring (Fig. III.4d). The oil in surface sediments, however, is very distinct as it is characterized by a lack of *n*-alkanes and isoprenoids and the presence of an elevated UCM in the range of C_{12} to C_{35} compounds (Fig. III.4e). This is an indication of severe biodegradation at these depth intervals. An increase in the UCM can additionally be caused by the production of biodegradation metabolites such as naphthenic acids (cf. AITKEN ET AL., 2004). In surface sediments anaerobic hydrocarbon degrading bacteria are most likely stimulated by the downward diffusion of sulfate from the overlying seawater.

The asphalts and oils of the sediments have matching distributions of triterpenoids, which can be used as source-related biomarkers (Fig. III.4f) and confirm their origin from Upper Jurassic, Thitonian, source rocks as known from other oils from the Campeche area (GUZMAN-VEGA AND MELLO, 1999; SCHOLZ-BÖTTCHER ET AL., 2009).

III.4.2. Porewater geochemistry of the sediments

The heterogeneity of near-surface petroleum seepage at the Chapopote is reflected in the geochemical profiles of the two oil-impregnated PUCs from sites GeoB10619 and GeoB10625, both situated in the immediate vicinity of the asphalt beds (<100 m; Fig. III.1a). Surrounding site GeoB10619, tubeworm bushes were found in patches on the seafloor (BOHRMANN ET AL., 2008). In comparison to site GeoB10625, which is situated closer to the main asphalt site, the sediments of GeoB10619 contain comparably lower concentrations of petroleum-derived HCs (130 to 170 mg g^{-1} sediment) and HC gases (~5 to 25 µmol kg^{-1} sediment, Fig. III.3a). Sulfate is present throughout the sediment core, however, gradual sulfate depletion and the presence of IPLs (~20 µg g^{-1} sediment) are indicative of microbial activity throughout the core. Sulfate concentrations, exceeding that of seawater (>40 mM) in the upper cm of PUC GeoB 10619 could be either due to local intrusions of brines or recent formation of gas hydrates close to the sediment surface. In contrast, site GeoB10625 contains three times higher concentration of petroleum-derived HC (15 to 520 mg g^{-1} sediment) and up to two orders of magnitude higher concentrations of HC gases (1 and 1.5 mmol kg^{-1}), seemingly stimulating microbial activity, which results in sulfate depletion after already 10 cm sediment depth (Fig. III.3b). At this site bacterial mats covering the seafloor were observed, which is further evidence of increased microbial activity (Bohrmann et al., 2008). Correspondingly, elevated IPL concentrations of up to 40 µg g^{-1} sediment are found in the upper 10 cm. Methane and higher HC gases are constantly supplied from the oil and are present throughout both sediment cores. Higher HC gases in PUC GeoB10619 could only be detected after alkaline leaching, indicating that these gases may also be sorbed to the sediments (cf. Hinrichs et al., 2006). There is no obvious shift in the HC gas isotopic composition throughout the shallow sediments at both sites. Low $\delta^{13}C$ values of methane (60‰ to 68‰) in both PUCs are indicative of a sizeable fraction of methane being derived from biological methanogenesis (Whiticar, 1999), whereas the $\delta^{13}C$ values of the C_2 to C_6 HC gases mainly reflect a thermogenic origin. Microbial activity is also reflected in the isotopic composition of the dissolved inorganic carbon (DIC) pool: In the surface sediments of site GeoB10619 the values are those of the seawater and with increasing sediment depth the values become increasingly depleted indicating a substantial contribution of heterotrophic CO_2 production. TOC remains constant at -27‰ throughout the sediment column of both PUCs, resembling the isotopic composition of the oil (Table III.1). Elevated IPL concentrations in surface sediments indicate an increase in microbial activity closer to the sediment-water interface, where input of nutrients and electron acceptors stimulate and enhance microbial hydrocarbon degradation.

The subsurface sediments of GRC GeoB10610, taken ~1 km northeast of the asphalt site are also influenced by oil, which was found in the core catcher at 7.6 mbsf. The presence of oil at 7.6 mbsf is reflected in the comparably low $C_1/(C_2+C_3)$ ratio, high overall HC gas concentrations (7 mmol kg^{-1} sediment) and $\delta^{13}C$ values for methane of -50‰, indicating a mainly thermogenic origin for methane (Whiticar, 1999; Fig. III.2c). Methane concentrations dramatically decline to <0.2 mmol/kg sediment at 6 mbsf, coinciding with a depletion of downward diffusing sulfate. At this SMTZ, depleted $\delta^{13}C$ DIC values (-27‰) confirm anaerobic methane oxidation as the dominating geochemical process. Notably, the SMTZ potentially extends over 1 m from 6 to 7 mbsf, as sulfate is still detected in low amounts (< 1 mM) until 7.2 mbsf. Towards the SMTZ methane $\delta^{13}C$ values become increasingly depleted in ^{13}C, reaching values of up to -75‰, indicating biogenic methane production (Borowski et al., 1997), potentially stimulated by oil-degrading bacteria (Zengler et al., 1999). Above the SMTZ methane becomes steadily enriched in ^{13}C, exhibiting a more diffusive profile. Depth profiles of $\delta^{13}C$ values of higher HC gases do not show marked differences, however ethane values of 40‰ are roughly 10‰ depleted in ^{13}C compared to ethane values in the surface sediments of site GeoB10619 and GeoB10625, which could be indicative of a partly biogenic origin of ethane as has been proposed for other deeply buried sediments (Hinrichs et al., 2006).

III.4.3. Diversity of intact polar lipids (IPLs) in asphalts and sediments – insights on microbial community composition

A variety of IPLs comprised of ether- and ester-linked glycerolipids with phospho-, glyco-, and amino-based head groups are detected in the asphalts and the oil-impregnated sediments (Figs. III.5, III.6, III.7, Table III.3, III.4). Their assignment to different groups of bacteria and archaea are discussed here.

III.4.3.1. Bacterial IPLs

III.4.3.1.1. Asphalts. In asphalt samples that contained gas hydrates phospholipids with diacylglycerol (DAG) and dietherglycerol (DEG) core structures are abundantly detected and can be assigned to bacterial sources (Fig. III.6a). Phospho-based head groups are composed of phosphatidylethanolamine (PE) and phosphatidyl-(N)-methylethanolamine (PME). IPL concentrations range from 280 to 500 ng g^{-1} asphalt, PME head groups were only detected in the sample with higher IPL concentrations. The PE and PME core lipids consist of mainly saturated and monounsaturated acyl and alkyl side chains with total sum of carbon chains between C_{30} and C_{34} (cf. Table III.4). PE and PME-DAG are common lipids in bacteria (Kates, 1966, Goldfine, 1984); and are commonly observed in marine sediments (e.g., Rossel et al., 2008; Schubotz et al., 2009, *Chapter II*). PE-DEG has so far only been found in thermophilic sulfate-reducing bacteria (Sturt et al., 2004) and Myxobacteria (Caillon et al., 1983), however, the

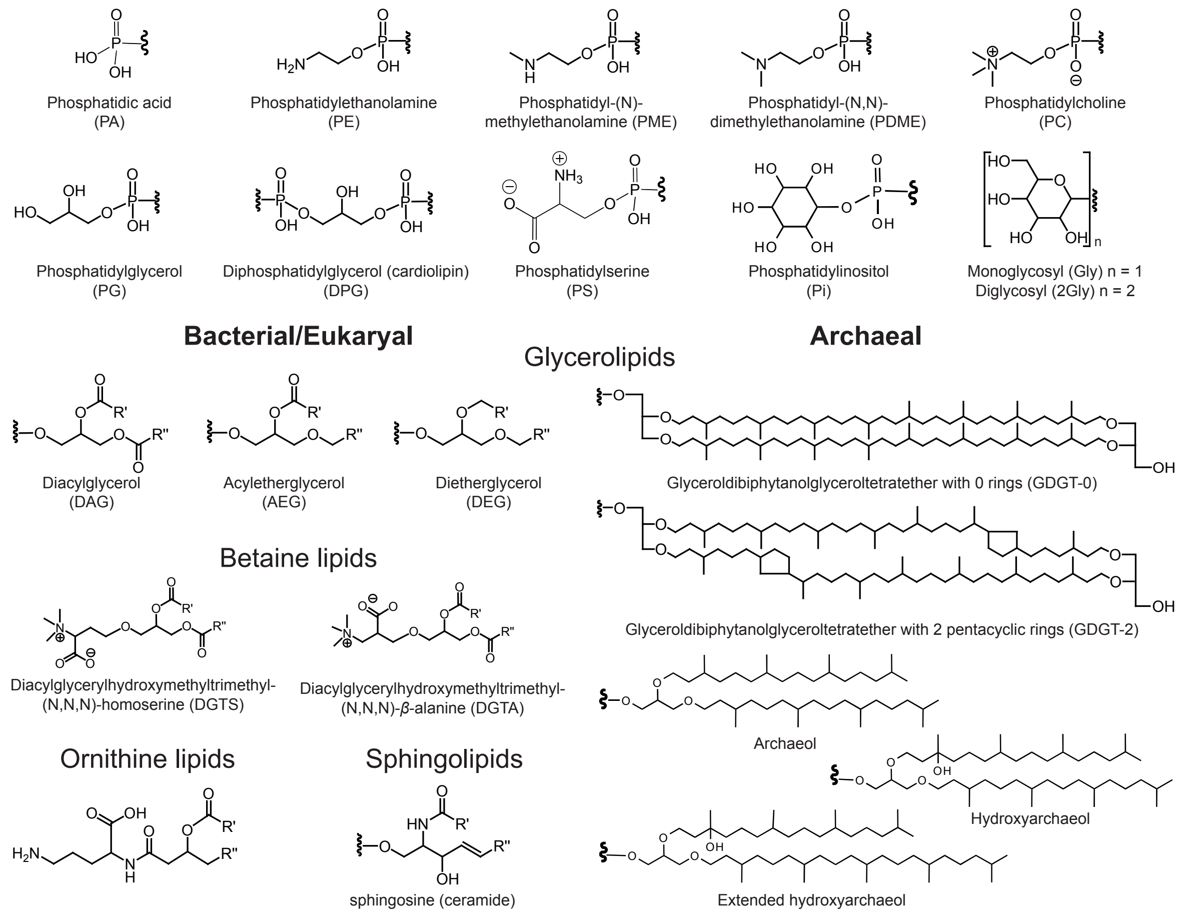
Phosphatidic acid (PA)
Phosphatidylethanolamine (PE)
Phosphatidyl-(N)-methylethanolamine (PME)
Phosphatidyl-(N,N)-dimethylethanolamine (PDME)
Phosphatidylcholine (PC)
Phosphatidylglycerol (PG)
Diphosphatidylglycerol (cardiolipin) (DPG)
Phosphatidylserine (PS)
Phosphatidylinositol (Pi)
Monoglycosyl (Gly) n = 1
Diglycosyl (2Gly) n = 2
Bacterial/Eukaryal
Glycerolipids
Archaeal
Diacylglycerol (DAG)
Acyletherglycerol (AEG)
Dietherglycerol (DEG)
Glyceroldibiphytanolglyceroltetratether with 0 rings (GDGT-0)
Glyceroldibiphytanolglyceroltetratether with 2 pentacyclic rings (GDGT-2)
Betaine lipids
Diacylglycerylhydroxymethyltrimethyl-(N,N,N)-homoserine (DGTS)
Diacylglycerylhydroxymethyltrimethyl-(N,N,N)-β-alanine (DGTA)
Archaeol
Hydroxyarchaeol
Ornithine lipids
Sphingolipids
sphingosine (ceramide)
Extended hydroxyarchaeol

Fig. III.5. Structures of core lipids and head groups of the identified intact polar membrane lipids.

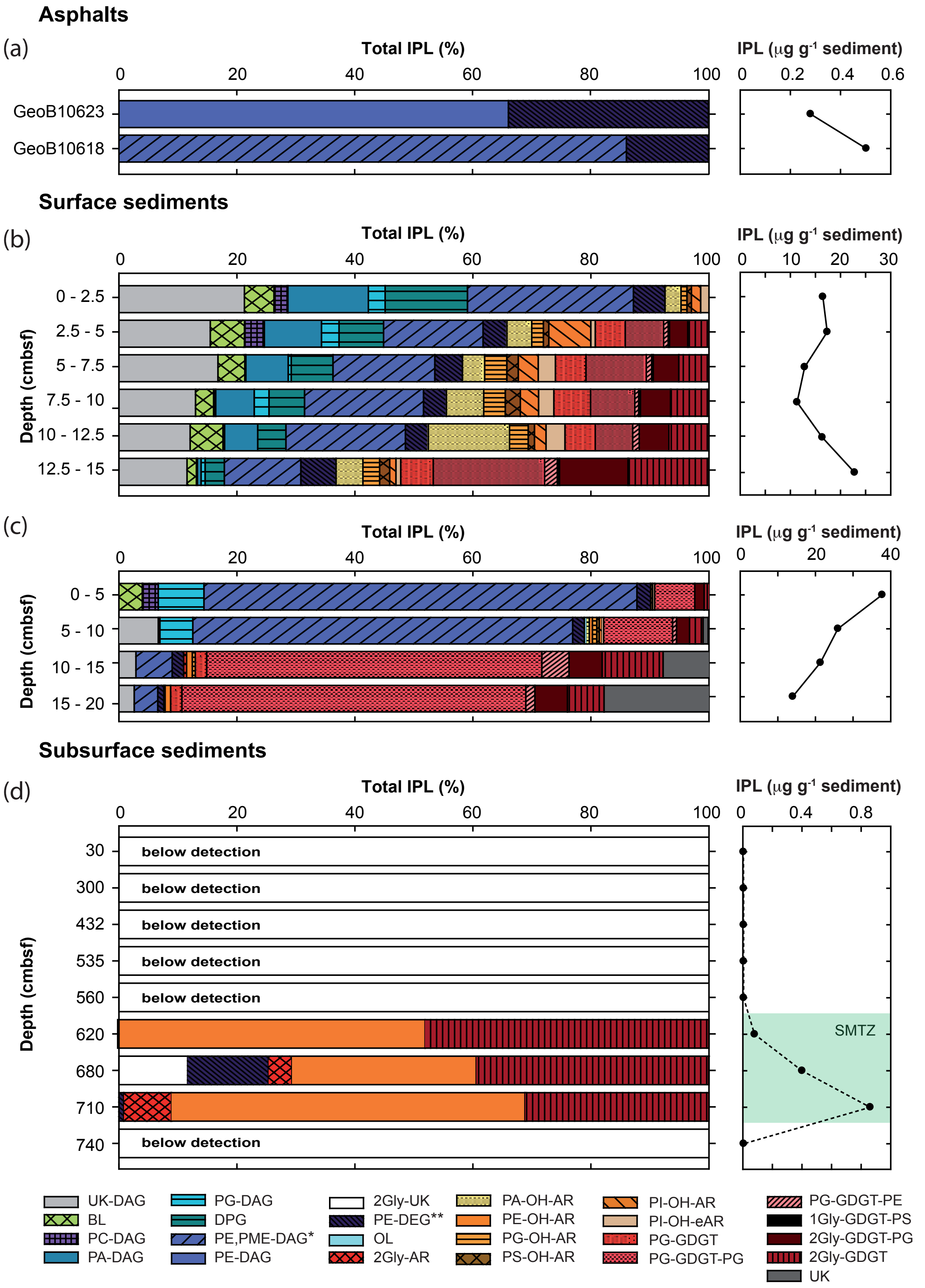

Fig. III.6. Distribution and absolute concentrations of intact polar membrane lipids (IPLs) in (**A**) deep asphalt samples associated to gas hydrates, (**B**) surface sediments from site GeoB10619, and (**C**) GeoB10625, and subsurface sediments from site GeoB10610. * At some depths, also PDME-DAG was observed (see main text), ** In the subsurface sediments (GeoB10610) also PME-DEG was observed.

GC-amenable apolar derivatives are frequently observed in marine sediments, where they have been assigned to uncultered mesophilic sulfate-reducing bacteria (e.g., Hinrichs et al., 2000, Pancost et al., 2001; Arning et al., 2008). Hence, likely sources for the bacterial phospholipids in the asphalts are sulfate-reducing bacteria (SRB) but also other oil-degrading bacteria, e.g., *Synthrophus sp.*, which were detected in these asphalts (G. Wegener, K. Knittel et al., pers. comm.) could be a potential biological source. Notably, only the gas hydrate containing asphalt contained detectable bacterial IPLs, thus indicating that elevated bacterial biomass is associated to the presence of gas hydrate.

III.4.1.1.2. Surface sediments. In the oil-impregnated surface sediments a more diverse suite of bacterial IPLs is observed (Figs. III.6b,c, III.7). Sites GeoB10619 and GeoB10625 contain similar IPLs, albeit in different relative and absolute concentrations. DAG-based IPLs with phospho head groups make up the majority of IPLs in the upper sediment layers of both PUCs (up to 70% of total IPLs). The head groups of these phospholipids at site GeoB10619 are composed of PE, followed by PME, diphosphatidylglycerol (DPG, cardiolipin), phosphatidic acid (PA), phosphatidylglycerol (PG), phosphatidyl-(N,N)-dimethylethanolamine (PDME) and phosphatidylcholine (PC). Sediments of station GeoB10625 contain mainly PE-, PME-, and PG-DAG with minor amounts of PC-DAG. The total abundance of DAG phospholipids in both cores decreases with increasing depth from 7.5 to 3 µg g^{-1} sediment (GeoB10619) and from 21 to 1 µg g^{-1} sediment (GeoB10625; Fig. III.3a,b, III.6). The acyl moieties of the phospholipids are mainly composed of combinations of C$_{14:0}$, C$_{15:0}$, C$_{16:0}$ and C$_{16:1}$ and C$_{18:0}$ fatty acids (FAs) (Table III.4). The bacterial origin of the DAG phospholipids is supported by the dominance of odd-carbon numbered FAs (Lechevalier, 1977; Fulco, 1983). Considering the geochemical conditions, it is likely that most of the phospholipids are derived from SRB, as they are frequently

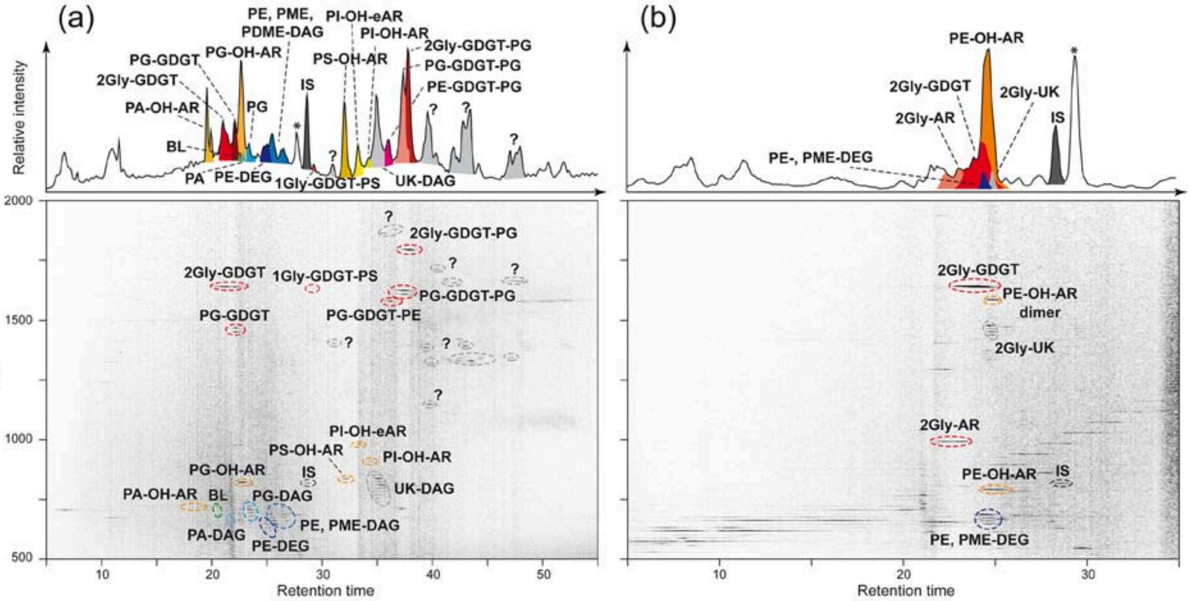

Fig. III.7. Density maps and chromatograms showing the distribution of intact polar lipids in (**A**) 12.5 to 15 cmbsf at site GeoB10619 and (**B**) 680 cmbsf at site GeoB10610. For abbreviations of lipid names refer to the text. * denotes contaminant; ? denotes unknown compounds.

Table III.3. Examples of characteristic fragmentation patterns in positive and negative ion mode of the intact polar membrane lipids (IPLs) observed in this study. All values in *m/z*.

IPL		Positive ion mode			Negative ion mode	
Head group	Core	MS^1 (adduct)	MS^2	MS^3	MS^1 (adduct)	MS^2
		Bacteria				
UK	15:0/15:1-DAG	784 (NH_4^+)	523	nd	765 (H^-)	241, 299
BL	16:0/17:1-DAG	724 (H^+)	456, 464, 486, 236	nd	nd	nd
PC	18:1/18:1-DAG	786 (H^+)	184	nd	830 ($HCOO^-$)	770, 281
PG	16:0/16:1-DAG	738 (NH_4^+)	549		719 (H^-)	253, 255
DPG	16:1/16:1-DAG-16:1/16:0-DAG	1364 (NH_4^{2+})	nd	nd	1345 (H^-)	779, 645, 643, 391, 389
PE	15:0/16:1-DAG	676 (H^+)	535	nd	674 (H^-)	241, 253
PE	16:1/17:1-DEG	688 (H^+)	645, 408	nd	686 (H^-)	643
PME	15:0/16:1-DAG	690 (H^+)	535	nd	688 (H^-)	241, 253
PDME	15:0/16:1-DAG	702 (H^+)	535	nd	700 (H^-)	241, 253
OL	3-OH-15:0/16:0	597 (H^+)	355, 335, 319	115	595 (H^-)	nd
		Archaea				
PA	OH-AR	749 (H^+)	453	nd	nd	nd
PG	OH-AR	823 (H^+)	527	nd	nd	nd
PG	GDGT-2	1470 (NH_4^+), 1452 (H^+)	1298, 1280	nd	nd	nd
PG-PG	GDGT-2	1623 (NH_4^+), 1606 (H^+)	1451, 1377	1298	1604(H^-)	1513, 1450
PE	OH-AR	792 (H^+)	496, 453	nd	nd	nd
PG-PE	GDGT-1	1577 (H^+)	1423, 1379	1300	nd	nd
PS	OH-AR	836 (H^+)	540, 522, 453	nd	834	747
PI	OH-AR	911 (H^+)	615	nd	nd	nd
PI	OH-eAR	961 (H^+)	685	nd	979	241
Gly-PS	GDGT-0	1632 (H^+)	1469	1302	nd	nd
2Gly-PG	GDGT-2	1794 (NH_4^+)	1451	1298	nd	nd
2Gly	AR	994 (NH_4^+)	653	nd	nd	nd
2Gly	GDGT-3	1637 (NH_4^+)	1296	nd	nd	nd
UK	GDGT-1	1655 (NH_4^+)	1413	1300	1637 (H^-)	1514, 1452
		Eukarya				
1Gly	d28:2/16:0-Cer	850 (NH_4^+)	688, 670, 654, 266	nd	894	848
PE	18:0p/20:4 Plasmalogen	752 (H^+)	611, 392, 359	nd	nd	nd
PE	17:0-*lyso*	510 (H^+)	184	nd	554 ($HCOO^-$)	494
PC	$C_{20:5}$/$C_{18:0}$-DAG	808 (H^+)	184	nd	852 ($HCOO^-$)	301
UK	-DAG	650 (NH_4^+)	nd	nd	631 (H^-)	nd

nd not detected

observed in oil-contaminated sediments (e.g., Rueter et al., 1994; Widdel et al., 2003). Indeed, PE, PG and DPG, the most abundant IPLs in core GeoB10619, are the main membrane-forming lipids in SRB (Makula and Finnerty 1975; Rütters et al., 2001; Sturt et al., 2004). Potential source organisms for PME-, PDME- and PC-DAG, which are predominantly found in the upper 5 cm of both sites could be denitrifying bacteria (Hagen et al., 1966; Goldfine and Hagen, 1968), which are also known to degrade aromatic oil-compounds (e.g., Rabus and Widdel, 1995). Other clades of bacteria that are known to produce PC and potentially PME and PDME belong to alpha- and gammaproteobacteria, bacteroides-flavobacteria, and some gram-positive bacteria (Sohlenkamp et al., 2003). PA, which is abundantly observed at site

GeoB10619 (up to 10% of total IPLs) cannot be clearly linked to a certain organism, as it is an intermediate in general phospholipid synthesis (Christie, 2003).

PE glycerolipids also occur as DEGs in shallow sediments at both PUC sites. PE-DEGs increase in concentration with depth from 0.7 to 1.3 µg g^{-1} sediment at site GeoB10619, and decrease from 1 to 0.2 µg g^{-1} sediment at site GeoB10625. Their core lipids contain combinations of ether-bound $C_{15:0}$, $C_{16:0,}$ $C_{16:1}$ and $C_{17:1}$ alkyl chains. Although DEG-based phospholipids have to date only been observed in thermophilic SRB (Langworthy et al., 1974; Sturt et al., 2004) and Myxobacteria (Caillon et al., 1983), their abundant distributions in cold marine sediments and microbial mats point to a more widespread occurrence of these lipids in mesophilic bacteria (e.g., Rütters et al., 2002; Schubotz et al., 2009, *Chapter II*; Seidel, 2009). For instance, at seep sites the presence of DEG-based phospholipids has been associated to SRB of AOM-mediating consortia (Sturt et al., 2004; Rossel et al., 2008). Likewise, their strongly ^{13}C depleted GC-amenable degradation products have been interpreted as products of SRB associated with AOM (e.g., Hinrichs et al., 2000; Pancost et al., 2001; Elvert et al., 2003, 2005). Further taxonomic information on the source organism can be gained by the analysis of core lipids by GC. However, due to analytical difficulties caused by the interference of oil-derived compounds we were not able to readily analyze the composition of phospholipid-derived fatty acids and alkyl moieties nor gain further information on their isotopic values in order to confirm SRB as the most likely source organism.

Table III.4. Major core lipid composition of intact polar membrane lipids (IPL) in the asphalts and at different sediment depths.

Sample	IPL	Major core structure
Asphalt	PE-DAG	C30:0[a], C30:1[a], C31:0[a], C32:1[a], C33:1[a]
	PME-DAG	C36:3[a], C34:2[a]
	PE-DEG	C34:2, C32:1, C31:1 [a]
Surface sediments (0 – 20 cmbsf)	UK-DAG	15:0/15:1
	BL	16:0/18:1, 16:0/17:1, 17:0/17:1
	PA-DAG	16:0/16:1, C34:1[a]
	PG-DAG	C34:1[a], C34:2[a], C32:1[a]
	DPG	16:1/16:1/16:1/16:0
	PE-, PME-, PDME-DAG	15:0/15:0; 15:0/16:1, 16:0/16:1, 15:0/14:0, 14:0/14:0
	PC-DAG	C36:2[a], C34:2[a], C33:2[a], C31:1[a]
	OL	OH-15:0/15:0
	UK-GDGT	1[b]
	2Gly-GDGT	3 > 2 >> 0,1[b]
	2Gly-GDGT-PG	3 > 2 >> 0,1[b]
	Gly-GDGT-PS	0 > 1[b]
	PG-GDGT	2 > 1[b]
	PG-GDGT-PG	2 > 3 >> 0,1[b]
	PG-GDGT-PE	1 > 0[b]
Subsurface sediments (620 -710 cmbsf)	PE, PME-DEG	16:1/17:1
	2Gly-GDGT	1 > 0,2[b]

[a]denotes sum of core lipid carbon chain length
[b]denotes number of pentacyclic rings in the GDGT core structure

Non-phosphorous fatty acid-containing IPLs observed in the sediments are betaine lipids (BL), and ornithine lipids (OL, only detected in PUC GeoB10625). BLs make up <10% of total IPLs and decrease in absolute abundance with depth from 0.7 to 0.3 µg g^{-1} sediment at site GeoB10619 and are not detectable below 5 cmbsf at station GeoB10625 (Fig. III.6). Their acyl moieties are mainly composed of $C_{16:0}/C_{18:1}$ and minor amounts of $C_{16:0}/C_{17:1}$ and $C_{17:0}/C_{17:1}$. BL are known to occur abundantly in algae and aquatic environments (e.g., Dembitsky, 1996; Ertefai et al., 2008; Van Mooy et al., 2009). In surface sediments they could potentially be incompletely degraded remnants associated with rapidly sinking plankton detritus (Fowler and Knauer, 1986; Ertefai et al., 2008). However, the fatty acid distribution of the BL does not indicate an algal source, as polyunsaturated fatty acids, typical for marine algae (Brett and Müller-Navarra, 1997), are absent. Instead, the presence of odd carbon-numbered fatty acid combinations such as $C_{17:0}$ and $C_{17:1}$ point to a bacterial source (Lechevalier, 1977; Fulco, 1983). Only recently BL were found in a number of studies in anoxic marine settings inferring an unknown mesophilic bacterial source for these lipids (Rossel, 2009; Schubotz et al., 2009, *Chapter II*; Seidel, 2009). Potential source organisms for BL in the bacterial domain belong to the alphaproteobacteria (Benning et al., 1995; López-Lara et al., 2003). OL, detected in small amounts in PUC GeoB10625, are minor IPLs found in SRB (Makula and Finnerty, 1975; Seidel, 2009), which are likely biological sources in these sediments. Additionally some IPLs with unknown head groups were observed, they were assigned to Bacteria due to the presence of fatty acids in their side chains (UK-DAG; Table III.2)

In context of the geochemical conditions and biomarker distributions we conclude that SRB are the predominant source organisms for a majority of the bacteria-derived IPLs in both shallow sediment sites. Sulfate is present throughout the sediment core in the shallow sediments and is therefore an easily accessible electron acceptor during hydrocarbon oxidation. It has been demonstrated *in-vitro* that a variety of SRB are capable to degrade a wide range of oil-derived hydrocarbons under anoxic conditions and they are among the most frequently isolated bacteria from oil-contaminated sediments (Rueter et al., 1994; Rabus et al., 1993; So and Young, 1999; Musat et al., 2009). SRB are also involved as synthrophic partners in AOM, which is likely to occur in these sediments. One striking difference between the two shallow PUCs is the higher diversity of IPLs at Site GeoB10619, whereas site GeoB10625 is mainly dominated by bacterial PE-DAG in the top 10 cmsbf and by archaeal PG-GDGT-PG in the deeper 10 to 20 cmbsf. As site GeoB10625 contains higher amounts of petroleum-derived hydrocarbons, these observations suggest that higher upward fluxes of hydrocarbons select for a simpler microbial community synthesizing more uniform IPLs whereas lower fluxes support a more diverse microbial community with a more complex IPLs distribution.

III.4.1.1.3. Subsurface sediments. In subsurface sediments at site GeoB10610 IPLs could only be detected in the SMTZ from 6 to 7 mbsf, with highest concentrations of 800 ng g^{-1} sediment at 7.1 mbsf. PE- and PME-DEG are the only IPLs that could be assigned to bacteria (Fig. III.6d). Furthermore an unknown IPL with a diglycosidic head group and core lipids in the mass range of *m/z* 1438 to 1480 was observed (2Gly-UK). Differences of 14 mass units indicate different chain lengths as known from Bacteria. PE and PME-DEGs have highest relative (up to 10% of total IPLs) and absolute (~60 ng g^{-1} sediment) abundances at 6.8 mbsf, and are observed in low amounts (~8 ng g^{-1} sediment) at 7.1 mbsf, but are below the detection limit at other depths. Similarly, the 2Gly-UK is observed only at 6.8 mbsf, comprising almost 10% of total IPLs. The core structures of PE-DEG mainly consist of ether-bound $C_{16:1}$ and $C_{17:1}$ alkyl chains. At 6.8 to 7.1 mbsf the DEG phospholipids are possibly derived from SRB operating at low levels of sulfate and could be potentially linked to AOM since no bacterial lipids were detectable above or below the SMTZ.

It is noticeable that the ratio from bacterial DAG to DEG increases with increasing burial depth. In subsurface sediments, microbial communities must cope with severe energy limitation that results from low supply of nutrients and electron acceptors and the presence of recalcitrant organic matter. VALENTINE (2007) has suggested that the archaeal membrane lipid architecture, consisting of mainly diether and tetraether lipids (cf. KOGA AND NAKANO, 2008) and the resulting low permeability would favor Archaea relative to Bacteria in coping with chronic energy limitation as encountered in subsurface sediments. In analogy to the chemical robustness of archaeal membrane lipids, we suggest that the dominance of bacterial DEG lipids in subsurface sediments reflects the selection of Bacteria that have adapted to the harsher conditions of the deep biosphere by mainly synthesizing ether lipids.

III.4.3.2. Archaeal IPLs

Although bacterial IPLs were observed inside the asphalts, archaeal IPLs were not detectable. However, in surface and subsurface sediments a wide variety of IPLs are present that can be assigned to Archaea

III.4.3.2.1. Surface sediments. In the shallow sediments at sites GeoB10619 and GeoB10625 diether and tetraether glycerolipids are abundantly detected which could be assigned to Archaea due to their isoprenoid-based core structure (Figs. III.5, III.6a,b). Observed archaeal diether lipids are C_{20}/C_{20} archaeol (AR), C_{20}/OH-C_{20} hydroxyarchaeol (OH-AR), and C_{25}/OH-C_{20} extended hydroxyarchaeol (OH-eAR). The dominant archaeal diethers in GeoB10619 are hydroxyarchaeol lipids (>99% of total isoprenoidal ether lipids, 0-2.5 cmbsf) with the tentatively identified phosphate-based head groups PG, PA, phosphatidylinositol (PI) and phosphatidylserine (PS); OH-eAR is only observed with PI as head group (cf. Fig. III.5). Archaeol is only detected in the deeper layers of site GeoB10625 (<1%, 1520 cmbsf) and contains diglycosydic head groups (2Gly). Maximum concentrations of total isoprenoidal diether IPLs range between 1 (GeoB10625) and 3 µg g^{-1} sediment (GeoB10619). Their relative abundance ranges between 7 to 20% of total IPLs at site GeoB10619 and at site GeoB10625 they make up ~2% of total IPL in surface sediments and decrease to <1% in the deeper layers. OH-AR derivatives are commonly found in methanogenic archaea, particularly of the genera *Methanosarcinales* and *Methanococcales* (KOGA ET AL., 1998; KOGA AND NAKANO, 2008), and are also often observed at seep sites where they have been linked to methanotrophic ANME-2 archaea that are affiliated with the *Methanosarcinales* (e.g., Blumenberg et al., 2004; Rossel et al., 2008). In both methanogenic and methanotrophic archaea, OH-ARs are present as PG, PE, PI and PS (Koga et al., 1998, Rossel et al., 2008), as observed in this study. OH-eAR has only recently been reported to be present at seep sites, where it was suggested to be indicative of halophilic ANME-2 archaea (Stadnitskaia et al., 2008). In agreement with observations at other AOM-dominated sites, the polar derivative is PI-OH-eAR (Rossel, 2009). We therefore conclude that the most likely biological source for PA-, PG-, PI-, and PS-OH-AR and PI-OH-eAR in the surface sediments are ANME-2 archaea, however also some contributions from methanotrophic archaea is possible. Notably 2Gly-AR and PE-OH-AR, which are only observed below the sulfate depletion depth at site GeoB10625 are more likely to be mainly derived from methanogenic archaea as they would not be expected in the sulfate-reduction zone (Kristjannson et al., 1982; Schönheit et al., 1982).

Membrane-spanning archaeal glyceroldibiphytanyltetraethers (GDGT) with acyclic structure or containing one, two or three pentacyclic rings (GDGT-0, GDGT-1, GDGT-2, GDGT-3) become the dominant IPLs towards the bottom of both PUCs. In the surface sediments of site GeoB10619, they are below detection limit and increase to 11 µg g^{-1} sediment at 15 cmbsf. In core GeoB10625 their relative abundance increases from 15% to 90% of total sediments with increasing sediment depth and absolute abundances of 15 µg g^{-1} sediment at 15 cm sediment depth. In both PUCs, the archaeal GDGT are linked to a diverse suite of phosphate- and sugar-based head groups that were tentatively identified by MS fragmentation patterns (Fig. III.8, Table III.3). At site GeoB10619 the most abundant GDGT throughout the sediment core contains as head group two PG (PG-GDGT-PG), followed by diglycoside (2Gly-GDGT), one PG (PG-GDGT), and mixtures of PG and diglycoside (2Gly-GDGT-PG). Less abundant IPL-GDGTs are PG-GDGT-PE and Gly-GDGT-PS. The IPL-GDGT distribution is similar at site GeoB10625, however, PG-GDGT-PG is by far the most abundant IPL and in deeper sediment layers an unknown tentatively identified GDGT was observed (Fig. III.6c, Table III.3). The core lipids of 2Gly-GDGT, 2Gly-GDGT-PG, and PG-GDGT-PG are predominantly bi- and tricyclic with minor contributions of acyclic and monocyclic GDGTs. PG-GDGT is mainly composed of bi- and monocyclic GDGT. PG-GDGT-PE and Gly-GDGT-PS consist of acyclic and monocyclic GDGTs (Table III.4). GDGTs are prominent membrane constituents in cultured members of the two archaeal kingdoms euryarchaeaota and crenarchaeaota. Mesophilic euryarchaeaota contain acyclic GDGT (GDGT-0) as the most dominant core structure, next to mainly monocyclic and bicyclic GDGTs (e.g., Koga and Morii 2005). Uncultured methanotrophic archaea of the ANME-1 cluster where shown to contain GDGT-0, GDGT-1 and GDGT-2 core lipids (Blumenberg et al., 2004) and IPLs of ANME-1 archaea are mainly composed of 2Gly-GDGT (Rossel et al., 2008). On the contrary methanogenic archaea of the order *Methanomicrobiales* and *Methanobacteriales* contain often phosphate-based head groups (Koga et al., 1998; Koga and Nakano, 2008; Strapoc et al., 2008, *Chapter VId*). However, at some seep settings where ANME-1 archaea dominate, diverse suites of phospho- and mixed

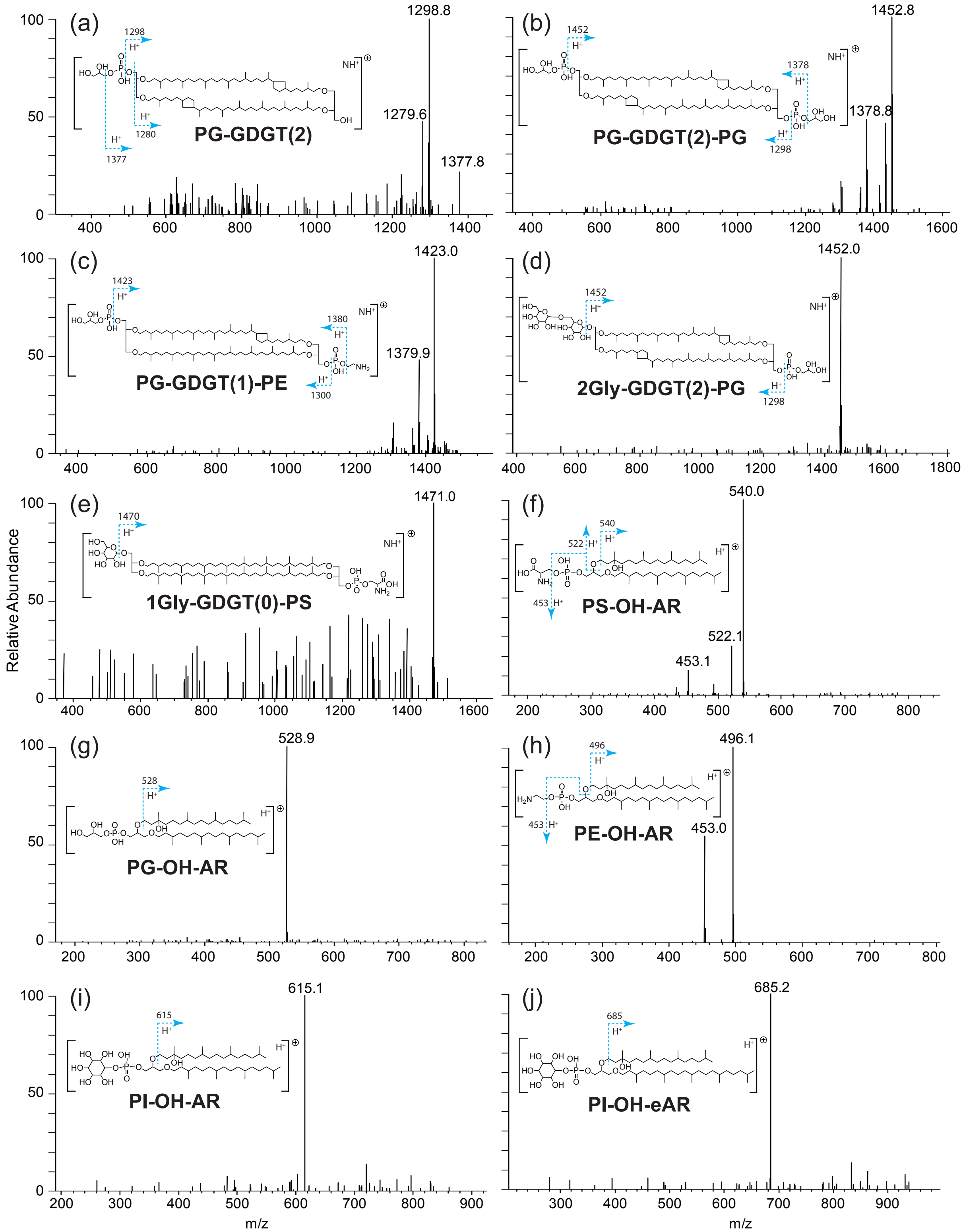

Fig. III.8. Mass spectra of tentatively identified intact archaeal isoprenoidal ether lipids in positive ion mode. (**A**) MS^2 of base peak ion *m/z* 1452, identified as PG-GDGT(2), (**B**) MS^2 of base peak ion *m/z* 1623, identified as PG-GDGT(2)-PG, (**C**) MS^2 of base peak ion *m/z* 1577, identified as PG-GDGT-PE, (**D**) MS^2 of base peak ion *m/z* 1794, identified as 2Gly-GDGT-PG, (**E**) MS^2 of base peak ion *m/z* 1632, identified as 1Gly-GDGT-PS, (**F**) MS^2 of base peak ion *m/z* 836, identified as PS-OH-AR, (**G**) MS^2 of base peak ion *m/z* 823, identified as PG-OH-AR, (**H**) MS^2 of base peak ion *m/z* 792, identified as PE-OH-AR, (**I**) MS^2 of base peak ion *m/z* 911, identified as PI-OH-AR, (**J**) MS^2 of base peak ion *m/z* 981, identified as PI-OH-eAR.

phospho- and glyco-GDGTs, similar to this study were found (Rossel, 2009). It is therefore not clear whether a distinction into methanotrophic and methanogenic archaea can be made on the basis of their phosphate of glycoside containing head group.

In summary, in surface sediments OH-ARs and OH-eAR with phospho head groups are most likely derived from ANME-2 archaea, whereas GDGT-based IPLs are indicative of ANME-1 methanotrophs. Increased abundances of 2Gly-AR and GDGTs with phospho head groups below depletion of sulfate could be indicative of the additional presence of methanogenic archaea. Noticeable, GDGT-based IPLs become more abundant than OH-AR-based IPLs, with sediment depth. This shift is most obvious in core GeoB10625, which exhibits a similaryl pronounced shift in the geochemical profile. At 15-20 cmbsf, OH-AR derivatives are present only in trace concentrations and PG-GDGT-PG becomes the most abundant lipid. These changes in IPL composition are likely reflective of a community shift from ANME-2 to ANME-1 archaea (Rossel et al., 2008) and/or methanogenic archaea.

III.4.3.2.2. Subsurface sediments. In the subsurface sediments at site GeoB10610 archaeal IPLs are composed of both diether and tetraether glycerolipids, and - like the bacterial IPLs - are only detectable within the SMTZ between 6 and 7 mbsf. The most abundant isoprenoidal diether lipid is PE-OH-AR, followed by 2Gly-AR. Highest abundances of both archaeol-based IPLs are observed at 7.1 mbsf (570 ng g^{-1} sediment, total sum) at the bottom of the SMTZ. The presence of archaeol-derived IPLs in and below the SMTZ could either point to ANME-2 archaea or the presence of methanogenic archaea. Remarkably, OH-AR is mostly present as PE derivative, whereas in surface sediments at sites GeoB10619 and GeoB10625 OH-AR are only observed as PA, PG, PS, and PI derivatives; in both cases PE-OH-AR, as well as 2Gly-AR are only detected after sulfate is depleted (Fig. III.6). A plausible explanation is that PE-OH-AR and 2Gly-AR are associated with methanogenic archaea, which would explain the increasingly depleted $\delta^{13}C$ values of methane at these depths.

The most abundant intact tetraether lipid is 2Gly-GDGT with maximum concentrations of 260 ng g^{-1} sediment at 7.1 mbsf and relative abundances of 35 to 50% of total IPLs. The core structure of 2Gly-GDGTs is mainly composed of GDGT-1 with small amounts of GDGT-0 and -2. In deeply buried sediments off Peru 2Gly-GDGT containing GDGT-0 to GDGT-3 or crenarchaeol as core lipid were attributed to uncultured benthic, heterotrophic eury- and crenarchaeota (Biddle et al., 2006; Lipp and Hinrichs, 2009), however, also methanotrophic ANME-1 (Rossel et al., 2008) or methanogenic archaea (Koga et al., 2008) could be potential sources, given the indications of porewater geochemistry.

It is notable that both GDGT-based lipids and PE-OH-AR were found in nearly equal concentrations in the deep sediments of site GeoB10610. This is surprising since the most abundant lipids previously found in deep subsurface sediments were GDGT-based glycolipids (Lipp et al., 2008; Lipp and Hinrichs, 2009). A possible explanation for this observation is that the deeper layers of the sediments from Chapopote are not only influenced by large quantities of oil, but also by high salinities due to advection of saline fluids (Zabel et al., 2009). At

7.6 mbsf chlorinity values are around 1.5 M and declined to almost 1 M at 5 mbsf shortly above the SMTZ. Such high salinity values fall within the range of brines, where microbial cells are exposed to additional osmotic stress. Recent studies in seep environments in the northern Gulf of Mexico showed that mainly ANME-1 archaea were adapted to hypersaline conditions (Lloyd et al., 2006). A predominance of ANME-1 archaea would account for the presence of 2Gly-GDGT, but does not explain the large quantities of OH-ARs. Notably, isoprenoidal DEG lipids are typically the most abundant lipids in halophilic archaea (De Rosa and Gambacorta, 1988), which could additionally explain the abundant presence of PE-OH-AR. Hydroxyarchaeol lipids have also been found in hypersaline seep environments of the Mediterranean Sea, where they have been attributed to ANME-2 archaea (Stadnitskaia et al., 2008).

In summary, the IPL distribution along the SMTZ at Site GeoB10610 is quite distinct from other SMTZs settings targeted in previous studies (Biddle et al., 2006; Lipp and Hinrichs, 2009). At the Chapopote, petroleum and associated hydrocarbon gases provide easily accessible substrates and clearly stimulate microbial activity. The anaerobic oxidation of methane (AOM) is likely the dominating process in the SMTZ as reflected by porewater sulfate, methane, and $\delta^{13}C$ values of DIC, but we furthermore suggest that the presence of oil in deeper sediment layers (at 7.6 mbsf) is the most likely cause to stimulate microbial biomass production, possibly in the form of methanogenic oil degradation, also indicated in the biogenic formation of methane.

III.4.3.3. Community shifts: Bacteria vs Archaea

A general shift from Bacteria to Archaea with increasing sediment depth can be observed in all three sediment cores: In surface sediments (0-5 cmbsf) bacterial IPLs decline from almost 90% to less than 60% of total IPLs and account for less than 20% at 20 cmbsf. At site GeoB10619 where concentrations of HC gases and petroleum-derived HCs are about two orders of magnitude lower than at site GeoB10625 bacterial lipids also decrease with depth, but the transition to archaeal lipid dominance is more gradual due to the presence of sulfate throughout the core. Increased bacterial biomass in subsurface sediments seems to be controlled by two factors, the presence of oil and sulfate, nevertheless bacterial IPLs comprise only 1 to 22% of total IPLs in the deeply buried SMTZ. This observation is consistent with a previous study in a wide range of marine environments where archaeal IPL dominance is pervasive in sediments buried deeper than ~10 cmbsf (Lipp et al., 2008). Inside the asphalts only bacterial IPLs were detected, supporting the observation that methanogenesis is only of minor importance inside the asphalts and that hydrocarbon degradation is mainly carried out by Bacteria.

III.4.4. Carbon and energy transfer: from petroleum to macrobenthos

The surface of the asphalt beds is widely colonized by benthic macrofauna, such as sea cucumbers, crabs, and symbiotic tubeworms and mussels. Holothuria, identified as *Chiridota heheva* species, were collected close to dense microbial mats and were analyzed for their lipid content in digestive tracks to gain insights on their dietary behavior (Fig. III.1c). The distribution of IPLs and core lipids are similar for both analyzed animals: IPLs are mainly composed of glycosyl ceramides (Gly-Cer), PC-DAG, PE-*lyso*DAG and PE-plasmalogen-DAGs (Fig. III.9a). The free fatty acids are dominated by polyunsaturated fatty acids ($C_{20:5}$, $C_{20:4}$, $C_{20:2}$, $C_{18:2}$) and monounsaturated and saturated C_{16} and C_{18} fatty acids and correspond to the distributions of acyl moieties in IPLs (Fig. III.9c). Minor compounds are $C_{14:0}$, $C_{22:1}$, $C_{20:1}$, $C_{17:1}$ and methyl-branched $C_{15:0}$ and $C_{17:0}$ fatty acids. The alcohol fraction contains saturated, branched and monounsaturated monoalkylglycerolethers (MAGE) in the carbon number range C_{14}-C_{20}. The dominating MAGE are $C_{16:1\omega7}$, $C_{16:1\omega5}$, $C_{16:0}$, $C_{18:1\omega7}$, $C_{18:0}$ and $C_{14:0}$, but also small amounts of *ai*-$C_{15:0}$, *i*-$C_{15:0}$ and methyl-branched C_{17} were present. Various sterols, including cholesterol and 4-methyl sterols, some pentacyclic triterpenoids (tetrahymanol, diplopterol, Δ2-diplopterol), and also isoprenoidal archaeol and *sn*2-hydroxyarchaeol were also detected. The hydrocarbon fraction is dominated by a similar UCM, triterpenoid and *n*-alkane distribution as observed in the surface asphalts (Fig. III.9b).

The major IPLs found in the digestive tracks, i.e., Gly-Cer, PC-DAG, lyso-PE-DAG, and plasmalogen PE are typical constituents of eukaryotic soft tissue (Kent, 1995; Lahiri and Futerman, 2007; Nagan and Zoeller, 2001) and are thus most probably derived from the holuthuria. Corresponding alkyl and acyl chains of these IPLs include the C_{20} PUFAs, most of the C_{16} and C_{18} fatty acids and the C_{18} and C_{20} MAGEs, which are derived from the ether-bond alkyl chain of plasmalogen PE. Core lipids assigned to bacterial sources include $C_{16:1\omega5}$, $C_{18:1\omega7}$ and branched C_{15} and C_{17} fatty acids and MAGEs. Branched fatty acids are specific biomarkers for SRB and gram-positive bacillus and actinomycetes (Fulco, 1983; Kaneda, 1991), the $C_{16:1\omega5}$ fatty acid could be a product of SRB living in close association with ANME-2 archaea (cf. Elvert et al., 2003). Similarly, the corresponding C_{15}, C_{16} and C_{17} MAGE are likely derived from AOM-associated SRB (Rütters et al., 2001). Additional potential sources for the bacterial fatty acids could be type I methylotrophic bacteria (Bowman et al., 1993) and nitrite-oxidizing bacteria (Lipski et al., 2001). $\delta^{13}C$ values of the fatty acids and MAGE further support these assignments. Weighted means of C_{15}-C_{17} FAs and C_{15} to C_{17} MAGE are up to 5‰ depleted in ^{13}C compared to the C_{18}-C_{22} FA and C_{18}-C_{20} MAGE, indicating a different carbon source and metabolism for these lipids (Fig. III.9c). Most of the sterols, such as cholesterol can be assigned to the holothuria, which is consistent with similar $\delta^{13}C$ values to the holothurian-derived FAs and MAGEs (~38‰). 4me-sterols have very different $\delta^{13}C$ values, they are 15‰ depleted in ^{13}C compared to the other sterols. 4me-sterols are abundantly synthesized by methanotrophic bacteria (Bouvier et al., 1976; Ourisson et al., 1987), which explains their depletion in ^{13}C compared to the other sterols. The presence of methanogenic bacteria is further confirmed by ^{13}C-depleted diplopterol and Δ^2diplopterol, which have been both identified as markers for methanotrophic bacteria (cf. Summons et al., 1994; Hinrichs et al., 2003, Elvert and Niemann, 2008). Isoprenoidal AR and OH-AR are exclusive archaeal biomarkers and they exhibit maximal $\delta^{13}C$ depletion with values ranging from -104‰ to -94‰, i.e., values typically found for methanotrophic archaea (Hinrichs et al., 1999, 2000; Blumenberg et al., 2004). Tetrahymanol is probably derived from ciliates that graze on the microbial mats or from rumen

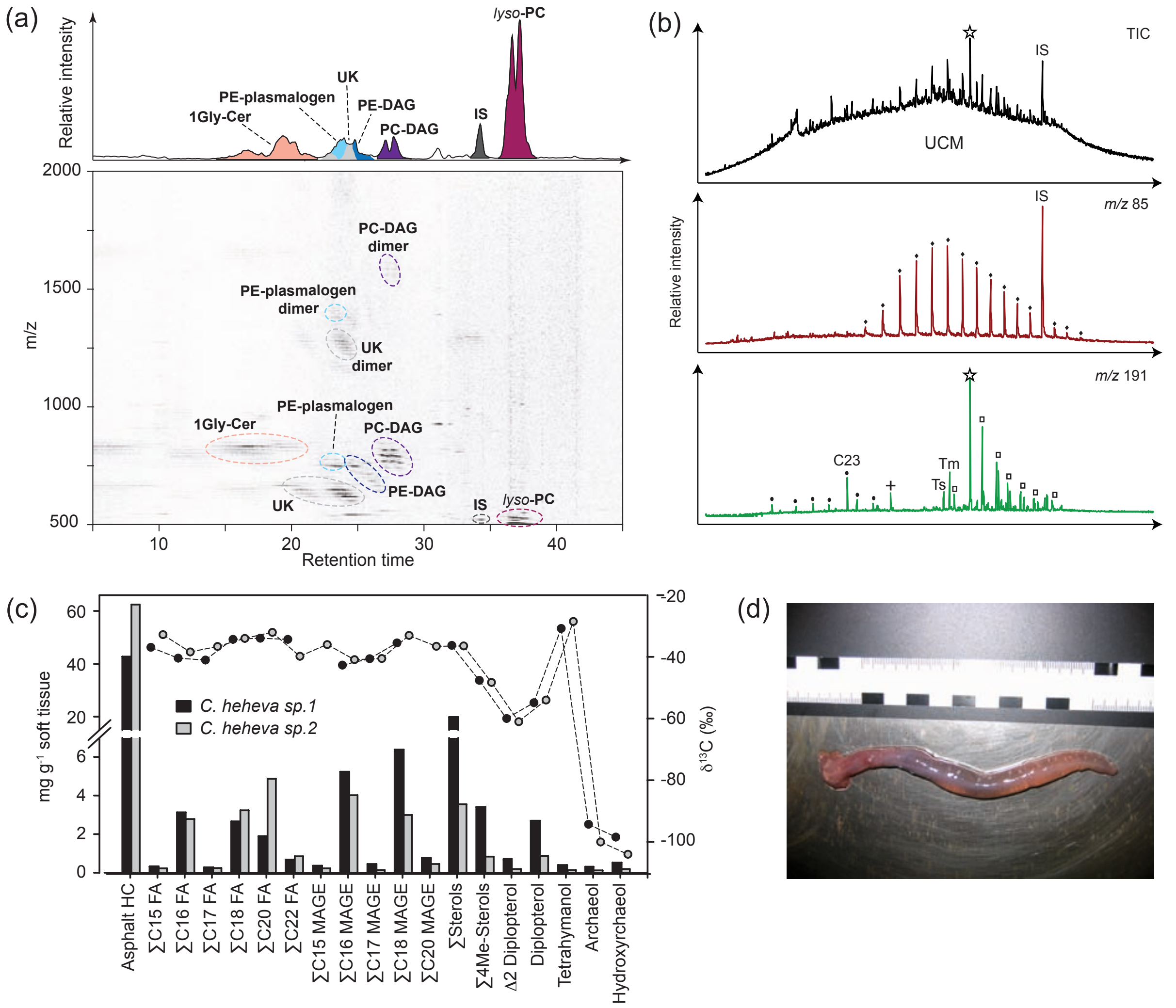

Fig. III.9. (**A**) Density map and chromatogram showing the distribution of intact polar membrane lipids in one of the analyzed holuthurian digestive tracks. For abbreviations refer to the text. (**B**) Total ion chromatogram (TIC), and extracted mass chromatogram *m/z* 85 and 191 of the hydrocarbon fraction of one of the guts. UCM – unresolved complex mixture, IS – internal standard, filled diamonds – *n*-alkanes (C_{24}- C_{39}), filled circles – tricyclic terpanes (C_{19}-C_{25}), cross – C_{24} tetracyclic terpane, Ts - trisnorneohopane, Tm - trisnorhopane, open squares – 17α21β R and S hopane series (C_{28}-C_{35}), star – norhopane. (**C**) Concentrations (bars) and stable carbon isotopic compositions (circles) of lipid biomarkers found in both holuthurian digestive tracks. HC-hydrocarbons, FA – fatty acids, MAGE – monoalkyglycerolether. (**D**) Picture of holothuria species *Chiridota heheva*.

fungi (Kemp et al., 1984). Enriched δ^{13}C values in comparison the animal derived lipids further support a different origin for tetrahymanol (Fig. III.9c).

The detection of asphalt-derived hydrocarbons (40 to 60 mg/g soft tissue) that resemble surficial asphalt, as demonstrated in the *n*-alkane and hopane distribution (Fig. III.9b), additionally indicates that the holothuria are grazing on the mats covering the asphalt surface. Isotopically depleted diplopterol, Δ^2-diplopterol, 4me-sterols, archaeol and hydroxyarchaeol indicate that the microbial mats are composed of both aerobic methanotrophic bacteria and anaerobic methanotrophic archaea. Only slightly δ^{13}C depleted values for SRB associated biomarkers indicate that only a minor part of the SRB are involved in AOM and that they are instead mainly involved in the degradation of asphalt hydrocarbons (δ^{13}C of asphalt TOC = 27‰, Fig. III.2b).

III.5. SUMMARY AND CONCLUSIONS

This study gives a comprehensive view on the function of a unique ecosystem fueled by seepage of heavy oil. Geochemical profiles and stable carbon isotopic composition of methane indicate that in oil-impregnated sediments sulfate reduction, methanogenesis, and methanotrophy are the dominating biologically mediated processes. A wide number of bacterial and archaeal IPLs detected in the sediments, show that microbial life is extensively stimulated at geochemical interfaces, and that microbial biomass is mainly controlled by the presence of oil (Fig. III.10). Sedimentary IPL profiles suggest that Archaea become the dominant microbes with depth. The only detectable bacterial IPLs in deeper sediments are composed of diether lipids, which is possibly reflective of membrane adaptation to low-energy conditions. In the gas hydrate containing asphalts bacterial hydrocarbon-degradation is indicated by a selective removal of biodegradation diagnostic hydrocarbons, and by the detection of bacterial diester and diether phospholipids. However, biological methanogenesis seems to be only a minor process, reflected in $\delta^{13}C$ of gas hydrate-derived methane of only 55‰ and a lack of archaeal IPLs within the asphalts. It could be shown that Holothuria found on top of the asphalt beds are grazing on microbial mats that colonize the asphalt surface, demonstrating a close link between the microbial to the macrofaunal world.

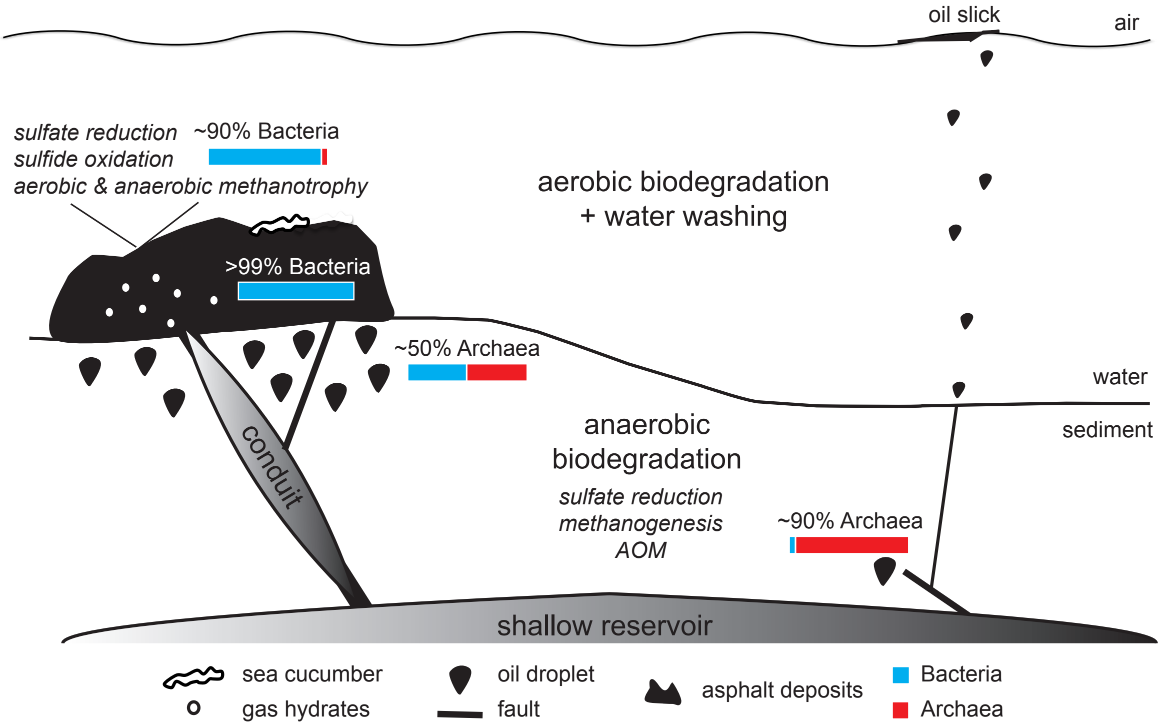
oil slick
air
sulfate reduction
sulfide oxidation
aerobic & anaerobic methanotrophy
~90% Bacteria
aerobic biodegradation
+ water washing
>99% Bacteria
~50% Archaea
water
sediment
conduit
anaerobic
biodegradation
sulfate reduction
methanogenesis
AOM
~90% Archaea
shallow reservoir
sea cucumber
gas hydrates
oil droplet
fault
asphalt deposits
Bacteria
Archaea

Fig. III.10. Schematic of hydrocarbon seepage and associated chemosynthetic life at the Chapopote Knoll.

III.6. ACKNOWLEDGEMENTS

We thank the shipboard crew and scientific crew of Meteor expedition M67/2 to the Campeche Knolls, Gulf of Mexico. Thorsten Wilhelm is thanked for sampling and pore water retrieval/analyses. Xavier Prieto-Mollar, Kevin Becker, Tim Kahs, and Christine Berndmeyer are thanked for their help in the laboratory. This work was funded by the Deutsche Forschungsgemeinschaft (DFG) through MARUM - Center for Marine Environmental Sciences and the graduate school GLOMAR.

III.7. REFERENCES

Aitken, C.M., Jones, D.M., Larter, S.R. (2004) Anaerobic hydrocarbon biodegradation in deep reservoirs. *Nature* **431**: 291-294.

Arning, E.T., Birgel, D., Schulz-Vogt, H.N., Holmkvist, L., Jørgensen, B.B., Larson, A., Peckmann, J. (2008) Lipid biomaker patterns of phosphogenic sediments from upwelling regions. *Geomicrobiol J* **25**: 69-82.

Benning, C., Huang, Z.H., Gage, D.A. (1995) Accumulation of a novel glycolipid and a betaine lipid in cells of *Rhodobacter sphaeroides* grown under phosphate limitation. *Arch Biochem Biophys* **317**: 103-111.

Berner, U., Faber, E. (1996) Empirical carbon isotope/maturity relationships for gases from algal kerogens and terrigenous organic matter, based on dry, open-system pyrolysis. *Org Geochem* **24**: 947-955.

Biddle, J.F., Lipp, J.S., Lever, M.A., Lloyd, K.G., Sørensen, K.B. Anderson, R., Fredricks, H.F., Elvert, M., Kelly, T.J., Schrag, D.P., Sogin, M.L., Brenchley, J.E., Teske, A., House, C.H., Hinrichs, K.-U. (2006) Heterotrophic Archaea dominate sedimentary subsurface ecosystems off Peru. *Proc Natl Acad Sci USA* **103**: 3846-3851.

Blumenberg, M., Seifert, R., Reitner, J., Pape, T., Michaelis, W. (2004) Membrane lipid patterns typify distinct anaerobic methanotrophic consortia. *Proc Natl Acad Sci USA* **101**: 11111-11116.

Boetius, A., Ravenschlag, K., Schubert, C.J., Rickert, D., Widdel, F., Gieseke, A., Amann, R., Jørgensen, B.B., Witte, U., Pfannkuche, O. (2000) A marine microbial consortium apparently mediating the anaerobic oxidation of methane. *Nature* **407**: 623-626.

Bohrmann, G., Spiess, V., M67/2 Cruise Participants (2008) Report and preliminary results of R/V Meteor cruise M67/2a and 2b, Balboa – Tampico – Bridgetown, 15 March – 24 April 2006. Fluid seepage in the Gulf of Mexico, Berichte, No.263, Fachbereich Geowissenschaften, Universität Bremen, Bremen, Germany.

Borowski, W.S., Paull, C.K., Ussler III, W. (1996) Marine pore-water sulfate profiles indicate in situ methane flux from underlying gas hydrate. *Geology* **24**: 655-658.

Borowski, W.S., Paull, C.K., and Ussler III, W. (1997) Carbon cycling within the upper methanogenic zone of continental rise sediments: An example from the methane-rich sediments overlying the Blake Ridge gas hydrate deposits. *Mar Chem* **57**: 299-31..

Bouvier, P. Rhomer, M., Benveniste, P., Ourisson, G. (1976) Δ8(14)-Steroids in the bacterium *Methylococcus capsulatus*. *Biochem J* **159**: 267-271.

Bowman, J.P., Jiménez, L., Rosario, I., Hazen, T., Sayler, G. (1993) Characterization of the methanotrophic bacterial community present in a trichloroethylene-contaminated subsurface groundwater site. *Appl Environ Microbio* **59**: 2380-2387.

Brett, M.T., Müller-Navarra D.C. (1997) The role of highly unsaturated fatty acids in aquatic foodweb processes. *Freshw Biol* **38**: 483-499.

Brooks, J.M., Kennicutt II, M.C., Fay, R.R., T.J. MacDonald (1984) Thermogenic gas hydrates in the Gulf of Mexico. *Science* **225**: 409-411.

Brüning, M., Sahling, H., MacDonald, I. R, Ding, F, Bohrmann, G. Origin, distribution, and alteration of asphalts at Chapopote Knoll, Southern Gulf of Mexico. *Marine and Petroleum Geology*, accepted September 16, 2009.

Caillon, E., Lubochinsky, B., and Rigomier, D. (1983) Occurrence of dialkyl ether phsopholipids in *Stigmatella aurantiaca*. *J Bacteriol* **153**: 1348-1351.

Christie, W.W. (2003) Lipid Analysis. 3rd edition. Oily Press, Bridgewater, UK.

Chung, H.M., Gormly, J.R., Squires, R.M. (1988) Origin of gaseous hydrocarbons in subsurface environments: Theoretical considerations of carbon isotope distribution. *Chem Geol* **71**: 97-103.

Dembitsky, V.M. (1996) Betaine ether-linked glycerolipids: chemistry and biology. *Prog Lipid Res* **35**: 1-51.

De Rosa, M., Gambacorta, A. (1988) The lipids of archaebacteria. *Prog Lipid Res* **27**: 153-175.

Ding, F., Spiess, V., Brüning, M., Fekete, N., Keil, H., Bohrmann, G. (2008) A conceptual model for hydrocarbon accumulation and seepage processes around Chapopote asphalt site, southern Gulf of Mexico: From high resolution seismic point of view. *J Geophys Res*:**113**.

Elvert, M., Boetius, A., Knittel, K., Jørgensen, B.B. (2003) Characterization of specific membrane fatty acids as chemotaxonomic markers for sulfate-reducing bacteria involved in anaerobic oxidation of methane. *Geomicrobiol J* **20**: 403-419.

Elvert M., Hopmans, E.C., Treude T., Boetius A., Suess E. (2005) Spatial variations of methanotrophic consortia at cold methane seeps: implications from a high-resolution molecular and isotopic approach. *Geobiology* **5**: 195-209.

Elvert, M., Niemann, H. (2008) Occurrence of unusual steroids and hopanoids derived from aerobic methanotrophs at an active marine mud volcano. *Org Geochem* **39**: 167-177.

Ertefai, T.F., Fisher, M.C., Fredricks, H.F., Lipp, J.S., Pearson, A., Birgel, D., Udert, K.M., Cavanaugh, C.M., Gschwend, P.M., Hinrichs, K.-U. (2008) Vertical distribution of microbial lipids and functional genes in chemically distinct layers of a highly polluted meromictic lake. *Org Geochem* **39**: 1572-1588.

Fowler, S.W., Knauer, G.A. (1986) Role of large particles in the transport of elements and organic compounds through the oceanic water column. *Prog Oceanogr* **16**: 147-194.

Fulco, A. (1983) Fatty acid metabolism in bacteria. *Prog Lipid Res* **22**: 133-160.

Garrison, L.E., Martin, R.G. (1973) Geologic structures in the Gulf of Mexico Basin, *US Geological Survey Professional Paper*, vol. 773, US Gov. Print. Off., Washington, D.C.

Goldfine, H., Hagen, P.-O. (1968) N-methyl groups in bacterial lipids. *J Bacteriol* **95**: 367-375.

Goldfine, H. (1984) Bacterial membranes and lipid packing theory. *J Lip Res* **25**: 1501-1507.

Guzman-Vega, M.A., Mello, M.R. (1999) Origin of oil in the Sureste basin, Mexico. *AAPG Bulletin* **83**: 1068-1095.

Hagen P.-O., Goldfine, H., Williams, P.J. (1966) Phospholipids of bacteria with extensive intracytoplasmic membrane. *Nature* **151**: 1543-1544.

Harvey, H.R., Fallon, R.D., Patton, J.S. (1986) The effect of organic matter and oxagen on the degradation of bacterial membrane lipids in marine sediments. *Geochim Cosmochim Acta* **50**: 795-804.

Hayes, J.M. (2001) Fractionation of the isotopes of carbon and hydrogen in biosynthetic processes. *Rev Mineral Geochem* **43**: 225-277.

Hinrichs, K.-U., Hayes, J.M., Sylva, S.P., Brewer, P.G., DeLong, E.F. (1999) Methane-consuming archaeabacteria in marine sediments. *Nature* **398**: 802-805.

Hinrichs, K.-U., Summons, R.E., Orphan, V., Sylva, S.P., Hayes, J.M. (2000) Molecular and isotopic analysis of anaerobic methane-oxidizing communities in marine sediments. *Org Geochem* **31**: 1685-1701.

Hinrichs, K.-U., Hmelo, L.R., Sylva, S. (2003) Molecular fossil record of elevated methane levels in late Pleistocene coastal waters. *Science* **299**: 1214-1217.

Hinrichs, K.-U., Hayes, J.M., Bach, W., Spivack, A.J., Hmelo, L.R., Holm, N.G., Johnson, C.G., and Sylva, S.P., (2006) Biological formation of ethane and propane in the deep marine subsurface. *Org Geochem* **31**: 1685-1701.

Itoh, Y.H., Sugai, A., Uda, I., Itoh, T. (2001) The evolution of lipids. *Adv Space Res* **4**: 719-724.

Joye, S.B., Boetius, A., Orcutt, B.N., Montoya, J.P., Schulz, H.N., Erickson, M.J., Lugo, S.K. (2004) The anaerobic oxidation of methane and sulfate reduction in sediments from Gulf of Mexico cold seeps. *Chem Geol* **205**: 219-238.

Joye, D.B., Samarkin, V.A., Orcutt, B.N., MacDonald, I.R., Hinrichs, K.-U., Elvert, M., Teske, A., Lloyd, K.G., Lever, M.A., Montoya, J.P., Meile, C.D. (2009) Metabolic variability in seafloor brines revealed by carbon and sulphur dynamics. *Nature Geosci* **2**: 349-354.

Kaneda, T. (1991) Iso- and anteiso-fatty acids in bacteria: Biosynthesis, function, and taxonomic significance. *Microbiol Rev* **55**: 288-302.

Kates, M. (1966) Biosynthesis of lipids in microorganisms. *Annu Rev Microbiol* **20**: 13-44.

Kemp, P., Lander, D., Orpin, C. (1984) The lipids of the rumen fungus *Piromonas communis*. *J Gen Microbiol* **130**: 27-37.

Kennicutt II, M.C., Brooks, J.M., Denoux, G.J. (1988) Leakage of deep, reservoired petroleum to the near surface on the Gulf of Mexico continental slope. *Marine Chem* **24**: 39-59.

Kent, C. (1995) Eukaryotic phospholipid biosynthesis. *Annu Rev Biochem* **64**: 315-343.

Klapp, S.A., Bohrmann, G., Kuhs, W.F., Murshed, M.M., Pape, T., Klein, H., Techmer, K.S., Heeschen, K., Abegg, F. (2009) Microstructures of structure I and II gas hydrate from the Gulf of Mexico. *Marine and Petroleum Geology* doi:10.1016/j.marpetgeo.2009.03.004

Kristjansson, J.K., Schönheit, P., Thauer, R.K. (1982) Different K_p values for hydrogen of the methanogenic bacteria and sulfate-reducing bacteria: An explanation for the apparent inhibition of methanogenesis by sulfate. *Arch Microbiol* **131**: 278-282.

Koga, Y., Morii, H., Akagawa-Matsushita, M., Ohga, M. (1998) Correlation of polar lipid composition with 16S rRNA phylogeny in methanogens. Further analysis of lipid component parts. *Biosci Biotechnol Biochem* **69**: 230-236.

Koga, Y., Morii, H. (2005) Recent advances in structural research in ether lipids from archaea including comparative and physiological aspects. *Biosci Biotechnol Biochem* **69**: 2019-2034.

Koga, Y., Nakano, M. (2008) A dendrogram of archaea based on lipid component parts composition and ist relationship to rRNA phylogeny. *Syst Appl Microbiol* **31**: 169-182.

Lahiri, S., Futerman, A.H. (2007) The metabolism and function of sphingolipids and glycosphingolipids. *Cell Mol Life Sci* **64**: 2270-2284.

Lechevalier, M.P., Moss, C.W. (1977) Lipids in bacterial taxonomy – a taxonomist's view. *Crit Rev Microbiol* **5**: 109-210.

Langworthy, T.A., Mayberry, W.R., and Smith, P.F. (1974) Long-chain glycerol diether and polyol dialkyl glycerol triether lipids of *Sulfolobus acidocaldarius*. *J Bacteriol* **119**: 106-116.

Langworthy, T.A., Pond, J.L. (1986) Archaeabacterial ether lipids and chemotaxonomy. *Syst Appl Microbiol* **7**: 253-257.

Lipp, J.S., Morono, Y., Inagaki, F., Hinrichs, K.-U. (2008) Significant contribution of Archaea to extant biomass in marine subsurface sediments. *Nature* **454**: 991-994.

Lipp, J.S., Hinrichs K.-U. (2009) Structural diversity and fate of intact polar lipids in marine sediments. *Geochim Cosmochim Acta,* DOI:10.1016/j.gca.2009.08.003.

Lipski, A., Spieck, E., Makolia, A., Altendorf, K. (2001) Fatty acid profiles of nitrite-oxidizing bacteria reflect their phylogenetic heterogeneity. *Syst Appl Microbiol* **24**: 377-384.

Lloyd, K.G., Lapham, L., Teske, A. (2006) An anaerobic methane-oxidizing community of ANME-1b Archaea in Hypersaline Gulf of Mexico sediments. *Appl Environ Microbiol* **72**: 7218-7230.

López-Lara, I.M., Sohlenkamp, C., Geiger, O. (2003) Membrane lipids in plant-associated bacteria: Their biosyntheses and possible functions. *Mol Plant Microbe Int* **16**: 567-579.

MacDonald, I.R., Guinasso, N.I., Reilly, J.F., Brooks, J.M., Callender, W.R., Gabrielle, S.G. (1990) Gulf of Mexico hydrocarbon seep communities: VI. Patterns in community structure and habitat. *Geo-Marine Lett* **10**: 244-252.

MacDonald, I.R., Guinasso, N.I., Ackleson, S.G., Amos, J.F., Duckworth, R., Sassen, R., and Brooks, J.M. (1993) Natural oil slicks in the Gulf of Mexico visible from space. *J Geophys Res* **98**: 16,351-16,364.

MacDonald, I.R., Bohrmann, G., Escobar, E., Abegg, F., Blanchon, P., Blinova, V., Brückmann, W., Drews, M., Eisenhauer, A., Han, X., Heeschen, K., Meier, F., Mortera, C., Naehr, T., Orcutt, B., Bernard, B., Brooks, J., de Faragó, M. (2004) Asphalt volcanism and chemosynthetic life in the Campeche Knolls, Gulf of Mexico. *Science* **304**: 999-1002.

Makula, R.A., Finnerty, W.R. (1975) Isolation and characterization of an ornithine-containing lipid from *Desulfovibrio gigas*. *J Bacteriol* **123**: 523-529.

Martin, R.G., and Case, J.E. (1975) Geophysical studies in the Gulf of Mexico. IN: A.E.M. Nairn and F.G. Stehli (eds), Ocean Basins and Margins, Vol. 3, Gulf of Mexico and Caribbean. Plenum, New York, pp. 65-106.

Musat, F., Galushko, A., Jacob, J., Widdel, F., Kube, M., Reinhardt, R., Wilkes, H., Schink, B., Rabus, R. (2009) Anaerobic degradation of naphthalene and 2-methylnaphthalene by strains of marine sulfate-reducing bacteria. *Environ Microbiol* **11**: 209-219.

Nagan, N., Zoeller, R.A. (2001) Plasmalogens: biosynthesis and functions. *Prog Lipid Res* **40**: 199-229.

ODP Leg 201 Shipboard Scientific Party. Explanatory Notes (2003) *In* S.L. D'Hondt, B.B. Jørgensen, D.J., Miller *et al.*, Proc. ODP, Init. Repts., 201 [Online]. http://www-odp.tamu.edu/publication/201_IR/chap_05/chap_05.htm.

Orcutt, B., Boetius, A., Elvert, M., Samarking, V., and Joye, S.B. (2005) Molecular biogeochemistry of sulfate reduction, methanogenesis and the anaerobic oxidation of methane at Gulf of Mexico cold seeps. *Geochim Cosmochim Acta* **69**: 4267-4281.

Orphan, V.J., House, C., Hinrichs, K.-U., McKeegan, K.D., DeLong, E.F. (2001) Methane-consuming archaea revealed by directly coupling isotopic and phylogenetic analysis. *Science* **293**: 484-487.

Ourisson, G., Rhomer, M., Poralla, K. (1987) Prokaryotic hopanoids and other polyterpenoid sterol surrogates. *Annu Rev Microbiol* **41**: 301-333.

Pancost, R.D., Bouloubassi, I., Aloisi, G., Sinninghe Damsté, J.S., the Medinaut Shipboard Scientific Party (2001) Three series of non-isoprenoidal dialkyl glycerol diether cold-seep carbonate crusts. *Org Geochem* **32**: 695-707.

Peters, K.E., and Moldowan, J.M. (1993) The Biomarker Guide. Prentice Hall, New York.

Rabus, R., Nordhaus, R., Ludwig, W., Widdel, F. (1993) Complete oxidation of toluene under strictly anoxic conditions by a new sulfate-reducing bacterium. *Appl Environ Microbiol* **59**: 1444-1451.

Rabus, R., Widdel, F. (1995) Anaerobic degradation of ethylbenzene and other aromatic hydrocarbons by new denitrifying bacteria. *Arch Microbiol* **163**: 96-103.

Riedinger, N., Pfeifer, K., Kasten, S., Garning, J.F.L., Vogt, C., Hensen, C. (2005) Diagentic alteration of magnetic signals by anaerobic oxidation of methane related to a change in sedimentation rate. *Geochim Cosmochim Acta* **69**: 4117-4126.

Rossel, P.E., Lipp, J.S., Fredricks, H.F., Arnds, J., Boetius, A., Elvert, M., Hinrichs, K.-U. (2008) Intact polar lipids of anaerobic methanotrophic archaea and associated bacteria. *Org Geochem* **39**: 992-999.

Rossel, P.E. (2009) *Dissertation*, University of Bremen, Bremen, Germany.

Rueter, P., Rabus, R., Wilkes, H., Aeckersberg, F., Rainey, F.A., Jannasch, H.W., Widdel, F. (1994) Anaerobic oxidation of hydrocarbons in crude oil by new types of sulphate-reducing bacteria. *Nature* **372**: 455-458.

Rütters, H., Sass, H., Cypionka, H., Rullkötter, J. (2001) Monoalkylether phospholipids in the sulfate-reducing bacteria *Desulfosarcina variabilis* and *Desulforhabdus amnigenus*. *Arch Microbiol* **176**: 435-442.

Rütters, H., Sass, H., Cypionka, H., Rullkötter, J. (2002) Phospholipid analysis as a tool to study complex microbial communities in marine sediments. *J Microbiol Meth* **48**: 149-160.

Sassen, R., Roberts, H.H., Aharon, P., Chinn, E.W., Carnay, R. (1993) Chemosynthetic bacterial mats at cold hydrocarbon seeps, Gulf of Mexico continental slope. *Org Geochem* **20**: 77-89.

Sassen, R., Milkov, A.V., Roberts, H.H., Sweet, S.T., DeFreitas, D.A. (2003) Geochemical evidence of rapid hydrocarbon venting form a seafloor-piercing mud diapir, Gulf of Mexico continental shelf. *Marine Geology* **198**: 319-329.

Sassen, R., Roberts, H.H., Aharon, P., Carnay, R., Milkov, A.V., DeFreitas, D.A., Lanoil, B., Zhang, C. (2004) Free hydrocarbon gas, gas hydrate, and authigenic minerals in chemosynthetic communities of the northern Gulf of Mexico continental slope: relation to microbial processes. *Chem Geol* **205**: 195-217.

Scholz-Böttcher, B.M., Ahlf, S., Gutiérrez, F.V., Rullkötter, J. (2009) Correlation of shallow- and deep-water asphalts from the Campeche Sound, Gulf of Mexico, with the type 2 oil family. *Abstract International Meeting on Organic Geochemistry (IMOG)*, Bremen 2009.

Schönheit P., Kristjansson J.K., Thauer, R.K. (1982) Kinetic mechanism for the ability of sulfate-reducers to out-compete methanogens for acetate. *Arch Microbiol* **132**: 285-288.

Schubotz, F., Wakeham, S.G., Lipp, J.S., Fredricks, H.F., Hinrichs, K.-U. (2009) Detection of microbial biomass by intact polar membrane lipid analysis in the water column and surface sediments of the Black Sea. *Environ Microbiol* **11**: 2720-2734 (DOI:10.1111/j.1462-2920.2009.01999.x), *see also Chapter II*.

Schubotz, F., Ventura, G.T., Nelson, R.K., Reddy, C.M., Hinrichs, K.-U. Determining total petroleum hydrocarbon degradation and weathering by comprehensive GC×GC at an asphalt seep in the southern Gukf of Mexico. *In prep., see also Chapter V.*

Sohlenkamp, C., López-Lara, I.M., Geiger, O. (2003) Biosynthesis of phosphatidycholine in bacteria. *Prog Lipid Res* **42**: 115-162.

Solomon, E.A., Kastner, M., MacDonald, I.R., Leifer, I. (2009) Considerable methane fluxes to the atmosphere from hydrocarbon seeps in the Gulf of Mexico. *Nature Geosci* **2**: 561-565.

So, C.M., and Young, L.Y. (1999) Isolation and characterization of a sulfate-reducing bacterium that anaerobically degrades alkane. *Appl Environ Microbiol* **65**: 2969-2976.

Seidel, M. (2009) *Dissertation*, Carl-von-Ossietzly University of Oldenburg, Oldenburg, Germany.

Stadnitskaia, A., Bouloubassi, I., Elvert, M., Hinrichs, K.-U., Sinninghe Damsté, J.S. (2008) Extended hydroxyarchaeol, a novel lipid biomarker for anaerobic methanotrophy in cold seepage habitats. *Org Geochem* **39**: 1007-1014.

Strąpoć, D., Picardal, F.W., Turich, C., Schaperdoth, I., Macalady, J.I., Lipp, J.S., Lin, Y.-S., Ertefai, T.F., Schubotz, F., Hinrichs, K.-U., Mastalerz, M., Schimmelmann, A. (2008) Methane-producing microbial community in a coal bed of the Illinois Basin. *Appl Environ Microbiol* **74**: 2424-2432 (*see also Chapter VIe*).

Sturt, H.F., Summons, R.E., Smith, K., Elvert, M., Hinrichs, K.U. (2004) Intact polar membrane lipids in prokaryotes and sediments deciphered by high-performance liquid chromatography/electrospray ionization multistage mass spectrometry – new biomarkers for biogeochemistry and microbial ecology. *Rap Comm Mass Spec* **18**: 617-628.

Summons, R.E., Jahnke, L.L., Roksandic, Z. (1994) Carbon isotopic fractionation in lipids from methanotrophic bacteria: relevance for interpretation of the geochemical record of biomarkers. *Geochim Cosmochim Acta* **58**: 2853-2863.

U.S. Department of Commerce, National Oceanic and Atmospheric Administration, National Geophysical Data Center, 2001. 2-minute Gridded Global Relief Data (ETOPO2).

Valentine, D.L. (2007) Adaptations to energy stress dictate the ecology and evolution of the Archaea *Nature Rev Microbiol* **5**: 316-323.

Van Mooy, B.A.S., Fredricks, H.F., Pedler, B.E., Dyhrman, S.T., Karl, D.M., Koblízek, M, Loma, M.W., Mincer, T.J., Moore, L.R., Moutin, T., Rappé, M.S., Webb, E.A. (2009) Phytoplankton in the ocean use non-phosphorous lipids in response to phosphorous scarcity. *Nature* **458**: 69-72.

Vieth, A., Wilkes, H., (2006) Deciphering biodegradation effects on light hydrocarbons in crude oils using their stable carbon isotope composition: A case study from the Gullfaks oil field: offshore Norway. *Geochim Cosmochim Acta* **70**: 651-665.

Wardlaw, G.D., Arey, J.S., Reddy, C.M., Nelson, R.K., Ventura, G.T., Valentine, D.L. (2008) Disentangling oil weathering at a marine seep using GCxGC: Broad metabolic specificity accompanies subsurface petroleum biodegradation. *Environ Sci Tech* **42**: 7166-7173.

Welte, D.H., Kratochvil, H., Rullkötter, J., Ladwein, H., Schaefer, R.G. (1982) Organic geochemistry of crude oils from the Vienna Basin and an assessment of their origin *Chem Geol* **35**: 33-68.

Wenger, L.M., Isaksen, G.H. (2002) Control of hydrocarbon seepage intensity on level of biodegradation in sea bottom sediments. *Org Geochem* **33**: 1277-1292.

White, D.C., Davis, W.M., Nickels, J.S., King, J.D., Bobbie, R.J. (1979) Determination of the sedimentary microbial biomass by extractable lipid phosphate. *Oecologia* **40**: 51-62.

Whiticar, M.J. (1999) Carbon and hydrogen isotope systematics of bacterial formation and oxidation of methane. *Chem Geol* **161**: 291-314.

Widdel, F., Boetius, A., Rabus, R. (2003) Anaerobic biodegradation of hydrocarbons including methane, p.1028-1049. *In* A Balows, H.G. Trüper, W. Dworkin, W. Harder, and K.-H. Schleifer (ed.) *The prokaryote*, 3rd ed. Springer-Verlag, New York, N.Y.

Zabel, M., Kasten, S. (2009) Geochemical characterization and origin of high saline pore fluids from the Chapopote asphalt volcano - Southern Gulf of Mexico. *Geochim Cosmochim Acta* **73**, Goldschmidt Conference Abstracts, A1494.

Zengler, K., Richnow, H.H., Rosselló-Mora, R., Michaelis, W., Widdel, F. (1999) Methane formation from long-chain alkanes by anaerobic microorganisms. *Nature* **401**: 266-269.

Chapter IV

Sulfate-reduction, methanotrophy, and methanogenesis at the Chapopote asphalt volcano deciphered by head group-specific stable carbon isotopic analysis of intact polar membrane lipids

Florence Schubotz[1*], Julius Sebastian Lipp[1], Marcus Elvert[1], Kai-Uwe Hinrichs[1]

In preparation for *Geochimica et Cosmochimica Acta*

**Corresponding author. Tel: +49-421-218-65711; Fax: +49-421-218-65715*

E-mail address: schubotz@uni-bremen.de

[1]Department of Geosciences and MARUM Center for Marine Environmental Sciences, University of Bremen, D-28359 Bremen, Germany

IV.1. ABSTRACT

Seepage of solidified asphalt forms the basis of a cold seep system at 3000 m water depth at the Chapopote Knoll in the Southern Gulf of Mexico. Anaerobic microbial life is stimulated in the oil-impregnated sediments as evidenced by the presence of intact polar membrane lipids (IPL) of Archaea and Bacteria at depths up to 7 m below the seafloor. Detailed investigation of stable carbon isotope composition ($\delta^{13}C$) of alkyl and acyl moieties derived from head group-specific IPL precursors revealed a variety of carbon fixation pathways for both Bacteria and Archaea. In surface sediments most of the polar lipid-derived fatty acids could be assigned to autotrophic sulfate-reducing bacteria, with a substantial proportion involved in the anaerobic oxidation of methane. Abundant heterotrophic oil-degrading bacteria were also observed that contained different phospholipid head groups. Archaeal IPLs with phosphate-based hydroxyarchaeols and diglycosidic glyceroldibiphytanylglyceroltetraethers (GDGTs) in surface sediments were assigned to methanogenic archaea, whereas $\delta^{13}C$ values of phosphate-based archaeols and mixed phosphate and diglycosidic based GDGTs were best explained by methanotrophic archaea. In deeper sediments at a sulfate-methane transition zone at 6 to 7 meter below the seafloor, $\delta^{13}C$ values of phosphate-based hydroxyarchaeols and diglycosidic archaeol and GDGTs showed a mixed signal of methanotrophic and methanogenic archaea. Here, diglycosidic GDGTs also contained crenarchaeol, which could be assigned to heterotrophic crenarchaea. This study extends previous compound-specific isotope studies by distinguishing between major IPL classes and reveals highly complex patterns in carbon-flow in versatile microbial communities associated with seepage of heavy oil and asphalt.

IV.2. INTRODUCTION

Methane is an important greenhouse gas and although it is abundantly produced in marine sediments, oceanic methane emissions amount to less than 2% of the global methane budget (cf. Reeburgh et al., 2007). The abundance and distribution of methane in the marine realm is effectively controlled by biological processes as microorganisms both produce and consume methane in marine sediments. Anaerobic methanotrophy recycles an estimated 7 to 25% of the global methane production within marine sediments (Hinrichs and Boetius, 2002; Reeburgh, 2007; Knittel and Boetius, 2009). The anaerobic oxidation of methane, which is responsible for up to 90% of methane consumption within marine sediments, was first evidenced by archaeal biomarkers that were highly depleted in ^{13}C (Elvert et al., 1999; Hinrichs et al., 1999) and was later confirmed to be mediated by a syntrophic consortium of methane-oxidizing archaea and sulfate-reducing bacteria (Boetius et al., 2000; Hinrichs et al., 2000; Orphan et al., 2001). AOM is also a widespread phenomenon in diffusive systems of deeply buried sediment and is often evidenced by an increase in cell counts in sediment horizons where sulfate and methane intercept (e.g., D'Hondt et al., 2004). Increased rates of AOM are observed at cold seeps where advective flux of reduced fluids and methane intensively stimulate microbial activity (cf. Knittel and Boetius, 2009). Cold seeps also pose the highest potential for release of methane from the seafloor into the ocean and subsequently to the atmosphere and are therefore of vital scientific interest.

The cold seeps of the Gulf of Mexico (GoM) are particularly unique to study as fluid and gas seepage is primarily controlled by salt tectonic movements and is often accompanied by the expulsion of oil and high amounts of higher hydrocarbon gases due to the large subsurface petroleum reservoirs (Kennicutt et al., 1988; Aharon et al., 1992; Sassen et al., 1999). Due to the presence of petroleum-derived hydrocarbons sulfate-reduction is not strictly coupled to AOM (Joye et al., 2004; Orcutt et al., 2004; Lloyd et al., 2006) on the continental slopes of the northern GoM. In the less studied southern GoM, MacDonald et al. (2004) discovered a hitherto novel form of petroleum seepage at 3000 m water depth, which was termed asphalt volcanism. Here, asphalt deposits cover the top of a salt knoll, the Chapopote, which is situated at the Campeche Knolls and is accompanied by abundant chemosynthetic communities and cold seep fauna. In 2006 this site was revisited to gain more insights into the geophysical, biological and geochemical processes associated with the asphalt seepage (Bohrmann et al., 2008; Ding et al., 2008; Brüning et al., 2009; Nähr et al., 2009). Investigations using intact polar membrane lipids (IPLs) revealed the presence of abundant microbial communities within oil-impregnated sediments surrounding the asphalt deposits (Schubotz et al., *in prep., Chapter III*). The composition of the IPLs in surface sediments is a balanced mixture from Archaea and Bacteria, whereas deeply buried sulfate-methane transition zones (SMTZ) in 6 meters below the seafloor (mbsf) were dominated by archaeal IPLs.

In this study we will focus on sediments that were retrieved from a zone with higher fluid flow where petroleum is seeping out of the seafloor and from a more diffusive site with a deeply buried SMTZ, which is characterized by the presence of oil in ca. 8 m sediment depth. We will investigate the effect of oil on the microbial community composition, their metabolic capabilities, and the sedimentary carbon flow. An extended analytical approach was developed to enable compound-specific isotope analysis based on separation of individual IPLs according to head group polarity before analysis of $\delta^{13}C$ values of their apolar derivatives. This extension provides more detailed insights into the complexity of the microbial community structure than previous studies that analyzed the IPL derivatives as bulk lipid biomass.

IV.3. MATERIAL AND METHODS

IV.3.1. Sampling

Sediment samples were retrieved during Meteor expedition M67/2 in March to April 2006. Sediment cores were recovered by gravity coring and by ROV operated push coring. Push core GeoB10619 (21°54.333'N, 93°26.497'E) was recovered in close vicinity of the main asphalt site (Brüning et al., 2009; Schubotz et al., *in prep., Chapter III*). The deep core GeoB10610 (21°54.25'N, 93°25.88'E) was retrieved approximately ~1 km northwest of the main asphalt site, in the trough of the Chapopote Knoll 'crater', where oil slicks were observed on the surface of the water.

IV.3.2. Lipid biomarkers

IV.3.2.1. Extraction of intact polar membrane lipids

Intact polar lipids (IPLs) were extracted from freeze-dried sediments with a modified Bligh and Dyer method according to the description in Schubotz et al. (*in prep., Chapter III*). In brief, 2 to 50 g of freeze-dried sediment were dispersed in 4 mL per gram sediment of a solvent mixture of dichloromethane:methanol:buffer (DCM:MeOH:buffer, 1:2:0.8; v/v/v) and ultrasonicated for 10 min in four steps. In the first two extraction steps a phosphate buffer was used (pH 7.4), and the last two steps were done with a trichloroacetic acid buffer (50 g/L, pH 2.0). After each ultrasonication step the mixture was centrifuged and the supernatants collected in a separatory funnel. The solvent composition was adjusted to achieve a final ratio of DCM/MeOH/buffer of 1:1:0.8 (v:v:v) by further adding DCM and deionized MilliQ water. The organic phase was washed three times with MilliQ water, carefully reduced to dryness under a stream of nitrogen at 37°C, and stored as total lipid extract (TLE) at -20°C until analysis.

IV.3.2.2. Analysis of IPLs by LC-MS

The analysis of IPLs was previously described in Sturt et al. (2004) and Schubotz et al. (in prep., *Chapter III*). Briefly, an aliquot of the TLE was re-dissolved in DCM:MeOH (5:1) and injected on to a ThermoFinnigan Surveyor HPLC System equipped with a LiChrosphere Diol-100 column (2.1 x 150 mm; Alltech, Germany) coupled to a ThermoFinnigan LCQ Deca XP Plus ion trap mass spectrometer using an electrospray ionization (ESI) interface. Instrument settings were previously described in Sturt et al. (2004). Identification of compounds was based on mass spectral information including complementary fragmentation patterns in positive and negative ionization mode and verification with standards and previously published data (Schubotz et al. *in prep., Chapter III*). Absolute concentrations were calculated from the relative response of the analyte compared to an injection standard (di-C_{19}-PC) and corrected by relative response factors of different IPL classes relative to the injection standard.

IV.3.2.3. Preparation of fractions enriched in IPL classes

Preparation of IPL-enriched fractions and simultaneous removal of petroleum hydrocarbons was achieved by preparative HPLC following the protocol by Biddle et al. (2006). A preparative LiChrosphere Si60 column (250 x 10 mm, 5 um, Alltech, Germany) was connected to a ThermoFinnigan Surveyor HPLC equipped with a Gilson FC204 fraction collector. The flow rate was set to 1.5 mL min^{-1}, and the eluent gradient was: 100%A to 100% in 120 min, hold at 100%B for 30 min, then 30 min column re-equilibration with 100%A, where eluent A was composed of *n*-hexane/2-propanol (79:20, v:v) and eluent B was 2-propanol/MilliQ water (90:10, v:v). In order to determine the fraction collection time windows, a micro-splitter was placed between column and fraction collector and part of the flow was splitted to a ThermoFinnigan LCQ Deca XP Plus mass spectrometer after post-column infusion of ammonium formate in methanol with a tee-piece and a syringe pump. In total, 14 fractions were collected over 120 min (Table IV.1).

Table IV.1. Recovered fractions after preparative LC, containing IPLs separated according to head group polarity. See methods for compound separation, and refer to text for abbreviations.

	Fraction	Abbreviation	Full name
	F1	no IPLs detected	
	F2	apolar lipids: petroleum hydrocarbons, free fatty acids	
	F3	core GDGTs, archaeol, hydroxyarchaeol	
	F4	no IPLs detected	
	F5	no IPLs detected	
	F11	no IPLs detected	
	F12	no IPLs detected	
	F13	no IPLs detected	
Archaeal IPLs	F6	1Gly-GDGT	monoglycosyl-glyceroldibiphytanylglyceroltetraether
	F7	2Gly-GDGT	diglycosyl-glyceroldibiphytanylglyceroltetraether
		2Gly-AR	diglycosyl-archaeol
	F8	3Gly-GDGT	triglycosyl-archaeol
		PG-GDGT	phosphatidylglycerol-glyceroldibiphytanylglyceroltetraether
		PE-AR	phosphatidylethanolamine-archaeol
		PG-AR	phosphatidylglycerol-archaeol
		PG-OH-AR	phosphatidylglycerol-hydroxyarchaeol
	F9	PG-AR	phosphatidylglycerol-archaeol
		PA-OH-AR	phosphatidic acid-hydroxyarchaeol
		PG-OH-AR	phosphatidylglycerol-hydroxyarchaeol
		PE-OH-AR	phosphatidylethanolamine-hydroxyarchaeol
		PI-OH-AR	phosphatidylinositol-hydroxyarchaeol
		PI-OH-eAR	phosphatidylinositol-extended hydroxyarchaeol
	F10	2Gly-GDGT-PG	diglycosyl-glyceroldibiphytanylglyceroltetraether-phosphatidylglycerol
		PG-GDGT-PG	phosphatidylglycerol-glyceroldibiphytanylglyceroltetraether-phosphatidylglycerol
		PG-GDGT-PE	phosphatidylglycerol-glyceroldibiphytanylglyceroltetraether-phosphatidylethanolamine
		PS-OH-AR	phosphatidylserine-archaeol
Bacterial IPLs	F8	PE-DAG	phosphatidylethanolamine-diacylglycerol
	F9	PE-DAG	phosphatidylethanolamine-diacylglycerol
		PE-DEG	phosphatidylethanolamine-dietherglycerol
		DPG	diphosphatidylglycerol
		PG-DAG	phosphatidylglycerol-diacylglycerol
		PA-DAG	phosphatidic acid-diacylglycerol
		UK-DAG	unknown-diacylglycerol
	F10	PME-DAG	phosphatidyl-(N)-methylethanolamine-diacylglycerol
		PDME-DAG	phosphatidyl(N,N)-dimethylethanolamine-diacylglycerol
		PA-DAG	phosphatidic acid-diacylglycerol
	nr	PC-DAG	phosphatidylcholine-diacylglycerol
		BL	betaine lipids

nr: not recovered

IV.3.2.4. Preparation of phospholipid-derived fatty acids (PLFA) and -alcohols (MAGE, DAGE, AR, OH-AR)

Apolar derivatives of IPLs were prepared according to the method described by Elvert et al. (2003). In brief, an aliquot of the polar fraction was dissolved in 2 mL of methanolic KOH (6% KOH in MeOH, w/v) and the reaction took place for 3 h at 80°C in an oven. The mixture was vortexed from time to time. After cooling down to room temperature, 2 mL of a 0.05M KCl solution were added and phospholipid-derived alcohols were extracted by three times shaking with 2 mL *n*-hexane. The pH value was adjusted to pH 1 with 25% HCl and fatty acids were extracted by three times shaking with 2 mL *n*-hexane. After drying under a nitrogen stream, the reaction products were stored at -20°C until derivatization and analysis.

IV.3.2.5. Preparation of hydrocarbon derivatives from IPLs

Preparation of apolar derivatives of ether-bound IPLs was conducted following the procedure by Jahnke et al. (2002). In brief, an aliquot of the polar fraction was dissolved in 200 µL of BBr_3 in DCM (SigmaAldrich, Germany). The cleavage reaction took place under argon atmosphere at 60°C for 2 h. After cooling, the mixture was carefully evaporated under an argon stream before 200 µL of a reaction mixture of superhydride in THF (SigmaAldrich, Germany) was added under argon atmosphere. The mixture was put in an oven for 2 h at 60°C before cooling down to room temperature. 200 µL of deionized MilliQ water was added for quenching of the reaction and the hydrocarbons were extracted by washing in three steps of each 500 µl hexane. After evaporation under a nitrogen stream, the reaction mixture was separated on a silica column (500 mg, Supelco, Germany) using 5 mL of hexane to prepare a clean hydrocarbon fraction.

IV.3.2.6. GC-MS, GC-FID, and GC-irMS

The apolar derivatives of IPLs were analyzed by gas chromatography using three different detectors: (*i*) GC-MS for identification of compounds, (*ii*) GC-FID for quantification of compounds, and (*iii*) GC-irMS for determination of the stable carbon isotopic composition. Gas chromatographic conditions are described in detail in Schubotz et al. (*in prep.*, *Chapter III*). Prior to analysis, an aliquot of the sample was derivatized with bis-(trimethylsilyl)trifluoroacetamide (BSTFA, Merck, Germany) in pyridine at 70°C for 1 h to synthesize trimethylsilyl-(TMS)-derivatives. The derivatives were dissolved in hexane, squalane was added as injection standard, and the mixture was analyzed on a ThermoFinnigan TraceGC coupled to a ThermoFinnigan TraceMS for structural identification through mass spectral information. The MS was operated in electron impact mode at 70 eV with a full scan mass range of *m/z* 40-800. For quantification the GC was coupled to a flame ionization detector (FID) and concentrations were calculated relative to the known amount of injection standard. Compound-specific stable carbon isotopic compositions were measured on a ThermoFinnigan GC coupled to a ThermoFinnigan Deltaplus XP isotope ratio MS via GC-combustion interface. The isotopic compositions of the TMS-derivatives were corrected for the additional methyl groups introduced during derivatization (-29‰). The standard deviation of replicate analysis (n=2) was <1‰. All isotopic values are reported in the delta notation ($\delta^{13}C$) relative to the Vienna PeeDee Belemnite Standard. The initial oven temperature was held at 60°C for 1 min, increased to 150°C with a rate of 10°C min^{-1}, then raised to a temperature of 310°C with a rate of 4°C min^{-1} and held at 310°C for 35 min. The carrier gas was helium with a constant flow of 1.0 mL min^{-1}.

IV.4. RESULTS

IV.4.1. Geochemical profiles

Sediment geochemical profiles of site GeoB10610 and GeoB10619 are discussed in detail by Schubotz et al. (*in prep., Chapter III*) and are summarized in Fig. IV.1. Briefly, at the surface sediment of site GeoB10619 sulfate and methane are present throughout the sediment column and can be used as electron acceptor and carbon source, respectively, by the microbial communities. The surface sediments at 0 to 20 centimeters below seafloor (cmbsf) are strongly influenced by heavy oil migrating upwards from below, which is reflected in the $\delta^{13}C$ of TOC of -27‰ and resembles the $\delta^{13}C$ values of the pure oil and also the asphalts deposited on the seafloor (Fig. IV.1a; Schubotz et al., *in prep.*, *Chapter III*). DIC $\delta^{13}C$ is close to zero in the upper cm of the sediment column, reflecting seawater DIC values and becomes increasingly depleted with depth, with values of up to -23‰ indicating biological respiration. Methane $\delta^{13}C$ values are constant at ca. -65‰ which is reflective of a partly biogenic origin of methane. High concentrations of intact polar lipids (IPLs, 10-25 µg/g sediment) point to the presence of viable microbial biomass throughout the core. The microbial community is composed of both Archaea and Bacteria, with Archaea becoming increasingly more abundant with depth (Fig. IV.1).

The subsurface sediments at site GeoB10610 shows a sulfate-methane transition zone (SMTZ) at ca. 600 cmbsf (Fig. IV.1b). Sulfate is still detected in low amounts (<5 mM)

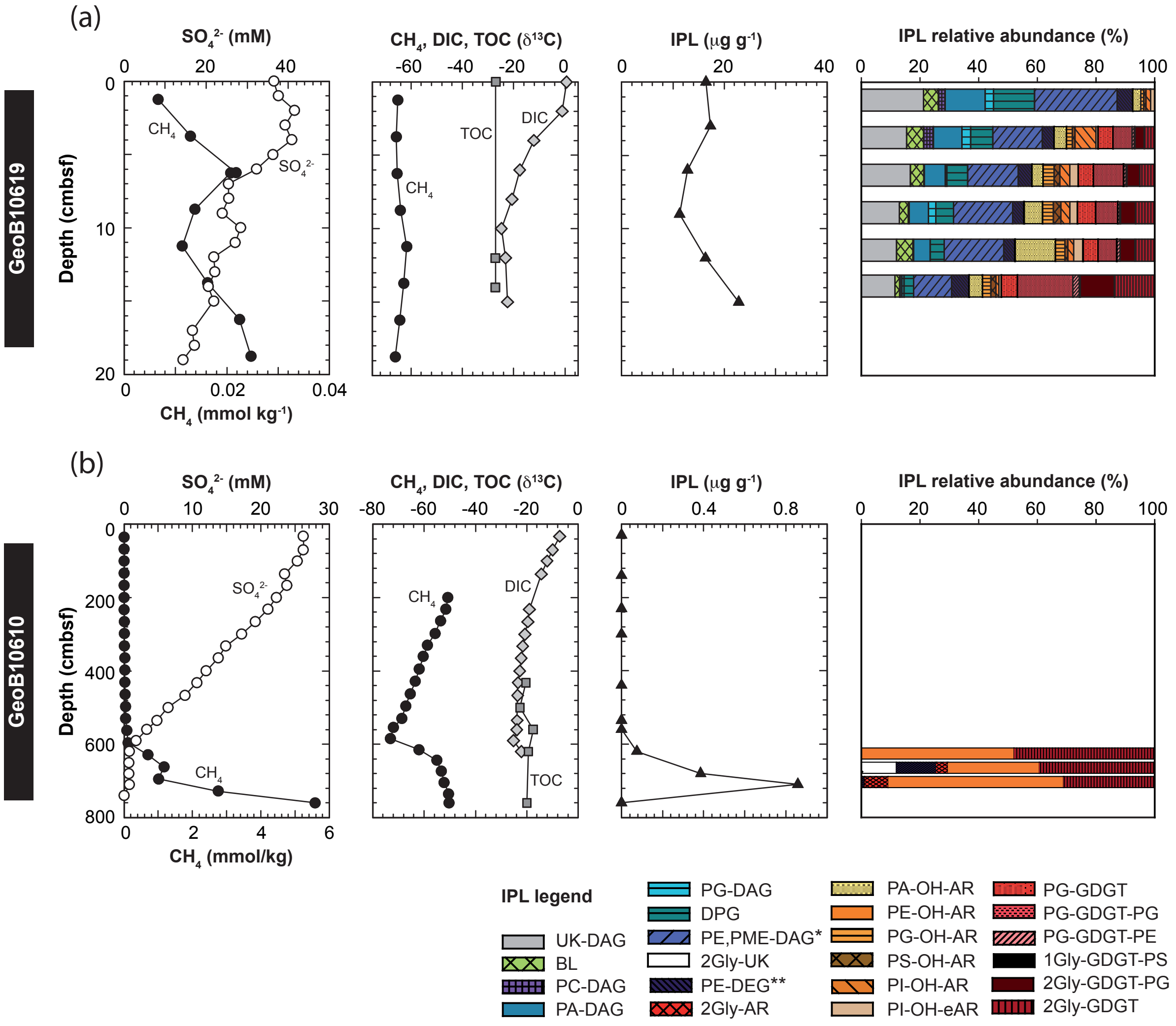

Fig. IV.1. Geochemical profiles of sulfate and methane concentrations, stable carbon isotope composition ($\delta^{13}C$) of methane (CH_4), dissolved inorganic carbon (DIC) and total organic carbon (TOC), and absolute and relative abundances of intact polar lipids (IPL) at site (**A**) GeoB10619 and (**B**) GeoB10610. For IPL abbreviations refer to the text and Table IV.1. *At some depths also PDME was observed. **At Site GeoB10610 also PME was observed. Data is taken from and modified after Schubotz et al. (*in prep., Chapter III*).

until 720 cmbsf and suggests a vertical extension of the SMTZ of more than 1 m. Methane concentrations are highest at 760 cmbsf, where oil droplets were visually observed in the sediment (Schubotz et al., *in prep., Chapter III*). Methane $\delta^{13}C$ values are around -50‰ at 760 cmbsf, pointing to a mainly thermogenic origin. Methane becomes increasingly depleted in ^{13}C in the SMTZ and reaches a minimum of -75‰ at the top of the SMTZ. Here, $\delta^{13}C$ values of DIC show a minimum of -25‰, indicating the contribution of methane oxidation to the DIC pool. TOC $\delta^{13}C$ values remain relatively constant throughout the depth at ca. -20‰. IPLs were only detected within the extended SMTZ, with highest concentrations (>800 ng/g sediment) at the base of the SMTZ where methane concentrations are highest. The IPL distribution is mainly dominated by archaeal compounds, suggesting a microbial community dominated by Archaea (70 to 99%).

IV.4.2. PLFA distribution of individual bacterial polar lipids

In order to gain more insights into the biological source organisms of the polar lipids at site GeoB10619 we separated the IPLs according to their head group by preparative HPLC and analyzed the respective polar lipid-derived fatty acid (PLFA) composition. We combined sediment samples from different depth intervals (2.5-10 cmbsf and 10-15 cmbsf) to have sufficient material for subsequent PLFA analysis. In total preparative LC yielded three different IPL fractions for each depth interval (Table IV.1). The first IPL fraction (F8) contains almost only phosphatidylethanolamine diacylglycerol (PE-DAG; >98%), the second fraction (F9) contains a mixture of PE (51 to 85%), phosphatidylglycerol (PG; 6 to 7%), diphosphatidylglycerol (DPG, cardiolipin; ~1%), phosphatidic acid (PA; 6 to 7%) and an IPL with an unknown head group (UK; 1 to 37%) with DAG structures. The last phospholipid fraction (F10) contains only phosphatidyl-(N)-methylethanolamine (PME, 30-98%), with small amounts of phosphatidyl-(N,N)-dimethylethanolamine (PDME) admixed and in the depth interval 2.5-10 cmbsf also PA-DAG (Table IV.2). PC-DAG, although previously detected during TLE analysis (Schubotz et al., *in prep., Chapter III*) could not be recovered in any of the fractions due to its retention on the preparative LC column.

Distinct differences in the fatty acid (FA) composition of the three fractions become apparent. Fraction 8 PLFAs, mainly derived from PE are dominated by $C_{16:0}$, *ai*-$C_{15:0}$ and $C_{14:0}$. Other major FAs are me$C_{15:0}$, $C_{16:1\omega7}$, $C_{15:0}$ and $C_{18:0}$ (Fig. IV.2). Notably, F8 also contains methyl branched FAs in the carbon number range $C_{14:0}$ to $C_{16:0}$. With depth the PLFA distribution remains similar, however $C_{18:1\omega7}$ and C_{17} fatty acids become abundant. There is some variety in the $\delta^{13}C$ of the PLFAs: saturated FAs $C_{14:0}$ to $C_{18:0}$ are most enriched in ^{13}C with values ranging from -33‰ to -25‰, and most depleted values are observed for $C_{17:1}$, cy$C_{17:0}$, and 10me$C_{16:0}$ ranging from -57 to -54‰ (Table IV.2). Fraction 9, composed of a mixture of four different head groups, has a very similar PLFA distribution to F8, however, $C_{16:0}$ is less abundant and monounsaturated C_{16} and C_{18} FA ($C_{16:1\omega7}$, $C_{16:1\omega5}$, $C_{18:1\omega7}$, and $C_{18:1\omega9}$) become more dominant. Similar to F8, the relative abundance of $C_{18:1\omega7}$ as well as $C_{16:1\omega7}$ and $C_{16:0}$ increase with depth. The distribution of $\delta^{13}C$ is also comparable to F8: most enriched values are observed for the

Table IV.2. Stable carbon isotopic composition and relative distribution (in parentheses) of most abundant fatty acids, MAGE and DAGE of bacterial IPLs, measured in duplicate (precision ±1‰).

	2.5-10 cmbsf			10-17.5 cmbsf		
	F8$^{(a)}$	F9$^{(b)}$	F10-F11$^{(c)}$	F8$^{(d)}$	F9$^{(e)}$	F10-F11$^{(f)}$
	δ^{13}C in ‰ (relative abundance in %)					
			Fatty acids (FA)			
C14:0	-30.8 (7.8)	-38.4 (3.8)	-35.9 (8.2)	-43.0 (6.9)	-42.5 (7.1)	-32.9 (6.7)
MeC14:0	nd (1.0)	-37.8 (1.4)	nd (0.5)	-38.9 (0.9)	-39.0 (2.2)	nd (0.8)
i-C15:0	nd (2.9)	-40.2 (1.9)	-37.6 (1.7)	-46.3 (3.2)	-47.7 (3.1)	nd (1.4)
ai-C15:0	-35.7 (12.6)	-40.4 (9.0)	-39.5 (5.3)	-50.8 (16.8)	-46.4 (19.6)	-45.3 (7.0)
C15:1	nd (0.7)	nd (0.3)	nd (0.5)	-47.3 (0.5)	-49.3 (0.7)	nd (0.5)
C15:0	-32.5(4.7)	-38.0 (1.9)	-33.0 (4.1)	-42.1 (4.6)	-45.0 (4.0)	-28.1 (3.5)
meC15:0	-34.5 (5.7)	-34.2 (1.9)	nd (0.0)	-40.9 (5.6)	-38.7 (2.7)	nd (0.0)
C16:1ω7	-29.6 (3.9)	-32.8 (4.6)	-28.9 (8.7)	-46.7 (5.4)	-30.1 (9.9)	-24.1 (8.5)
C16:1ω5	nd (3.4)	-40.7 (2.8)	-37.3 (4.3)	-46.4 (2.8)	-53.8 (5.8)	-37.5 (2.5)
C16:0	-25.2 (14.5)	-29.9 (57.5)	-26.3 (26.8)	-29.1 (17.9)	-26.1 (14.7)	-22.5 (31.2)
10meC16:0	nd (1.9)	-48.5 (1.0)	nd (0.7)	-53.7 (3.0)	-57.2 (2.3)	-46.0 (1.0)
meC16:0	nd (1.3)	-46.8 (0.6)	nd (1.4)	-50.8 (1.9)	-53.1 (1.9)	-47.4 (1.7)
C17:1	nd (0.0)	-61.6 (0.5)	nd (0.8)	-56.6 (1.5)	-42.6 (1.7)	-32.5 (1.4)
cyC17:0	nd (0.0)	nd (0.6)	nd (0.7)	-57.0 (0.8)	-57.9 (1.0)	-29.8 (0.4)
C17:0	nd (0.5)	-28.0 (0.2)	nd (0.7)	-28.5 (1.5)	-31.4 (0.8)	-31.0 (1.4)
C18:1ω9	nd	-30.2 (0.6)	-24.3 (5.6)	-30.4 (1.7)	-15.8 (1.1)	-23.0 (7.2)
C18:1ω7	nd	-31.3 (2.2)	-26.2 (5.4)	-30.9 (6.9)	-28.8 (7.3)	-19.1 (6.2)
C18:1ω5	nd	-29.6 (2.2)	-29.7 (7.0)	-40.7 (1.3)	-26.6 (2.5)	-23.5 (2.2)
C18:0	-27.5 (11.5)	-28.7 (1.2)	-24.7 (8.2)	-24.4 (5.9)	-26.4 (4.1)	-24.6 (12.8)
			Monoalkylglycerolether (MAGE)			
C14:0	nd	-46.6 (5.7)	nd	nd	-43.2 (6.7)	nd
i-C15:0	nd	-43.7 (5.4)	nd	nd	-42.6 (3.2)	nd
ai-C15:0	nd	-42.4 (22.0)	nd	nd	-43.5 (17.2)	nd
C15:0	nd	-44.9 (4.3)	nd	nd	-44.0 (8.2)	nd
meC15:0	nd	-43.9 (4.7)	nd	nd	-38.1 (4.5)	nd
C16:1ω7	nd	-60.0 (6.3)	nd	nd	-58.1 (5.3)	nd
C16:1ω5	nd	-67.6 (3.4)	nd	nd	nd (3.2)	nd
C16:0	nd	-49.1 (18.7)	nd	nd	-42.8 (18.2)	nd
10meC16:0	nd	-31.2 (9.2)	nd	nd	-36.5 (4.0)	nd
C17:1	nd	nd (2.6)	nd	nd	-56.5 (2.7)	nd
C17:0	nd	nd (4.9)	nd	nd	-59.0 (7.0)	nd
			Dialkylglycerolether (DAGE)			
ai-C15:0/*ai*-C15:0	nd	-50.5	nd	nd	-55.0	nd

(a) F8 contains >98% PE as main head group
(b) F9 contains 85% PE, 7% PG, 7% PA, 1% DPG and <1% unknown compounds as head group for fatty acids and PE as head group for MAGE and DAGE
(c) F10-F11 contains 70% PA and 30% PME as head groups
(d) F8 contains > 98% PE as main IPL
(e) F9 contains 51% PE, 6% PG, 6% PA, and 37% unknown compounds as head group
(f) F10-F11 contains >98% PME with admixtures of PDME as head groups
nd not detected or below detection limit

saturated C_{14} to C_{18} FAs, and most depleted values are found for $C_{17:1}$, cy$C_{17:0}$, 10me$C_{16:0}$ and $C_{16:1\omega5}$. Fraction 10 is very distinct from the other two fractions as it contains only minor amounts of methyl branched FAs and is almost solely dominated by $C_{16:0}$ (up to 30% of total FAs, Table IV.2). The FA *ai*-$C_{15:0}$ comprises only a minor part of PLFAs, and monounsaturated C_{18} FAs also contain $C_{18:1\omega5}$ (Fig. IV.2). The PME-PLFA distribution does not change with depth. The δ^{13}C values are also distinct from F8 and F9. Overall values are relatively enriched in ^{13}C, mainly ranging around -30‰, and most depleted values are observed for *ai*-$C_{15:0}$, 10me$C_{16:0}$,

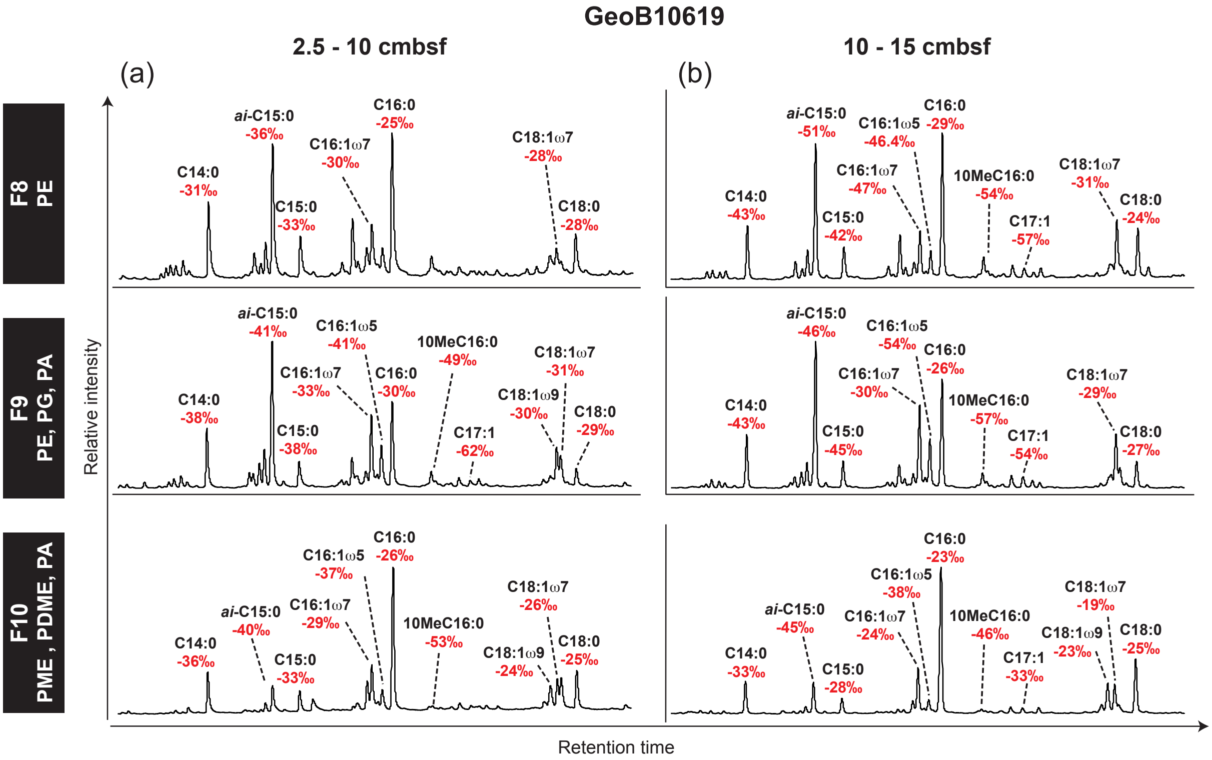

Fig. IV.2. Distribution of polar lipid-derived fatty acids of different head groups from fraction 8, 9 and 10 at site GeoB10619 at (**A**) 2.5 to 10 cm sediment depth, and (**B**) 10 to 15 cm sediment depth.

and $C_{16:0}$ (Table IV.2). Weighted means of the different compound classes were determined and show that F8 and F9 become about 10‰ depleted with depth, whereas F10 is ca. 5‰ enriched in the deeper layers of the surface sediments.

IV.4.3. Distribution of phospholipid-derived MAGE and DAGE

The monoalkylglycerolethers (MAGE) of PE and PME, collected in F9, resemble the chain distribution of the FAs: *ai*-$C_{15:0}$ and $C_{16:0}$ and $C_{14:0}$ are the dominating MAGE, followed by $C_{16:1\omega7}$, $C_{16:1\omega5}$, 10Me-$C_{16:0}$ and $C_{14:0}$. The δ^{13}C values of all MAGE are depleted in ^{13}C throughout the core and range from -67‰ to -31‰ (Table IV.2). The most abundant dialkylglycerolethers (DAGE) is composed of two *ai*-$C_{15:0}$ alkyl chains and its isotopic composition is -48‰ (2.5 to 10 cmbsf) and -52‰ (10 to 17.5 cmbsf). The weighted means of all MAGE and DAGE are more depleted ^{13}C compared to the PLFAs and their δ^{13}C composition becomes slightly enriched with sediment depth.

IV.4.4. Separation of archaeal diether and tetraether IPLs and core lipids

In the surface sediments at site GeoB10619 the most abundant archaeal diether lipid detected was hydroxyarchaeol (OH-AR) with the phosphate-based head groups PG, PA, phosphatidylinositol (PI) and phosphatidylserine (PS), followed by extended hydroxyarchaeol (OH-eAR) with PI as head group (SCHUBOTZ ET AL., *IN PREP.*, *CHAPTER III*). After fractionation of IPL classes with preparative HPLC, we were not able to completely separate all the OH-ARs according to their head group. In total we obtained three fractions: F8 comprised of PG-OH-AR, F9, which contains mixtures of PG- (26-37%), PA- (46-59%), and PI-OH-AR (9-14%), and a third fraction (F10) with solely PS-OH-AR (Table IV.1). Additionally, after preparative sample clean up we could detect intact archaeols (AR) with PG and PE head groups in the prepared fractions, that were not detected previously due to high limit of detection (LOD) during TLE analysis. IPL-ARs were separated into PG-AR in one fraction (F8) and a mixture of PG- (0-17%) and PE-AR (83-100%) in the other fraction (F9; cf. Table IV.1). Isotopic values for OH-ARs and AR with different head groups were very similar. For OH-ARs and OH-eARs, the δ^{13}C values ranged from -107‰ to -95‰ and PS was most enriched in ^{13}C. In comparison, ARs were enriched in ^{13}C with values around -70‰ to -67‰. The isotopic values did not change significantly with depth.

The main GDGTs in the surface sediments are 2Gly-GDGT, 2Gly-GDGT-PG and PG-GDGT-PG and PG-GDGT-PE. We were able to separate 2Gly-GDGT from PG-GDGT and the remaining IPL-GDGTs by preparative LC prior to δ^{13}C analysis. Ether cleavage of GDGT from the individual head group fractions revealed very depleted values for GDGT-derived biphytanes (bp). The most depleted values are observed for 2Gly-GDGT, where isotopic values of bp with 0 to 3 pentacyclic rings (bp0-bp3) ranged from -96‰ to -83‰. PG-GDGT is more enriched in ^{13}C with values ranging from -88‰ to -64‰. The remaining IPL-GDGTs contained bp0 to 2 with values spanning from -84‰ to -63‰. For all IPL-GDGT, bp0 is ca. 10‰ to 20‰ more enriched in ^{13}C compared to bp1 and bp2.

The most abundant diether archaeal IPLs in subsurface sediments from core GeoB10610 were PE-OH-AR and 2Gly-AR (Fig. IV.1). Saponification of the corresponding preparative fractions (F7 and F9) did not result in sufficient yields for isotopic analysis. Therefore we analyzed phytane after ether cleavage of the 2Gly-AR containing fraction (F7). For PE-OH-AR, not enough material was left after saponification to conduct ether cleavage, after saponification therefore we used the core lipid fraction (F3) where the presence of hydroxyarchaeol was confirmed by HPLC-APCI-MS analysis. The phytane of the ether cleaved F3 fraction represents a mixture of AR, derived from 2Gly-AR (<12%) and PE-OH-AR (>88%; Fig. IV.1). However, the values for phytane from the F3 and the F7 were very similar, therefore we assume that also the δ^{13}C values for 2Gly-AR and PE-OH-AR are similar (Table IV.4).

The most abundant intact tetraether lipid in the deep sediment is 2Gly-GDGT. After preparative LC we also detected small amounts of 1Gly- and 3Gly-GDGT at 710 and 680 cmbsf (<1% of total IPLs). 1Gly-, 2Gly-, and 3Gly-GDGT could be separated according to their head groups prior to δ^{13}C analysis (Table IV.1). For 3Gly-GDGT isotope values could be determined only for the sample from 710 cmbsf due to low concentration. Values for bp0 and bp1 are most depleted in all IPL-GDGTs (-96‰ to -74‰), most enriched values are observed for bp3c (-18‰ to -21‰), which is derived from crenarchaeol, a GDGT with four pentacyclic rings and one hexacyclic ring (Sinninghe-Damsté et al., 2002). Core GDGTs without head groups were found in F3, here isotopic values could only be determined for bp2 and bp3c at 560 and 620 cmbsf and range at ~18‰. At 680 and 710 cmbsf bp2 and bp3c become slightly depleted by 1 to 6‰ (Table IV.4). At these depths also bp0 and bp1 δ^{13}C values could be determined,

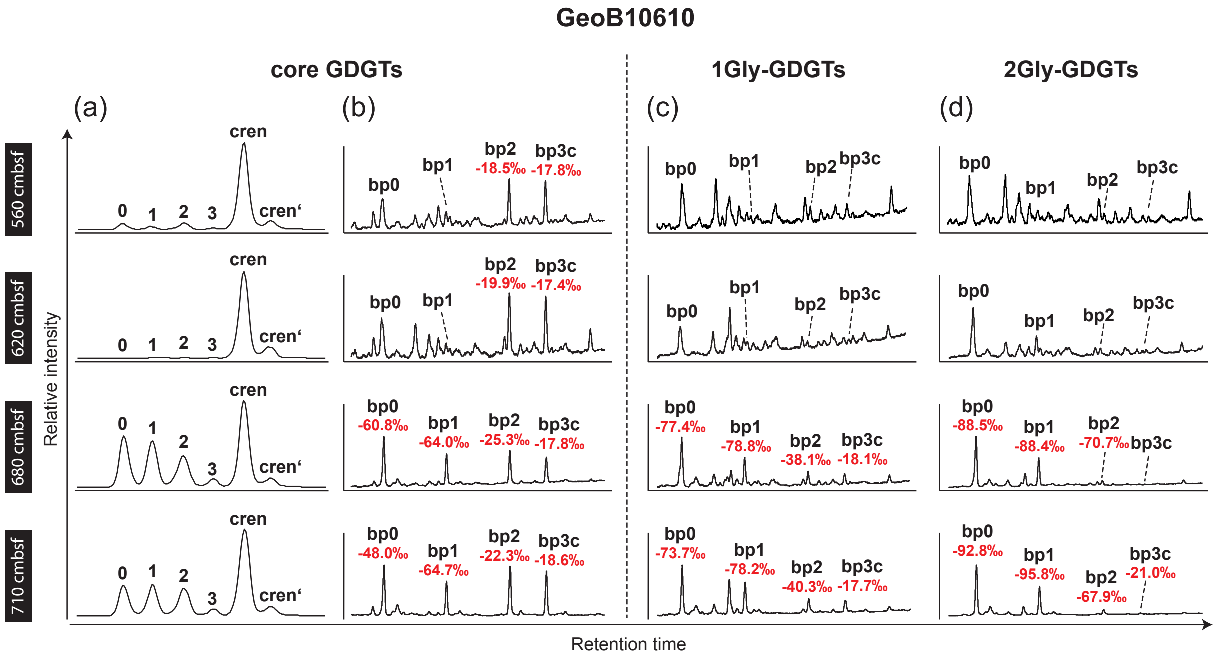

Fig. IV.3. Core and IPL-GDGT distribution in GRC GeoB10610. (**A**) HPLC-APCI-MS base peak plot of reconstructed mass chromatograms of GDGT-0, -1, -2, -3, -5, -5' of core GDGTs, (**B**) GC-FID chromatogram of core GDGT ether-cleaved biphytanes, (**C**) 1Gly-GDGT ether cleaved biphytanes, (**D**) and 2Gly-GDGT ether-cleaved biphytanes. In parentheses are $\delta^{13}C$ of individual compounds, see also Table IV.2.

which likely derive from GDGT-0, GDGT-1 and GDGT-2 that become increasingly abundant with depth (Fig. IV.3) and range around -64‰ to -50‰.

IV.5. DISCUSSION

IV.5.1. Distribution of heterotrophic and autotrophic sulfate-reducing bacteria in oily surface sediments

Bacterial DAG phospholipids in the oil-impregnated surface sediments of site GeoB10619 are dominated by PE and PME, PG, PA, DPG, PC, and PDME (Fig. IV.1). Furthermore an unknown IPL with a diacylglycerol core structure (UK-DAG) was identified. Schubotz et al. (*in prep.*, *Chapter III*) assigned most of these phospholipids to sulfate-reducing bacteria (SRB) on the basis of the IPL inventories found in cultures and of sulfate, as a likely electron acceptor during hydrocarbon degradation, being present throughout the sediment. IPL-specific PLFA analysis and subsequent $\delta^{13}C$ analysis confirms that SRB are indeed likely biological precursor of most of the bacterial IPLs, but pronounced differences in the carbon metabolism are observed. A distinct feature of the PLFA of IPLs with PE, PG, DPG, PA and the unknown head group (F8 and F9) is the abundance of branched $C_{14:0}$, $C_{15:0}$, and $C_{16:0}$ fatty acids (Fig. IV.2, Table IV.2). Branched and odd-carbon-numbered fatty acids are typical components in cultures of SRB (Boon et al., 1977, Taylor and Parkes, 1983; Dowling et al., 1986). The only other bacteria known to produce branched fatty acids, apart from SRB are gram-positive Bacillus and Actinomycetes (Kaneda 1991; Wallace et al., 1995). However, we can exclude the latter as potential source organism in these sediments since many Bacillus and Actinomycetes species contain additional unique IPLs in their cell membrane, such as surfactin (cf. HUE ET AL., 2001) and glycolipids (e.g., SHAW, 1970; GAMIAN ET AL., 1996) that were not detected in this study.

Some of the observed fatty acids are genus specific for certain SRB, for instance 10me$C_{16:0}$ and cy$C_{17:0}$ are main fatty acids in *Desulfobacter* (TAYLOR AND PARKES, 1983; DOWLING ET AL., 1986; KOHRING ET AL., 1994; LONDRY ET AL., 2004), *Desulfobacterium* (LONDRY ET AL., 2004) and *Desulfobacula* (KUEVER ET AL., 2001). Members of the *Desulfobacter* and *Desulfobacterales* are able to anaerobically degrade aromatic petroleum hydrocarbons (e.g., PHELPS ET AL., 1998; RUETER ET AL., 1994; MUSAT ET AL. 2009) and are thus likely to be present in the oil-impregnated sediments. Iso- and anteiso-C_{15} and C_{17} fatty acids are characteristic for *Desulfovibrio sp.* (BOON ET AL., 1977; UEKI AND SUTO, 1979; TAYLOR AND PARKES, 1983; VAINSHTEIN ET AL., 1992; KOHRING ET AL., 1994), and members of this group are also known to degrade oil compounds such as *n*-alkanes (cf. RABUS ET AL., 2006). The $C_{17:1}$ FAs, which are present in minor amounts have been mainly associated with *Desulfobulbus sp.* (TAYLOR AND PARKES, 1983; PARKES AND CALDER, 1985; KOHRING ET AL., 1994) and members of *Desulforhabdus* and *Desulforhopalus* (KNOBLAUCH ET AL., 1999; RÜTTERS ET AL., 2001). Another potential source organism for *ai*-$C_{15:0}$ and $C_{17:1}$ is also *Desulfosarcina variabilis* (RÜTTERS ET AL., 2001) which is a cultured representative of the *Desulfosarcina*/*Desulfoccocus* (DSS) group involved in AOM together with ANME-1 and ANME-2 methanotrophic archaea (BOETIUS ET AL., 2000; ORPHAN ET AL., 2001). The presence of sequences similar to *Desulfobacterium*, *Desulfobacula,* and *Desulfosarcina* was confirmed by *dsrA*-gene in the sediments of GeoB10619 (D. SANTILLANO ET AL., PERS. COMM.).

Within the PLFAs of F8, F9 and F10 there is considerable variation in $\delta^{13}C$. FAs with $\delta^{13}C$ values close to $\delta^{13}C$ TOC values are observed in all three phospholipid fractions and are comprised of saturated C_{16} to C_{18} and monounsaturated C_{18} fatty acids (Table IV.2). These FAs are considered as generic, however, they are often the most abundant FAs in oil-degrading bacteria (e.g., KOHRING ET AL., 1994, MACNAUGHTON ET AL., 1999; ARIES ET AL., 2001). Based on their $\delta^{13}C$ values, we assign these PLFAs to mainly heterotrophic oil-degrading bacteria, in accordance with observed fractionations of heterotrophic SRBs in laboratory studies of up to 14‰ (LONDRY ET AL., 2004). For some of the FAs, particularly for saturated and monounsaturated C_{18} FAs, an enrichment in ^{13}C relative to TOC is observed ranging from 0.5‰ to 8‰. Such enrichments relative to the substrate have been observed under substrate limitation during heterotrophic growth in the gram positive SRB *Desulfotomaculum acetooxidans* that utilizes the reversed TCA cycle during carbon assimilation (LONDRY ET AL., 2004). *Desulfotomaculum sp.* is a candidate source organism in these sediments since it is a known hydrocarbon degrader (cf. RABUS ET AL., 2006) with a generic fatty acid distribution composed of mainly saturated FAs and monounsaturated C_{18} (TAYLOR AND PARKES, 1993; KOHRING ET AL., 1994; LONDRY ET AL., 2004). Further support comes from *dsrA* gene sequences of *Desulfotomaculum* relatives that were detected in the sediments (D. SANTILLANO ET AL., PERS. COMM.).

In all bacterial phospholipid fractions, the FAs that are most depleted relative to DIC with a mean fractionation of ca. -30‰ relative to DIC are *ai*-$C_{15:0}$, 10me$C_{16:0}$, me$C_{16:0}$, $C_{17:1}$ and cy$C_{17:0}$, and also almost all of the MAGEs and *ai*-$C_{15:0}$/*ai*-$C_{15:0}$ DAGE (Table IV.2). These are also the common lipids that have been associated with SRB involved in AOM (Hinrichs et al., 2000; Pancost et al., 2001; Elvert et al., 2003, Blumenberg et al., 2004, Niemann and Elvert, 2008). However, in other AOM-dominated systems, including the northern GoM, a typical offset of -40‰ to -50‰ in the FAs relative to DIC is observed (Hinrichs and Boetius, 2002; Zhang et al., 2002; Orcutt et al., 2005), in accordance with carbon isotopic fractionation by autotrophic SRB using the acetyl-CoA-carbon monoxide dehydrogenase pathway (Preuss et al., 1989; Londry and Des Marais, 2003; Londry et al., 2004). Autotrophic growth and recycling of depleted CO_2 generated during methane oxidation for bacteria during AOM has recently been confirmed in laboratory studies (Wegener et al., 2008). We consequently assign the more enriched $\delta^{13}C$ of these PLFAs to a mixed signal of autotrophic and heterotrophic bacteria synthesizing similar FAs. This is reasonable considering that *Desulfobacterium* and *Desulfobacula* also produce these FAs and are likely oil-degraders in these sediments. Monoalkylglycerolethers have not only been detected in the AOM associated *Desulfosarcina variabilis*, but also in *Desulforhabdus amnigenus*, a SRB capable of degradation of aromatic hydrocarbons (Rütters et al., 2001). Decoupling of sulfate reduction and AOM, evidenced by sulfate reduction rates exceeding AOM rates are known from seep sites, particularly in the GoM (e.g., Joye et al. 2004; Formolo et al., 2004; Orcutt et al., 2004; Lloyd et al., 2006). In those studies sulfate reduction was primarily coupled to the degradation of petroleum and other hydrocarbons next to AOM.

Comparison of the weighted means of the different phospholipid fractions indicates that heterotrophic and autotrophic bacteria seem to produce different head groups. Mean $\delta^{13}C$ values of PLFA from F8 and F9, consisting of PE, PG, DPG, PA, and the UK head groups, are consistently depleted relative to DIC by -15‰ to -18‰ (Fig. IV.4, Table IV.2), consistent with autotrophy as primary carbon metabolism (Londry et al., 2004). This observation is consistent with culture IPL studies where PE, PG and DPG are the most abundant IPLs observed in a wide range of gram-negative SRB of the Deltaproteobacteria, including *Desulfosarcina variabilis* (e.g., Rütters et al., 2001, Sturt et al., 2004, Makula and Finnerty, 1974; Seidel, 2009). In contrast, mean $\delta^{13}C$ values of PLFAs from F10, comprised of mainly PME and PDME head groups, more closely resemble those of TOC (Fig. IV.4, Table IV.2), suggestive of a predominant heterotrophic metabolism. Therefore we conclude that PLFAs with PME and PDME head groups are mainly synthesized by oil-degrading bacteria.

IV.5.2. Methanotrophic and methanogenic archaea in surface sediments

Abundant archaeal IPLs with OH-AR and GDGT core structures in surface sediments at site GeoB10619 were assigned to both methanotrophic and methanogenic archaea (Schubotz et al., *in prep., Chapter III*). Since methanotrophic and methanogenic archaeal are likely to produce very similar lipids (cf. Koga and Nakano, 2008; Rossel et al., 2008), $\delta^{13}C$ values of the lipids are required for assessing the relative importance of these two microbial groups in the sediments of the Chapopote asphalt seep.

Almost all archaeal IPLs in surface sediments are more depleted in ^{13}C than methane, indicating a major contribution of methanotrophic archaea at these depth intervals. However, there are strong variations in δ^{13}C of different archaeal diethers and tetraethers and also between lipids associated with different polar head group classes. Compounds that are most depleted in ^{13}C relative to methane by -40‰ to -43‰ are OH-ARs of F8 and F9 (Fig. IV.3). There are only little variations between different phospho-based head groups, apart from PS-OH-AR, which is ~10‰ more enriched in ^{13}C compared to PI-OH-AR, PA-OH-AR, and PG-OH-AR in the deeper sediments (Table IV.3). This strong depletion relative to methane is consistent with field observations where lipids assigned to methanotrophic archaea are typically depleted in ^{13}C relative to methane by 40‰ to 50‰ (Hinrichs and Boetius, 2002). AR with PG and PE head groups has substantially higher δ^{13}C values than OH-AR and is only -3‰ to -8‰ depleted in ^{13}C relative to methane. Therefore an exclusive methanotrophic source for these lipids is unlikely. Instead δ^{13}C values of IPL-AR covary with δ^{13}C values of DIC and show an apparent isotopic fractionation relative to DIC of -45‰ to -58‰ (Fig. IV.3). Methanogenic archaea have fractionation factors of 23‰ and 45‰ between biomass and CO$_2$ during CO$_2$-reducing methanogenesis (House et al., 2003). The fractionation factor from biomass to lipid in CO$_2$-reducing methanogens was observed to be around 18‰ (cf. Hayes, 2001), recent studies confirmed that fraction between lipid and CO$_2$ can be as high as -47‰ under H$_2$ limitation and around 14‰ with abundant H$_2$ present (Londry et al., 2008). δ^{13}C values of IPL-AR and their relationship to DIC are consistent with a primary origin of methanogenic archaea.

In the surface sediments (0 to 20 cmbsf), IPL-GDGTs were observed with both phospho-based and diglycosidic polar head groups or mixtures of both (Fig. IV.1a). The analysis of GDGT-derived bp of the different head groups revealed distinct patterns in δ^{13}C values.

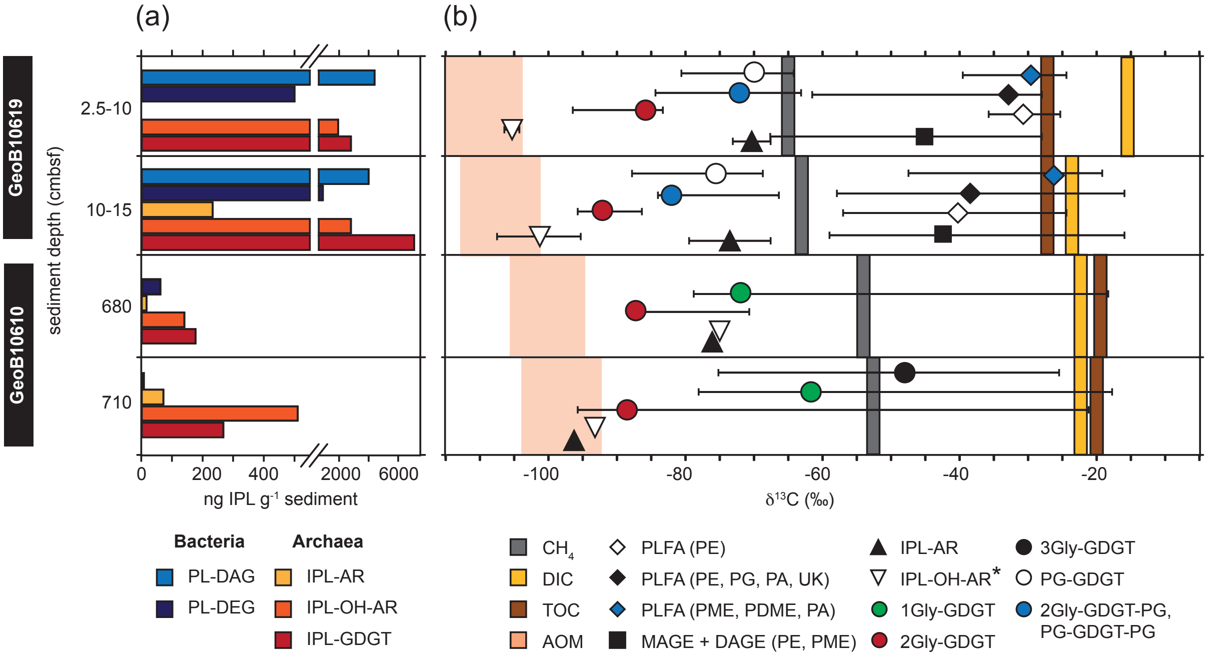

Fig. IV.4. (**A**) Depth profile of archaeal and bacterial IPL concentration at site GeoB10619 and GeoB10610. (**B**) Variations in δ^{13}C of IPL-derived apolar derivatives and carbon substrates TOC, DIC and methane. Symbols depict the weighted means of each individual IPL fraction and horizontal bars designate the range in δ^{13}C observed in the respective fraction. For IPL-AR and IPL-OH-AR the mean of the different head groups (F8 to F10) are depicted. *The δ^{13}C value for PE-OH-AR at site GeoB10610 could only be determined indirectly by analysis of the F3 core lipid fraction (see main text). For abbreviations of IPLs refer to the text and Table IV.1.

Biphytanes of 2Gly-GDGT were overall most depleted and ranged between -96‰ to -83‰ which is up to 30‰ enriched in ^{13}C compared to the IPL-OH-AR and up to 30‰ depleted in ^{13}C compared to the IPL-AR and thus most likely represents a mixed signal of methanotrophic and methanogenic archaea. ANME-2 archaea are known to produce phosphate-based OH-AR, whereas ANME-1 archaea mainly produce 2Gly-GDGTs (Rossel et al., 2008). The observation of a lower fractionation for ANME-1 compared to ANME-2 archaea is consistent with previous findings (cf. Niemann and Elvert, 2008), and is supported by analysis of single cells of ANME-1 (Orphan et al., 2002). A likely explanation is that archaea from the ANME-1 cluster, which are closely related to known methanogens, may be able to do both: methane oxidation and methanogenesis. Alternatively, the less depleted biphytanes are derived from a mixture of methanogenic and methanotrophic archaea. This is supported by an observed shift to lighter isotopic values with depth, mirroring the lighter values for DIC, and pointing to a connection to an autotrophic metabolism of the 2Gly-GDGT-producing archaea. The variation in δ^{13}C of the core lipids of GDGT is minimal, however, bp0 is up to 10‰ enriched in ^{13}C (Table IV.3), which would support the latter hypothesis. Culture studies of methanogenic archaea have shown that they mainly synthesize GDGT-0 (Koga et al., 1998) whereas methanotrophic archaea contain mainly GDGT-1, GDGT-2 and GDGT-3 (Blumenberg et al., 2004). The biphytanes of phospho-GDGTs and mixed phospho-glyco-GDGTs are more enriched in ^{13}C compared to 2Gly-GDGT. Minimal apparent fractionations relative to DIC are observed for bp0, ranging from 43‰ to 50‰, which is in a similar range as the IPL-ARs and can be thus partly assigned to

Table IV.3. Stable carbon isotopic composition of archaeal diether and tetraether IPL-derivatives in surface sediments, measured in duplicate (precision ±1‰).

	2.5-10 cmbsf					
	2Gly (100)	PG-PE (33) PG-PG (34), 2Gly-PG(33)	PG (100)	PE (83), PG (17)	PI (9), PA (59), PG (26), PS(5)	PI (100)
	δ^{13}C in ‰					
Archaeol	nd	nd	-72.9	-67.6	nd	nd
Hydroxyarchaeol	nd	nd	nd	nd	-106.0	nd
Ext. hydroxyarchaeol	nd	nd	nd	nd	nd	-104.5
Biphytane 0	-83.3	-63.2	-64.3	nd	nd	nd
Biphytane 1	-88.0	-74.4	-76.8	nd	nd	nd
Biphytane 2	-86.6	-84.3	-80.6	nd	nd	nd
	10-17 cmbsf					
	2Gly (100)	PG-PE (4), PG-PG (64), 2Gly-PG(32)	PG (100)	PE (100)	PI (14), PA (46), PG (37), PS(3)	PS (100)
	δ^{13}C in ‰					
Archaeol	nd	nd	-69.2	-79	nd	-678
Hydroxyarchaeol	nd	nd	-104.9	nd	-107	-95
Biphytane 0	-86.5	-66.3	-68.8	nd	nd	nd
Biphytane 1	-95.8	-84.1	-77.6	nd	nd	nd
Biphytane 2	-94.5	-83.6	-87.9	nd	nd	nd
Biphytane 3	-93.6	nd	nd	nd	nd	nd

nd – not detected

methanogenic archaea (Hayes, 2001; House et al., 2003; Londry et al., 2008). Biphytanes with increasing ring numbers become increasingly depleted in ^{13}C, indicating an increased contribution of methanotrophic archaea. The observation that methanotrophic and methanogenic archaea produce different head groups in the environment is novel, but is generally consistent with published data that show that 2Gly-GDGT is the main IPL in ANME-1 methanotrophic archaea (Rossel et al., 2008) and phospho- and mixed phospho and glyco-GDGTs, e.g., PG-GDGT, PG-GDGT-PG, and 2Gly-GDGT-PG, are abundantly observed IPLs in methanogenic archaea (Koga et al., 1998; Strapoc et al., 2008, *Chapter VId*).

IV.5.2.1. Distribution of ANME-1 and ANME-2 archaea

The mixture of δ^{13}C depleted phospho-OH-ARs and slightly less depleted 2Gly-GDGTs in the oil-impregnated surface sediments of GeoB10619 points to the presence of both ANME-2 and ANME-1 (cf. Rossel et al., 2008). Although subtle, we observe an increase in 2Gly-GDGT with depth, indicating that ANME-1 archaea become more important in the deeper layers. In a similar manner also the phospho-GDGTs increase, particularly PG-GDGT-PG and 2Gly-GDGT-PG. The δ^{13}C analysis, however, suggest that those compounds are predominantly derived from methanogenic archaea. A dominance of ANME-1 in the sediments of GeoB10619 also fits the PLFA profiles, as abundant *ai*-$C_{15:0}$ together with the presence of $C_{16:1\omega5}$ were mainly assigned to the DSS cluster associated with ANME-1 archaea (cf. Elvert et al., 2003). Furthermore it was observed that ANME-1-associated bacteria contain more DEG lipids (Blumenberg et al., 2004), which also fits our results where phospho-DEG increase in abundance with depth (Fig. IV.1). Finally, the increase in ANME-1 archaea with depth is accompanied by a decrease in sulfate concentration, consistent with previous studies where ANME-1 groups were observed at locations with reduced sulfate levels (Harrison et al., 2009; Knittel et al., 2005).

IV.5.3. Methanogenic, methanotrophic, and heterotrophic archaea in subsurface sediments

The ratio of archaeal to bacterial IPLs increases with sediment depth. This trend can already be seen in the surface sediments of site GeoB10619 and becomes most apparent in subsurface sediments at site GeoB10610 where more than 80% of IPLs are derived from Archaea (Fig. IV.1). Typically, this trend is expressed in an increase of membrane-spanning GDGTs containing diglycosidic head groups (Lipp et al., 2008; Lipp and Hinrichs, 2009), and with δ^{13}C lipid compositions reflecting a heterotrophic metabolism, even in deeply buried SMTZ (Biddle et al., 2006). However, at Chapopote abundant OH-ARs were observed in the deeply buried SMTZ and δ^{13}C values of most of the archaeal IPLs are very depleted (<-70‰), even in the deeper sediment layers in the SMTZ.

In contrast to surface sediments, IPL-ARs and IPL-GDGTs contain mainly glycosidic-based head groups, and IPL-OH-AR contains PE as head group, which was not observed in the surface sediments of site GeoB10619. This is an indication that the archaeal community is different from that in surface sediments. PE-OH-AR (determined through F3, see methods) and 2Gly-AR are very similar in their isotopic compositions: they are both ca. 20‰ more depleted

Table IV.4. Stable carbon isotopic composition of archaeal diether and tetraether lipid-derivatives in subsurface sediments, measured in duplicate (precision ±1‰).

	Depth (cmbsf)			
	560	620	680	710
	$\delta^{13}C$ in ‰			
	1Gly-GDGT			
Biphytane 0	nd	nd	-77.4	-73.7
Biphytane 1	nd	nd	-78.8	-78.2
Biphytane 2	nd	nd	-38.1	-40.3
Biphytane 3 cren	nd	nd	-18.1	-17.7
	2Gly-GDGT			
Phytane	nd	nd	-76.0	-96.2
Biphytane 0	nd	nd	-88.5	-92.8
Biphytane 1	nd	nd	-88.4	-95.8
Biphytane 2	nd	nd	-70.7	-67.9
Biphytane 3 cren	nd	nd	nd	-21.0
	3Gly-GDGT			
Biphytane 0	nd	nd	nd	-75.2
Biphytane 1	nd	nd	nd	-62.9
Biphytane 2	nd	nd	nd	-25.4
	Core lipids			
Phytane	nd	nd	-74.9	-93.2
Biphytane 0	nd	nd	-63.5	-50.1
Biphytane 1	nd	nd	-62.0	-63.5
Biphytane 2	-18.5	-19.9	-25.3	-22.3
Biphytane 3 cren	-17.8	-17.4	-17.8	-18.6

nd – not detected

at the bottom of the SMTZ than in the center, 30 cm above (Table IV.4). Towards the top of the SMTZ, methane becomes increasingly depleted in ^{13}C, suggesting the presence of methanogens that utilize ^{13}C depleted CO_2. It is conceivable that at the bottom of the SMTZ where abundant methane is present the archaea mainly gain energy by methane consumption, but as methane is consumed, some of the archaea switch their metabolism to autotrophy, i.e., CO_2-reducing methanogenesis.

The $\delta^{13}C$ values of the IPL-GDGT-derived biphytanes from different head groups are quite variable and likely reflect different carbon sources, source organisms, and/or mixing ratios of precursors with different metabolisms. In contrast to IPL-GDGTs from the surface sediments, the IPL-GDGT from the SMTZ also contain crenarchaeol as GDGT core lipid, besides GDGT-0, -1, -2, and -3. Crenarchaeol is considered to be a characteristic marker for crenarchaea (Sinninghe-Damsté et al., 2002) and its IPL-derivatives in subsurface sediments have been assigned to indigenous benthic crenarchaea (cf. Lipp and Hinrichs, 2009). Opposed to euryarchaea, including methanotrophic and methanogenic archaea, crenarchaea are not known to metabolize methane, instead they have been assigned a heterotrophic metabolism in subsurface sediments (Biddle et al., 2006). A mixture of euryarchaea and crenarchaea as potential source organisms is indeed reflected in $\delta^{13}C$ of the GDGT-derived biphytanes of 1Gly-and 2Gly-GDGT. Whereas bp0 and bp1 are always significantly depleted in ^{13}C with

-92‰ to -63‰ for 1Gly-, 2Gly- and 3Gly-GDGTs, bp3c has values around -21‰ to -17‰ and bp2 mixed $\delta^{13}C$ values of -25‰ to -70‰. The more depleted values resemble those of 2Gly-AR and PE-OH-AR and indicate methanotrophy or mixed methanotrophy and methanogenesis as carbon metabolism for the source organisms of bp0 and 1, whereas the most enriched values observed for bp3c reflect heterotrophy (Table IV.4, Fig. IV.3).

IV.5.3.1. Turnover of IPLs in subsurface sediments

There is an ongoing debate about the detection of crenarchaeol in deeply buried sediment with $\delta^{13}C$ values resembling those of TOC and planktonic archaea. Are these signals indeed derived from indigenous archaea and not a fossil signal (cf. Lipp and Hinrichs, 2009)? Comparison of the size of the IPL-GDGT pool (representing mostly live biomass) and the core GDGT pool (representing fossil material) has shown that the IPL-GDGT pool is 1 to 2 orders of magnitude smaller than the core GDGTs pool (Lipp and Hinrichs et al., 2009; Liu et al., 2009). We were interested if we could see an imprint of the IPL-GDGT pool in the fossil record. Above the SMTZ, where IPL-GDGTs were below the limit of detection, core GDGTs most likely represent a fossil signal derived from the water column. Stable carbon isotope values of -19‰ to -17‰ for bp2 and bp3c are consistent with a planktonic source for these lipids (Trumbore and Druffel, 1995). In sediments inside the SMTZ, however, the abundances of bp0 and bp1, which are also the most abundant biphytanes observed in the IPL fractions, also increases in the core GDGT fraction. As the concentration of these lipids increase with depth the isotopic composition becomes more depleted in a similar manner as for the biphytanes derived from the intact GDGTs. Bp1, which has the lowest values in the IPL-GDGT pool, shows very low $\delta^{13}C$ values around -66‰, and similarly bp0 of the core GDGTs is more depleted in ^{13}C in the SMTZ than above the SMTZ at 560 cmbsf. Values for bp3c, which was not observed in any of the intact lipids, remain constant at -17‰. Bp2 becomes slightly enriched by 2 to 5‰. These results clearly show that the core GDGT pool is significantly influenced and altered by turnover of IPLs derived from indigenous methanotrophic, methanogenic, and heterotrophic archaea in the SMTZ.

IV.6. SUMMARY AND CONCLUSIONS

This study provides detailed insight into the structure and function of microbial communities involved in hydrocarbon and methane turnover at an asphalt seep. We were able to obtain a more detailed view on the carbon flow by IPL-specific $\delta^{13}C$ analysis. Although head group separation was not always complete, pronounced differences in $\delta^{13}C$ composition were observed. These reflect differences in carbon assimilation of the respective source organism that would have been overlooked by conventional compound-specific carbon isotope analysis.

- The presence of SRB in surface sediments were confirmed by characteristic PLFA profiles, e.g., *ai*-$C_{15:0}$, 10me$C_{16:0}$, , $C_{16:1\omega5}$, *cy*$C_{17:0}$, could mostly be associated to AOM-performing SRB due to ^{13}C-depleted values. Distinct differences in $\delta^{13}C$ values of the PLFAs were observed for different polar head groups: (*i*) PLFAs derived from PE, PG, DPG, and PA head groups were on average 20 to 40‰ depleted relative to DIC and could thus be assigned to an autotrophic metabolism, and (*ii*) PLFAs derived from PME and PDME head groups were generally correlated to $\delta^{13}C$ TOC values and were therefore mainly associated to oil-degrading SRB.

- In surface sediments, phosphate-based OH-ARs and GDGTs with diglycosidic head groups were predominantly assigned to methanotrophic archaea, whereas phosphate-based ARs and GDGTs are more enriched in ^{13}C and were attributed to CO_2-reducing methanogenic archaea with an additional potential methanotrophic source.
- In surface sediments IPLs of both ANME-1 (2Gly-GDGT) and ANME-2 (phospho-OH-AR) were observed. ANME-1 archaea become dominant with increasing sediment depth, which is also reflected in the associated bacterial apolar derivatives, i.e., a dominance of *ai*-$C_{15:0}$, and mono- and dialkylglycerolethers.
- In the subsurface SMTZ methanotrophic and methanogenic archaea dominate the microbial community composition. Evidence for heterotrophic benthic crenarchaea is found in $\delta^{13}C$ values that resemble the $\delta^{13}C$ of TOC. Methanotrophic, methanogenic and heterotrophic archaea in the deeply buried sediment produce similar lipids as reflected in mixed methanotrophic and methanogenic signals for PE-OH-AR, 2Gly-AR and 1Gly-, 2Gly-, and 3Gly-GDGTs.
- Core GDGTs, presumably fossil remains of planktonic water column archaea, show an imprint of the indigenous archaea thriving at the SMTZ, as reflected in both the relative distribution of GDGTs and a shift to highly depleted $\delta^{13}C$ values. This is evidence for fast turnover of IPLs even in sediments that are buried in over 7 m sediment depth.

IV.7 ACKNOWLEDGEMENTS

We thank the Shipboard crew and scientific crew of Meteor expedition M67/2 to the Campeche Knolls, Gulf of Mexico. Xavier Prieto-Mollar, Kevin Becker, and Tim Kahs are thanked for their help in the laboratory and Enno Schefuß is gratefully thanked for providing access to GC-irMS. This work was funded by the Deutsche Forschungsgemeinschaft (DFG), through MARUM - Center for Marine Environmental Sciences and the graduate school GLOMAR, funded through the excellence initiative of the DFG.

IV.8. REFERENCES

Aharon, P., Roberts, H.H., Snelling, R.(1992) Submarine venting of brines in the deep Gulf of Mexico: observations and geochemistry. *Geology* **20**: 483-486.

Aries, E., Doumenq, P., Aertaud, J., Acquaviva, M., Bertrand, J.C. (2001) Effects of petroleum hydrocarbons on the phospholipid acid composition of a consortium composed of marine hydrocarbon-degrading bacteria. *Org Geochem* **32**: 891-903.

Biddle, J.F., Lipp, J.S., Lever, M.A., Lloyd, K.G., Sørensen, K.B. Anderson, R., Fredricks, H.F., Elvert, M., Kelly, T.J., Schrag, D.P., Sogin, M.L., Brenchley, J.E., Teske, A., House, C.H., Hinrichs, K.-U. (2006) Heterotrophic Archaea dominate sedimentary subsurface ecosystems off Peru. *Proc Natl Acad Sci USA* **103**: 3846-3851.

Blumenberg, M., Seifert, R., Reitner, J., Pape, T., Michaelis, W. (2004) Membrane lipid patterns typify distinct anaerobic methanotrophic consortia. *Proc Natl Acad Sci USA* **101**: 11111-11116.

Boetius, A., Ravenschlag, K., Schubert, C.J., Rickert, D., Widdel, F., Gieseke, A., Amann, R., Jørgensen, B.B., Witte, U., Pfannkuche, O. (2000) A marine microbial consortium apparently mediating the anaerobic oxidation of methane. *Nature* **407**: 623-626.

Bohrmann, G., Spiess, V., M67/2 Cruise Participants (2008) Report and preliminary results of R/V Meteor cruise M67/2a and 2b, Balboa – Tampico – Bridgetown, 15 March – 24 April 2006. Fluid seepage in the Gulf of Mexico, Berichte, No.263, Fachbereich Geowissenschaften, Universität Bremen, Bremen, Germany.

Boon, J.J., De Leeuw, J.W., V. D. Hoek, G.J., Vosjan, J.H. (1977) Significance and taxonomic value of iso and anteiso monoenoic fatty acids and branched *β*-hydroxy acids in *Desulfovibrio desulfuricans*. *J Bacteriol* **129**: 1183-1191.

Brüning, M., Sahling, H., MacDonald, I. R, Ding, F, Bohrmann, G. Origin, distribution, and alteration of asphalts at Chapopote Knoll, Southern Gulf of Mexico (2009) *Marine and petroleum Geology* accepted September 2009.

D'Hondt S., Jørgensen B.B., Miller D.J., Batzke A., Blake R., Cragg B.A., Cypionka H., Dickens G.R., Ferdelman T., Hinrichs K.-U., Holm N.G., Mitterer R., Spivack A., Wang G., Bekins B., Engelen B., Ford K., Gettemy G., Rutherford S.D., Sass H., Skilbeck C.G., Aiello I.W., Guèrin G., House C.H., Inagaki F., Meister P., Naehr T., Niitsuma S., Parkes R.J., Schippers A., Smith D.C., Teske A., Wiegel J., Padilla C.N., Acosta J.L.S. (2004) Distributions of Microbial Activities in Deep Subseafloor Sediments. *Science* **306**: 2216-2221.

Ding, F., Spiess, V., Brüning, M., Fekete, N., Keil, H., Bohrmann, G. (2008) A conceptual model for hydrocarbon accumulation and seepage processes around Chapopote asphalt site, sourthern Gulf of Mexico: From high resolution seismic point of view. *J Geophy Res* **113**: DOI:10.1029/2007JB005484.

Dowling, N.J.E., Widdel, F., White, D.C. (1986) Phospholipid ester-linked fatty acid biomarkers of acetate-oxidizing sulphate-reducing and other sulphide-forming bacteria. *J Gen Microbiol* **132**: 1815-1825.

Elvert, M., Suess, S., Whiticar, M.J. (1999) Anaerobic methane oxidation associated with marine gas hydrates: superlight C-isotopes from saturated and unsaturated C_{20} and C_{25} irregular isoprenoids. *Naturwissenschaften* **86**: 295-300.

Elvert, M., Boetius, A., Knittel, K., Jørgensen, B.B. (2003) Characterization of specific membrane fatty acids as chemotaxonomic markers for sulfate-reducing bacteria involved in anaerobic oxidation of methane. *Geomicrobiol J* **20**: 403-419.

Formolo, M.J., Lyons, T.W., Zhang, C., Kelley, C., Sassen, R., Horita, J., Cole, D.R. (2004) Quantifying carbon sources in the formation of authigenic carbonates at gas hydrate sites in the Gulf of Mexico. *Chem Geol* **205**: 253-264.

Gamian, A., Mordarska, H., Ekiel, I., Ulrich, J., Szponar, B., Defaye, J. (1996) Structural studies of the major glycolipid from *Saccharopolyspora* genus. *Carbohydr Res* **296**: 55-67.

Harrison, B.K., Zhang, H., Berelson, W., Orphan, J. (2009) Variations in archaeal and bacterial diversity associated with the sulfate-methane transition zone in continental margin sediments (Santa Barbara Basin, California). *Appl Environ Microbiol* **75**: 1487-1499.

Hayes, J.M. (2001) Fractionation of the isotopes of carbon and hydrogen in biosynthetic processes. *Rev Mineral Geochem* **43**: 225-277.

Hinrichs, K.-U., Hayes, J.M., Sylva, S.P., Brewer, P.G., DeLong, E.F. (1999) Methane-consuming archaeabacteria in marine sediments. *Nature* **398**: 802-805.

Hinrichs, K.-U., Summons, R.E., Orphan, V., Sylva, S.P., Hayes, J.M. (2000) Molecular and isotopic analysis of anaerobic methane-oxidizing communities in marine sediments. *Org Geochem* **31**: 1685-1701.

Hinrichs, K.-U., Boetius, A. (2002) The anaerobic oxidation of methane: New insights in microbial ecology and biogeochemistry. In *Ocean Margin Systems*, eds. Wefer G.,Billet, D., Hebbeln, D., Jørgensen, B. B., Schlüter, M. & van Weering, T. (Springer, Berlin), pp. 457–477.

House, C.H., Schopf, J.W., Stetter, K.O. (2003) Carbon isotopic fractionation by archaeans and other thermophilic prokaryotes. *Org Geochem* **34**: 345-356.

Hue, N., Serani, L., Laprévote, O. (2001) Structural investigation of cyclic peptidolipids from *Bacillus subtilis* by high-energy tandem mass spectrometry. *Rap Comm Mass Spec* **15**: 203-209.

Jahnke, L.L., Embaye, T., Summons, R.E. (2002). Lipid biomarkers for Methanogens in Hypersaline Cyanobacterial Mats for Guerrero Negro, Baja California Sur. NASA Technical report, Document ID: 20030014742.

Joye, S.B., Boetius, A., Orcutt, B.N., Montoya, J.P., Schulz, H.N., Erickson, M.J., Lugo, S.K. (2004) The anaerobic oxidation of methane and sulfate reduction in sediments from Gulf of Mexico cold seeps. *Chem Geol* **205**: 219-238.

Kaneda, T. (1991) Iso- and anteiso-fatty acids in bacteria: Biosynthesis, function, and taxonomic significance. *Microbiol Rev* **55**: 288-302.

Kennicutt II, M.C., Brooks, J.M., Denoux, G.J. (1988) Leakage of deep, reservoired petroleum to the near surface on the Gulf of Mexico continental slope. *Marine Chem* **24**: 39-59.

Knittel, K., Lösekann, T., Boetius, A., Kort, R., Amann, R. (2005) Diversity and distribution of methanotrophic archaea at cold seeps. *Appl Environ Microbiol* **71**: 467-479.

Knittel, K., Boetius, A. (2009) Anaerobic Oxidation of methane: Progress with an unknown process. *Annu Rev Microbiol* **63**: 311-334.

Knoblauch, C., Sahm, K., Jørgensen, B.B. (1999) Psychrophilic sulfate-reducing bacteria isolated from permantly cold Arctic marine sediments: description of *Desulfofrigus oceanense* gen. nov., sp. nov., *Desulfofrigus fragile* sp. nov., *Desulfofaba gelida* gen.

nov., sp. nov., *Desulfotalea psychrophila* gen. nov., sp. nov., *Desulfotalea arctiva* sp. nov. *Int J Syst Bacteriol* **49**: 1631-1643.

Koga, Y., Morii, H., Akagawa-Matsushita, M., Ohga, M. (1998) Correlation of polar lipid composition with 16S rRNA phylogeny in methanogens. Further analysis of lipid component parts. *Biosci Biotechnol Biochem* **69**: 230-236.

Koga, Y., Nakano, M. (2008) A dendrogram of archaea based on lipid component parts composition and its relationship to rRNA phylogeny. *Syst. Appl. Microbiol.* **31**: 169-182.

Kohring, L.L., Ringelberg, D.B., Devereux, R., Stahl, D.A., Mittelman, M.W., White, D.C. (1994) Comparison of phylogenetic relationships based on phospholipid fatty acid profiles and ribosomal RNA sequence similarities among dissimilatory sulfate-reducing bacteria. *FEMS Microbiol Lett* **119**: 303-308.

Kuever, J., Könneke, M., Galushko, A., Drzyga, O. (2001) Reclassification of *Desulfobacterium phenolicum* as *Desulfobacula phenolica* comb. nov. and description of strain SaxT as *Desulfotignum balticum* gen. nov., sp. nov. *Int J Syst Evol Microbiol* **51**: 171-177.

Lipp, J.S., Morono, Y., Inagaki, F., Hinrichs, K.-U. (2008) Significant contribution of Archaea to extant biomass in marine subsurface sediments. *Nature* **454**: 991-994.

Lipp, J.S., Hinrichs K.-U. (2009) Structural diversity and fate of intact polar lipids in marine sediments. *Geochim Cosmochim Acta* DOI:10.1016:j.gca.2009.08.003.

Liu, X., Lipp, J.S., Hinrichs, K.-U. (2009) Distribution of fossil and intact archaeal GDGTs I marine sediments. *Abstract International Meeting on Organic Geochemistry (IMOG)*, Bremen, 2009.

Lloyd, K.G., Lapham, L., Teske, A. (2006) An anaerobic methane-oxidizing community of ANME-1b Archaea in Hypersaline Gulf of Mexico sediments. *Appl Environ Microbiol* **72**: 7218-7230.

Londry, K.L., Des Marais, D.J. (2003) Stable carbon isotope fractionation by sulfate-reducing bacteria. *Appl Environ Microbiol* **69**: 2942-2949.

Londry, K.L., Jahnke, L.L., Des Marais, D.J. (2004) Stable carbon isotope ratios of lipid biomarker of sulfate-reducing bacteria. *Appl Environ Microbiol* **70**: 745-751.

Londry, K.L., Dawson, K.G., Grover, H.D., Summons, R.E., Bradley, A.S. (2008) Stable carbon isotope fractionation between substrates and products of *Methanosarcina barkeri* **39**: 608-621.

MacDonald, I.R., Bohrmann, G., Escobar, E., Abegg, F., Blanchon, P., Blinova, V., Brückmann, W., Drews, M., Eisenhauer, A., Han, X., Heeschen, K., Meier, F., Mortera, C., Naehr, T., Orcutt, B., Bernard, B., Brooks, J., de Faragó, M. (2004) Asphalt volcanism and chemosynthetic life in the Campeche Knolls, Gulf of Mexico. *Science* **304**: 999-1002.

MacNaughton, S.J., Stephen, J.R., Venosa, A.D., Davis, G.A., Chang, Y.-J., White, D.C. (1999) Microbial population changes during bioremediation of an experimental oil spill. *Appl Environ Microbiol* **65**: 3566-3574.

Makula, R.A., Finnerty, W.R. (1974) Phospholipid composition of *Desulfovibrio* species. *J Bacteriol* **120**: 1279-1283.

Musat, F., Galushko, A., Jacob, J., Widdel, F., Kube, M., Reinhardt, R., Wilkes, H., Schink, B., Rabus, R. (2009) Anaerobic degradation of naphthalene and 2-methylnaphthalene by strains of marine sulfate-reducing bacteria. *Environ Microbiol* **11**: 209-219.

Nähr, T.H., Birgel, D., Bohrmann, G., MacDonald, I.R., Kasten, S. (2009) Biogeochemical controls on authigenic carbonate formation at the Chapopote "asphalt volcano", Bay of Campeche. *Chem Geol* **266**: 399-411.

Niemann, H., Elvert, M. (2008) Diagnostic lipid biomarker and stable carbon isotope signatures of microbial communities mediating the anaerobic oxidation of methane with sulphate. *Org Geochem* **39**: 1668-1677.

Orcutt, B.N., Boetius, A., Lugo, S.K., MacDonald, I.R., Samarkin, V.A., Joye, S.B. (2005) Life at the edge of methane ice: microbial cycling of carbon and sulfur in Gulf of Mexico gas hydrates. *Chem Geol* **205**: 239-251.

Orcutt, B., Boetius, A., Elvert, M., Samarkin, V., Joye, S.B. (2005) Molecular biogeochemistry of sulfate reduction, methanogenesis and the anaerobic oxidation of methane at Gulf of Mexico cold seeps. *Geochim Cosmochim Acta* **69**: 4267-4281.

Orphan, V.J., House, C., Hinrichs, K.-U., McKeegan, K.D., DeLong, E.F. (2001) Methane-consuming archaea revealed by directly coupling isotopic and phylogenetic analysis. *Science* **293**: 484-487.

Orphan, V.J., House, C., Hinrichs, K.-U., McKeegan, K.D., DeLong, E.F. (2002) Multiple archaeal groups mediate methane oxidation in anoxic cold seep sediments. *Proc Natl Acad Sci USA* **99**: 7663-7668.

Pancost, R.D., Bouloubassi, I., Aloisi, G., Sinninghe Damsté, J.S., the Medinaut Shipboard Scientific Party (2001) Three series of non-isoprenoidal dialkyl glycerol diether cold-seep carbonate crusts. *Org Geochem* **32**: 695-707.

Parkes, R.J., Calder, A.G. (1985) The cellular fatty acids of three strains of Desulfobulbus, a propionate-utilising sulphate-reducing bacterium. *FEMS Microbiol Lett* **31**: 361-363.

Parkes, R.J., Cragg, B.A., Banning, N., Brock, F., Webster, G., Fry, J.C., Hornibrook, E., Pancost, R.D., Kelly, D., Knab, N., Jørgensen, B.B., Rinna, J., Weightman, A.J. (2007) Biogeochemistry and biodiversity of methane cycling in subsurface sediments (Skagerrak, Denmark). *Environ Microbiol* **9**: 1146-1161.

Phelps, C.D., Kerkhof, L.J., Young, L.Y. (1998) Molecular characterization of a sulfate-reducing consortium which mineralizes benzene. *FEMS Microbiol Ecol* **27**: 269-279.

Preuß, A., Schauder, R., Fuchs, G., Stichler, W. (1989) Carbon isotope fractionation by autotrophic bacteria with three different CO_2 fixation pathways. *Z Naturforsch* **44**: 397-402.

Rabus, R., Hansen, T.A., Widdel, F. (2006) Dissimilatory sulfate- and sulfur-reducing prokaryotes. *The Prokaryotes* **2**: 659-768.

Reeburgh. W.S. (2007) Oceanic methane biogeochemistry. *Chem Rev* **107**: 486-513.

Rossel, P.E., Lipp, J.S., Fredricks, H.F., Arnds, J., Boetius, A., Elvert, M., Hinrichs, K.-U. (2008) Intact polar lipids of anaerobic methanotrophic archaea and associated bacteria. *Org Geochem* **39**: 992-999.

Rueter, P., Rabus, R., Wilkes, H., Aeckersberg, F., Rainey, F.A., Jannasch, H.W., Widdel, F. (1994) Anaerobic oxidation of hydrocarbons in crude oil by new types of sulphate-reducing bacteria. *Nature* **372**: 455-45

Rütters, H., Sass, H., Cypionka, H., Rullkötter, J. (2001) Monoalkylether phospholipids in the sulfate-reducing bacteria *Desulfosarcina variabilis* and *Desulforhabdus amnigenus*. *Arch Microbiol* **176**: 435-442.

Sassen, R., Joye, S., Sweet, S.T., DeFreitas, D.A., Milkov, A.V., MacDonald, I.R. (1999) Thermogenic gas-hydrates and hydrocarbon gases in complex chemosynthetic communities, Gulf of Mexico, continental slope. *Org Geochem* **30**: 485-497.

Schubotz, F., Lipp, J., Elvert, M., Kasten, S., Zabel, M., Escobar, E., Bohrmann, G., Hinrichs, K.-U. Chemosynthetic life at the Chapopote asphalt volcano – insights from stable carbon isotopes and intact polar membrane lipid analyses. *In prep. for Geochim Cosmochim Acta (see also Chapter III).*

Seidel, M. (2009) Dissertation, Carl-von-Ossietzky University of Oldenburg, Oldenburg, Germany.

Shaw, N. (1970) Bacterial glycolipids. *Bacteriol Rev* **34**: 365-377.

Sinninghe Damsté, J.S., Schouten, S., Hopmans, E.C., van Duin, A.C.T., and Geenevasen, A.J. (2002b) Crenarchaeol: the characteristic core glycerol dibiphytanyl glycerol tetraether membrane lipid of cosmopolitan pelagic crenarchaeota. *J Lipid Res* **43**: 1641-1651.

Strapoc, D., Picardal, F.W., Turich, C., Schaperdoth, I., Macalady, J.I., Lipp, J.S., Lin, Y.-S., Ertefai, T.F., Schubotz, F., Hinrichs, K.-U., Mastalerz, M., Schimmelmann, A. (2008) Methane-producing microbial community in a coal bed of the Illinois Basin. *Appl Environ Microbiol.* **74**: 2424-2432 (*see also Chapter VId*).

Stadnitskaia, A., Bouloubassi, I., Elvert, M., Hinrichs, K.-U., Sinninghe Damsté, J.S. (2008) Extended hydroxyarchaeol, a novel lipid biomarker for anaerobic methanotrophy in cold seepage habitats. *Org Geochem* **39**: 1007-1014.

Sturt, H.F., Summons, R.E., Smith, K., Elvert, M., Hinrichs, K.U. (2004) Intact polar membrane lipids in prokaryotes and sediments deciphered by high-performance liquid chromatography/electrospray ionization multistage mass spectrometry – new biomarkers for biogeochemistry and microbial ecology. *Rap Comm Mass Spec* **18**: 617-628.

Taylor, J., Parkes, R.J. (1983) The cellular fatty acids of the sulphate-reducing bacteria, *Desulfobacter* sp., *Desulfobulbus* sp. and *Desulfovibrio desulfuricans*. *J Gen Microbiol* **129**: 3303-3309.

Trumbore, S. E., Druffel, E. R. M. (1995). *Carbon isotopes for characterizing sources and turnover of nonliving organic matter.* In: Role of Nonliving Organic Matter in Earth's Carbon Cycle (eds. Zepp, R. G., Sonntag, C.), 7-22, John Wiley & Sons, Chichester.

Ueki, A., Suto, T. (1979) Cellular fatty acid composition of sulfate-reducing bacteria. *J Gen Appl Microbiol* **25**: 185-196.

Vainshtein, M., Hippe, H., Kroppenstedt, R.M. (1992) Cellular fatty acid composition of Desulfovibrio species and its use in classification of sulfate-reducing bacteria. *Syst Appl Microbiol* **15**: 554-566.

Wallace, K.K., Zhao, B., McArthur, H.A.I., Reynolds, K.A. (1995) *In-vivo* analysis of straight-chain and branched-chain fatty acid biosynthesis in three actinomycetes. *FEMS Microbiol Lett* **131**: 227-234.

Wegener, G., Niemann, H., Elvert, M., Hinrichs, K.-U., Boetius, A. (2008) Assimilation of methane and inorganic carbon by microbial communities mediating the anaerobic oxidation of methane. *Environ Microbiol* **10**: 2287-2298.

Zabel, M., Kasten, S. (2009) Geochemical characterization and origin of high saline pore fluids from the Chapopote asphalt volcano - Southern Gulf of Mexico. *Geochim Cosmochim Acta* **73**, Goldschmidt Conference Abstracts, A1494.

Zhang, C.L., Li, Y., Wall, J.D., Larsen, L., Sassen, R., Huang, Y., Wang, J., Peacock, A., White, D.C., Horita, J., Cole, D.R. (2002) Lipid and carbon isotopic evidence of methane-oxidizing and sulfate-reducing bacteria in association with gas hydrates from the Gulf of Mexico. *Geology* **30**: 239-242.

Chapter V

Determining total petroleum hydrocarbon degradation and weathering by comprehensive GC×GC at an asphalt seep in the southern Gulf of Mexico

Florence Schubotz[1*], G. Todd Ventura[2†], Robert K. Nelson[2], Christopher M. Reddy[2],
Kai-Uwe Hinrichs[1]

In preparation for *Environmental Science and Technology*

*Corresponding author. Tel: +49-421-218-65711; Fax: +49-421-218-65715
E-mail address: schubotz@uni-bremen.de
[1] Department of Geosciences and MARUM Center for Marine Environmental Sciences, University of Bremen, D-28359 Bremen, Germany
[2] Department of Marine Chemistry and Geochemistry, Woods Hole Oceanographic Institution, MS#4, Woods Hole, Massachusetts 02543
[†] current affiliation: University of Oxford, Department of Geosciences, Oxford, UK

V.1. ABSTRACT

Oil pollution and the persistence of hydrocarbons in the marine environment is of high ecological significance and greatly depends on the composition of the respective oil. We used comprehensive two-dimensional gas chromatography to investigate long-term compositional changes of naturally occurring deposits of heavy oil at the Chapopote asphalt seep in the southern Gulf of Mexico. We could identify and quantify molecular changes in petroleum hydrocarbons between different asphalt types and associate them to combinations of biological and physical weathering processes. Asphalt degradation occurs in two steps, first slow anaerobic biodegradation and surficial aerobic biodegradation and water washing consumes selective compounds amounting up to 30% of total petroleum hydrocarbons (TPH) . Long-term dissolution of TPH, most likely aided by biological oil emulsions, disperse up to 77% of TPH into the ocean, yielding an estimated TPH emission potential of 1,540 ± 770 tons. The Chapopote asphalt seep forms a natural ecosystem where most of the hydrocarbons are already efficiently recycled by metabolic processes at the source site. This study provides unique insights into long-term anaerobic and aerobic hydrocarbon degradation of heavy oils.

V.2. INTRODUCTION

Global estimates of petroleum entering the world oceans from natural seepage are around 600,000 metric tons yr^{-1} (cf. Kvenvolden and Cooper, 2003), which equals that from human activities (NAS, 2003). However, these estimates are accompanied with a large error, which is partly due to the inaccessibility to study most of these offshore seep sites. Nevertheless, it is known from some of the well studied oil seeps, e.g., off the coast of California, that hydrocarbon emissions are within the range of anthropogenic petroleum input in the form of tanker oils spills (e.g., Farwell et al., 2009). Natural seepage often occurs in the form of heavy oil, as evidenced by tar balls washed onto the shores of Australia, California, and the Gulf of Mexico (GoM; e.g., Wilson et al., 1974; Anderson et al., 1983; Edwards et al., 1998). The transformation of petroleum into tars can be caused by a variety of alteration processes, including biodegradation, which is assumed to play an important role (cf. Atlas, 1981). Biodegradation likely already occurs in the subsurface during migration of petroleum to the sediment surface (Head et al., 2003) and is later accompanied by other weathering processes such as water washing, evaporation and photooxidation during transport through the ocean (Hunt, 1996). In order to access the toxicity potential of naturally and anthropogenic occurring oil spills, the processes affecting the petroleum composition need to be studied. Petroleum seeps provide an excellent natural laboratory for studying these transformations and the remediation efficiency of nature.

Within the global estimates the GoM is an important contributor to hydrocarbon emission with up to estimated 140,000 tons yr^{-1}, amounting to ~23% of global petroleum emissions (MacDonald et al., 1993; Kvenvolden and Cooper, 2003). However, wide regions in the southern GoM are poorly investigated in terms of hydrocarbon seepage and much of the data used for the global estimates are based solely on satellite data (MacDonald et al., 1993, 2002).

In this study we will investigate the recently discovered asphalt seeps of the Chapopote Knoll in the southern Gulf of Mexico (MacDonald et al., 2004). The Chapopote Knoll is located at the northwestern tip of the Campeche Knolls, which are formed by the up-doming of salt. Here hydrocarbon seepage has resulted in mysterious asphalt deposits that have a lava-flow like morphology and are extensively colonized by chemosynthetic communities (MacDonald et al., 2004; Bohrmann et al., 2008). This newly discovered cold seep system has been the focus of more detailed recent investigations (Ding et al., 2008; Brüning et al., 2009; Nähr et al., 2009; Schubotz et al., *in prep., Chapter III*). Oil from the southern Gulf of Mexico is known to be very heavy, with low API gravity and rich in sulfur (cf. Guzman-Vega et al., 2001). Consequently, these asphalt deposits are likely caused due to negative buoyancy caused by a high asphaltene and resin content in combination with a loss of lighter hydrocarbon compounds during migration and finally deposition on the seafloor. It is unclear on which timescales the seepage at the Chapopote has been occurring, however, according to the maximum length of vestimentiferan tubeworms the oldest asphalt fields must have been deposited at least more than two decades ago (Brüning et al., 2009). The asphalt seepage at the Chapopote therefore provides the possibility to study long-term weathering and degradation processes of asphalt exposed on the sea floor.

Preliminary investigations have shown that the oils from the Chapopote asphalt seep are characterized by an unresolved complex hydrocarbon mixture (UCM) in the elution range of C_{14} to C_{40}, which could not be resolved with conventional gas chromatography (Schubotz et al., *in prep., Chapter III*). A promising alternative technique with an increased chromatographic resolution is comprehensive two-dimensional gas chromatography (GC×GC). GC×GC has the potential to separate over thousands of individual peaks and is a method that is frequently applied when conventional methods fail to resolve the UCM (e.g., Frysinger and Gaines, 2001; Reddy et al., 2002). GC×GC has been established as a tool to track and quantify molecular changes and associate them to biological or physical processes (Arey et al., 2007; Wardlaw et al., 2009) and has been successful in identifying the source of spilled oil and deciphering mechanisms of weathering (Gaines et al., 1999; Nelson et al., 2006; Farwell et al., 2009). The goal of this study is to investigate molecular compositional changes that occurred after asphalt deposition at the Chapopote Knoll and to try to decipher the underlying biological or physical weathering processes.

V.3. EXPERIMENTAL

V.3.1 Study site and sampling of different asphalt types

Asphalt samples were collected by the remotely operated vehicle ROV Quest 4000 during R/V Meteor expedition M67/2 at the Chapopote Knoll in the southern Gulf of Mexico (Bohrmann et al., 2008). For a map and detailed sampling locations see Fig. V.S1, a detailed morphologic and bathymetric sampling map is published in Brüning et al. (2009). We retrieved asphalt samples from different locations that indicated visually different degrees of alteration (Fig. V.S1). Most of the asphalts are from a site called the main asphalt site (MAF, 21°53’95N 93°26’24W; cf. Brüning et al., 2009) where the deposited asphalt had a ropy morphology and flow-like structures. Upon sample retrieval these asphalts had a highly viscous texture and could be cut very easily (“like butter”) with a knife. Some of the asphalt-oils were still liquid and others were positively buoyant due to very high gas contents and occluded gas hydrates (Bohrmann et al., 2008; Schubotz et al., *in prep., Chapter III*). At some instances the fresher, more viscous asphalt with clearly visible flow-like structures seemingly overflowed older blocky asphalt material, indicating multiple stages of asphalt seepage (cf. Brüning et al., 2009; Nähr et al., 2009). Microbial mats, consisting of sulfide-oxidizing, sulfate-reducing and methanotrophic bacteria, but also minor amounts of anaerobic methanotrophic archaea (Schubotz et al., *in prep., Chapter III*; G. Wegener, K. Knittel et al., pers. comm.), cover less exposed areas of the ropy asphalts of the MAF, either in the cavities at the edges of the ropy asphalt or in some areas in meter-wide patches (Brüning et al., 2009). The second site is called bubble site (BS, 21°54’90N 93°26’12W) due to visually observed out-gassing and gas hydrate-enclosing asphalts on the seafloor (Bohrmann et al., 2008; Brüning et al., 2009). Here, the asphalts have a more rough appearance and are covered by corals, sponges and mussels that obviously use the asphalt as bedrock. The dense population of macrofauna indicates long-term deposition and weathering of the rough asphalt in comparison to the fresh asphalt from the MAF. The third site occurs in patches around the MAF and the BS and is composed of heavily weathered sedimented asphalt patches of brittle appearance. The asphalt patches (AP, 21°53’97N 93°26’19W) all have a thin sediment layer, indicating long-term exposure on the seafloor, considering sedimentation rates of 7.5 cm kyr^{-1}, which were determined for deep southern GoM Pleistocene sediments (Worzel et al., 1973). In total 12 samples were analyzed in this study: fresh asphalts from the MAF (7), rough asphalts from the BS (2), and brittle asphalts from the AP (3). Asphalt samples were stored frozen at -20°C or at 4°C in the dark to exclude photooxidation during sample storage.

V.3.2. δ^{13}C of TOC

Stable carbon isotope values of TOC were analyzed on pure asphalts (~1 mg) on a Leco CS200 analyzer.

V.3.3. Preparation of total petroleum hydrocarbon (TPH) extracts

10 to 60 mg of asphalt were cut out of bigger asphalt blocks with solvent rinsed knives and sterile scalpels and subsequently dissolved in dichloromethane (DCM) and methanol (MeOH; 9:1, v/v). Typically, the cut-out asphalt pieces were sampled 2 cm within the asphalt blocks and the small brittle asphalt pieces were dissolved as whole pieces. The asphalt-solvent mixture was separated into a hexane-soluble maltene fraction and a DCM-soluble asphaltene fraction by using a pasteur pipette filled with $NaSO_4^{2-}$. The maltene fraction was further subjected to column separation with silica gel (Silica Gel 60, 60-200 µm, Roth, Germany), preconditioned with DCM, to separate the total petroleum hydrocarbons (TPH) with 10 mL hexane:DCM (9:1, v:v) from the resins, eluted with 10 mL DCM:MeOH (2:1, v:v).

V.3.4. GC×GC-ToF-MS and GC×GC-FID analysis

Chapopote Knoll samples were analyzed by comprehensive two dimensional time-of-flight mass spectrometry (GC×GC-ToF-MS) on a system that employed a dual stage cryogenic modulator (Leco, Saint Joseph, Michigan) installed in an Agilent 6890N gas chromatograph configured with a 7683B series split/splitless auto-injector, two capillary gas chromatography columns, and coupled to a time of flight mass spectrometric detection system. Each extract was injected in splitless mode and the purge vent was opened at 0.5 minutes. The inlet temperature was 300°C. The first-dimension column and the dual stage cryogenic modulator reside in the main oven of the Agilent 6890N gas chromatograph (Agilent, Wilmington, Delaware). The second-dimension column is housed in a separate oven installed within the main GC oven. With this configuration, the temperature profiles of the first-dimension column, dual stage thermal modulator and the second-dimension column can be independently programmed. The first-dimension column was an apolar Restek Rtx-1 Crossbond, (15 m length, 0.25 mm ID, 0.25 µm film thickness) that was programmed to remain isothermal at 90°C for 10 minutes and then ramped from 90 to 315°C at 1.75°C min^{-1}. Compounds eluting from the first dimension column were cryogenically modulated on deactivated fused silica (0.5 m length, 0.22 mm ID). The modulator cold jet gas was dry $N_{2,}$ chilled with liquid nitrogen. The thermal modulator hot jet air was heated to 80°C above the temperature of the main GC oven. The hot jet was pulsed for 1 second every 12 seconds with a 5 second cooling period between stages. Second-dimension separations were performed on a 50% phenyl polysilphenylene-siloxane column (SGE BPX50, 0.90 m length, 0.10 mm ID, 0.1 µm film thickness) that was programmed to remain isothermal at 115°C for 10 minutes and then ramped from 115 to 340°C at 1.75°C min^{-1}. The carrier gas was Helium at a constant flow rate of 1.3 mL min^{-1}. The Leco ToF-MS detector signal was sampled at 50 spectra per second and the mass range was 50-675 amu. The transfer line from the second oven to the ToF-MS was deactivated fused silica (0.5 m length, 0.18 mm ID) which was held at a constant temperature of 280°C. The ToF source temperature was 230°C and the detector voltage was 1575 Volts. For quantification purposes, the GC×GC was coupled to an FID with a sampling rate of 100 Hz.

TPH were identified according to their retention time on the first and second dimension axis, their fragmentation patterns and by comparison with previously published data (e.g., GAINES ET AL., 1999; FRYSINGER AND GAINES, 2001). The quantification of individual peaks and compound classes and the generation of difference chromatograms followed the protocol described in detail by WARDLAW ET AL. (2008).

V.3.4.1 Quantification with FID vs. ToF-MS

All samples were analyzed by GC×GC-ToF-MS to aid structural identification of TPH. Quantification with ToF-MS according to compound classes was possible and differences between asphalt samples from different sampling sites were statistical robust. However, for a more robust quantification selected samples were run on GC×GC-FID, since FID detection has a higher scan rate and therefore better resolution power and thus should be better suited for quantitative analysis (cf. Frysinger et al., 1999). The direct comparison of samples quantified with ToF-MS and FID revealed profound differences in the relative distribution between samples analyzed with both techniques (Fig. V.S2). These differences particularly affect the alkylcycloalkanes and the alkylbenzenes. For instance, in sample GeoB10617-6 #3 these compound classes are much less abundant in the FID (30-40% of total TPH) than compared to the ToF-MS analyses (60-70% of total TPH; cf. Fig. V.S2). This discrepancy is likely caused by the resolving power of these two detection methods. The ToF-MS detector is unable to resolve individual peaks, particularly in the elution range of the alkylcycloalkanes and alkylbenzenes, which results in an overestimate of these compound classes in the TPH quantification. This observation is important for future studies of highly degraded oils and highlights the importance to further improve techniques with very high resolving power to obtain robust estimates on compound class distribution and quantification. Consequently in the discussion we will mainly focus on the three samples that were analyzed by GC×GC FID, where peak resolution was satisfactory.

V.4. RESULTS AND DISCUSSION

V.4.1. Chemical characterization and source correlations of the asphalts

All asphalt samples have high contents of asphaltenes (>50%), and the asphaltene content increases from samples recovered from the MAF and the BS to the AP (>70%; Table V.1). The biomarker distributions and bulk $\delta^{13}C$ values around -27‰ are similar within all asphalt samples pointing to a common source reservoir (Table V.S1, Fig. V.S1). The hopane distribution is characterized by a high C_{29}/C_{30} hopane ratio, abundant extended hopanes, high C_{35}/C_{34} extended hopane ratios, and the presence of hexahydrobenzohopanes and 17α(H)-29,30-bisnorhopane. Furthermore, all asphalts contain C_{30} steranes, have a high abundance of C_{29} relative to C_{27} steranes but very low abundance of extended diasteranes and a regular sterane to homohopane ratio of <1. A comparison of these data with the literature from the Campeche area reveals that the Chapopote asphalts match oils from the Campeche Shelf of the Tithonian marine

Table V.1. Sample list and asphaltene content of analyzed asphalts.

Sample location	Sample ID (GeoB)	Depth (cm)	Sample description	Asphaltenes	Maltenes
				%	
MAF	10617-6 #2	1	Fresh	44	56
MAF	10617-6 #3	2	Fresh	46.5	53.5
MAF	10617-6 #4	3	Fresh	43	57
MAF	10621-1 #2	100	Fresh, almost liquid	50	50
MAF	10623 #2	100	Fresh, outgassing upon retrieval	52	48
MAF	10625-18 #1	Surface	Brittle	48	52
MAF	10625-16 #1	2	Fresh, outgassing upon retrieval	51	49
BS	10622-4 #1	Surface	Rough, covered with sponge	58	42
BS	10622-4 #2	2	Rough, covered with sponge	52	48
AP	10617-7 #2	surface	Brittle	61	39
AP	10619-17 #1	surface	Brittle	90	10
AP	10619-17 #2	surface	Brittle	79	21
sediment	10613-1 #1	2	Brittle	50	50

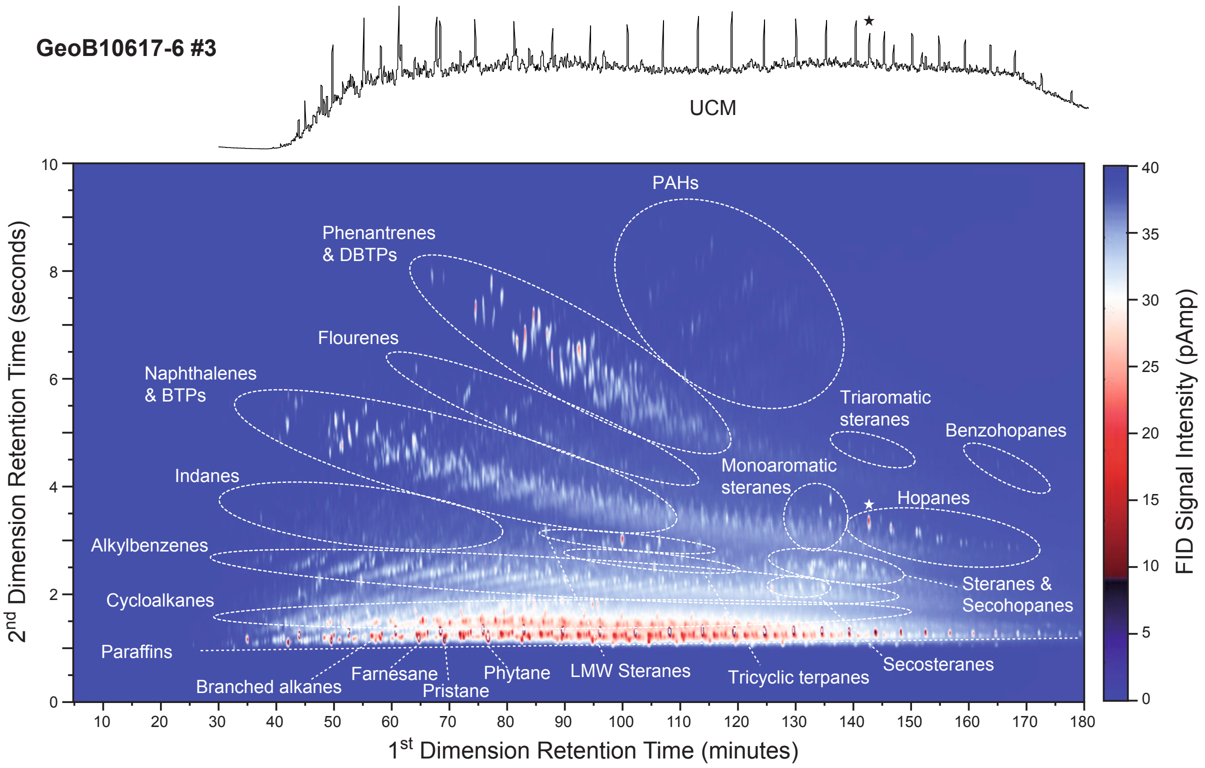

Fig. V.1. Comparison of conventional GC-MS chromatogram, showing an unresolved complex mixture (UCM, top) and GCxGC chromatogram of an asphalt sample from the main asphalt field (GeoB10617-6 #3) showing the distribution of the compound classes determined in this study. Star denotes Norhopane.

marl-dominated source oil group (Guzmán-Vega et al., 2001). The biomarker distribution is consistent with a carbonate depositional environment, possibly under hypersaline conditions and with a high relative contribution of bacterial biomass (Connan et al., 1986; Mello et al., 1988). High C_{29}/C_{30} hopane ratios can be related to oils derived from organic-rich carbonate or evaporitic rocks (cf. Zumberge, 1984; Connan et al., 1986). In summary, we can confidently state that all samples can be assigned to a common source; hence differences in the molecular composition are reflective of different degrees of alterations.

V.4.2. Classification of asphalts according to compound classes

Upon GC-MS analysis all asphalt samples contained a prominent unresolved complex mixture (UCM) in the boiling range of C_{14} to C_{40}. (Schubotz et al., *in prep., Chapter III*). This UCM was completely resolved using the GC×GC technique (Fig. V.1). Previous studies (e.g., Gaines et al., 1999; Frysinger et al., 1999; Nelson et al., 2006; Wardlaw et al., 2008) have shown that TPH can be classified into different compound classes according to the retention time in both chromatographic dimensions. In combination with structural information from ToF-MS, this form of classification facilitates the comparison of different samples that contain up to 10,000 compounds or more. Fig. V.1 demonstrates the classification into compound classes of an asphalt sample from the MAF, where the main UCM-forming compounds are comprised of *n*-alkanes, branched alkanes, acyclic isoprenoids, alkylcycloalkanes, alkylbenzenes, sulfur containing alkylbenzothiophenes (C_n-BT) and alkyldibenzothiophenes (C_n-DBT), and polyaromatic hydrocarbons, including alkyl-substituted naphthalenes (C_n-N), phenantrenes

(C_n-P), and anthracenes. These compound classes were detectable in all analyzed asphalt samples, albeit in varying relative abundances. For sample comparison we quantified the different compound classes with GC×GC ToF-MS and subjected all samples to a cluster analysis. The resulting dendrogram illustrates that the analyzed asphalts can be classified into three categories, which correspond to the three sampling locations (Fig. V.2a): (A) the fresh asphalts from the MAF, (B) the rough asphalts from the BS, and (C) the brittle asphalts from the sedimented AP. Relative distributions of the compound classes within category A, i.e., the fresh asphalts, are mainly found in the paraffins, composed of *n*-alkanes, branched alkanes and isoprenoids in the carbon range C_{14} to C_{40} (10 to 20% of TPH), alkylcycloalkanes (40 to 60% of TPH), and alkylbenzenes (15 to 25%). Category B differs from A due to a decrease in the amount of paraffins (<10% of TPH) and an increase in the alkylcycloalkanes (> 60% of TPH). Category C, i.e., the brittle asphalts, is clearly distinguished from the other categories by the lack of alkylcycloalkanes and alkylbenzenes (together <30%) and an increase in the biomarkers, i.e., steranes and hopanes (together >40%).

V.4.3. TPH transformation from the fresh to the rough asphalt site

Asphalts from the MAF still have a full suite of *n*-alkanes, branched alkanes and acyclic isoprenoids, despite the presence of a broad UCM in conventional GC-MS analyses. This is surprising as UCMs are typically observed in oils that have already been highly biodegraded, where usually all alkanes are degraded and the UCM is composed of the remaining biodegradation-recalcitrant compounds (Connan et al., 1984; Wenger et al., 2002). To explain this observed discrepancy we suggest that oil mixing in the form of recharge of hydrocarbons from more

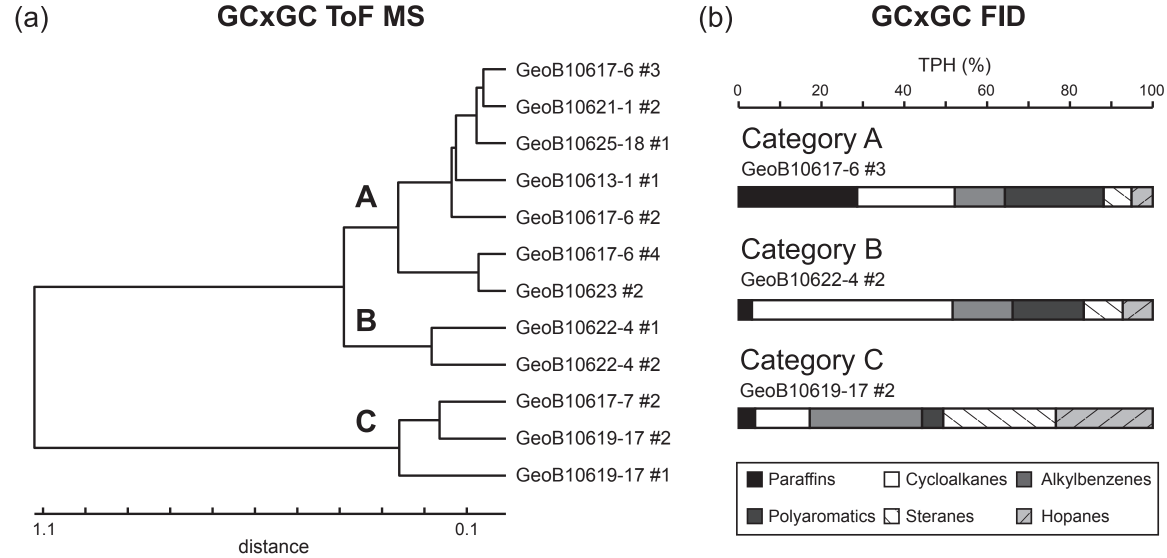

Fig. V.2. (**A**) Dendrogram of compound classes in all GC×GC ToF-MS analyzed asphalt samples. Cluster A are samples from the main („fresh") asphalt field, Cluster B are samples from the bubble (rough) asphalt field, and Cluster C asphalt samples are all brittle asphalts.. (**B**) Compound class quantification of three selected samples from cluster A, B and C with GC×GC FID. Compound classes were simplified as follows: parraffins include *n*-alkanes, branched and isoprenoidal alkanes; aromatics include all alkyl-substituted PAHs, including the sulfur-organic compounds; hopane includes tricyclic terpane, benzohopanes, regular hopanes and homohopanes; sterane includes regular steranes, short chain steranes, secohopanes, mono- and triaromatic steranes.

pristine oil has been occurring after initial biodegradation (Barnard and Bastow, 1991; Horstad and Larter, 1997). This suggests that seepage might still be occurring in the asphalt beds of the MAF, although a seepage source could not be identified during site exploration (Bohrmann et al., 2008). Biodegradation inside the asphalts is indicated by substantial variations in pristane (Pr) to n-C_{17} ratios of 0.3 to 0.7, this is a very wide range (cf. Peters and Moldowan, 1993; Wenger et al., 2002) and shows a considerable heterogeneity in different asphalts samples within the MAF (Schubotz et al., *in prep., Chapter III*), showing that alkane degradation is occurring within the asphalts. Next to aliphatic hydrocarbon degradation, GC×GC analysis showed that also low molecular weight (LMW) aromatics, such as naphthalene, benzene, toluene, and the xylene isomers are being degraded inside the asphalts. These compounds were either not detectable or only present in trace amounts in most of the samples from the MAF. These LMW aromatic compounds are known to be degradable by microorganisms under denitrifying, sulfate reducing, iron reducing or methanogenic conditions (cf. Widdel and Rabus, 2001). Biological activity inside the asphalts is furthermore confirmed by the detection of intact phospholipids in gas hydrate-containing asphalts and the observation of slightly depleted $\delta^{13}C$ values for methane (-55‰; Schubotz et al., *in prep., Chapter III*) together with 16S rDNA of a methanogenic alkane-degrading consortia consisting of *Synthrophus sp.* bacteria and *Methanosaeta sp.* archaea (G. Wegener, K. Knittel et al., pers. comm.).

To compare biodegradation patterns within asphalts from different sites we created a difference chromatogram between one of the fresh asphalts from the MAF (category A) and one of the rough asphalts from the BS (category B). This difference chromatogram visualizes pronounced changes in molecular distribution between these two samples (Fig. V.3). Compounds that are absent in the rough compared to the fresh asphalt include the whole series of n-alkanes, branched alkanes and acyclic isoprenoids in the carbon range C_{14} to C_{35} as well as low molecular weight (LMW) PAHs, such as C_1-N to C_4-N, P, BTP, DBT and their C_1-C_3 alkyl substituted counterparts (Fig. V.3). It is well established that microbial hydrocarbon degradation involves a variety of specialized bacteria with different levels of substrate specificity that operate simultaneously, but at different rates (cf. Head et al., 2006). This consequently results in a successive removal of compounds, where the order of disappearance is first the short chain n-alkanes, followed by the mid-chain then long chain n-alkanes and branched alkanes; subsequently the isoprenoidal alkanes are removed and finally cyclic and aromatic compounds (cf. Connan et al., 1984; Peters and Moldowan, 1993; Head et al., 2003).

In the rough asphalt samples from the BS the microbial hydrocarbon degradation has already reached an advanced state, where the paraffins, including all C_{14} to C_{35} n-alkanes, branched alkanes and acyclic isoprenoids have been removed. Compared to the selective loss of the paraffins, the loss of the LMW alkylated PAHs was rather unselective and showed a removal of compounds along a path perpendicular to solubility contours established by Arey et al. (2007). These solubility contours, or "dissolution lines" follow the observation that small - more water-soluble - aromatic compounds are primarily removed by water washing, followed by more aliphatic compounds which are less water soluble (Reddy et al., 2002; Nelson et al.,

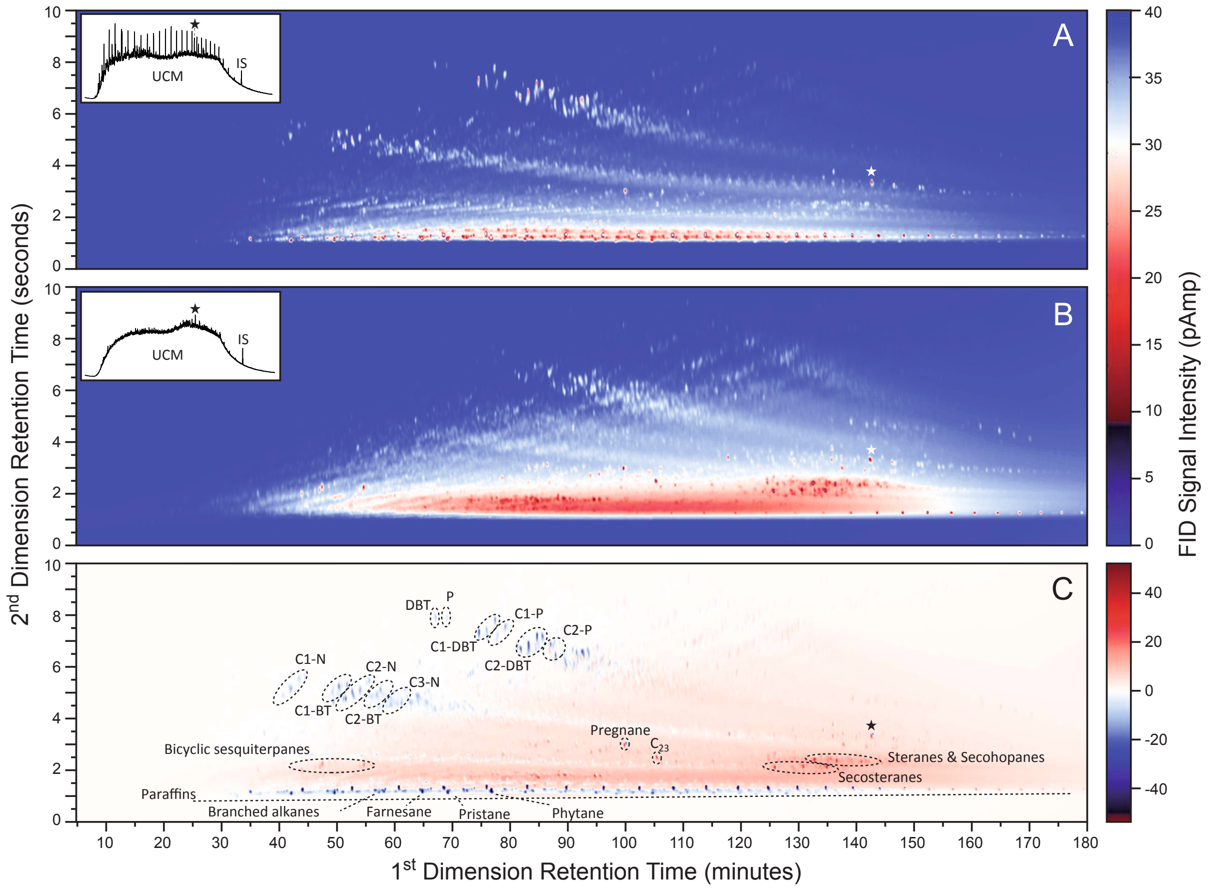

Fig. V.3. Chromatogram of a fresh asphalt sample from the main asphalt field (**A**) and a rough asphalt sample from the bubble asphalt field (**B**) and the generated difference chromatogram between the two chromatograms (**C**). Relative losses of compounds are depicted in blue and recalcitrant compounds in red. Star denotes Norhopane, which was used for normalization. The inserts in **(A)** and **(B)**, top left, show chromatograms of conventional GC analyses, UCM – unresolved complex mixture, IS – injection standard.

2006; Farwell et al., 2009). Water washing as main cause of the removal of the alkylated PAHs, could probably be accompanied by aerobic degradation. *Cycloclasticus sp.*, an efficient and widely distributed (Geiselbrecht, 1998) aerobic degrader of aromatic hydrocarbons, including alkyl-substituted PAHs (Kasai et al., 2002) was found as a symbiont in mussels and sponges on the surface of the rough asphalts at BS (Raggi et al., *in prep.*, *Chapter VIc*, G. Wegener, K. Knittel et al., pers. comm.).

Anaerobic degradation cannot be ruled out as cause for the observed losses. It is known from both culture studies (cf. Chakraborty and Coates, 2004; Musat et al., 2009) and field observation in petroleum reservoirs and oil spills (Larter et al., 2003; Wang et al., 1998; Ohshiro and Izumi, 1999; Meckenstock et al., 2004) that anaerobic bacteria are also capable of degrading PAHs such as the naphthalenes, phenantrenes, BT, DBT and their alkyl-substituted derivatives. The degradation of these compounds also occurs in a successive manner and could thus be responsible for a similar pattern as observed during the water washing process. It is often observed in oil spill studies that anaerobic biodegradation seems to come to a halt under certain conditions, leading to a persistence of hydrocarbons in the environment over several decades (Blumer and Sass, 1972; Reddy et al., 2002; Peacock et al., 2007). In this case we believe that it is plausible that the rough asphalts from the BS represent the end member of anaerobic degradation: all alkanes and isoprenoidal alkanes have been degraded as well as the LMW alkylated PAHs leaving behind most of the alkylcycloalkanes and alkylbenzenes forming together with the recalcitrant biomarkers the undegradable UCM.

V.4.4. Molecular changes from fresh to brittle asphalts

A comparison of fresh asphalts from the MAF to sedimented brittle asphalts of the AP by creating a difference chromatogram revealed most profound changes in the TPH composition (Fig. V.4). Most of the UCM-forming compounds have been completely removed, including most of the alkylated PAHs, alkylcycloalkanes and alkylbenzenes, the remaining compounds are aliphatic and aromatic steranes and hopanes, and tricyclic terpanes as well as higher *n*-alkanes. Physical processes such as water washing likely enhance the dissolution and dispersion of TPHs, however, it seems unlikely that water washing alone accounts for the removal of these apolar compounds due to their very low water solubility (e.g., AREY ET AL., 2007). Other processes such as photooxidation and evaporation can be excluded at 3000 m water depth. Instead, we suggest that biological activity further enhances the solubility of the apolar petroleum hydrocarbons. Many hydrocarbon-degrading bacteria and fungi produce biosurfactants to increase the bioavailability of hydrophobic water-insoluble substrates (ZAJIC

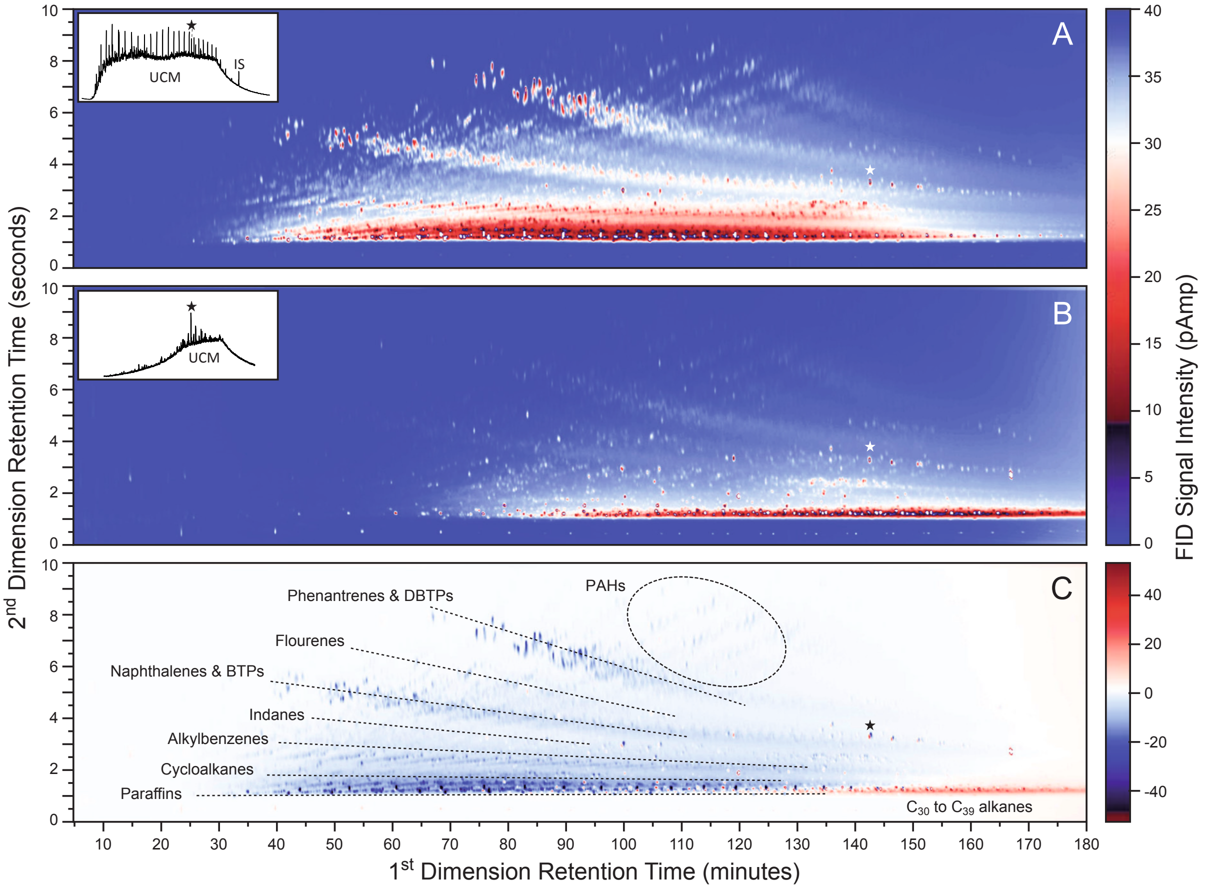

Fig. V.4. Chromatogram of a fresh asphalt sample from the main asphalt field (**A**) and a brittle asphalt sample from the sedimented asphalt patches (**B**) and the generated difference chromatogram between the two chromatogramns (**C**). Relative losses of compounds are depicted in blue and recalcitrant compounds in red. Star denotes Norhopane, which was used for normalization. The inserts in **(A)** and **(B)**, top left, show chromatograms of conventional GC analyses, UCM – unresolved complex mixture, IS – injection standard.

and Supplisson, 1972; Oberbremer and Müller-Hurtig, 1989; Zon and Rosenberg, 2002). Emulsification of the TPH could account for the observed total mass loss of TPH in samples from the AP, including the long chain methyl-substituted cycloalkanes. Furthermore, we consider aerobic biodegradation to be the main driver of emulsification as it is more effective and occurs on shorter timescales than anaerobic processes (e.g., Grishchenkov et al., 2000). We conclude that a combination of biodegradation, probably under aerobic conditions, and water washing is responsible for the almost complete TPH mass removal observed in the brittle asphalt. This process likely takes place on even longer time scales as indicated by the asphalt sediment coverage. Considering a sedimentation rate of 7.5 cm kyr^{-1} (Worzel et al., 1973) the time scales are on the order of decades to centuries.

V.4.5. Recalcitrance of biomarkers

As a consequence of the selective removal of compounds, more recalcitrant compounds are enhanced in relative abundance. Among the most recalcitrant compounds in both rough and brittle asphalts are steranoid- and hopanoid-derived biomarkers, which are comprised of hopanes, methyl-hopanes, regular steranes, C_{21} pregnane, monoaromatic and triaromatic steranes, benzohopanes, secohopanes, secosteranes, but also bicyclic sesquiterpanes, and tricyclic terpanes dominated by C_{23}. This is consistent with the persistence of these biomarkers during biodegradation and long-term weathering, as observed in previous studies on weathering of heavy oil in the marine environment (Volkman et al., 1984; McKirdy et al., 1994; Burns et al., 1999; Farwell et al., 2009) and laboratory-based biodegradation studies (Wehner et al., 1985). Biodegradation can affect the distribution of biomarkers in reservoir oils, however, this process takes place on geological timescales over millions of years (e.g., Head et al., 2003; Larter et al., 2003). Further support that this group of biomarkers is not greatly affected by selective removal during biodegradation processes can also be seen in the consistent biomarker ratios within the different asphalt samples (Fig. V.S1).

Compounds such as the bicyclic terpanes and secosteranes that were identified among the most recalcitrant biomarkers, are not often reported in the literature. This is because they are not used as regular target compounds during source rock correlations or maturity evaluations. By GC×GC analysis we demonstrate that these compounds become dominant hydrocarbons in the otherwise unresolved UCM. Bicyclic sesquiterpanes are known to be unaffected by biodegradation (cf. Philp, 1985), and were recently proposed as useful biomarkers in environmental forensics and oil spill correlations (Yang et al., 2009). Secosteranes were tentatively based on mass spectral data and by comparison with literature date (Fig. V.S3, e.g., Maurer, 2004). Secosteranes are very rarely reported in the literature (Li et al., 1990; Ma et al., 1991). However, they have been suggested to be widely distributed in oils from around the world (Maurer, 2004). In this study these compounds become most abundant in rough asphalts from the BS due to their recalcitrance to biodegradation. They are also still present in brittle asphalts from the AP, which are strongly affected by weathering processes.

Table V.2. Relative abundance of total petroleum hydrocarbons (TPH) in the three asphalts analyzed with GC×GC-FID and percentages of TPH losses of compound classes relative to the fresh asphalt (refer to main text for details).

Compound class	fresh asphalt Category A	rough asphalt Category B		brittle asphalt Category C	
	% of TPH	% of TPH	% loss from fresh site	% of TPH	% loss from fresh site
Paraffins	29	3.2	92	4.0	97
Alkylcycloalkanes	24	49	-47[a]	13	87
Alkylcyclobenzenes	12	15	15	27	47
Indanes	2.4	2.2	36	1.9	81
Naphthalanes	9.0	3.7	71	0.6	98
Flourenes	2.5	1.9	47	0.9	92
Phenantrenenes	7.9	7.3	34	1.6	95
Anthracenes	2.0	2.2	24	0.03	100
Steranes+hopanes	11.8	16.7	0	50.6	0
TPH	100	100	29	100	77

[a]negative values represent relative mass gains

V.4.6. Estimation of TPH emission

The recalcitrance of the biomarkers discussed in the previous section can be used for normalization and enables estimation of relative TPH mass losses within the different asphalt types (Fig. V.5, Table V.2). Accordingly, the mass loss of paraffins (including *n*-alkanes, branched alkanes and acyclic isoprenoids) from fresh asphalt of the MAF to the rough asphalt from the BS amounts to more than 90%. Furthermore, more than 70% of the naphthalenes and more than two thirds of the phenantrenes are lost in the rough asphalt from the BS. This is a substantial amount, considering that these aromatic compounds have comprised a significant fraction of TPHs in the fresh asphalt from the MAF (~30%). On the contrary, cycloalkanes show a relative increase of 47%. This can be interpreted to be partly due to the addition of intermediates generated during biological transformation of petroleum (cf. Aitken et al., 2004). In the brittle asphalt the almost complete removal of the UCM amounts to a TPH loss of 77% (Table V.2), where not only

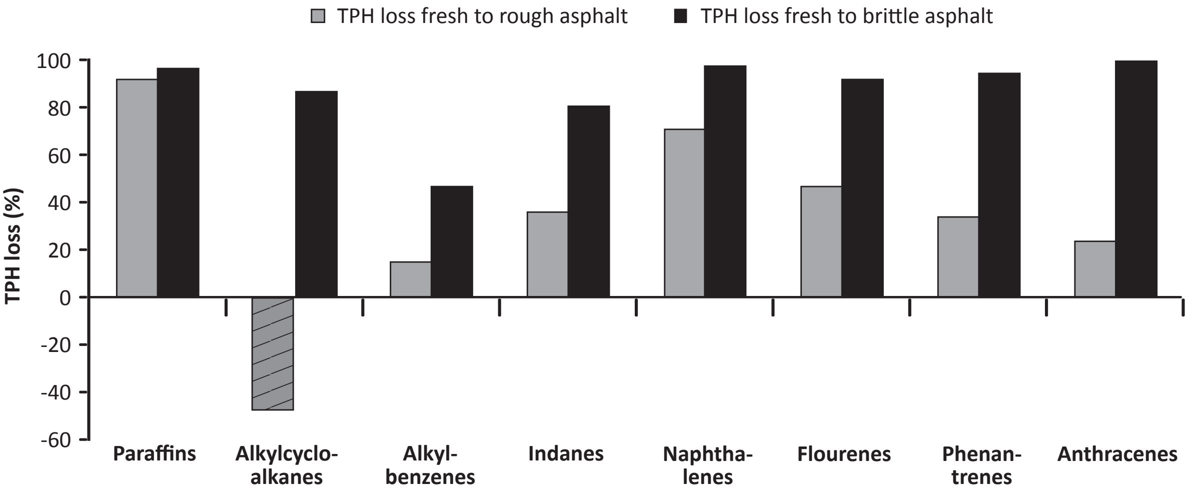

Fig. V.5. Estimated total petroleum hydrocarbon (TPH) mass losses between fresh asphalts from the main asphalt field and rough asphalts from the bubble site (gray) and brittle asphalts from the sedimented asphalt patches (black). Negative values, (gray, black stripes) represent relative gains.

the alkylated PAH have been removed (>95% mass losses for naphthalenes, phenantrenes and anthracenes), but also the alkylcycloalkanes (87% mass loss) and other less polar compounds (99% of the paraffins and 47% of the alkylbenzenes; Fig. V.5, Table V.2).

Based on the calculated TPH mass losses during post-depositional asphalt degradation and weathering we can establish a TPH emission potential at the Chapopote asphalt seeps. Estimates of the total asphalt deposits at the Chapopote range at ca. 4,000 ± 2,000 m^3 (Brüning et al., 2009) amounting to >4,000 ± 2,000 tons assuming a density >1 g/mL. This amounts to ca. 1-2% the size of a modern day supertanker, but also to a little less than 1% of the annually estimated input of natural seepage into the marine environment (Kvenvolden and Cooper, 2003). This study can only account for the potential TPH loss of the GC×GC-amenable hydrocarbon fraction, i.e. not the asphaltenes which amount to roughly 50% of the total asphalt deposits (cf. Table V.1). Of the >2,000 ± 1,000 tons TPH, ca. 77% (or >1,540 ± 770 tons; total loss of TPH from fresh to brittle asphalt, Table V.2) have the potential to be released into the ocean by dissolution and dispersion. A substantial amount, however, is already likely consumed by anaerobic biological uptake (up to 29%; total loss of TPH from fresh to rough asphalt, Table V.2). Notably, in this rough estimate we did not account for the more diffuse petroleum seepage through oil-impregnated sediments in an area of ca. 1 km^2 where TPH comprise between 3 and 10% wt in the sediments and where anaerobic biodegradation is also taking place (Schubotz et al., *in prep., Chapter III*). The timescales of this emission are currently not well constrained, but seepage at the Chapopote must have occurred for at least two decades based on tubeworm age determinations (Brüning et al., 2009). Most likely these processes are taking place over centuries, based on sedimentation rates and asphalt sediment cover.

With an emission of more than 1,540 ± 770 tons TPH over a time span of decades to centuries, the contribution of the Chapopote asphalt seep to global seepage budgets is quite small compared to other major natural oil seeps (Wardlaw et al., 2008; Farwell et al., 2009). However, considering the Chapopote is only one of the smaller Knolls of the 40 Campeche Knolls and satellite imaging has shown that active petroleum seepage is also occurring at the other knolls, the Campeche Knolls could have a substantial contribution to TPH emissions in the GoM.

V.5. ACKNOWLEDGEMENTS

We would like to acknowledge the ROV team and shipboard and scientific members of R/V Meteor expedition M67/2b for obtaining the samples. J.S. Lipp and M. Elvert are thanked for help with data interpretation; T. Hörske and S. Sylva for help in the laboratory; M. Brüning and F. Ding for continuous fruitful discussions, and J.S. Lipp for helpful comments on the manuscript. This work was supported by the Deutsche Forschungsgemeinschaft (through MARUM Center for Marine Environmental Sciences, and the Bremen International Graduate School for Marine Sciences, GLOMAR), and the Woods Hole Oceanographic Institution.

V.6. REFERENCES

Aitken, C.M., Jones, D.M., Larter, S.R. (2004) Anaerobic hydrocarbon biodegradation in deep subsurface oil reservoirs. *Nature* **43**: 291-294.

Anderson, R.K., Scalan, R.S., Parker, P.L. (1983) Seep oil and gas in Gulf of Mexico slope sediment. *Nature* **222**: 619-621.

Arey, J.S., Nelson, R.K., Reddy, C.M. (2007) Disentangling oil weathering using GC×GC. 1. Chromatogram analysis. *Environ Sci Technol* **41**: 5738-5746.

Atlas, R.M. (1981) Microbial degradation of petroleum hydrocarbons: an environmental perspective. *Microbiol Rev* **45**: 180-209.

Barnard, P.C., Bastow, M.A. (1991) Hydrocarbon generation, migration and alteration, entrapment and mixing in the central and northern N. Sea. In. England, W.A., Fleet, A.J. (eds) Geological Society Special Publication, No. 59, Petroleum Migration. The Geological Society, London, pp. 167-190.

Blumer, M, Sass, J. (1972) Oil pollution: persistence and degradation of spilled fuel oil. *Nature* **176**: 1120-1122.

Bohrmann, G., Spiess, V., M67/2 Cruise Participants (2008) Report and preliminary results of R/V Meteor cruise M67/2a and 2b, Balboa – Tampico – Bridgetown, 15 March – 24 April 2006. Fluid seepage in the Gulf of Mexico, Berichte, No.263, Fachbereich Geowissenschaften, Universität Bremen, Bremen, Germany.

Brüning, M., Sahling, H., MacDonald, I. R, Ding, F, Bohrmann, G. (2009) Origin, distribution, and alteration of asphalts at Chapopote Knoll, Southern Gulf of Mexico. *Mar Petrol Geol*, accepted September 16, 2009.

Burns, K.A., Codi, S., Pratt, C., Duke, N.C. (1999) Weathering of hydrocarbons in mangrove sediments: testing the effects of using dispersants to treat oil spills. *Org Geochem* **30**: 1273-1286.

Chakraborty, R., Coates, J.D. (2004) Anaerobic degradation of monoaromatic hydrocarbons. *Appl Microbiol Biotechnol* **64**: 437-446.

Connan, J. (1984) Biodegradation of crude oils in reservoirs. In: Brooks, J., Welte, D. (eds.) Advances in petroleum geochemistry, Vol. 1. Academic Press, London, pp. 299-335.

Connan, J., Bouroullec, J., Dessort, T.D., Albrecht, P. (1986) The microbial input in carbonate-anhydrite facies of a sabkha palaeoenvironment from Guatemala; a molecular approach, In: D. Leythaeuser and J. Rullkötter (eds.) Advances in organic geochemistry 1985: Pergamon Press, Inc. Oxford, UK, pp. 29-50.

Ding, F., Spiess, V., Brüning, M., Fekete, N., Keil, H., Bohrmann, G. (2008) A conceptual model for hydrocarbon accumulation and seepage processes around Chapopote asphalt site, southern Gulf of Mexico: From high resolution seismic point of view. *J Geophy Res* **113**: DOI:10.1029/2007JB005484.

Edwards D.S., McKirdy D.M. and Summons R.E. (1998) Enigmatic asphaltites from the Southern Australian Margin: Molecular and carbon isotopic composition. *Petroleum Exploration Society of Australia Journal* **26**: 106-129.

Farwell, C., Reddy, C.M., Peacock, E., Nelson, R.K., Washburn, L., Valentine, D.L. (2009) Weathering and the fallout plume of heavy oil from strong petroleum seeps near coal point, CA. *Environ Sci Technol* **43**: 3542-3548.

Frysinger, G.S., Gaines, R.B., Ledford, E.B. Jr. (1999) Quantitative determination of BTEX and total aromatic compounds in gasoline by comprehensive two-dimensional gas chromatography (GC×GC). *J High Res Chrom* **22**: 195-200.

Frysinger, G.S., Gaines, R.B. (2001) Separation and identification of petroleum biomarkers by comprehensive two-dimensional gas chromatography. *J Sep Sci* **24**: 87-96.

Gaines, R.B., Frysinger, G.S., Hendrick-Smith, M.S., Stuart, J.D. (1999) Oil spill source identification by comprehensive two-dimensional gas chromatography. *Environ Sci Technol* **33**: 2106-2112.

Geiselbrecht, A.D., Hedlung, B.P., Tichi, M.A., Staley, J.T. (1998) Isolation of marine polycyclic aromatic hydrocarbon (PAH)-degrading *Cycloclasticus* strains from the Gulf of Mexico and comparison of their PAH degradation ability with that of Puget sound *Cycloclasticus* strains. *Appl Environ Microbiol* **64**: 4703-4710.

Grishchenkov, V.G., Townsend, R.T:, McDonald, T.J., Autenrieth, R.L., Bonner, J.S., Boronin, A.M. (2000) Degradation of petroleum hydrocarbons by facultative anaerobic bacteria under aerobic and anaerobic conditions. *Proc Biochem* **35**: 889-896.

Guzmán-Vega et al., M.A., Castro Ortíz, L., Román-Ramos, J.R., Medrano-Morales, L., Valdéz, L.C., Vázquez-Covarrubias, E., Ziga-Rodriguez, G. (2001). Classification and origin of petroleum in the Mexican Gulf Coast Basin: An overview, In: C. Bartolini, R.T. Buffler, and A. Cantú-Chapa (eds) The western Gulf of Mexico Basin: Tectonics, sedimentary basins, and petroleum systems: AAPG Memoir 75, pp.127-142.

Head, I.M., Jones, D.M., Larter, S.R. (2003) Biological activity in the deep subsurface and the origin of heavy oil. *Nature* **426**: 344-352.

Head, I.M., Jones, D.M., Röling, W.F.M. (2006) Marine microorganisms make a meal of oil. *Nat Rev Micro* **4**: 173-182.

Horstad, I., Larter, S.R. (1997) Petroleum migration, alteration, and remigration within Troll Field, Norwegian North Sea. *AAPG Bulletin* **81**: 222-248.

Hunt, J.S. (1996) Petroleum Geochemistry and Geology; W.H. Freeman: New York, 1996.

Kasai, Y., Kishira, H., Harayama, S. (2002) Bacteria belonging to the genus *Cyclocasticus* play a primary role in the degradation of aromatic hydrocarbons released in a marine environment. *Appl Environ Microbiol* **68**: 5625-5633.

Kvenvolden, K.A., Cooper, C.K. (2003) Natural seepage of crude oil into the marine environment. *Geo-Mar Lett* **23**: 140-146.

Larter, S., Wilhelms, A., Head, I., Koopmans, M., Aplin, A., Di Primio, R. Zwach, C., Erdmann, M., Tenaes, N. (2003) The controls on the composition of biodegraded oils in the deep subsurface-part 1: biodegradation rates in petroleum reservoirs. *Org Geochem* **34**: 601-613.

Li, T.S., Li, Y.L., Liang, X.T. (1990) Synthesis of 5α-(17R,20R)-14,15-*seco*-cholestane. *Chin Chem Lett* **1**: 215-218.

Ma, J.G., Li, T.S., Li, Y.L. (1991) Synthesis of 4,5-*seco*-cholestane and 4-methyl-4,5-*seco*-cholestane. *Chin Chem Lett* **2**: 521-522.

MacDonald, I.R., Guinasso, N.L. Jr., Ackleson, S.G., Amos, J.F., Duckworth, R., Sassen, R., Brooks, J.M. (1993) Natural oils slicks in the Gulf of Mexico visible from space. *J Geophys Res* **98**: 16,351-16,364.

MacDonald, I.R., Leifer, I., Sassen, R., Stine, P., Mitchell, R., Guinasso, N. Jr. (2002) Transfer of hydrocarbons from natural seeps to the water column and atmosphere. *Geofluids* **2**: 95-107.

MacDonald, I.R., Bohrmann, G., Escobar, E., Abegg, F., Blanchon, P., Blinova, V., Brückmann, W., Drews, M., Eisenhauer, A., Han, X., Heeschen, K., Meier, F., Mortera, C., Naehr, T., Orcutt, B., Bernard, B., Brooks, J., de Faragó, M. (2004) Asphalt volcanism and chemosynthetic life in the Campeche Knolls, Gulf of Mexico. *Science* **304**: 999-1002.

Maurer, J. (2004) Dissertation, Carl-von-Ossietzky University of Oldenburg, Oldenburg, Germany.

McKirdy, D.M., Summons. R.E., Padley, D., Serafini, K.M., Boreham, C.J., Struckmeyer, H.I.M. (1994) Molecular fossils in coastal bitumens from southern Australia: signatures of precursor biota and source rock environments. *Org Geochem* **21**: 265-286.

Meckenstock R.U., Safinowski, M., Griebler, C. (2004) Anaerobic degradation of polycyclic aromatic hydrocarbons. *FEMS Microbiol Ecol* **49**: 27-36.

Mello, M.R., Gaglianone, P.C., Brassel, S.C., Maxwell, J.R. (1988) Geochemical and biological marker assessment of depositional environment using Brazilian offshore oils. *Mar Petrol Geol* **2**: 205-223.

Musat, F., Galushko, A., Jacob, J., Widdel, F., Kube, M., Reinhard, R., Wilkes, H., Schink, B., Rabus, R. (2009) Anaerobic degradation of naphthalene and 2-methylnaphthalene by strains of marine sulfate-reducing bacteria. *Environ Microbiol* **11**: 209-219.

NAS (2003) Oil in the sea III: inputs, fates and effects. National Academy of Sciences, National Academy Press, Washington, DC.

Nähr, T.H., Birgel, D., Bohrmann, G., MacDonald, I.R., Kasten, S. (2009) Biogeochemical controls on authigenic carbonate formation at the Chapopote “asphalt volcano”, Bay of Campeche. *Chem Geol* **266**: 399-411.

Nelson, R.K., Kile, B.M., Plata, D.L., Sylva, S., Xu, L., Reddy, C.M., Gaines, R.B., Frysinger, G.S., Reichenbach, S.E. (2006) Tracking the weathering of an oil spill with comprehensive two-dimensional gas chromatography. *Environ Foren* **7**: 33-44.

Oberbremer, A., Müller-Hurtig, R. (1989) Aerobic stepwise hydrocarbon degradation and formation of biosurfactants by an original soil population in a stirred reactor. *Appl Microbiol Biotechnol* **31**: 582-586.

Oshihro, T. Izumi, Y. (1999) Microbial Desulfurization of Organic Sulfur Compounds in Petroleum. *Biosci Biotechnol Biochem* **63**: 1-9.

Peacock, E.E., Hampson, G.R., Nelson, R.K., Xu, L., Frysinger, G.S:, Gaines, R.B., Farrington, J.W., Tripp, B.W., Reddy, C.M. (2007) The 1974 spill of the *Bouchard 65* oil barge: Petroleum hydrocarbons persist in Windsor Cove salt marsh sediments. *Mar Pollut Bull* **54**: 214-225.

Peters, K.E., Moldowan, J.M. (1993) *The Biomarker Guide*. Prentice Hall, New York, 1993.

Philp, R.P. (1985) Biological markers in fossil fuel production. *Mass Spectrom Rev* **4**: 1-54.

Raggi, L., Schubotz, F., Hinrichs, K.-U., Dubilier, N. Bacterial symbionts of *Bathymodiolus* mussels and *Escarpia* tubeworms from an asphaltic deep-sea environment in the southern Gulf of Mexico. *in preparation for Mar Ecol Progr Ser (see also Chapter VIc)*.

Reddy, C.M., Eglinton, T.I., Hounshell, A., White, H.K., Xu, L., Gaines, R.B., Frysinger, G.S. (2002) The West Falmouth oil spill after thirty years: The persistence of petroleum hydrocarbons in marsh sediments. *Environ Sci Technol* **36**: 4754-4760.

Schubotz, F., Lipp, J., Elvert, M., Kasten, S., Zabel, M., Escobar, E., Bohrmann, G., Hinrichs, K.-U. Chemosynthetic life at the Chapopote asphalt volcano – insights from stable carbon isotopes and intact polar membrane lipid analyses. *In prep. for Geochim Cosmochim Acta* (*see also Chapter III*).

Volkman, J.K. (1984) Biodegradation of aromatic hydrocarbons in crude oils from the Barrow Sub-basin of Western Australia. *Org Geochem* **6**: 619-632.

Wang, Z., Fingas, M., Blenkinsopp, S., Sergy, G., Landriault, M., Sigouin, L., Foght, J., Semple, K., Westlake, D.W.S (1998) Comparison of oil composition changes due to biodegradation and physical weathering in different oils. *J Chrom A* **809**: 89-107.

Wardlaw, G.D.; Arey, J.S.; Reddy, C., M.; Nelson, R.K.; Ventura, G.T.; Valentine D.L. (2008) Disentangling oil weathering at a marine seep using GC×GC: Broad metabolic specificity accompanies subsurface petroleum biodegradation *Environ Sci Technol* **41**: 5865.

Wehner, H., Teschner, M., Bosecker, K. (1985) Chemical reactions and stability of biomarkers and stable isotope ratios during *in vitro* biodegradation of petroleum. *Org Geochem* **10**: 463-471.

Wenger, L.M., Isaksen, G.H. (2002) Control of hydrocarbon seepage intensity on level of biodegradation in sea bottom sediments. *Org Geochem* **33**: 1277-1292.

Widdel, F., Rabus, R. (2001) Anaerobic biodegradation of saturated and aromatic hydrocarbons. *Curr Opin Biotechnol* **12**: 259-276.

Wilson, R.D., Monaghan, P.H., Osanik, A., Price, L.C., Rogers, M.A. (1974) Natural marine oil seepage. *Science* **184**: 857-865.

Worzel, L.J., Bryant, William R., Beall jr., A.O., Capo, R., Dickinson, K., Foreman, H.P., Laury, R., McNeely, B.W., Smith, L.A., 1973. Site 88. In: L.J. Worzel and W.R. Bryant (eds), Init. Report of DSDP. National Science Foundation, Washington, pp. 55-70.

Yang, C., Wang, Z., Hollebone, B.P., Brown, C.E., Landiault (2009) Characteristics of bicyclic sesquiterpanes in crude oils and petroleum products. *J Chrom A* **1216**: 4475-4484.

Zajic, J.E., Supplisson, B. (1972) Emulsification and degradation of “Bunker C” fuel oil by microorganisms. *Biotech Bioeng* **14**: 331.343.

Zon, E., Rosenberg, E. (2001) Biosurfactants and oil remediation. *Curr Opin Biotechnol* **13**: 249-252.

Zumberge, J.E. (1984) Source rocks of the La Luna Formation (Upper Cretaceous) in the Middle Magdalena Valley, Colombia, In: J.G. Palacas (ed) Petroleum geochemistry and source rock potential of carbonate rocks: AAPG Studies in Geology **18**, pp. 127-134.

V.S1. SUPPLEMENTARY MATERIAL

Table V.S1. Biomarker ratios, bulk $\delta^{13}C$ values of the analyzed asphalt samples. SGoM-southern Gulf of Mexico, MAF-main asphalt site, BS- bubble site, AP-asphalt patches. Biomarker ratios: C_{29}/hop - 17α,21β (H)-30-norhopane (*m/z* 191) to 17α,21 β (H)- hopane (*m/z* 191), *H*h-C_{35}/C_{36} - 17α,21β (H)-30-pentakishomohopane 22S+22R (*m/z* 191) to 17α,21b (H)-30-tetrakishomohopane 22S+22R to (*m/z* 191), Olean. - 18a (H)-oleanane over peak are of 17a, 21b (H)-hopane (*m/z* 191), C_{24}-tetra/C_{26}-tri - tetracyclic terpane (C_{24}; *m/z* 191) to tricyclic terpane (C_{26}; *m/z* 191), Ts/Tm - 18α (H)-22,29,30-trisnorneohopane (*m/z* 191) to 17α (H)-22,29,30-trisnorhopane (*m/z* 191), Dia/Ster - sum of C_{27} 20R and 20S 13β,17α (H) diasteranes (*m/z* 217) over sum of C_{29} 20S and 20R 5α (H),14β(H),17β(H),24-ethylcholestane (*m/z* 217).

Sample location	Sample ID (GeoB)	Depth (cm)	C_{29}/hop	*H*h-C_{35}/C_{36}	Olean.	C_{24}-tetra/ C_{26}-tri	Ts/Tm	Dia/Ster	$\delta^{13}C$ TOC
SGoM[a]	Macuspana	nd	0.6	0.3	0.6	0.9	1.1	0.7	-27.2
SGoM[a]	Campeche Shelf	nd	1.1	0.9	0.0	1.6	0.5	0.10	-27.2
MAF	10617-6 #4	3	1.6	1.3	0.0	1.4	0.6	0.11	nd
MAF	10617-6 #3	2	1.5	1.0	0.0	1.2	0.5	0.07	-27.3
MAF	10617-6 #2	1	1.4	1.1	0.0	1.1	0.6	0.09	-27.3
BS	10622-4 #2	2	1.8	0.8	0.0	1.4	0.4	0.10	nd
AP	10619-17 #2	Surface	1.5	1.3	0.0	1.5	0.6	0.06	nd
MAF	10623	100	1.4	0.9	0.0	1.3	0.6	0.08	nd
MAF	10621-1	100	1.4	0.9	0.0	1.0	0.6	0.09	-27.6
MAF	10625-16	2	1.5	0.8	0.0	1.6	0.5	0.08	nd

[a] biomarker ratios adapted from GUZMÁN-VEGA ET AL., 2001
nd-not determined

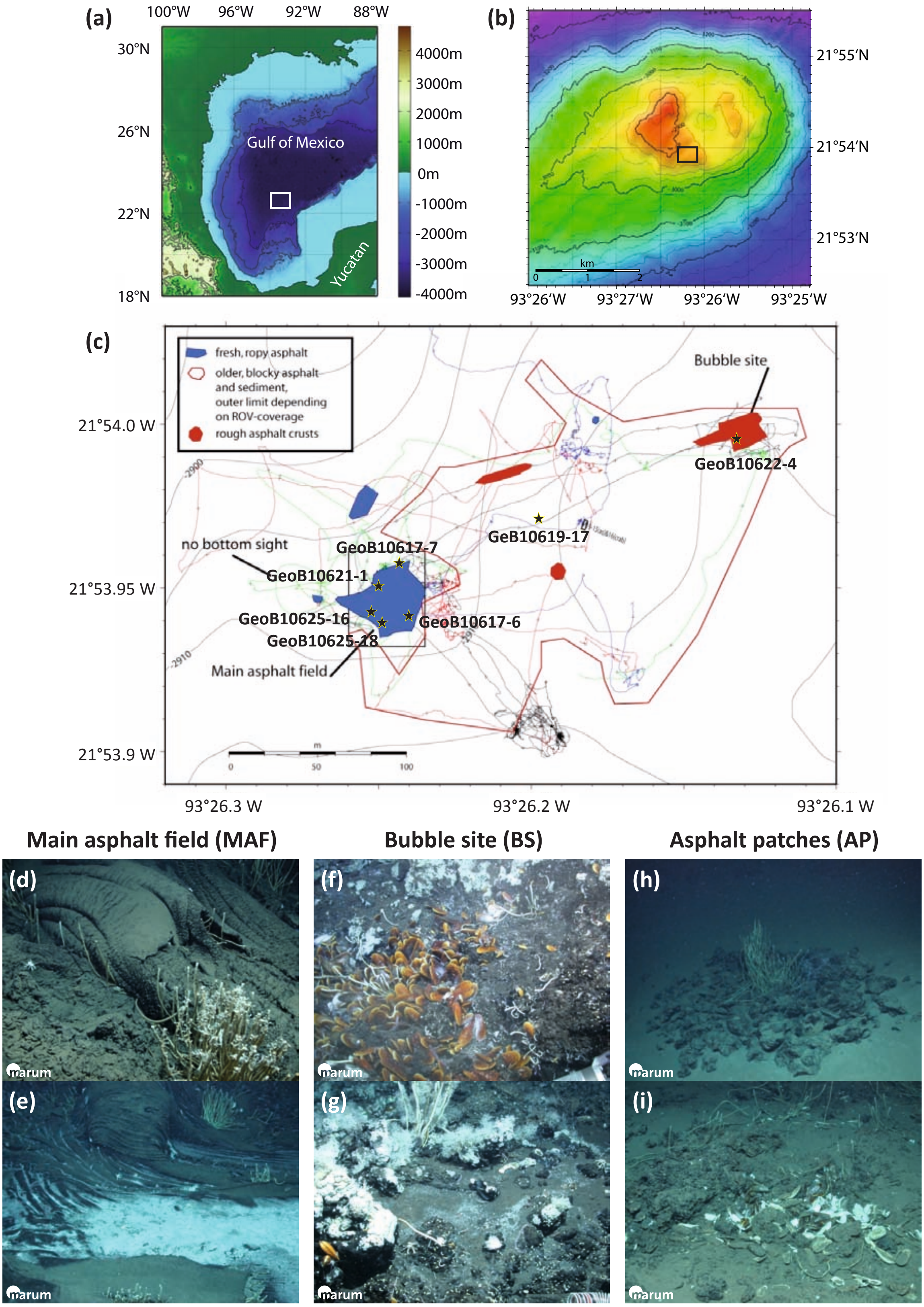
(a)
100°W
96°W
92°W
88°W
30°N
26°N
22°N
18°N
Gulf of Mexico
Yucatan
4000m
3000m
2000m
1000m
0m
-1000m
-2000m
-3000m
-4000m
(b)
21°55'N
21°54'N
21°53'N
km
0
1
2
93°26'W
93°27'W
93°26'W
93°25'W
(c)
fresh, ropy asphalt
older, blocky asphalt and sediment, outer limit depending on ROV-coverage
rough asphalt crusts
Bubble site
GeoB10622-4
21°54.0 W
GeB10619-17
no bottom sight
GeoB10617-7
GeoB10621-1
21°53.95 W
GeoB10625-16
GeoB10625-18
GeoB10617-6
Main asphalt field
-2900
-2910
21°53.9 W
m
0
50
100
93°26.3 W
93°26.2 W
93°26.1 W
Main asphalt field (MAF)
Bubble site (BS)
Asphalt patches (AP)
(d)
(e)
(f)
(g)
(h)
(i)
marum

Fig. V.S1. Map of the asphalt seeps at the Chapopote Knoll. (**A**) Location of the Chapopote Knoll (square) in the southern Gulf of Mexico, (**B**) detailed bathymetry of the Chapopote Knoll, square shows asphalt site sampling area (modified after BOHRMANN ET AL., 2008 and SCHUBOTZ ET AL., *IN PREP., CHAPTER III*). (**C**) Map of the asphalt seep site at the Chapopote Knoll, with locations of ROV collected asphalt samples (modified after BRÜNING ET AL., 2009). (**D**) – (**E**) Images of the flow-like structures of asphalt at the main asphalt field with associated chemosynthetic communities, e.g., microbial mats (in white) and, crabs, sea cucumbers and tube worm bushes. (**F**) – (**G**) Images of the bubble site where asphalts were covered with mussels, sponges and corals. (**H**) – (**I**) Sedimented asphalt patches with tube worm bushes and clam shells.

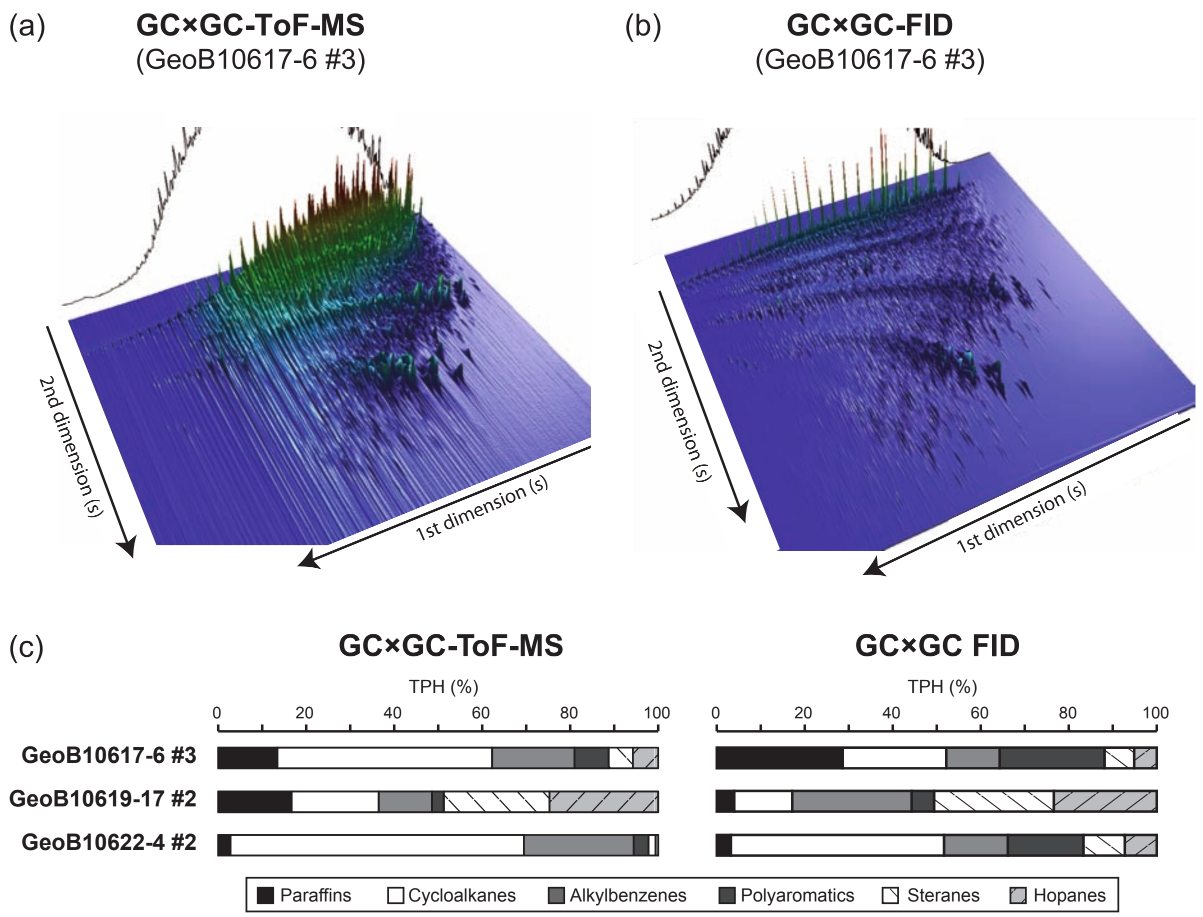

Fig. V.S2. Comparison of GC×GC chromatogram of an asphalt sample from the main asphalt field (GeoB10617-6 #3) analyzed with (**A**) GC×GC ToF-MS and (**B**) GC×GC-FID, showing higher peak resolution with GC×GC-FID. (**C**) Differences in quantification of compound classes with GC×GC ToF-MS and GC×GC-FID.

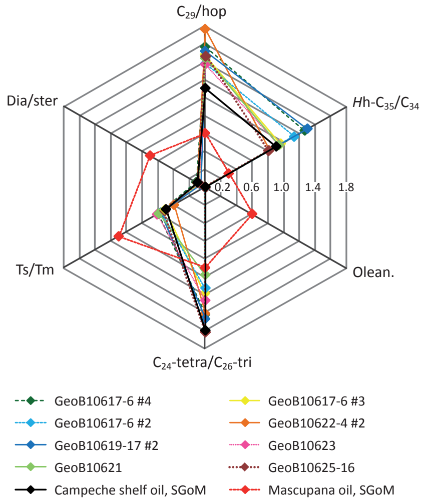

Fig. V.S3. Spider diagram showing the biomarker ratios of a selection of the analyzed asphalt samples and two oils from the Campeche Shelf and the Sureste Basin (published in GUZMÁN-VEGA ET AL., 2001). Biomarker ratios (clockwise): C_{29}/hop - 17α,21β (H)-30-norhopane (*m/z* 191) to 17α,21 β (H)- hopane (*m/z* 191), *Hh*-C_{35}/C_{36} - 17α,21β (H)-30-pentakishomohopane 22S+22R (*m/z* 191) to 17α,21b (H)-30-tetrakishomohopane 22S+22R to (*m/z* 191), Olean. - 18a (H)-oleanane over peak are of 17a, 21b (H)-hopane (*m/z* 191), C_{24}-tetra/C_{26}-tri - tetracyclic terpane (C_{24}; *m/z* 191) to tricyclic terpane (C_{26}; *m/z* 191), Ts/Tm - 18α (H)-22,29,30-trisnorneohopane (*m/z* 191) to 17α (H)-22,29,30-trisnorhopane (*m/z* 191), Dia/Ster - sum of C_{27} 20R and 20S 13β,17α (H) diasteranes (*m/z* 217) over sum of C_{29} 20S and 20R 5α (H),14β(H),17β(H),24-ethylcholestane (*m/z* 217).

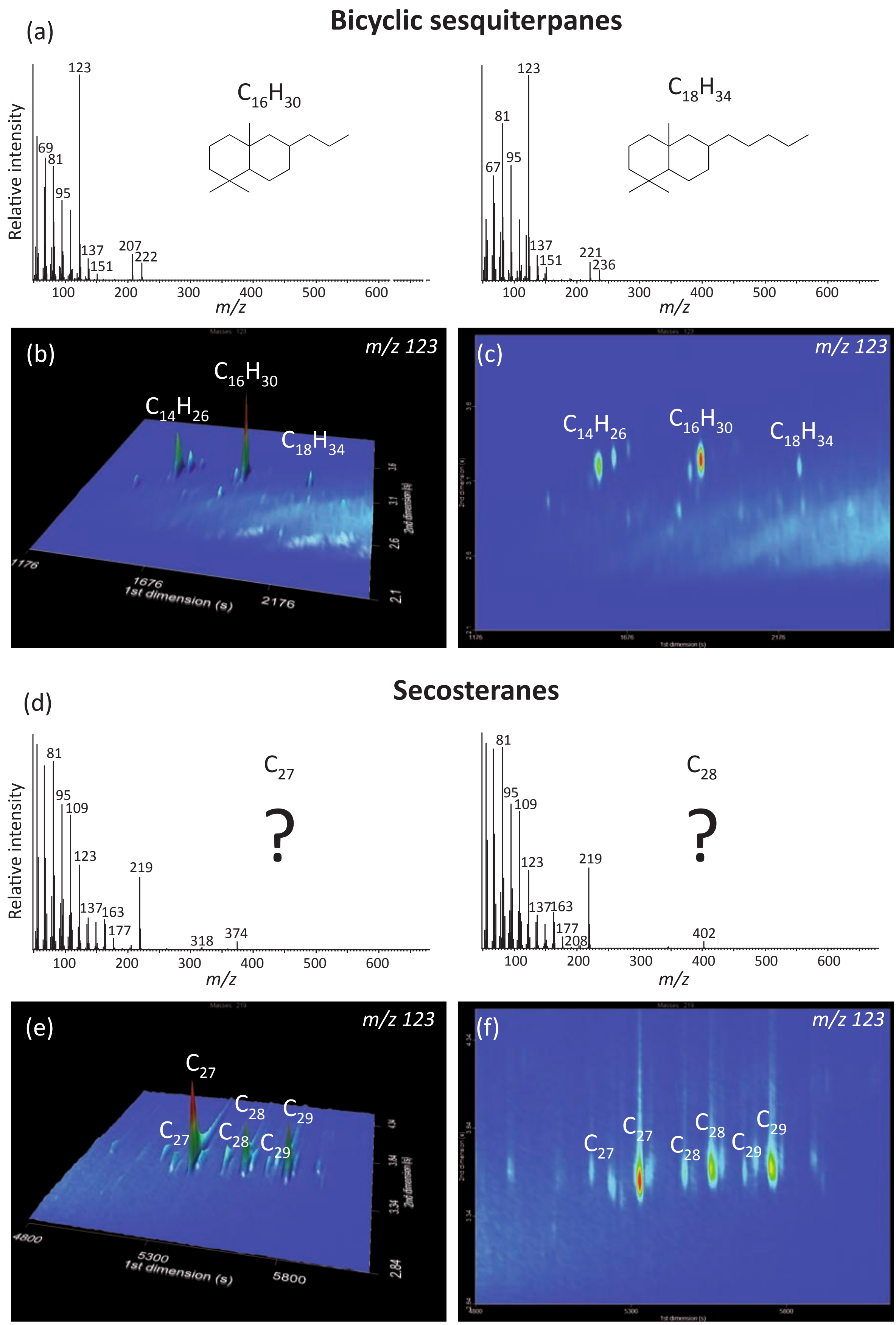

Fig. V.S4. (**A**) Mass spectra of bicyclic sesquiterpanes identified in this study, and their distribution depicted as (**B**) a mountain plot and (**C**) contour plot of in the GC×GC-MS m/z 123 mass chromatogram. (**D**) Mass spectra of the tentatively identified secohopanes, exact structures could not be identified, and their distribution depicted as (**E**) a mountain plot and (**F**) contour plot of in the GC×GC-MS m/z 219 mass chromatogram.

V.S2. SUPPLEMENTARY REFERENCES

Bohrmann, G., Spiess, V., Cruise Participants (2008) Report and preliminary results of R/V Meteor cruise M67/2a and 2b, Balboa – Tampico – Bridgetown, 15 March – 24 April 2006. Fluid seepage in the Gulf of Mexico, Berichte, No.263, Fachbereich Geowissenschaften, Universität Bremen, Bremen, Germany.

Brüning, M., Sahling, H., MacDonald, I. R, Ding, F, Bohrmann, G. Origin, distribution, and alteration of asphalts at Chapopote Knoll, Southern Gulf of Mexico. *Mar Petrol Geol*, accepted September 16, 2009.

Guzmán-Vega et al., M.A., Castro Ortíz, L., Román-Ramos, J.R., Medrano-Morales, L., Valdéz, L.C., Vázquez-Covarrubias, E., Ziga-Rodriguez, G. (2001). Classification and origin of petroleum in the Mexican Gulf Coast Basin: An overview, In: C. Bartolini, R.T. Buffler, and A. Cantú-Chapa (eds) The western Gulf of Mexico Basin: Tectonics, sedimentary basins, and petroleum systems: AAPG Memoir 75, pp.127-142.

Schubotz, F., Lipp, J., Elvert, M., Kasten, S., Zabel, M., Escobar, E., Bohrmann, G., Hinrichs, K.-U. Chemosynthetic life at the Chapopote asphalt volcano – insights from stable carbon isotopes and intact polar membrane lipid analyses. *In prep. for Geochim Cosmochim Acta, see also Chapter III.*

Chapter VIa

Methane and sulfide fluxes in permanent anoxia: *in-situ* studies at the Dvurechenskii mud volcano (Sorokin Trough, Black Sea)

Anna Lichtschlag[1*], Janine Felden[1,], Frank Wenzhöfer[1,2], Florence Schubotz[3], Tobias Ertefai[3+], Antje Boetius[1,2], Dirk de Beer[1]

Submitted to *Geochimica et Cosmochimica Acta*

* corresponding author, +49 (0)421 2028843, alichtsc@mpi-bremen.de

[1]*Max-Planck-Institute for Marine Microbiology, Celsiusstrasse 1, 28359 Bremen, Germany*

[2]*HGF MPG Research Group on Deep Sea Ecology and Technology, Alfred Wegener Institute for Polar and Marine Research, Am Handelshafen 12, 27570 Bremerhaven, Germany*

[3]*MARUM, University Bremen,* Leobener Strasse, *28359 Bremen, Germany*

[+]*current address: Department of Applied Chemistry, Curtin University of Technology, Kent St, Perth, Australia*

ABSTRACT

Benthic fluxes of methane and sulfide, and the factors controlling transport, consumption and production of both compounds within the sediment were investigated at a cold seep in permanently anoxic waters (Dvurechenskii mud volcano (DMV), 2060 m water depth, Black Sea). The otherwise pie shaped mud volcano showed temperature anomalies as well as solute and gas fluxes indicating high fluid flow at a small elevation north of the geographical center. This is probably the missing source of the previously reported methane flares above the DMV. The anaerobic oxidation of methane (AOM) coupled to sulfate-reduction (SR) was excluded from this zone due to fluid-flow induced sulfate limitation. Consequently the biological methane consumption by AOM did not function at this site, hence methane escaped into the water column with a rate of 0.44 mol m^{-2} d^{-1}. Fluid flow and total methane flux decreased towards the outer edge of the mud volcano, correlating with an increase in sulfate penetration into the sediment, and with higher SR and AOM rates. Additional signs of seepage were seen at the edges of the mud volcano. Outside the summit area between 50-70% of the methane flux (0.07-0.1 mol m^{-2} d^{-1}) was consumed within the upper 10 cm of the sediment. The total amount of dissolved methane released from the DMV into the water column was still significant with a discharge of 1.4 x 10^7 mol yr^{-1}. The DMV maintains also high areal rates of methane-fueled sulfide production of on average 0.05 mol m^{-2} d^{-1}. However, we concluded that sulfide and methane emission into the hydrosphere from deep water mud volcanoes does not significantly contribute to the sulfide and methane inventory of the Black Sea.

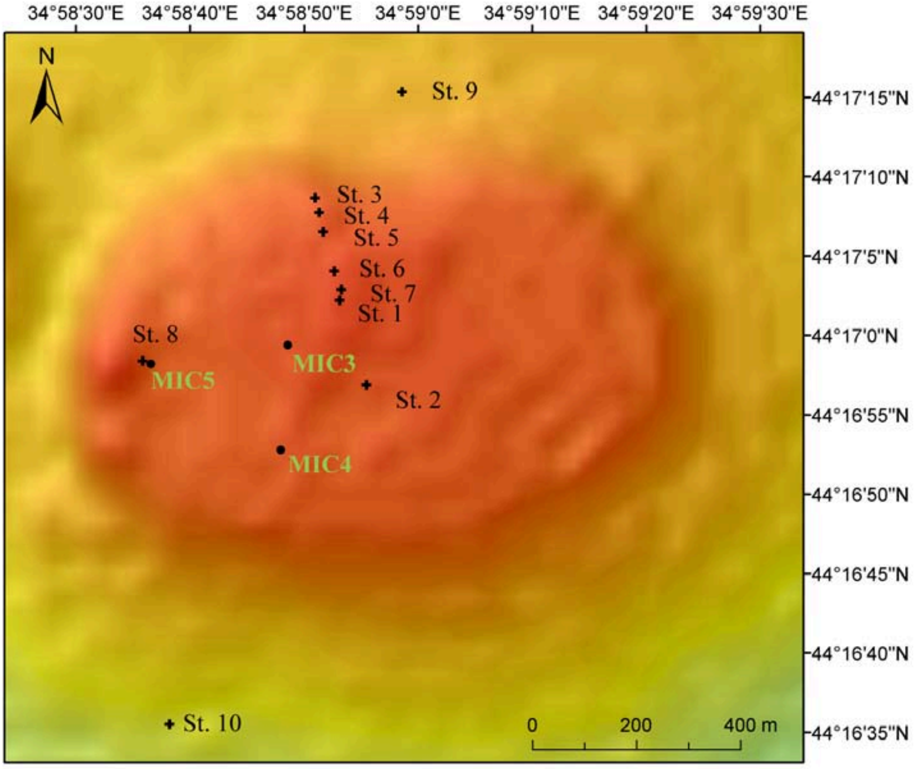

Fig. VIa. Bathymetric map of the DMV generated during the M72-2 cruise with sampling stations (St. 1-St. 10, displayed as **+**). Additionally, sampling positions MIC 3-5 from Wallmann et al. (2006; *Earth Planet Sci Lett* **248**: 545-560) and Aloisi et al. (2004; *Earth Planet Sci Lett* **225**: 347-363) are displayed as **o**.

Chapter VIb

Bacterial symbionts of *Bathymodiolus* mussels and *Escarpia* tubeworms from an asphaltic deep-sea environment in the southern Gulf of Mexico

Luciana Raggi[1*], Florence Schubotz[2], Kai-Uwe Hinrichs[2] and Nicole Dubilier[1]

In preparation for *Marine Ecology Progress Series*

* corresponding author. lraggi@mpi-bremen.de
[1]*Max-Planck Institute for Marine Microbiology, D-28359 Bremen, Germany*
[2]*Department of Geosciences, University of Bremen, D-28359 Bremen, Germany*

Keywords
Endosymbionts, thiotrophic, methanotrophic, *Bathymodiolus* mussels, *Escarpia* tubeworms, asphalt, cold seep, Gulf of Mexico

ABSTRACT

Chemosynthetic life was recently discovered in the southern Gulf of Mexico (GoM) where lava-like flows of solidified asphalt cover a large area at 3000 m depth, with oil seeps and gas hydrate deposits also present. This site, called Chapopote, is colonized by animals with chemosynthetic symbionts such as vestimentiferan tubeworms, mussels, and clams. Based on morphological and molecular analyses (COI gene), two mussel species are present at Chapopote, *Bathymodiolus heckerae* and *B. brooksi*, and a single *Escarpia laminata* tubeworm species. Comparative 16S rRNA sequence analysis and FISH showed that all three host species harbor intracellular sulfur-oxidizing symbionts that are highly similar or identical to the symbionts found in the same host species from northern GoM sites. The mussels also harbor methane-oxidizing symbionts, and these are identical to their northern GoM conspecifics. Unexpectedly, we discovered a novel symbiont in *B. heckerae* that is closely related to hydrocarbon degrading bacteria of the genus *Cycloclasticus*. We found in *B. heckerae* the phenol hydroxylase gene and stable carbon isotope analyses of lipids typical for heterotrophic bacteria were consistently heavier in *B. heckerae* by 3‰ than in *B. brooksi.*, indicating that the novel symbiont might use isotopically heavy hydrocarbons from the asphalt seep as an energy and carbon source. The discovery of a novel symbiont that may be able to metabolize hydrocarbons is particularly intriguing because until now only methane and reduced sulfur compounds have been identified as energy sources in chemosynthetic symbioses. The large amounts of hydrocarbons available at Chapopote would provide these mussel symbioses with a rich source of nutrition.

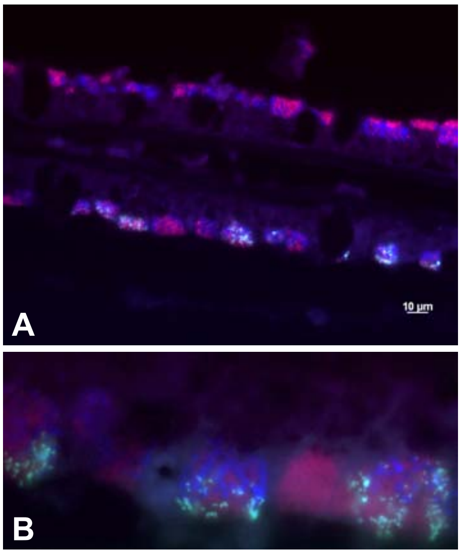

Fig. VIb.1. Fluorescence *in-situ* hybridization (FISH) identification of bacterial symbionts in *Bathymodiolus heckerae* (**A**) Cross-section through gill filament of *B. heckerae*. Methanotrophic-related bacteria (blue), thiotrophic-related (red) and *Cycloclasticus*-related (green). The auto fluorescence of the tissue is visible in purple. (**B**) Inset shows an amplification of bacteriocytes highly populated by the three bacterial phylotypes.

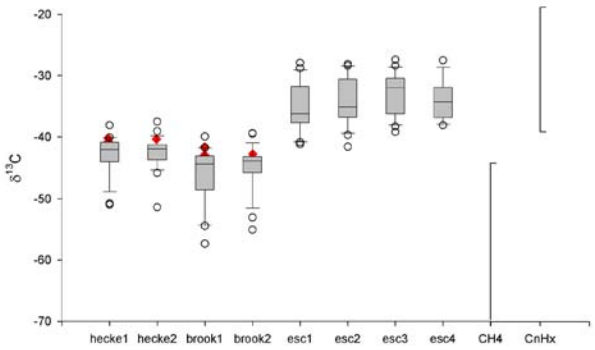

Fig. VIb.2. Stable carbon isotope composition of fatty acids extracted from *B. heckerae*, *B. brooksi*, and *Escarpia sp.* tubeworms tissue. PLFA (circles and bars) and bulk tissue (diamonds) carbon isotope values from *Bathymodiolus spp.* tissue.

Chapter VII

Concluding Remarks and Outlook

VII.1 SUMMARY AND CONCLUSIONS

The study of microorganisms in the environment greatly relies on culture-independent molecular techniques (cf. AMANN ET AL., 1995; SCHLOSS AND HANDELSMANN, 2004). A powerful technique is the analysis of intact polar membrane lipids (IPLs) that uses the taxonomic information encoded in lipid molecules. Analysis of IPLs is thought to reflect live biomass as the covalently-bound head group is enzymatically quickly degraded upon cell death (cf. WHITE ET AL. 1979; HARVEY ET AL., 1986). However, studies of IPLs in the marine environment are still scarce and further research is necessary. The main focus of this study was to decipher patterns in environmental IPL compositions and link changes to the dominating microbial communities. An additional objective was to extend compound-specific carbon isotopic analysis to head group-specific core lipids. Furthermore, comprehensive two-dimensional gas chromatography (GC×GC) was applied to study biodegradation and weathering of asphalt deposits on the sea floor.

To investigate if IPLs are useful biomarkers to trace community changes in the marine environment I investigated the distribution of IPLs in the stratified water column of the Black Sea. Here, distinct changes in microbial community composition are coupled to the geochemical stratification and are likely also observed in the composition of IPL (cf. WAKEHAM ET AL., 2007). Indeed, the expected stratification of IPLs was observed within the oxic, suboxic and anoxic water layers (*CHAPTER II*). Oxygenated surface waters were dominated by glycolipids with diacylglycerol core structures that were mainly composed of polyunsaturated fatty acids (PUFAs). The glycolipids could be identified as mono- and diglycosyl-diacylglycerols (1Gly-, and 2Gly-DAG) and sulfoquinovosyl diacylglycerols (SQ-DAG). Additional phospholipids were phosphatidylglycerol (PG) and phosphatidylcholine (PC) with diacylglycerol core structures. The core lipids of PG contained mainly combinations of saturated and monounsaturated C_{14}, C_{16} and C_{18} fatty acids (FAs), whereas the core lipids of PC also comprised the long chain polyunsaturated FAs $C_{20:5}$ and $C_{22:6}$, which are characteristic for marine algae (BRETT AND MÜLLER-NAVARRA, 1997). The presence of marine algae could be confirmed by betaine lipids with even-numbered fatty acids, which are prominent constituents in algae (e.g, DEMBITSKY, 1996). The observed glycolipids and PG-DAG could also be assigned to be derived mainly of phototrophic organisms, as glycolipids are widespread among this group and they are the most abundant lipids observed in cyanobacteria (SIEGENTHALER ET AL., 1998; WADA AND MURATA, 1998).

The IPL composition abruptly changes after depletion of oxygen and below 60 meter below sea level (mbsl) the first intact archaeal lipids were observed. These archaeal lipids were comprised of monoglycosidic and diglycosidic glyceroldibiphytanyltetraethers (1Gly- and 2Gly-GDGTs). 1Gly-GDGT contained predominantly acyclic GDGTs structures or GDGTs with 5 rings, which was identified to be crenarchaeol (WAKEHAM ET AL., 2007), a putative biomarker for crenarchaea (SINNINGHE-DAMSTÉ ET AL., 2002). 2Gly-GDGT mainly consisted of core structures with 2 and 3 rings. These differences in core lipid composition are indicative of different source organisms, however, recent IPL studies on one of the only cultured member of marine crenarchaea, also observed differences in the core lipid composition within this one culture (Schouten et al., 2008). The observed IPL composition greatly resembled that of the cultured planktonic member, apart from the observation that phospho-hexose based GDGTs were not identified in this study. We assigned the increase in IPL-GDGTs close to the nitrification zone to the presence of nitrifying crenarchaea (e.g., Lam et al., 2007).

Another distinct change below the oxygenated zone was a steep increase in 1Gly-DAG IPLs. The finding of such high abundances of glycolipids at this depth (77 to 100 mbsl) was at first surprising because synthesis of this glycolipid is mainly known from phototrophic organisms. However, it was shown that anoxygenic phototrophic green-sulfur bacteria are indeed capable to grow photoautotrophically within the chemocline of the Black Sea up to 100 mbsl (Manske et al., 2005) and are thus a likely source for the observed glycolipids. Another sharp transition in the IPL distribution was observed below 100 msbl. This depth also marks the beginning of the sulfidic anoxic zone. Here, the IPL composition was composed to one third of PE and PME head groups that contained either diacyl or diether (DEG) core structures with short chain odd-carbon numbered fatty acids. Together with PG, which was also observed in the anoxic zone, these IPLs were mainly assigned to SRB. This was also supported by the core lipid composition consisting predominantly of $C_{15:0}$, $C_{17:0}$ and $C_{16:1}$ fatty acids or ether bond alkyl chains (e.g., Rütters et al., 2001).

The most surprising observations in the anoxic zone were twofold: (*i*) the presence of unexpected bacterial lipids, such as betaine lipids and sphingolipids with glycosidic head groups, as well as the glycolipid 1Gly-DAG, and (*ii*) only very small amounts of archaeal lipids. According to determined methane oxidation rates, methane consumption in the Black Sea amounts up to 2 nM per day (Reeburgh et al., 1991), however recent studies have shown that ANME cells, which are known anaerobic methane oxidizers, cannot account for such high rates (Schubert et al., 2006). Our observation of low abundance of archaeal biomass in the lower anoxic part support the findings by Schubert et al. (2006), and it still remains to be solved which organisms are responsible for the high methane oxidation rates. The presence of betaine lipids and glycosidic cerebrosides (Gly-Cer) cannot be specifically assigned to a biological precursor. To date betaine lipids have only been observed in anoxygenic phototrophic bacteria and plant symbiosis-associated bacteria (Benning et al., 1995; Geiger et al., 1999). Similarly, sphingolipids are not reported for strictly anaerobic bacteria (cf. Olsen and Jantzen, 2001). These results thus demonstrate a considerable lack in knowledge on the distribution of IPLs in environmentally important microorganisms.

This study could show that IPLs within oxic and anoxic water columns indeed can be used as a tracer to track changes in the microbial community composition. An additional aspect was to test if IPLs are exported to the sediment and to examine how stable IPLs are in anoxic sediments. Evidence for export of surficial IPLs to the sediment was found by the presence of 1Gly-DAG, SQ-DAG, betaine lipids and PC in the top fluff layer. Export of IPLs could occur in association with algal material via rapidly sinking particles (Fowler and Knauer, 1986). However, we also found evidence for abundant *in-situ* production of IPLs below the fluff zone, i.e., PE-DEG lipids were only detected below a sedimentary fluff layer and archaeal IPLs composed of 2Gly-GDGT and unknown head group were first detected below 2 cm, resembling previously detected benthic archaea (LIPP ET AL., 2008; LIPP AND HINRICHS, 2009). These findings show that IPLs can monitor changes in microbial community composition already within the upper centimeters of marine sediments, even under permanently anoxic conditions.

In a second study the distribution of IPLs in a methane- and hydrocarbon-fueled cold seep system was investigated, which was newly discovered by MACDONALD ET AL. (2004). This system is characterized by seepage of heavy oils and asphalts and is densely populated by chemosynthetic communities. Here, elevated concentrations of IPLs were observed in sediments surrounding the asphalts, particularly where higher amounts of oil and methane were present (*CHAPTER III*). Bacterial IPLs could be detected inside the deposited asphalts and were composed of phosphatidylethanolamine (PE) and phosphatidyl-(N)-methylethanolamine (PME) head groups with diacyl and diether core structures. The presence of Bacteria inside the asphalts could be confirmed by 16S gene sequences (WEGENER, KNITTEL ET AL., PERS. COMM.), and were observed in conjunction with methanogenic archaea. A slight biogenic contribution to the methane occluded inside the asphalts was confirmed by slightly depleted δ^{13}C values of -55‰. The top of the asphalts was at some locations colonized by dense layers of microbial mats and BRÜNING ET AL. (2009) suggested that these sites reflect the freshest seepage area. Analysis of digestive tracts of sea cucumbers showed that the benthic fauns is directly feeding on the microbial mats. Compound-specific stable carbon isotope analysis indicated that the mats are composed of methanotrophic bacteria and archaea and oil-degrading sulfate-reducing bacteria.

In oil-impregnated surface sediments a wide array of IPLs from both Bacteria and Archaea was detected. Bacteria were mainly comprised of diacylglycerol-based phospholipids containing predominantly PE and PME head groups. Other observed head groups were phosphatidylglycerol (PG), phosphatidic acid (PA), diphosphatidylglycerol (DPG), phosphatidylcholine (PC), and betaine lipids. PE was also observed with diether core structures. Archaeal IPLs were composed of phosphate-based hydroxyarchaeols and to a minor extend archaeols and GDGTs with mixed phospho- and glycosidic head groups. Generally, bacterial IPL abundance decreased with depth and archaeal IPLs increased, comprising up to 80% of total IPLs at around 15 cm. This trend was particularly obvious in one core where the sulfate-depletion zone was situated at ca. 10 cm. In the deeper sediments the most abundant archaeal IPL was comprised of PG-GDGT-PG. In the course of this thesis an extended method was developed to investigate the IPL-specific core lipid δ^{13}C values to unravel the carbon flow in this presumably highly active system (*CHAPTER IV*). Separation according to head group polarity was achieved by preparative HPLC. This separation proved very useful as it also efficiently separated the IPLs from oil-derived hydrocarbon compounds. In earlier studies the interference of an unresolved complex mixture (UCM) derived from the oil have made δ^{13}C analysis of archaeal lipids almost impossible (e.g., ZHANG ET AL., 2002; ORCUTT ET AL., 2005). Head group-specific δ^{13}C analysis in the oil-impregnated surface sediments in concert with identification of group-specific fatty acids could show that a majority of the bacterial IPLs were assigned to SRBs involved in the degradation of the oil. This observation is consistent with previous results from seep sites in the northern GoM (e.g., Joye et al., 2004). More depleted $\delta^{13}C$ values were observed for fatty acids that are typically found in SRB involved in the anaerobic oxidation of methane (AOM), these fatty acids included 10me$C_{16:0}$, cy$C_{17:0}$, and *ai*-$C_{15:0}$ (cf. Elvert et al., 2003). Some of the observed $\delta^{13}C$ of fatty acids were enriched relative to TOC, which could best explained by the presence of oil-degrading SRB that use the reversed TCA cycle during carbon assimilation (Londry et al., 2004). Archaeal IPLs in the surface sediments could be both assigned to methanotrophic and methanogenic archaea. Phosphate-based OH-AR contained the most depleted values and were assigned to ANME-2 archaea based on previous findings by Rossel et al. (2008). However, phosphate-based AR were isotopically more enriched by up to 50‰ and were consequently mainly assigned to methanogenic archaea. Similary, IPL-GDGTs showed pronounced differences. 2Gly-GDGTs were isotopically most depleted and were consistent with an ANME-1 signal (Rossel et al., 2008), whereas phosphate-based GDGTs, such as 2Gly-GDGT-PG and PG-GDGT-PG where consistently 10 to 20‰ enriched in ^{13}C compared to 2Gly-GDGTs. Consequently, phosphate-containing GDGTs were primarily assigned a methanogenic source.

Studies in deep sediments that were influenced by oil, as evidenced by the presence of oil at 8 m sediment depth, showed the presence of a sulfate-methane transition zone (SMTZ) at 6 m depth. Methanogenic activity within this zone was evidenced by depleted $\delta^{13}C$ values of methane (up to -75‰) and anaerobic oxidation of methane to CO_2 was indicated by slightly depleted $\delta^{13}C$ values of dissolved inorganic carbon in the SMTZ. IPLs could only be detected within the SMTZ and were below the detection limit above and below this activity zone. Bacterial IPLs only comprised a minor fraction of total IPLs (<20%). Archaeal IPLs composed of almost equal amounts of phosphate based OH-ARs and diglycosidic GDGTs were the most abundant IPLs. Head group-specific core lipid $\delta^{13}C$ analysis revealed that most of the OH-AR and ARs are from a similar archaeal source, as opposed to the surface sediments. 2Gly-GDGTs could be assigned to be a mixture of methanotrophic, methanogenic and heterotrophic archaea. Hereby, core lipids derived from crenarchaeol are most enriched in $\delta^{13}C$ closely resembling the values of TOC (around -20‰). We therefore assigned crenarchaeol containing IPL-GDGTs to be derived from benthic crenarchaea as observed in previous studies (Biddle et al., 2006).

As a third aim this thesis applied comprehensive two-dimensional gas chromatography (GC×GC) to decipher asphalt degradation and weathering on the ocean floor (*Chapter V*). Compositional differences of three different asphalt types that visually showed different degrees of alterations were determined and were also associated to different biocommunities on the seafloor. Asphalt samples that were presumably freshly deposited still contained the full suite of *n*-alkanes. Application of biodegradation indices, however, showed that anaerobic biodegradation is already occurring within the asphalts. Asphalts that were densely colonized by biocommunities, such as sponges, corals, and mussels distributed a complete loss of all *n*-alkanes, branched alkanes and isoprenoids, as well as a loss of low molecular weight polyaromatic hydrocarbons, including alkyl-substituted naphthalenes, phenantrenes, benzothiophenens and dibenzothiophenes. We assigned these processes to be a mixture of biodegradation and weathering, according to Arey et al. (2007). The presence of aerobic aromatic hydrocarbon degraders in symbiotic relationship with mussels (*Chapter VIc*) and sponges (Wegener, Knittel, Boetius et al., pers. comm.) showed that the aromatic compounds of the asphalts are a carbon source for the microbial communities. Highly degraded and brittle asphalt samples that have likely been deposited on the seafloor decades to centuries ago have lost more than 77% of their petroleum-compounds. The only petroleum hydrocarbon compounds left were biomarkers such as steranes and hopanes. The observation of the persistence of these hydrocarbons in the environment were also shown in other oil spill studies (e.g., Hofstettler and Kvenvolden, 1994). Comparative analysis of the different asphalt samples allowed the estimation of total petroleum hydrocarbon losses in the environment. According to these results the Chapopote asphalt deposits have a total petroleum hydrocarbon emission potential of the currently deposited asphalts at the Chapopote of 1,540 ± 770 tons. Most of which is however already efficiently recycled by the activity of hydrocarbon-degrading bacteria.

VII.2 OUTLOOK

This thesis considerably contributed to the understanding on the distribution of IPLs in the environment and its association to the dominating groups of microbes. However, these investigations have also opened up new questions that need to be tackled by both laboratory-based and *in-situ* studies

- Methane oxidation in the Black Sea anoxic water column is still enigmatic and the presence of betaine lipids and glycosidic sphingolipids with currently unknown biological precursors calls for a more detailed investigation of this site. To further unravel the metabolic capabilities of these unknown microbes I suggest to conduct preparative LC on the individual head group classes in order to study the detailed carbon flow in this system. Preparative-LC could also potentially help to elucidate potentially different sources of 1Gly- and 2Gly-GDGTs in the suboxic and anoxic water column.
- To further study the complex methanogenic and methanotrophic communities in the oil-impregnated sediments of the Gulf of Mexico I suggest to conduct ^{13}C-substrate labeling experiments in order to test uptake of methane or CO_2 and link those to specific IPLs.
- ^{13}C-labeling experiments can also be used to investigate the capabilities of the SRB to degrade certain compounds of the oil, e.g., compare the uptake of aliphatic vs. aromatic compounds and also to compare time scales of aerobic vs. anaerobic biodegradation.
- Another interesting observation was the detection of PE-OH-AR in the subsurface sediments as well as the exclusive detection of PE-DEG as bacterial IPL. Typically subsurface environments are dominated by the presence of glycosidic GDGTs. Hereby,

questions of membrane adaptation arise and it would be interesting to test more oil-influenced subsurface environments, including some that are not influenced by brines, to test if this membrane distribution is a common feature for such systems.

- Fur future studies it would also be interesting to monitor other organic intermediates, such as acetate. In this study we were constrained by sample size and could not detect sufficient amounts of acetate, indicating that this is a rapidly metabolized substrate.
- Although GC×GC proved to be a very powerful tool in deciphering degradation and weathering processes of the asphalts and estimating total petroleum hydrocarbon emission rates, future studies should also focus on compositional changes of the asphaltenes, as these comprised more than 50% of the asphalts and likely contain a multitude of environmentally toxic hydrocarbons.
- Anaerobic degradation of the asphalts could also be investigated by laboratory-based incubation studies and could be subsequently measured with GC×GC to see if the observed compositional changes from the fresh to the more degraded and weathered asphalts can be indeed mainly caused by anaerobic degradation.

VII.3 REFERENCES

Amann, R. I., Ludwig, W., Schleifer, K.-H. (1995). Phylogenetic Identification and *In-Situ* Detection of Individual Microbial Cells without Cultivation. *Microbiol. Rev.* **59**,:143-169.

Arey, J.S., Nelson, R.K., Reddy, C.M. (2007) Disentangling oil weathering using GC×GC. 1. Chromatogram analysis. *Environ Sci Technol* **41**: 5738-5746.

Benning, C., Huang, Z.H., Gage, D.A. (1995) Accumulation of a novel glycolipid and a betaine lipid in cells of *Rhodobacter sphaeroides* grown under phosphate limitation. *Arch Biochem Biophys* **317**: 103-111.

Biddle, J.F., Lipp, J.S., Lever, M.A., Lloyd, K.G., Sørensen, K.B. Anderson, R., Fredricks, H.F., Elvert, M., Kelly, T.J., Schrag, D.P., Sogin, M.L., Brenchley, J.E., Teske, A., House, C.H., Hinrichs, K.-U. (2006) Heterotrophic Archaea dominate sedimentary subsurface ecosystems off Peru. *Proc Natl Acad Sci USA* **103**: 3846-3851.

Brett, M.T., Müller-Navarra D.C. (1997) The role of highly unsaturated fatty acids in aquatic foodweb processes. *Freshw Biol* **38**: 483-499.

Brüning, M., Sahling, H., MacDonald, I. R, Ding, F, Bohrmann, G. Origin, distribution, and alteration of asphalts at Chapopote Knoll, Southern Gulf of Mexico (2009). *Mar Petrol Geol,* accepted September 2009.

Dembitsky, V.M. (1996) Betaine ether-linked glycerolipids: chemistry and biology. *Prog Lipid Res* 35: 1-51.

Elvert M., Boetius, A., Knittel, K., Jorgensen, B.B. (2003) Characterization of specific membrane fatty acids as chemotaxonomic markers for sulfate-reducing bacteria involved in anaerobic oxidation of methane. *Geomicrobiol J* **20**: 403-419.

Fowler, S.W., Knauer, G.A. (1986) Role of large particles in the transport of elements and organic compounds through the oceanic water column. *Progr Oceanogr* **16**: 147-194.

Geiger O., Röhrs, V., Weissenmayer, B., Finan, T.M., Thomas-Oates, J.E. (1999) The regulator gene *phoB* mediates phosphate stress-controlled synthesis of the membrane lipid diacylglyceryl-N,N,N-trimethylhomoserine in *Rhizobium (Sinorhizobium) meliloti*. *Mol*

Microbiol **32**: 63-73.

Harvey, H.R., Fallon, R.D., Patton, J.S. (1986) The effect of organic matter and oxygen on the degradation of bacterial membrane lipids in marine sediments. *Geochim Cosmochim Acta* **50**: 795-804.

Hostettler, F.D., Kvenvolden, K.A. (1994) Geochemical changes in crude oil spilled from the Exxon Valdez supertanker into Prince William Sound, Alaska. *Org Geochem* **21**: 927-936.

Joye, S.B., Boetius, A., Orcutt, B.N., Montoya, J.P., Schulz, H.N., Erickson, M.J., Lugo, S.K. (2004) The anaerobic oxidation of methane and sulfate reduction in sediments from Gulf of Mexico cold seeps. *Chem Geol* **205**: 219-238.

Lam, P., Jensen, M.M., Lavik, G., McGinnis, D.F., Müller, B., Schubert, C.J., Amann, R., Thamdrup, B., Kuypers, M.M.M (2007) Linking crenarchaeal and bacterial nitrification to anammox in the Black Sea. *Proc Natl Acad Sci USA* **104**: 7104-7109.

Lipp, J.S., Morono, Y., Inagaki, F., Hinrichs, K.-U. (2008) Significant contribution of Archaea to extant biomass in marine subsurface sediments. *Nature* **454**: 991-994.

Lipp, J.S., Hinrichs K.-U. (2009) Structural diversity and fate of intact polar lipids in marine sediments. *Geochim Cosmochim Acta* DOI:10.1016/j.gca.2009.08.003.

Londry, K.L., Jahnke, L.L., Des Marais, D.J. (2004) Stable carbon isotope ratios of lipid biomarker of sulfate-reducing bacteria. *Appl Environm Microbiol* **70**: 745-751.

MacDonald, I.R., Bohrmann, G., Escobar, E., Abegg, F., Blanchon, P., Blinova, V., Brückmann, W., Drews, M., Eisenhauer, A., Han, X., Heeschen, K., Meier, F., Mortera, C., Naehr, T., Orcutt, B., Bernard, B., Brooks, J., de Faragó, M. (2004) Asphalt volcanism and chemosynthetic life in the Campeche Knolls, Gulf of Mexico. *Science* **304**: 999-1002.

Manske, A.K., Glaeser, J., Kuypers, M.M., Overmann, J. (2005) Physiology and phylogeny of green sulfur bacteria forming a monospecific phototrophic assemblage at a depth of 100 meters in the Black Sea. *Appl Environ Microbiol* **71**: 8049-8060.

Olsen, I., Jantzen, E. (2001) Sphingolipids in bacteria and fungi. *Anaerobe* **7**: 103-112.

Orcutt, B., Boetius, A., Elvert, M., Samarkin, V., Joye, S.B. (2005) Molecular biogeochemistry of sulfate reduction, methanogenesis and the anaerobic oxidation of methane at Gulf of Mexico cold seeps. *Geochim Cosmochim Acta* **69**: 4267-4281.

Reeburgh, W.S., Ward, B.B., Whalen, S.C., Sandbeck, K.A., Kilpatrick, K.A., Kerkhof, L.J. (1991) Black Sea methane geochemistry. *Deep-Sea Res* **38**: 1189-1210.

Rossel, P.E., Lipp, J.S., Fredricks, H.F., Arnds, J., Boetius, A., Elvert, M., Hinrichs, K.-U. (2008) Intact polar lipids of anaerobic methanotrophic archaea and associated bacteria. *Org Geochem*. **39**: 992-999.

Rütters, H., Sass, H., Cypionka, H., Rullkötter, J. (2001) Monoalkylether phospholipids in the sulfate-reducing bacteria *Desulfosarcina variabilis* and *Desulforhabdus amnigenus*. *Arch Microbiol* **176**: 435-442.

Schloss, P. D., Handelsmann, J. (2004). Status of the microbial census. *Microbiol. Mol. Biol. Rev.* **68**: 686-691.

Schouten, S., Hopmans, E. C., Baas, M., Boumann, H., Standfest, S., Könneke, M., Stahl, D. A., Damste, J. S. S. (2008). Intact Membrane Lipids of „*Candidatus Nitrosopumilus maritimus*“, a Cultivated Representative of the Cosmopolitan Mesophilic Group I Crenarchaeota. *Appl. Environ Microbiol* **74**: 2433-2440.

Schubert, C.J., Coolen, M.J.L., Neretin, L.N., Schippers, A., Abbas, B., Durisch-Kaiser, E., Wehrli, B., Hopmans, E.C., Sinninghe Damsté, J.S., Wakeham, S.G., Kuypers, M.M.M. (2006) Aerobic and anaerobic methanotrophs in the Black Sea water column. *Environ*

Microbiol **8**: 1844-1856.

Siegenthaler, P.-A. (1998) Molecular organization of acyl lipids in photosynthetic membranes of higher plants. In Lipids in photosynthesis. Siegenthaler P.-A., Murata, N. (eds). Kluwer Academic Publishers, Dordrecht, The Netherlands, pp 199-144.

Sinninghe Damsté, J.S., Schouten, S., Hopmans, E.C., van Duin, A.C.T., and Geenevasen, A.J. (2002) Crenarchaeol: the characteristic core glycerol dibiphytanyl glycerol tetraether membrane lipid of cosmopolitan pelagic crenarchaeota. *J Lipid Res* **43**: 1641–16451.

Wada, H., Murata, N. (1998) Membrane Lipids in cyanobacteria. In: Lipids in photosynthesis: structure, function and genetics. Siegenthaler P., Murata N. (eds.) Kluwer Academic Publishers, pp. 65-81.

Wakeham, S.G., Amann, R., Freeman, K.H., Hopmans, E.C., Jørgensen, B.B., Putnam, I.F., Schouten, S., Sinninghe Damsté, J.S., Talbot, H.M., Woebken, D. (2007) Microbial ecology of the stratified water column of the Black Sea as revealed by a comprehensive biomarker study. *Org Geochem* **38**: 2070-2097.

White, D.C., Davis, W.M., Nickels, J.S., King, J.D., Bobbie, R.J. (1979) Determination of the sedimentary microbial biomass by extractable lipid phosphate. *Oecologia* **40**: 51-62.

Zhang, C.L., Li, Y., Wall, J.D., Larsen, L., Sassen, R., Huang, Y., Wang, J., Peacock, A., White, D.C., Horita, J., Cole, D.R. (2002) Lipid and carbon isotopic evidence of methane-oxidizing and sulfate-reducing bacteria in association with gas hydrates from the Gulf of Mexico. *Geology* **30**: 239-242.

ACKNOWLEDGEMENTS

My foremost thanks go to my supervisor Kai-Uwe Hinrichs. I feel very fortunate to have had the opportunity to be a PhD student under Kai's supervision, who is not only a great scientist, but also an exceptionally good motivator and someone who made me push my goals into the right direction. I also want to thank Stuart G. Wakeham for volunteering to be my very patient and enduring second supervisor, and for his very enjoyable visits to Bremen and a hopefully fruitfully continuing collaboration.

I would also like to thank my thesis committee members Antje Boetius and Matthias Zabel who supported me throughout my PhD years with helpful comments and scientific expertise.

There are many people that have accompanied me throughout my PhD years and have contributed to the outcome of this work in one way or the other. However there is one person who receives my greatest gratitude. Thanks to Julius Lipp for being there for me every day and for his invaluable help and support particularly throughout the last months of this thesis. Thank you not only for maintaining the HPLC-MS, but also for teaching me so many (big and small) things, for our extensive scientific – and non-scientific – discussions, and most importantly for your love and for making me smile every single day.

A special thanks goes to the wonderful Helen Fredricks (aka Sturt) who introduced me into the fascinating world of intact polar lipids. I couldn't have hoped for a better teacher.

An extra special thanks to Xavi Prieto-Mollar who is the irreplaceable soul of the work group and the "gute Fee" of the lab: thanks for keeping the instruments running, the lab clean and supply of solvents and nitrogen rolling in.

Thanks to my great office mates: Matthias Kellermann, Xiaolei Liu, Sitan Xie and Gerhard Versteegh for creating a great work atmosphere every day. I hereby also want to thank my "old" office mates for accompanying me throughout the years: Tobias Ertefai, Lars Hoffmann, Steffi Tille, Henning Peters, Corinna Harms, Jan Blees and many more! A very special thanks to Matti, Xiaolei and Tobi for keeping my plants alive! And thank you Matti for the games of catch ;)

I particularly want to thank Marcus Elvert, Daniel Birgel and Verena Heuer for the continuous support and supervision throughout the years. Yu-Shih Lin for sharing many late night work hours in the lab that were always fun and productive. I want to thank Marcos Yoshinaga for his great friendship and his interest in IPLs. Furthermore, I want to thank all the great current and past members of the Organic Geochemistry group, including Solveig Bühring, Pamela Rossel, Frauke Schmidt, Julio Sepulveda, Steffanie Lüers, Nadine Buchs, Marlene Bausch and Arne Leider! A very special thanks goes out to Birgit Schmincke for taking care of all the administrative things.

Thanks to the wonderful Woods Hole crew, most importantly to Chris Reddy, Todd Ventura and Bob Nelson, you guys are great! Thanks also for Sean and Sebastian for letting me share their office and the lab. Laura, Nadine, James, Kristin and Eoghan and many more are thanked for the nice times in the Kidd and everywhere else. I also want to acknowledge GLOMAR for funding my stay abroad: Especially Uta Brathauer, Carmen Murken, Gaby Rathmeyer and Dierk Hebbeln.

Thanks to all the participants on the Meteor cruises M67/2b and M72/2 and to my MPI colleagues: Gunter Wegener, Luciana Raggi, Janine Felden, Anna Lichtschlag, Thomas Holler, Daniel Santillano & many more. I also greatly valued the continuous meetings with my fellow RCOM E colleagues Feng Ding, Markus Brüning and Stephan Klapp.

I also want to send a special thanks to all the coming and going visiting scientists: Courtney Turich, Dariusz Strapoc, Carri-Ayne Jones, Mea Cook, John Pohlman, Beth! Orcutt, Roberta Hansman, Sean Sylva and of course Roger Summons and Yoshinori Takano. Additionally I want to send my thanks to the Oldenburg IPL-group: Micha Seidel and Jörn Logemann for extensive IPL-chats and helpful discussions of the data.

Thanks to the work group Geobiology for always providing enjoyable coffee chats. I am particularly thankful to my HiWis that have helped me with lab work throughout the years: Daniela Hitschel, Timo Hörske, Tim Kahs and Kevin Becker!

Additionally I would like to thank all my Bremen and non-Bremen friends for social distraction and years of support.

Ich würde diese Arbeit gerne meiner lieben Familie widmen, die mich durch all die Jahre hindurch immer liebevoll unterstützt haben: meine Oma, meine Eltern und mein lieber Bruder.

APPENDIX

Published manuscript I

Rock weathering creates oases of life in a High Arctic desert

Sara Borin[1], Stefano Ventura[2], Fulvia Tambone[3], Francesca Mapelli[1], Florence Schubotz[4], Lorenzo Brusetti[1§], Barbara Scaglia[3], Luigi P. D'Acqui[2], Bjørn Solheim[5], Silvia Turicchia[2], Ramona Marasco[1], Kai-Uwe Hinrichs[4], Franco Baldi[6], Fabrizio Adani[3], and Daniele Daffonchio[1*]

Accepted for publication in *Environmental Microbiology* (August 11, 2009)

doi:10.1111/j.1462-2920.2009.02059.x

* corresponding author. daniele.daffonchio@unimi.it

[1] *Department of Food Science and Microbiology, University of Milan, I-20133 Milan, Italy*

[2] *Istitute of Ecosystem Study, CNR, I-50019 Sesto Fiorentino, Italy*

[3] *Department of Crop Science, University of Milan, I-20133 Milan, Italy*

[4] *Department of Geosciences, University of Bremen, D-28359 Bremen, Germany*

[5] *Department of Biology, University of Tromsø, N-9037 Tromsø, Norway*

[6] *Department of Environmental Sciences, University of Venice "Ca' Foscari", I-30121 Venice, Italy*

[§] *Present address: Faculty of Science and Technology, Free University of Bozen/Bolzano, Via Sernesi 1, 39100 Bolzano, Italy*

ABSTRACT

During primary colonization of rock substrates by plants, mineral weathering is strongly accelerated under plant roots, but little is known on how it affects soil ecosystem development before plant establishment. Here we show that rock mineral weathering mediated by chemolithoautotrophic bacteria is associated to plant community formation in sites recently released by permanent glacier ice cover in the Midtre Lovénbreen glacier moraine (78°53'N), Svalbard. Increased soil fertility fosters growth of prokaryotes and plants at the boundary between sites of intense bacterial mediated chemolithotrophic iron-sulfur oxidation, and the common moraine substrate where carbon and nitrogen are fixed by cyanobacteria. Microbial iron oxidizing activity determines acidity and corresponding fertility gradients, where water retention, cation exchange capacity and nutrient availability are increased. This fertilization is enabled by abundant mineral nutrients and reduced forms of iron and sulfur in pyrite stocks within a conglomerate type of moraine rock. Such an interaction between microorganisms and moraine minerals determines a peculiar, not yet described model for soil genesis and crop formation with potential past and present analogues in other harsh environments with similar geochemical settings.

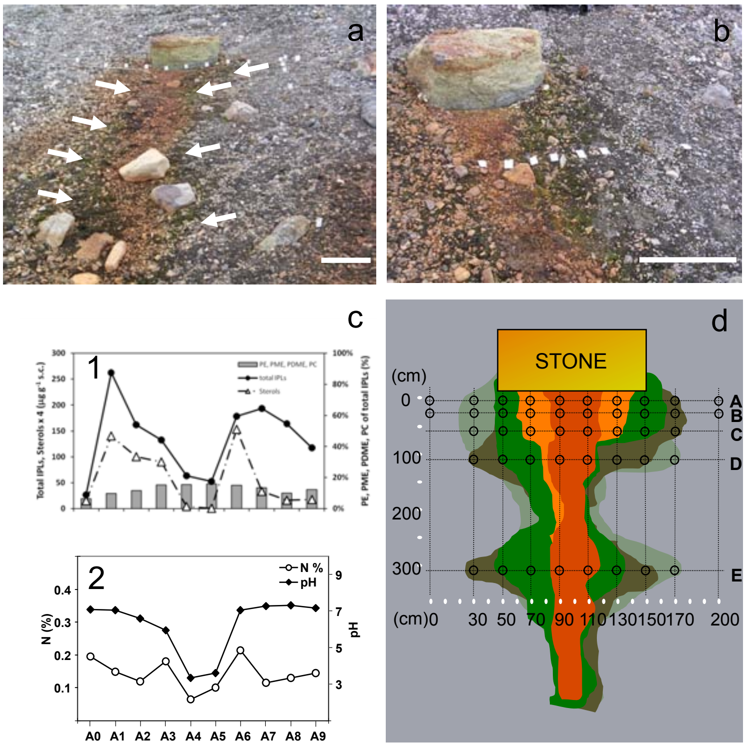

Fig. Appendix 1. The ML-RS1 site in the moraine of Midtre Lovénbreen glacier, Ny Ålesund, Svalbard. (**A**) A rusty leaching strip departs from a stone within the grey-colored moraine (white bar = 50 cm). White arrows indicate zones where dense plant biomass can be observed. A detail of an area densely-colonized by plants within the site is shown in (**B**) (white bar = 50 cm). (**C**) Relative and absolute abundance of different lipid biomarkers in soil crusts (s.c.) reflecting prokaryotic and eukaryotic biomass along transect A (**C1**) and B (**C2**). Shown are total intact polar lipids (IPLs), bacterially derived ornithine lipids (OL) and bacteriohopanepolyols (BHPs) consisting of bacteriohopane-32,33,34,35-tetrol (BHT) and 35-amino-bacteriohopane-32,33,34-triol (aminotriol) and plant sterols. Relative quantities of BHPs were normalized to the sample with maximum concentration. (**D**), map of the area showing the position of the sampling transects.

Published manuscript II

Methane-Producing Microbial Community in a Coal Bed of the Illinois Basin

Dariusz Strapoc[1], Flynn W. Picardal[2], Courtney Turich[3], Irene Schaperdoth[3], Jennifer L. Macalady[3], Julius Sebastian Lipp[4], Yu-Shih Lin[4], Tobias F. Ertefai[4], Florence Schubotz[4], Kai-Uwe Hinrichs[4], Maria Mastalerz[5], Arndt Schimmelmann[1]

Published in *Applied and Environmental Microbiology*,

vol. 74, no. 8, page 2424-2432, doi:10.1128/AEM.02341-07

© American Society for Microbiology, Apr. 2008

[1] *Department of Geological Sciences, Indiana University, Bloomington, IN, USA*

[2] *School of Public and Environmental Affairs, Indiana University, Bloomington, IN, USA*

[3] *Department of Geosciences, Pennsylvania State University, University Park, PA, USA*

Organic Geochemistry Group, Department of Geosciences and MARUM Center for Marine Environmental

[4] *Sciences, University of Bremen, D-28334 Bremen, Germany*

[5] *Indiana Geological Survey, Indiana University, Bloomington, IN, USA*

ABSTRACT

A series of molecular and geochemical studies were performed to study microbial, coal bed methane formation in the eastern Illinois Basin. Results suggest that organic matter is biodegraded to simple molecules, such as H_2 and CO_2, which fuel methanogenesis and the generation of large coal bed methane reserves. Small-subunit rRNA analysis of both the *in-situ* microbial community and highly purified, methanogenic enrichments indicated that *Methanocorpusculum* is the dominant genus. Additionally, we characterized this methanogenic microorganism using scanning electron microscopy and distribution of intact polar cell membrane lipids. Phylogenetic studies of coal water samples helped us develop a model of methanogenic biodegradation of macromolecular coal and coal-derived oil by a complex microbial community. Based on enrichments, phylogenetic analyses, and calculated free energies at the *in-situ* subsurface conditions for relevant metabolisms (H_2-utilizing methanogenesis, acetoclastic methanogenesis, and homoacetogenesis), H_2-utilizing methanogenesis appears to be the dominant terminal process of biodegradation of coal organic matter at this location.

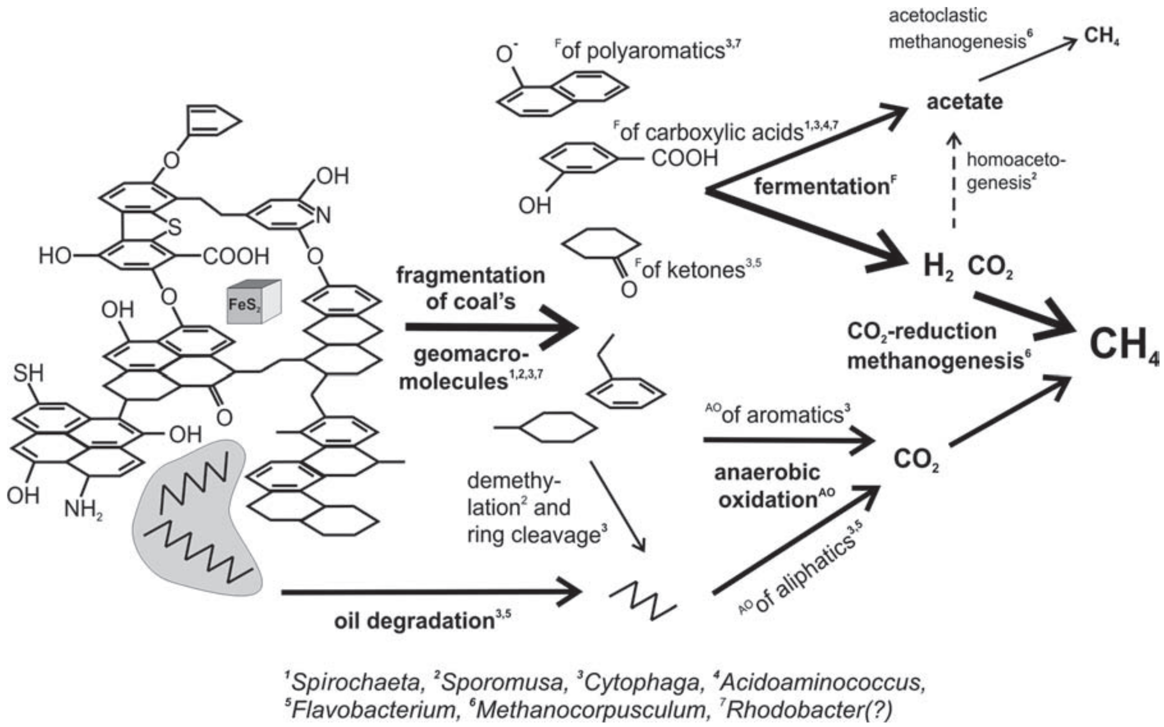
acetoclastic methanogenesis⁶
CH₄
O⁻
ᶠof polyaromatics³,⁷
acetate
ᶠof carboxylic acids¹,³,⁴,⁷
COOH
OH
fermentationᶠ
homoaceto-genesis²
OH
N
O
S
HO
COOH
O
FeS₂
OH
SH
O
OH
OH
NH₂
ᶠof ketones³,⁵
O
H₂ CO₂
fragmentation of coal's
geomacro-molecules¹,²,³,⁷
CO₂-reduction methanogenesis⁶
CH₄
ᴬᴼof aromatics³
CO₂
demethy-lation² and ring cleavage³
anaerobic oxidationᴬᴼ
ᴬᴼof aliphatics³,⁵
oil degradation³,⁵
¹Spirochaeta, ²Sporomusa, ³Cytophaga, ⁴Acidoaminococcus,
⁵Flavobacterium, ⁶Methanocorpusculum, ⁷Rhodobacter(?)

Fig. Appendix 2. Proposed mechanisms of stepwise biodegradation of OM in coal, annotated with microbes related to those found in the clone library and potentially capable of performing the indicated processes: (*i*) defragmentation of coal geomacromolecular structure predominately by fermentation targeted at oxygen-linked moieties and oxygen-containing functional groups (this process detaches some of the oxygen-linked aromatic rings and generates some short organic acids); (*ii*) anaerobic oxidation of available aromatic and aliphatic moieties, derived from coal defragmentation or from dispersed oil; (*iii*) fermentation of products available from step *i* described above to H_2, CO_2, and acetate; and (*iv*) methanogenesis utilizing H_2 and CO_2 likely predominating over homoacetogenesis and acetoclastic methanogenesis. The dark area represents a droplet of oil. The molecular model of coal is adapted from SAROJ ET AL. (2001; PROCEEDINGS OF THE 6TH U.S. MINE VENTILATION SYMPOSIUM).

CURRICULUM VITAE

Personal Information

Florence Schubotz, M.Sc.

Dept. of Geosciences
University of Bremen
PO Box 330 440
D-28334 Bremen

Tel: 0421-218-65711
Fax: 0421-218-65715
Email: schubotz@uni-bremen.de
Web: hhtp://www.marum.de/en/Florence_Schubotz.html

Born: September 27th, 1981 in Reutlingen (Germany)
Gender: female
Family status: single

Education

Mar. 2006 - Oct. 2009 (expected)	External PhD student of the GLOMAR graduate school (“Global Change in the Marine Realm”)
Jan. 2006 - Oct. 2009 (expected)	PhD candidate in the Organic Geochemistry Group at the MARUM Center for Marine and Environmental Sciences, Bremen, Germany (supervisor, Dr. K.-U. Hinrichs)
Nov. 1, 2005	Master of Science (M.Sc.), University of Bremen, Germany
Sept. 2003 - Oct. 2005	Graduate studies of the international master program Environmental and Marine Geosciences, University of Bremen, Germany
Sept. 2002 - July 2003	Graduate studies of Marine Sciences, Universidad the Las Palmas de Gran Canaria, Spain
Aug. 26, 2002	Vordiplom (undergraduate degree) in Marine Environmental Sciences, Carl-von-Ossietzky University Oldenburg, Germany
Oct. 2000 - Aug. 2002	Undergraduate studies of Marine Environmental Sciences, Carl-von-Ossietzky University Oldenburg, Germany
October 1996 - April 1999	Abitur (High school diploma)

Awards

2006 RCOM Research Award for best Master thesis. Thesis title: “Investigation of Intact Polar Lipids of Bacteria Isolated from the Deep Marine Subsurface”.

2002-2003 ERASMUS Grant for two semester academic studies in Spain, sponsored by the European Union and the DAAD (German Academic Exchange Service).

International Experience

June - Aug. 2008	Research visit at the Woods Hole Oceanographic Institution, MA, USA - collaboration with Dr. Chris Reddy
Dec. 2007	Research visit at the Skidaway Institute of Oceanography, Savannah, GA, USA - collaboration with Dr. Stuart Wakeham
Oct. - Dec. 2007	Research visit at the Woods Hole Oceanographic Institution, MA, USA - collaboration with Dr. Chris Reddy

Sea-going Experience

Feb. - Mar. 2007	RV Meteor 72/2, Black Sea - study of anoxic microbial habitats at the Crimea and Sorokin trough
Apr. 2006	RV Meteor 67/2b, Gulf of Mexico - investigation of asphalt volcanism at the Campeche Knolls
Nov. - Dec. 2004	RV Meteor 62/5a, Equatorial and South Atlantic - exploration of hydrothermal vent sites at the mid oceanic ridge

Student supervision and Teaching

Apr. - Sept. 2008	Co-supervision M.Sc. thesis of Marlene Bausch: "Molecular Signatures of Biological Soil Crusts and Salt Lakes of Southern Australia"
Apr. - Sept. 2008	Co-supervision M.Sc. thesis of Nadine Buchs: "Biogeochemical analysis of microbial biomass using HPLC/ESI-IT-MS^n"
July - Dec. 2007	Co-supervision M.Sc. thesis of Matthias Kellermann: "Lipid Biomarkers of Thiotrophic and Methanotrophic Symbionts in different *Bathymodiolus* mussel species: Chemical and Isotopic Analysis" (received 2008 MARUM award for best Master thesis)
Sept. - Mar. 2007	Co-supervision M.Sc. thesis of Corinna Harms: "Diversity of Intact Polar Lipids in an Extreme Acidic Environment: the Río Tinto, Spain"
June - July. 2006	Co-supervision of student lab course in Organic Geochemistry

Outreach and other Activities

Spring 2008	Deutsche Welle TV, short documentary on asphalts in the deep ocean "Die Geheimnisse des Asphalts" (*"Secrets of the asphalt"*)
Spring 2008	DFG Science TV, short documentary on asphalts in the deep ocean "Leben im Asphalt" (*"Life inside of asphalts"*)
Oct. 2005 - Oct. 2007	Mentor for foreign undergraduate and graduate students within the KOMPASS program, International Office, University of Bremen
Feb. - July 2005	Public relation assistant, City of Science 2005, Bremen

Erklärung gemäß § 6 Abs. 5 der Promotionsordnung der Universität Bremen für die mathematischen, natur- und ingenieurwissenschaftlichen Fachbereiche

Hiermit versichere ich, dass ich die vorliegende Arbeit

1. ohne unerlaubte fremde Hilfe angefertigt habe,

2. keine anderen als die von mir im Text angegebenen Quellen und Hilfsmittel benutzt habe, und

3. die den benutzten Werken wörtlich oder inhaltlich entnommenen Stellen als solche kenntlich gemacht habe.

Bremen, den 7.10.2009

Florence Schubotz